

**Algal dynamics in Lake Taihu, an example for shallow eutrophic lakes -  
from monitoring to modelling**

**Algendynamik im Taihu See, ein Beispiel für flache eutrophe Seen -  
vom Monitoring zur Modellierung**

Zur Erlangung des akademischen Grades einer  
DOKTORIN DER NATURWISSENSCHAFTEN  
von der KIT-Fakultät für  
Bauingenieur-, Geo- und Umweltwissenschaften

des Karlsruher Instituts für Technologie (KIT)

genehmigte

DISSERTATION

von

M. Sc. Jingwei Yang

aus Hubei, China

Tag der mündlichen Prüfung: 04. 12. 2020

Referent: Prof. Dr. Stefan Norra

Korreferent: Prof. Dr.-Ing. Stefan Hinz

Karlsruhe, den 24. 12. 2020

## **Erklärung**

Hiermit erkläre ich, dass ich die vorliegende Dissertation, abgesehen von der Benutzung der angegebenen Hilfsmittel, selbständig verfasst habe.

Alle Stellen, die gemäß Wortlaut oder Inhalt aus anderen Arbeiten entnommen sind, wurden durch Angabe der Quelle als Entlehnungen kenntlich gemacht.

Diese Dissertation liegt in gleicher oder ähnlicher Form keiner anderen Prüfungsbehörde vor.

Karlsruhe den 24. 12. 2020

Jingwei Yang

Some great mottos get me out of mental doldrums and spur me on in science.

## **Mottos**

The best part about science is that it never ends.

— Ashmita Acharyya

Patience passes science

Patience surpasses knowledge.

— Motto under Coat of Arms of Viscount Falmouth

Your assumptions are your windows on the world. Scrub them off every  
once in a while, or the light won't come in.

— Isaac Asimov

## Acknowledgements

I want to thank the China Scholarship Council (CSC) for financial support to pursue my Ph.D. study in Germany for four years and KIT Graduate School for Climate and Environment (GRACE) for three months doctoral extension. The research project I was embedded was funded by the Federal Ministry of Education and Research of Germany (BMBF, grant no. 02WCL1336B). Further, I very much appreciate GRACE to offer various courses and summer school for developing personal skills and providing funds for me to attend and give a talk at the 34<sup>th</sup> International Society of Limnology conference held in Nanjing, China. I have also received GRACE funds for the two and half months research stay at Taihu Laboratory for Lake Ecosystem Research (TLLER) in China and the University of North Carolina at Chapel Hill (UNC-CH) in the US. Thanks also to the Karlsruhe House of Young Scientists (KHYS), providing one-month funds for me to stay at the University of Melbourne (UoM) in Australia.

This Ph.D. thesis is the output of the efforts and support of several people to whom I am extremely grateful. First and foremost, I would like to extend my deepest gratitude to my supervisors Professor Dr. Stefan Norra, Professor Dr. Stefan Hinz and Dr. Andreas Holbach, for their helpful advice on my Ph.D. study and scientific career. Professor Dr. Stefan Norra, thanks for guiding and teaching me how to be a good researcher and fieldworker and thanks for your concern about my life in Germany. I appreciated all your contributions of time, ideas and funding to make my Ph.D. experience wonderful, productive and stimulating. Professor Dr. Stefan Hinz, thanks for your valuable comments on my presentations and the thesis. Special thanks to Andreas for teaching me how to use instruments and analyse data patiently at the beginning of my Ph.D. and always supported and nurtured me to get through different kinds of problems, even when you are in Denmark. You taught me by your actions to keep calm and seek new solutions when sampling and researches facing difficulties.

I also wish to express my gratitude to my colleagues at AGW for daily accompany, sharing work and lives, exchanging ideas and keep me in a motivating mood. They enriched my time in Germany. Thank you, Andre Wilhelms, Nicolas Börsig, Jonas Bauer, Hongyan Wang, Xiaohui Tang, Flavia Digiaco, Andrew Thomas, and Van Cam Pham. I am very glad to express my sincere gratitude and thanks to lab technicians, Elisabeth Eiche, Claudia Mößner, Beate Oetzel, Ralf Wachter,

Chantalle Kotschenreuther, Kristian Nikoloski, and Gesine Preuß, for their immense and constant support, information and timely help. I affectionately thank secretaries, Andrea Friedrich, Victoria Weist and Ilse Engelmann, for assisting me in many different ways. Especially, Andrea Friedrich, you are always so friendly and patient to help me. I also want to thank Andreas Schenk, who was helping me applying for GRACE funds.

Thanks to the nice colleagues from the SIGN-project group. I enjoy the time of sampling with you together and thanks for your friendly help during sampling and lab work in China: Charlotte Schäfer, Cora Schmid, Tim aus der Beek, Anna-Lena Schneider, Lara Stelmaszyk, Aili Li and Yunlu Jia. Special thanks to Andre Wilhelms, I received great support, physical help and warm encouragement from you.

I gratefully acknowledge the help of Peter Haushahn, Christian Moldaenke, and André Zaake for offering remote help when instruments were having troubles in the field. I learned sensor technology from you.

The work presented in this thesis has been critically assessed and approved by an outstanding committee to whom I am more than grateful: Prof. Dr. Stefan Norra, Prof. Dr. Stefan Hinz, Prof. Dr. Franz Nestmann, Prof. Dr. Thomas Neumann, PD Dr. Ulf Mohrlök, Prof. Dr. Olivier Eiff, and Prof. Dr. Florian Wittmann. Thanks for serving as my committee members even at these hard Corona times.

At last, I am deeply thankful to my family and friends for their love, encourage and support, which enable me to enjoy the research life to the fullest. Without them, this thesis would never have been finished.

## **Abstract**

Algal blooms are frequently observed in eutrophic lakes and have become a widespread concern in many countries in the world. Algal blooms are never absent and appear many times every year in shallow and eutrophic Lake Taihu, China. The drinking water crisis that happened in 2007 has been a wake-up call for government, researchers and civilians. For more than a decade, many measures were taken to alleviate this problem. However, the result is not satisfactory, until now. It urgently needs to understand the algal dynamics in shallow and eutrophic Lake Taihu in different seasons and the driving factors for the algal bloom. Developing better policies and solutions must be based on these pieces of knowledge and background.

Traditional methods for water quality measurement always generate delayed data, which can not resolve real-time situations. Moreover, most studies ignore the vertical difference in water quality, especially when studying shallow water bodies. This study applied a stationary online high-frequency multi-sensor system (BIOLIFT) to measure the water quality changes across the whole water column. A real-time weather station was connected to the BIOLIFT to record meteorological data at the same time. Moreover, a boat dragged online multi-sensor system (BIOFISH) was used to measure the water quality's spatial distribution. Water and sediment samples were also taken at the same time to understand the nutrients and trace metals status and dynamics in Lake Taihu. A simulation model and conceptual model was created based on this knowledge, which aims to contribute to an early warning system for water management and drinking water plants in the near future. Moreover, online measurement data were compared with data from the deeper and less eutrophic Lake Westensee, Germany.

From the results, eutrophication and lake shallowness create better conditions for algal growth and also aggravate the remobilization of metals. Oxygen depletion was observed, caused by algal decomposition and sunlight reduction in the water by algal scums. It will kill aquatic animals and reduce biodiversity. Algal dynamic, meteorological changes, and water quality (e.g., nutrients, water temperature, etc.) variation have seasonal differences. Even in shallow Lake Taihu, stratification was observed in summer and sometimes in autumn, which indicates the necessity of vertical depth-profile monitoring. The vertical distribution of algae varied between species and is

influenced by the wind-induced mixing and resuspension. Specifically, resuspension is one of the nutrient sources and it can help the benthic algae get better living conditions as well as bring the surface blue-green algae scums back to deeper layers. Blue-green algae prefer to accumulate on the water surface in summer and autumn to get better light conditions, especially in the afternoon. Light is important for algal growth, however, fluorescence quenching and/or photoinhibition caused by the strong sunlight will increase algae fluorescence signals at night due to the recovery of light damage. In general, shallow lakes have better light availability, however, easier to be reduced by wind-induced resuspension. Except for the resuspension, blue-green algae scums will also influence the light conditions in the water.

In general, blue-green algal blooms prefer to happen under warm, sunny, calm, and high pH conditions. There is a high probability that it will happen after a strong wind. Blue-green algae can also tolerate low-light conditions by their capability to move to the water surface by buoyancy changes. Therefore, preventive work can be done beforehand.

From the result, models were developed based on high-frequency multi-sensor and weather data to simulate chlorophyll-a fluorescence changing rate of green algae and diatoms and phycocyanin fluorescence of blue-green algae on the water surface layer. Taking into account weather forecast data, these models furthermore have the potential to predict chlorophyll-a and phycocyanin fluorescence over short-term periods (2-3 days). This can be used in the drinking water plant for further decision-making of water treatment procedures and the amount of water pumped in different intake areas.

This dissertation provides new methods to measure and analyse water quality in shallow and eutrophic lakes. Besides Lake Taihu, the system can also be applied in other surface waters (e.g., Lake Westensee). The pieces of knowledge and models about the water and algal dynamics can also be transferred to other lakes in the world as well.

## **Zusammenfassung**

Algenblüten kommen häufig in eutrophen Seen vor und sind in vielen Ländern der Welt zu einem großen Problem geworden. Ein Beispiel hierfür ist der flache und eutrophe Taihu-See in China. Im Taihu-See treten Algenblüten oft mehrmals im Jahr auf und führen zu wachsenden Herausforderungen bei der Trinkwasserversorgung. Besonders die Trinkwasserkrise im Jahr 2007 war ein Weckruf für die Regierung, Zivilbevölkerung und Forscher, weshalb über die letzten Jahre verschiedenste Maßnahmen ergriffen wurden, um diesem Problem entgegenzuwirken. Die Ergebnisse dieser Maßnahmen sind jedoch bis heute nicht zufriedenstellend. Es ist daher dringend erforderlich, die Algendynamik im Taihu-See in den verschiedenen Jahreszeiten zu verstehen sowie die treibenden Faktoren der Algenblüten zu identifizieren, um auf Basis dieses Wissens angepasste Strategien und Lösungen zu entwickeln.

Herkömmliche traditionelle Methoden zur Messung der Wasserqualität liefern in der Regel verzögerte Messdaten, die meist nie die Echtzeit-Situation eines Gewässers widerspiegeln. Zudem ignorieren die meisten Messverfahren vertikale Unterschiede der Wasserqualität, die insbesondere bei flachen und geschichteten Wasserkörpern einen großen Einfluss haben können. In dieser Studie wurde daher ein stationäres Online-Hochfrequenz-Multisensorsystem (BIOLIFT) eingesetzt, um die Veränderungen der Wasserqualität über die gesamte Wassersäule zu analysieren. Gleichzeitig wurde eine an den BIOLIFT angeschlossene Wetterstation genutzt, um meteorologische Echtzeit-Daten zu erfassen. Zur Messung der räumlichen Verteilung der Wasserqualität kam zudem ein Online-Multisensorsystem (BIOFISH) zum Einsatz, welches von einem Boot aus betrieben wurde. Parallel zu diesen Aktivitäten wurden Wasser- und Sedimentproben entnommen, um den Zustand und die Dynamik der im Taihu-See auftretenden Nährstoffe und Spurenmetalle zu charakterisieren. Auf Basis dieser Erkenntnisse wurde anschließend ein Simulationsmodell sowie ein konzeptionelles Modell erstellt, das in naher Zukunft dazu beitragen soll, ein Frühwarnsystem für das Wassermanagement am Taihu-See und den Betrieb von Trinkwasseranlagen zu entwickeln. Darüber hinaus wurden die ermittelten Online-Messdaten mit entsprechenden Daten des tieferen und weniger stark eutrophierten Westensees in Deutschland verglichen.

Aus den Ergebnissen dieser Arbeit geht hervor, dass die Eutrophierung in Kombination mit geringen Wassertiefen vorteilhafte Bedingungen für das Algenwachstum schafft und auch die



Remobilisierung von Metallen verstärkt. Es wurde ein Sauerstoffmangel beobachtet, der durch die Zersetzung von Algen und die Reduzierung des ins Wasser einfallenden Sonnenlichts durch Algenschäume verursacht wurde. Dieser Sauerstoffmangel führt zum Tod von Wassertieren und zur Verringerung der Artenvielfalt. Die Algendynamik, die Klima- und Witterungsbedingungen sowie die Wasserqualität (z.B. Nährstoffgehalte, Wassertemperatur, etc.) weisen außerdem starke jahreszeitliche Unterschiede auf. Selbst im flachen Taihu-See wurde im Sommer und zeitweilig im Herbst eine Stratifizierung beobachtet, was auf die Notwendigkeit eines vertikalen Tiefenprofil-Monitorings der Wasserqualität hinweist. Die vertikale Verteilung der Algen variiert in Abhängigkeit der Algenarten und wird durch windinduzierte Vermischungs- und Resuspensions-Ereignisse beeinflusst. Resuspensionsprozesse stellen eine der zentralen Nährstoffquellen dar und können insbesondere den benthischen Algen zu besseren Lebensbedingungen verhelfen sowie nahe der Wasseroberfläche auftretende Blaualgenkolonien in tiefere Wasserschichten zurückbringen. Blaualgen sammeln sich im Sommer und Herbst, vor allem am Nachmittag, bevorzugt an der Wasseroberfläche an. Sonnenlicht ist wichtig für das Algenwachstum, jedoch führen Fluoreszenzlöschung- und/oder Photoinhibitionseffekte durch das starke Sonnenlicht zu einem Anstieg der Algenfluoreszenz in der Nacht, aufgrund der Erholung von Lichtschäden. Im Allgemeinen weisen flache Seen wie der Taihu eine bessere Lichtverfügbarkeit auf, allerdings kann diese auch leichter durch windbedingte Resuspensionsprozesse reduziert werden. Neben der Resuspension beeinflussen auch Blaualgenschäume die Lichtverhältnisse im Wasser.

Grundsätzlich treten Blaualgenblüten vorzugsweise an warmen, sonnigen und ruhigen Tagen auf, wenn das Wasser außerdem einen hohen pH-Wert aufweist. Es besteht zudem eine höhere Wahrscheinlichkeit, dass Blaualgenblüten nach einem starken Windereignis auftreten. Blaualgen tolerieren auch Schwachlichtbedingungen, indem sie sich durch Auftriebsänderungen an die Wasseroberfläche bewegen. Daher kann präventive Arbeit im Vorfeld geleistet werden.

Mit den Ergebnissen dieser Studie wurde ein Modell entwickelt, mit dem auf Basis von hochfrequenten Multisensor- sowie Wetterdaten die Chlorophyll-a-Fluoreszenz-Veränderungsraten von Grün- und Kieselalgen sowie die Phycocyanin-Fluoreszenz von Blaualgen an der Wasseroberfläche simuliert werden können und sich darüber hinaus über einen kurzfristigen Zeitraum (2-3 Tage) vorhersagen lassen. Dies kann in Trinkwasseranlagen zur weiteren

Entscheidungsfindung über notwendige Wasseraufbereitungsverfahren und die Menge des in verschiedene Einzugsgebiete gepumpten Rohwassers genutzt werden.

Diese Dissertation zeigt neue Methoden zur Messung und Analyse der Wasserqualität in flachen und eutrophen Seen. Neben dem Taihu-See kann dieses System auch in anderen Oberflächengewässern (z.B. den Westensee) angewendet werden. Die Erkenntnisse und Modelle über die Wasser- und Algendynamik lassen sich zudem auf andere Seen in der Welt übertragen.

## Table of Contents

<i>Erklärung</i> .....	<i>I</i>
<i>Mottos</i> .....	<i>II</i>
<i>Acknowledgements</i> .....	<i>III</i>
<i>Abstract</i> .....	<i>V</i>
<i>Zusammenfassung</i> .....	<i>VII</i>
<i>Table of Contents</i> .....	<i>X</i>
<i>List of Figures</i> .....	<i>XII</i>
<b>1 Context of this dissertation</b> .....	<b>15</b>
<b>1.1 Introduction</b> .....	<b>16</b>
1.1.1 Eutrophication in the world and Lake Taihu region .....	16
1.1.2 Algal monitoring and modelling .....	19
1.1.3 Metal pollution .....	22
<b>1.2 Research objectives</b> .....	<b>23</b>
<b>1.3 The “SIGN” project</b> .....	<b>25</b>
<b>1.4 Study area — Northern Lake Taihu, China</b> .....	<b>26</b>
1.4.1 Location and morphological characteristics.....	26
1.4.2 Hydrology and Climate .....	27
1.4.3 Pollution and Eutrophication.....	28
1.4.4 Characteristic of Northern Lake Taihu .....	30
<b>1.5 Synoptic summary of field works and experiment methods</b> .....	<b>33</b>
1.5.1 Stationary depth-profile multi-sensor system (BIOLIFT) for <i>in situ</i> water and meteorological parameter measurements.....	33
1.5.2 Spatial-temporal multi-sensor system (BIOFISH) for <i>in situ</i> water quality measurements at certain depth .....	34
1.5.3 Performed fieldwork and chemical analytics .....	35
1.5.4 Sample collection and chemical analytics .....	36
1.5.5 Statistical methods .....	38
<b>2 Results</b> .....	<b>40</b>
<b>2.1 Published results and discussion</b> .....	<b>40</b>
2.1.1 Highly time-resolved analysis of seasonal water dynamics and algal kinetics based on in-situ multi- sensor-system monitoring data in Lake Taihu, China.....	40

2.1.2 Identifying spatio-temporal dynamics of trace metals in shallow eutrophic lakes on the basis of a case study in Lake Taihu, China .....	42
2.1.3 Simulating chlorophyll-a fluorescence changing rate and phycocyanin fluorescence at one location by using a multi-sensor system in Lake Taihu, China .....	45
<b>2.2 Further results and discussions .....</b>	<b>47</b>
2.2.1 Water quality vertical distribution at different times and seasons.....	47
2.2.2 Nutrients spatial distribution and temporal dynamics .....	51
2.2.3 Water quality comparison of Lake Westensee in Germany and Lake Taihu in China .....	65
<b>3 Synoptic discussion.....</b>	<b>70</b>
3.1 Algal biomass dynamics .....	70
3.2 Algal species changes.....	73
3.3 Influence of algal dynamic, lake eutrophication and shallowness to the water quality and aquatic life.....	76
<b>4. Conclusions and outlook.....</b>	<b>77</b>
4.1 Conclusions .....	77
4.2 Outlook.....	78
4.2.1 Early-warning system for drinking water plants .....	78
4.2.2 Transferred the knowledge and technology to other aquatic systems.....	79
<b>References.....</b>	<b>80</b>
<b>Appendix A-List of publications during my Ph.D. study as first author .....</b>	<b>93</b>
<b>Appendix B-Full articles of scientific publications as first author .....</b>	<b>94</b>

## List of Figures

Figure 1 Trophic state classification of global inland waters in the austral and boreal summers of 2012 assessed using the FUI-based method. Reprinted by permission from Fig.13 in Wang et al. (2018) . © Elsevier & Remote Sensing of Environment. ....	17
Figure 2 Most concerned keywords in publications related to lakes (1955 - 2019) a) Chinese lakes; b) worldwide drinking water c) worldwide policy development. Adapted by permission from Fig. 3, 8, 10 in Ho and Goethals (2020). © Springer Nature & Scientometrics. ....	19
Figure 3 Lake Taihu area within China and the specific study areas of northern Lake Taihu .....	26
Figure 4 COD <sub>Mn</sub> , TP and TN changes from 1988 to 2018 in Lake Taihu. Adapted by permission from Qin (2008). © Springer Nature & Springer eBook. Adapted from The health status report of Taihu Lake (2019) in <a href="http://www.tba.gov.cn/slbthlyglj/sj/sj.html">http://www.tba.gov.cn/slbthlyglj/sj/sj.html</a> . ....	29
Figure 5 Trophic status index changes in recent years. Adapted from The health status report of Taihu Lake (2019) in <a href="http://www.tba.gov.cn/slbthlyglj/sj/sj.html">http://www.tba.gov.cn/slbthlyglj/sj/sj.html</a> .....	30
Figure 6 Changes of TN and TP distribution in recent years (2007, 2012, 2017, 2018). Adapted from The health status report of Taihu Lake (2019) in <a href="http://www.tba.gov.cn/slbthlyglj/sj/sj.html">http://www.tba.gov.cn/slbthlyglj/sj/sj.html</a> .....	31
Figure 7 Algal bloom distribution in 2018 (the darker the colour, the greater the density). Adapted from The health status report of Taihu Lake (2019) in <a href="http://www.tba.gov.cn/slbthlyglj/sj/sj.html">http://www.tba.gov.cn/slbthlyglj/sj/sj.html</a> .....	32
Figure 8 Spatial distribution of (left) agriculture and (right) industry pollution. Reprinted by permission from Zhao et al. (2013).© Springer Nature & Chinese Geographical Science.....	32
Figure 9 Structure of BIOLIFT-buoy system (left) and its application in Lake Taihu (right) .....	34
Figure 10 BIOFISH measuring spatial water quality at certain depth by using float body.....	35
Figure 11 Timeline of fieldworks conducted within the SIGN project. Note: the campaigns conducted by other colleagues were with dark background (2014 April, 2015 May & November, 2019 August).....	35
Figure 12 The developments of BIOLIFT-buoy system.....	36

Figure 13 Depth-profile of water temperature and air temperature changes in three days in different campaigns in 2018 .....	48
Figure 14 Vertical distributions of a) - c) $Chl_{a-f}$ , d) - f) Phycocyanin, g) - i) photosynthetically active radiation at different water depths (IRR), as well as j) - l) wind direction and speed in three days in three different campaigns in 2018 .....	49
Figure 15 Percentage of $Chl_{a-f}$ of blue-green algae, diatoms and green algae measured by PhycoLA in three campaigns in 2018. ....	50
Figure 16 Seasonal changes of a) TN, b) $NO_3-N$ and $EC_{25}$ , c) $NH_4-N$ and wind speed.....	53
Figure 17 Time series of chlorophyll-a fluorescence, phycocyanin fluorescence (blue-green algae), CDOM, turbidity, $PAR_{water}/PAR_{air}$ , wind speed, wind direction and TN in 2018 November .....	54
Figure 18 Seasonal changes of a) dissolved P, Oxygen-sat., wind speed, b) particulate P and wind speed, c) total P at TLLER station .....	55
Figure 19 Spatial distribution of a) P in the surface sediment; b) dissolved P in the surface water samples in northern Lake Taihu.....	57
Figure 20 Time series of $Chl_{a-f}$ _PhycoLA, TN and $NH_4-N$ changes in a) 2018 November; b) 2019 March .....	58
Figure 21 a)-c) Time series of $Chl_{a-f}$ _PhycoLA, dissolved P and $NO_3-N$ changes in 2018 March/April, 2018 November and 2019 March; d) summarized variation curve of $Chl_{a-f}$ and nutrients.....	59
Figure 22 Location of River Ludianqiaobang (LD) and River Xinhuzhuangtianbang (XH).....	60
Figure 23 Concentration of $NO_3-N$ , $NH_4-N$ , TN and dissolved P in different locations and two different days (30 <sup>th</sup> March and 1 <sup>st</sup> April) .....	61
Figure 24 Ratio changes of algal classes within two days at the TLLER station.....	62
Figure 25 Ratio changes of algal classes in different location along River LD and XH.....	63
Figure 26 Geographic location of Lake Westensee and Lake Taihu .....	66
Figure 27 Color map and time series of parameters measured by BIOLIFT in Lake Westensee and Lake Taihu .....	68

Figure 28 Conceptual model of algal biomass and species changes .....	71
Figure 29 Variation curve of Chl <sub>a-f</sub> changing rate and a) temperature, b) wind speed .....	72
Figure 30 Typical seasonal variations of algal concentration. Reprinted from Fig.5.1.2 in Ji (2017). © John Wiley and Sons & Wiley Books. ....	73
Figure 31 Correlation between a) pH and Chl <sub>a-f</sub> of blue-green algae, b) PAR and ratio of Chl <sub>a-f</sub> of blue-green algae .....	74
Figure 32 Diurnal changes of $\Delta\text{Chl}_{a-f}\%$ and PAR in a) 2016 June/July; June 29 <sup>th</sup> - July 1 <sup>st</sup> , b) 2016 June/July; July 3 <sup>th</sup> - 5 <sup>th</sup> , c) 2017 February/March; February 26 <sup>th</sup> - 28 <sup>th</sup> , d) summarized diurnal variation curve of $\Delta\text{Chl}_{a-f}\%$ and PAR. ....	75
Figure 33 Structure diagram of algal early warning system for drinking water plants .....	79

## List of Tables

Table 1 TN and TP in different trophic status of water bodies. Reprinted by permission from Table 1 in Bhagowati and Ahamad (2019) . © Elsevier (2018). ....	16
Table 2 Comparison of different algal monitoring methods (Ogashawara, 2019; Principles, 2017) .....	20
Table 3 The instruments and technologies used for sample analysis .....	37
Table 4 The software and statistic methods used in the study .....	38
Table 5 Campaign information and measured parameters at TLLER station .....	52
Table 6 Basic information and annual air temperature, wind speed, wind direction, rainfall in Lake Westensee and Lake Taihu .....	66
Table 7 Comparison of annual TP, TN and chlorophyll-a concentraton in Lake Taihu and Lake Westensee in 2017 .....	67

## **1 Context of this dissertation**

Lake Taihu, located in Yangtze Delta, China, is a key drinking water source for the local human population (estimated to be ~10 million), with tourism, fisheries, and shipping being additionally important economic functions (Qin et al., 2010). However, it is also a well-known algae-plagued large and shallow lake due to serious eutrophication, which caused hampered water supply in surrounding areas (Zhang et al., 2008). In shallow water, light condition is better and the temperature is higher at the bottom, which creates better conditions for the algal growth and bloom (Janssen et al., 2014). Moreover, water levels and conditions can be subject to strong fluctuations resulting from climatic variability in shallow lakes (Scheffer and Van Nes, 2007). Detailed introduction of these issues follows in section 1.1. In this context, this dissertation aims to understand the algal dynamics in shallow eutrophic Lake Taihu and explore the possibility of modeling the algal dynamics based on high-frequency multi-sensor data. The specific research objectives are in section 1.2.

This dissertation is based on the cumulation of three first-author scientific publications (Section 2.1) and three other parts: water quality vertical distribution (section 2.2.1), nutrient dynamic (section 2.2.2), and comparison of Lake Westensee and Lake Taihu (Section 2.2.3). The research papers are all based on fieldwork, physical analyses, biogeochemical analyses, statistic and mathematical modelling, and experiences that were all performed and gained within the frame of “Sino-German research (SIGN) project” funded by the ‘Federal Ministry of Education and Research of Germany’ (BMBF) as well as the ‘Ministry of Science and Technology of China’ (MOST). The project is introduced in section 1.3. The specific characters of the study area (Lake Taihu) are illustrated in section 1.4 to better understand the purposes of this study. All the sampling and analytical instruments and methods used in this study are summarized in section 1.5.

In the cumulated publications of this dissertation, I revolved around the shallow and eutrophic characteristics of Taihu Lake discussing the vertical distribution and dynamics of algae (section 2.1.1), the influence of shallowness and eutrophication to the metal dynamics (section 2.1.2), and algal simulation models in shallow and eutrophic lakes (Section 2.1.3). Section 2.2.1 is about water quality vertical distribution in different seasons. In section 2.2.2, the nutrients status and dynamics in Lake Taihu across different seasons are analyzed. Furthermore, geographic location, local



climate, land use and water quality of the eutrophic Lake Taihu (China) and Lake Westernsee (Germany) were compared (section 2.2.3). Combining complementary information of algal and chemical spatial-vertical dynamics is a prerequisite to understanding the full complexity of biogeochemical processes in shallow eutrophic lakes, to develop efficient water management and prevention measures and to create an algal forecast model for the drinking water plant.

## 1.1 Introduction

### 1.1.1 Eutrophication in the world and Lake Taihu region

Environmental risk due to water pollution is an ongoing everyday problem in many lakes, coastal areas and rivers of the World. Eutrophication, during the last decades, has emerged as one of the leading causes of water quality impairment due to human activities (Vinçon-Leite and Casenave, 2019). It is an ecological state of aquatic ecosystems when the water environment becomes enriched with nutrients (Ansari et al., 2010; Boyd, 2015; Smith et al., 1998). The nutrient status of the water body is usually classified into three classes: oligotrophic, mesotrophic, eutrophic (Carlson, 1977) (Table 1). Lakes with extreme trophic indices may also be considered "hypertrophic".

**Table 1 TN and TP in different trophic status of water bodies. Reprinted by permission from Table 1 in Bhagowati and Ahamad (2019). © Elsevier (2018).**

Trophic status	Total P ( $\mu\text{g/L}$ )	Total N ( $\mu\text{g/L}$ )
Oligotrophic	5-10	250-600
Mesotrophic	10-30	500-1100
Eutrophic	30-100	1000-2000
Hypertrophic	>100	>2000

In the Lake Taihu region, wastewater discharge, agriculture and other anthropogenic activities generally override natural processes and substantially increase N and P concentrations (Wurtsbaugh et al., 2019). Excess phosphorus inputs to lakes mainly come from agriculture, and industrial discharges, sewage, urban areas, and construction sites (Bennett et al., 2001). Particulate P is the dominant fraction of total P loss by runoff, as the P is widely considered to be firmly fixed onto the soil particles (Zhang et al., 2003). Similar to P, applied fertilizers are also the primary source of N inputs and runoff is the major pathway to transport into aquatic systems (Lian et al.,

2018; Zhao et al., 2012). In addition, domestic sewage, livestock, and poultry farm sewage incorporates more ammonium-N ( $\text{NH}_4\text{-N}$ ) and get into the water body during rainfall events (H. Xu et al., 2008). In the Lake Taihu region, production and/or processing of textiles, paper, petroleum, chemicals, medicines, and fibers are the six major polluting industries, with around 1.04 million factories in Jiangsu province, where Lake Taihu is located (Dai, 2014). The soil in Jiangsu province is intensively cropped, with over 4 million hectares of irrigated area and ca. 3 million tons of applied chemical fertilizers in 2017 (National Bureau of Statistics of China, 2018), and primarily under a rice-wheat rotation (Wang et al., 2015).

Wang et al. (2018) assessed the trophic state of global inland waters in 2012 (Fig.1). Of the 2058 water bodies considered, eutrophic water bodies accounted for 63.1% of the total number and 30.5% of the total surface area, mesotrophic water bodies accounted for 26.2% of the total number and 39.4% of the total surface area, and oligotrophic water bodies accounted for 10.7% of the total number but 30.1% of the total surface area. Eutrophication is no longer a local issue. Instead, it turned out to be a global problem.

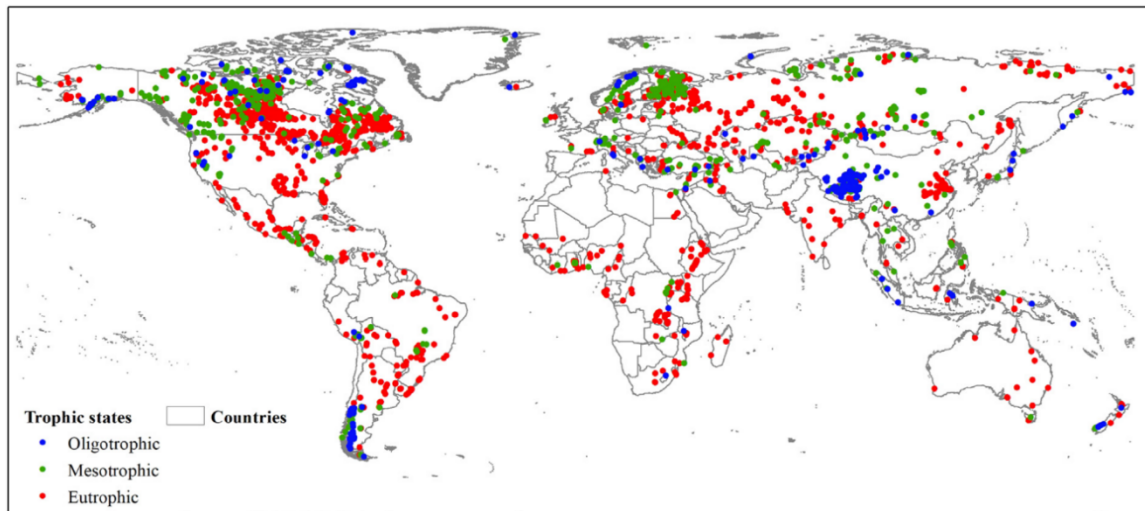


**Figure 1 Trophic state classification of global inland waters in the austral and boreal summers of 2012 assessed using the FUI-based method. Reprinted by permission from Fig.13 in Wang et al. (2018) . © Elsevier & Remote Sensing of Environment.**

Eutrophication stimulates an array of symptomatic changes, including increased phytoplankton and resulting in high turbidity, less light penetration and anoxic conditions, which leads to fish kills (Schindler et al., 2008; Wang and Wang, 2009). Eutrophication may lead to fisheries and

water quality deterioration, drinking water crisis and other undesirable changes that interfere with water use (Bhagowati and Ahamad, 2019; Prepas and Charette, 2003) and threaten human and animal health. In some areas, these environmental crises have become an urgent societal issue. Qin et al. (2010) reviewed the Wuxi drinking water crisis in 2007 at the northern shore of Taihu Lake due to bloom-forming cyanobacterial genus *Microcystis* contamination, which affected more than 1 million citizens. Another example is the toxic algal bloom in Lake Erie in 2014, which forced 0.4 million people to drink bottled water for three days (Smith et al., 2015).

Besides, environmental factors might also stimulate eutrophication, including long water residence times, high temperatures and a sufficient amount of irradiation (light). From Izmailova and Rumyantsev's study (2016), anthropogenic eutrophication processes have presently affected not only small-sized and middle-sized lakes, but also most of the large shallow lakes (surface areas exceeding 1000 km<sup>2</sup>) in the world due to their specific physiographic conditions. Since sediments are frequently disturbed by wind-induced resuspension in shallow lakes, leading to massive nutrients release and increased eutrophication. Moreover, the large lakes contain the most important freshwater reserves on the planet. It is very important to have a clear idea of their ecological conditions, and the changes that have taken place in them during the past decades.

Ho et al. (2020) retrieved research hotspots of 147,811 publications about lakes and reservoirs from the database of the Science Citation Index Expanded from 1955 to 2019. Lake Taihu is the most studied lake in China and eutrophication is one of the most concerned subjects in drinking water and policy development research in the world (Fig.2).

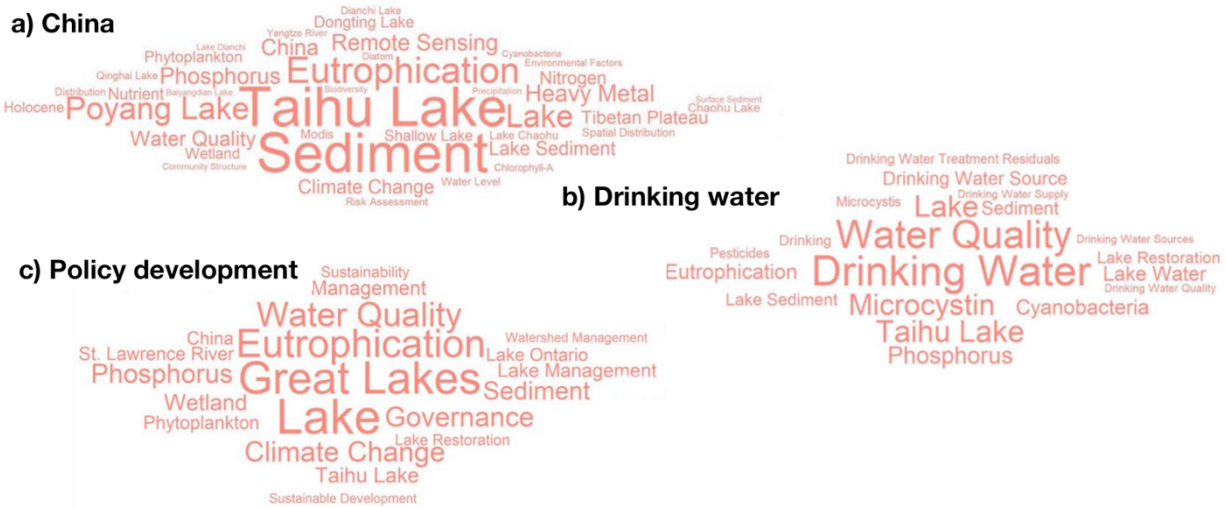


**Figure 2** Most concerned keywords in publications related to lakes (1955 - 2019) a) Chinese lakes; b) worldwide drinking water c) worldwide policy development. Adapted by permission from Fig. 3, 8, 10 in Ho and Goethals (2020). © Springer Nature & Scientometrics.

### 1.1.2 Algal monitoring and modelling

Blue-green algae that feed on nutrients grow into unsightly scums on the water surface, decreasing recreational value and clogging water-intake pipes. Decaying mats of dead algae can produce foul tastes and odors in the water; their decay by bacteria consumes dissolved oxygen from the water, sometimes causing fish kills. Algae, as primary producers, produce food via photosynthesis for themselves and most other aquatic animals. So far, 158,241 algal species are included in the online taxonomic database AlgaeBase (<http://www.algaebase.org>). Lee (2008) classified algae into two groups Prokaryota and Eukaryota, which were further divided into divisions. Prokaryota has just one division, Cyanophyta (blue-green algae), whereas Eukaryota is further divided on the basis of the nature of chloroplast membrane (including green algae, diatoms).

Algae need suitable temperatures, enough sunlight and nutrients to grow. When conditions turn favorable for algal growth, such as an excess of nutrients (eutrophication), rapid algal growth occurs and algal blooms develop (Klemas, 2012). Algal blooms of blue-green algae, which might produce toxins, are considered to be Harmful Algal Blooms (HABs) (Benayache et al., 2019; Glibert et al., 2006; National Rivers Authority, 1990). Monitoring algae presence for water supplies is an important aspect to reduce the risk of algal blooms forming. Qualitative and quantitative analyses of the microorganisms are the key steps, including microscopic analysis,

online measurement by phycocyanin probe, molecular techniques, high-throughput sequencing, etc. The most common methods used include manual cell counting as well as photosynthetic pigment concentration analysis (mainly chlorophyll-a, phycocyanin and phycoerythrin) (Ahn et al., 2007; Sahoo and Seckbach, 2015). The advantages and limitations of each method are listed in Table 2.

**Table 2 Comparison of different algal monitoring methods (Ogashawara, 2019; Principles, 2017)**

Methods	Advantages	Limitations
Microscopy	low cost easy operation	prone to misidentification time-consuming
Spectrometer (chlorophyll-a)	low cost easy operation	time-consuming limited sensitivity
HPLC (chlorophyll-a)	accurate	time-consuming
Molecular Techniques (Polymerase Chain Reaction (PCR) and Real-Time Quantitative PCR (qPCR))	highly sensitive	little contamination produce misleading results, only identify known pathogen/gene
Fluorescence <i>in-situ</i> probes (chlorophyll-a, phycocyanin)	online, rapid, sterilizable, stable, selective, fast, accurate	interfered by cell physiology, light condition, water quality
Satellite (spectral reflectance)	cost-effective cover large spatial area benefits for surface scums	limited by transmittance challenge for proper calibration

Many planktonic cyanobacterial species are positively buoyant and therefore have a tendency to accumulate at the water surface, with aggregations often reinforced by light winds and flow-mediated processes (Hunter et al., 2008). This can make sampling and monitoring of cyanobacteria and cyanotoxins problematic. Cell concentrations can vary rapidly with changing meteorological conditions, which lead to shifts in water temperature and mixing and transport processes. Traditional sampling practices (e.g., grab samples taken at a regular monitoring site) provide only a snapshot of cyanobacteria present at that one point in time and may miss areas or times of highest risk. Online measurement of water quality and meteorological data at the same time is very important. Field data loggers equipped with phycocyanin-specific sensors have been developed to monitor cyanobacterial populations and can provide early warning signals, for example, in drinking water supplies (Izydorczyk et al., 2005).

Therefore, in this Ph.D. work, I used *in-situ* fluorescence probes to measure the total chlorophyll-a (diatoms and green algae) and phycocyanin (blue-green algae). Moreover, an *ex-situ*

fluorescence instrument was used to detect chlorophyll-a of five different algal species (diatoms, green algae, blue-green algae, planktothrix and cryptophyta). Moreover, chlorophyll-a extraction was performed in the laboratory and measured by UV-vis Spectrometer.

Algal models can tease apart the dynamics underlying observations, simulate and predict bloom events, and are increasingly used as management tools. Integrating data from traditional and emerging techniques into deterministic models has the potential to improve knowledge of algal processes rapidly and ultimately enable more accurate risk assessment and mitigation strategies. These models are classified into different categories, including conceptual, empirical-statistical, process, diagnostic, predictive simulation, and management (Glibert et al., 2006). While observational technologies have advanced rapidly in recent years, there has been considerably less effort devoted to advancing or developing new models.

Conceptual models are the first step in all subsequent models, particularly useful in synthesizing observations into a coherent description of the system. Since the publication of Margalef's (Margalef et al., 1979) mandala phytoplankton conceptual model, there have been massive advances in the understanding of phytoplankton arise under different environmental conditions. Glibert (Glibert, 2016) has updated Margalef's conceptual model to 12 dimensions, including oxidation state of nitrogen, inorganic nitrogen and phosphorus, high light, motility, ambient turbulence, size and etc. Boyle (O'Boyle et al., 2015) created a conceptual model for shallow Irish estuaries based on the monitoring data, which showed different nutrient limitations (N, P or Si) in different seasons and gave suggestions of nutrient reduction strategy. Conceptual models thus serve as a simplified structure for synthesizing information about a complex system. This structure can then be used to motivate further research, as well as the basis for formulating mathematical models of the system. I combined the monitoring data and pieces of knowledge from the literature review to build a conceptual model for algal dynamics and species changes, which is presented in the synoptic discussion.

Empirical-Statistical models are built up through statistical analyses of observations. They may not include any cause-effect dynamics, but rather describe the system through statistical correlations. Such models are most often used as predictive or management tools. This is due to their relative tractability compared to the more numerically intensive dynamic models. Empirical-statistical models are only interpretable within the limits of the data used to create them; this presents a strong constraint to prediction in the face of changing conditions such as those driven

by anthropogenic climate change. Many different statistic methods have been used in algal models, including multiple linear regressions (Çamdevýren et al., 2005; Lamon, 1995), machine learning approaches (Kown et al., 2018), neural networks (Guzel, 2019; Nazeer et al., 2017; Tian et al., 2017), M5P model-tree (Yi et al., 2019), and support vector machines (Wang et al., 2017). Empirical-statistical models are powerful tools when sufficient data are available. Though they are static in the sense that they do not include dynamic relationships among variables, with sufficient data (which usually means many bloom/non-bloom cycles), they can reveal relationships among environmental and ecological forcing and HAB responses.

Algal models face challenges for emergency prediction because algal growth and location alternated very fast, especially as ecosystems are challenged by climatic shifts, severe weather, and anthropogenic influences. Therefore, a high-frequency online monitoring system was applied to observe as much information as possible for algal dynamic processes (section 2.1.1, 2.2.1, 2.2.3). Moreover, online monitoring data were used to create an algal simulation model (section 2.1.3).

### **1.1.3 Metal pollution**

Trace metals originate primarily from urban runoff and industrial discharge, such as from electrical machinery, pharmaceutical industry, chemical production, automobile exhausts, and waste incineration (Cai et al., 2015b; Cheung et al., 2003). Once metals have entered the lakes, they are easily deposited on the sediment surfaces through adsorption and coagulation and react as a source of secondary pollution (Liu et al., 2017).

However, the dynamics of trace metals are not independent. The algal dynamics will influence metal dynamics. In eutrophic lakes, heavy metal remobilization is often closely related to nutrient remobilization as both regularly adsorb to similar mineral fractions in the sediments (Bolan et al., 2003; Chen et al., 2017; Zan et al., 2011). Phosphate likely adsorbs on Ca-, Fe-, Mn-, Mg- and Al-complexes in sediments, which are relatively insoluble and mostly transported in particulate forms (Selig, 2003; Weihrauch and Opp, 2018; Xu et al., 2017). Moreover, algal blooms may decrease the concentrations of dissolved metals in the water due to uptake by algae (Chen et al., 2008; Sunda, 2012).

Besides, the lake characters will affect not only the dynamics of algae but also metals. Most of the suspended matter is due to resuspended surface sediments and algal biomass in the shallow

eutrophic Lake Taihu, which is characterized by high resuspension rates and high biological activity (Wang et al., 2001; Yang et al., 2019; Zhu et al., 2015).

Therefore, it can be supposed that the improvement of eutrophication and alleviating of blue-green algal blooms will also help mitigate the metal pollution problem.

## **1.2 Research objectives**

Fishing, recreation, drinking water supplies, the protection of aquaculture regions, as well as measuring progress towards water quality targets, are just some of the reasons that improvements in monitoring and prediction of algae have become necessary in freshwaters worldwide. The goal of this Ph.D. work is to show, how the state of the art tools and technologies for detecting algal dynamics, their associated environmental conditions, can help to understand the impacts of eutrophication on shallow eutrophic lakes. Afterwards, incorporating those new high-frequency data to understand the water quality dynamics better and creating new types of algal forecast models. This leads to the following objectives:

- 1) Implementing and adapting high-frequency multi-sensor systems in shallow eutrophic Lake Taihu to understand the seasonal water dynamics and algal kinetics at different water depths, combing with meteorological data.** Traditional laboratory-based monitoring methods cannot reflect the real-time water quality and algal changes (section 1.1.2). Its limitation is substantial for fast-growing algae and rapidly changing environments. Therefore, building an online monitoring system to offer high-frequency real-time data is the first step for further water quality and dynamic analysis and modelling (section 2.1.1). A deep understanding of the algal vertical distribution, seasonal dynamics and its correlation with physicochemical meteorological parameters are fundamental for the further one-location algal model (section 2.1.1, 2.1.3, 2.2.1). To extract as much useful information as possible from a large amount of sensor data is the challenge and goal. Chlorophyll-a concentrations measured by different devices and methods were compared to verify the data accuracy for making confident estimates of algal dynamics, as well as calibrating and validating algal simulation models (section 2.1.3). Nutrients' changes will influence algal concentrations on a long time scale. To get an overview of the algal dynamics and its future trends, I discussed the relations between nutrients and algae in different seasons (section 2.2.2). Trace metal pollution is a



problem that cannot be ignored. However, very few studies were done for it in eutrophic Lake Taihu and there is a lack of criteria of suspended particles and sediment in Chinese surface water standard. Trace metal pollution status in shallow eutrophic Lake Taihu as well as how the shallowness and algal dynamics affect the metal dynamics were explored in this study. Those pieces of knowledge offer new ideas for metal and algal pollution prevention, management, and treatment (section 2.1.2).

- 2) **Creating an algal simulation model based on high-frequency multi-sensor data and discussing the possibility of predicting the algal bloom.** The rapid growth of algae and Cyanobacteria blooms are a big concern for the drinking water plants. The ultimate goal is to implement a multi-sensor system in the intake area of drinking water plants and combining *in-situ* sensor data and weather forecast data to estimate algal changing rate or maximum concentrations within 2-3 days. The predictive result can help decision makers in drinking water plants to decide the amount of water to pump in different intake areas and alternate the water treatment procedures and time if necessary. A preliminary study is needed to address the possibilities (section 2.1.3).
- 3) **Comparing the geology location and physicochemical parameters of eutrophic Lake Taihu and Lake Westensee.** To explore the universality of applying the high-frequency multi-sensor system, the same instruments were applied in a lake in northern Germany. It is a lake deeper than Lake Taihu and is faced with fewer eutrophication problems (section 2.2.3).

### 1.3 The “SIGN” project

The Sino-German research project SIGN (phase I and II) runs from 2015 to 2021, aimed to contribute towards improving water quality in the Taihu region. The SIGN-Project is a joint research and development project formed by a Sino-German scientific consortium and bilaterally funded by BMBF and MOST. All together, more than 15 partners from German and Chinese industrial, university and research institutes take part in the project and are focusing on different parts like urban catchment area, monitoring, lake processes, water treatment, water distribution, dissemination, market implementation and action priorities.

Within SIGN, the sub-project DYNAQUA (phase I, BMBF grant-no. 02WCL1336B) was designed and supervised by Prof. Dr. Stefan Norra at the KIT Institute of Applied Geoscience (AGW). Moreover, sub-project AMORIS (phase II) was designed by Dr. Andreas Holbach and supervised by Prof. Dr. Stefan Norra at KIT-AGW. The main development objective of the two projects is to build a profiling buoy, which will carry *in situ* and online multi-sensor equipment for stationary and long-term water quality and meteorological measurements to create an algal early warning system (DYNAQUA) and assessing ecological risks of sediment resuspension events (AMORIS). The initial ideas of the projects were created by Prof. Dr. Stefan Norra and Dr. Andreas Holbach from the KIT-AGW, and Prof. Binghui Zheng from the Chinese Research Academy of Environmental Sciences (CRAES) in Beijing, China.

Personally, I was involved in the project from June 2016 until December 2020. My responsibilities mainly focused on the operation of the *in situ* multi-sensor systems (BIOLIFT) and primarily included the following tasks: 1) Applying and improving the BIOLIFT system to be adapted to field conditions in Lake Taihu, China; 2) preparing and conducting fieldwork in Lake Taihu in different seasons; 3) laboratory works for water and sediment samples collected in Lake Taihu; 4) analyzing water quality spatial-temporal dynamics with different statistical and geostatistical methods; 5) creating algal early warning model by using BIOLIFT data.

## 1.4 Study area — Northern Lake Taihu, China

### 1.4.1 Location and morphological characteristics

Lake Taihu is one of the five major freshwater lakes in the Yangtze River Basin and the third largest freshwater lake in China. It is located at the southern of the Yangtze River Delta and belongs to the lower reaches of the Yangtze valley (Fig.3).

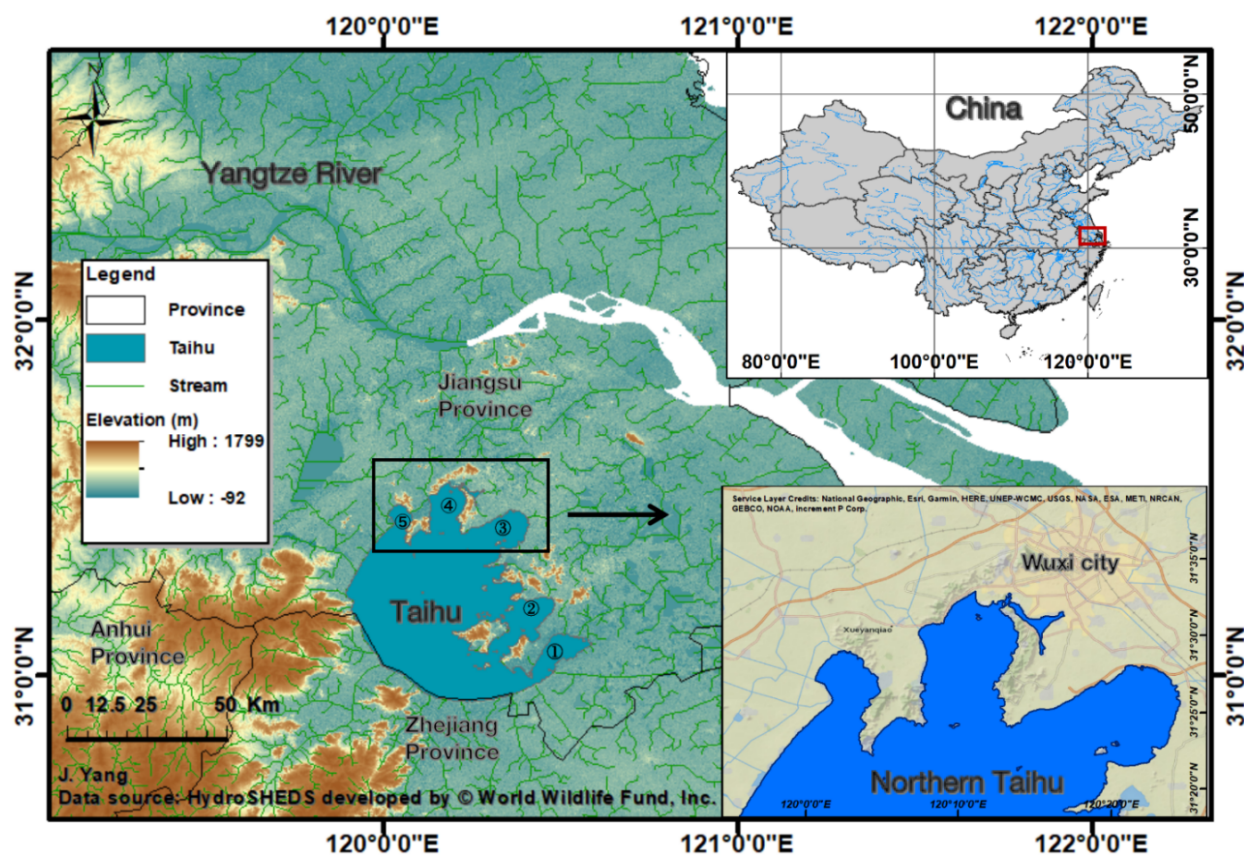


Figure 3 Lake Taihu area within China and the specific study areas of northern Lake Taihu

The lake is situated on the border of the two provinces Jiangsu and Zhejiang in East China between  $30^{\circ}55'40''\text{N}$  and  $31^{\circ}32'58''\text{N}$  and  $119^{\circ}52'32''\text{E}$  and  $120^{\circ}36'10''\text{E}$ . Lake Taihu is 68.5 km long in the north-south direction and on average 34 km wide from east to west. Its total water area is 2,338.1 km<sup>2</sup> (Qin et al., 2007b). Low hill and massif region (ground above 12 m), situated at the west of the basin. The eastern parts are lowland plains. From natural and anthropogenic causes,

Lake Taihu has five bays: Eastern Taihu Bay, Xukou Bay, Gonghu Bay, Meiliang Bay, and Zhushan Bay from east to west (number one to five in Fig.3).

As a typical shallow lake, the mean water level of Lake Taihu is 3.0 m above sea level (a.s.l.). The maximum depth and mean depth are 2.6 m and 1.9 m, respectively. The topography of the lake bottom is flat, with a mean declivity of 0°0'19.66. The mean elevation of the lake bottom is 1.1 m above sea level (a.s.l.) (Qin, 2008).

## **1.4.2 Hydrology and Climate**

The total length of rivers in the Taihu basin is about 12,000 km (Qin et al., 2007b). Evidence of its prior topographic character, rivers tend to flow from west to east. West of the basin is the riverhead or upstream zone of most rivers feeding Lake Taihu. The lake has a complex watercourse with around 200 rivers enter into the lake. The annual mean runoff into the lake is around 4.1 billion m<sup>3</sup> (Xu et al., 2009). Most of the runoff (33%) occurs in summer (from June to August); the least (11%) occurs in winter (December–February). Runoff volume varies greatly from year to year (Qin, 2008). The discharges of most rivers in the Taihu basin are very small. The maximum mean discharge of the tributary is 26.8 m<sup>3</sup>/s. In general, the water retention time of Lake Taihu is about 300 days (Mao et al., 2008). Lake Taihu has approximately the same amount of inflow and outflow in flooding years as in normal years. In recent decades, the Lake Taihu water regime has changed as sluice gates have been built to control the outflowing watercourses. Presently, Lake Taihu has the characteristics of a reservoir as the water balance can be brought under human control (Qin, 2008).

Taihu Lake region is dominated by a subtropical monsoon climate. In summer, between June and September, the main precipitation appears during the rainy season (Zhao, 2013). The historical floods are caused by strong summer precipitation and the variation of the lake water level has a close relationship with changes in the monsoon precipitation (Li et al., 2013). The annual mean precipitation and evaporation are 1000 – 1400 mm and 941 mm, respectively. The annual mean air temperature is varying from 14.9 to 16.2 °C. The water temperature ranges from 0 to 38 °C, with the minimum temperature happening in January and the maximum in August (Li et al., 2008).

Moreover, the monsoon climate is responsible for dominant southeast winds in summer, and west and northwest winds in winter (Qin, 2008). The waves in Lake Taihu are caused by surface wind disturbance, and their characteristics mainly depend on wind speed, wind fetch, and water depth (Qin, 2008).

### **1.4.3 Pollution and Eutrophication**

Lake Taihu plays multifunction roles, including navigation, tourist interest, water resource of drinking, aquaculture, agriculture and industry (Yang and Liu, 2010). The Lake Taihu region is located in one of China's most important economic areas; the GDP of Jiangsu province has consistently ranked among the top three in China in the past 60 years. To achieve this, urbanization, developed industries, and agriculture made significant contributions. However, economic success led to vast resource depletion and environmental pollution. Lake Taihu has been suffering from problems such as industrial and agricultural pollution, flooding, eutrophication, aquaculture, overfishing (Wang et al., 2009). The discharge of the wastewater from these industries introduced heavy metals into Lake Taihu.

Nutrient contamination and eutrophication are considered to be the main water quality problem in Taihu Lake, as they frequently cause algal blooms, which threaten the drinking water supply. The soil in Jiangsu province is primarily under a rice-wheat rotation (Wang et al., 2015). Rice is planted in mid-June and harvested in late October, while wheat is grown from early November to late May (Yu et al., 2018). Applied fertilizers are also the primary source of N and P inputs and runoff is the major pathway of transport into aquatic systems (Bennett et al., 2001; Lian et al., 2018; Zhao et al., 2012). Excess P inputs to lakes are also coming from industrial discharges, sewage, urban areas, and construction sites. Particulate P was the dominant fraction of total P loss by runoff, as the P is widely considered to be firmly fixed onto the soil particles (Zhang et al., 2003). For N, domestic sewage, livestock, and poultry farm sewage can incorporate ammonium-N ( $\text{NH}_4\text{-N}$ ) and get into the water body during rainfall events (H. Xu et al., 2008).

The governments (national and regional) have implemented a series of economic, technological, and industrial policies during the past decades, such as establishing a pollution levy system, stricter emission standards, supporting environmental-friendly industries and so on, to control and improve the water quality of Lake Taihu (Environmental Protection Department of Jiangsu

Province, 2016; Köster, 2019). With the strengthening of supervision, the amount of fertilizer applied slightly decreased in these three years (National Bureau of Statistics of China, 2018).

Nitrogen exports from Wuxi city decreased in recent decades, due to the agricultural production structure changes and farm management improvements (Lian et al., 2018). The total P input from Jiangsu province had slightly decreased in 2017 ( $1.8 \times 10^3$  ton) compared to 2016 ( $2 \times 10^3$  ton). However, the expected reduction of algal blooms in Lake Taihu did not occur, yet. Contrarily, the intensity and frequency of algal blooms increased in 2017 compared to that of 2016. The largest algal bloom area reached up to 1403 km<sup>2</sup> in May 2017, which was the maximum observed since 2009 (Qin et al., 2019). However, the pollution and eutrophication status in Lake Taihu has not been greatly improved. The changes in COD<sub>Mn</sub>, TP, and TN over 30 years from 1988 to 2018 were shown in Fig.4. In 2007, COD<sub>Mn</sub>, TP, and TN dramatically increased compared with that of 1988. In recent years, COD<sub>Mn</sub> and TN decreased and TP fluctuates around 0.078 mg/L. The pollution and eutrophication of the lake will cause serious economic and social harm.

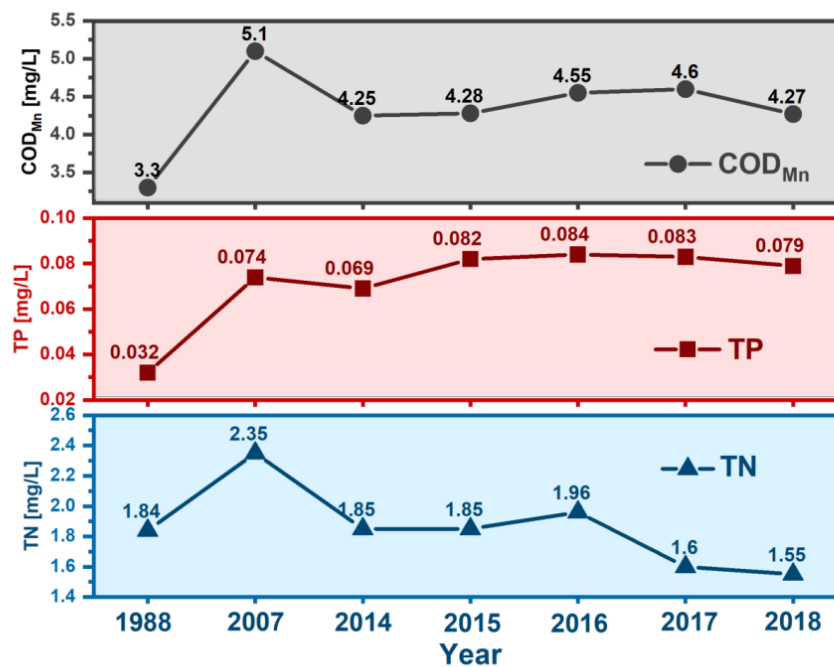


Figure 4 COD<sub>Mn</sub>, TP and TN changes from 1988 to 2018 in Lake Taihu. Adapted by permission from Qin (2008). © Springer Nature & Springer eBook. Adapted from The health status report of Taihu Lake (2019) in <http://www.tba.gov.cn/slbthlyglj/sj/sj.html>.

The trophic status index over the last 11 years was larger than 60 and belonged to middle eutrophic status (Fig.5). Pollution control is necessary but cannot instantly solve the problem. Besides the

external P input, sediments can also act as an internal P source, releasing P-species by diffusion under anoxia and calm conditions (typical for summer) and by sediment resuspension under windy conditions (Selig, 2003).

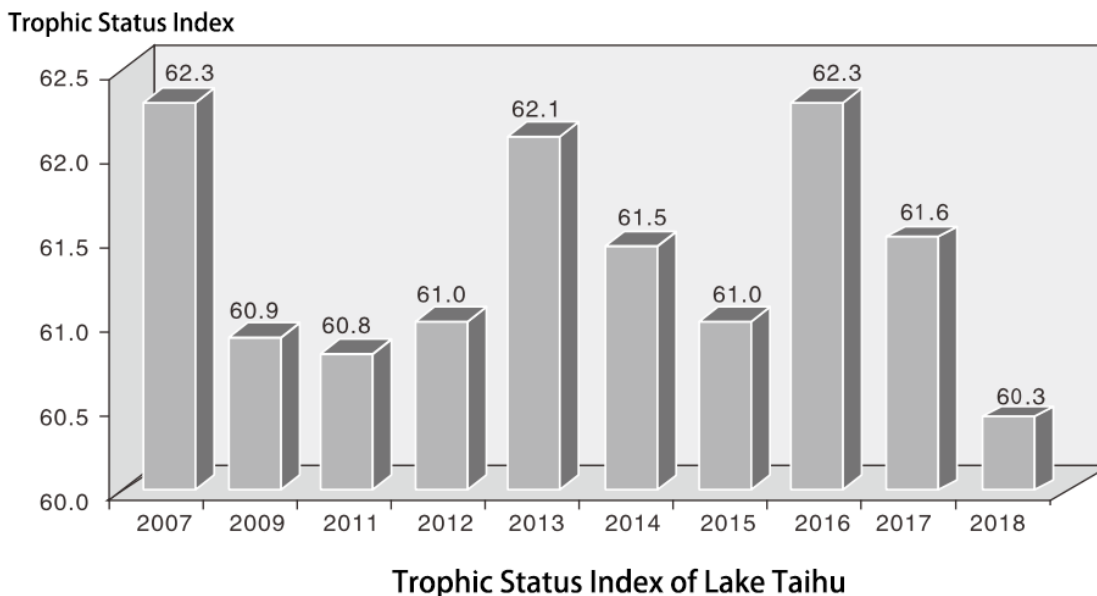


Figure 5 Trophic status index changes in recent years. Adapted from The health status report of Taihu Lake (2019) in <http://www.tba.gov.cn/slbthlyglj/sj/sj.html>

#### 1.4.4 Characteristic of Northern Lake Taihu

The study was conducted in northern Lake Taihu, which contains three major bays. These are Zhushan Bay, Meiliang Bay, and Gonghu Bay (Fig.6). Northern Lake Taihu, and especially its northern bays, are the most polluted area with nutrients, Microcystin, antibiotics, pharmaceuticals, and heavy metals (Li et al., 2011; Tao et al., 2012; Wilhelm et al., 2011; Xu et al., 2014). The distribution of nutrients in 2018 is shown in Fig.6 (Zhang et al., 2019). The northern Lake Taihu is highly polluted because the main pollutant loads are input from external sources with the Taihu tributaries in the north and cause poor water quality (Qin et al., 2007b).

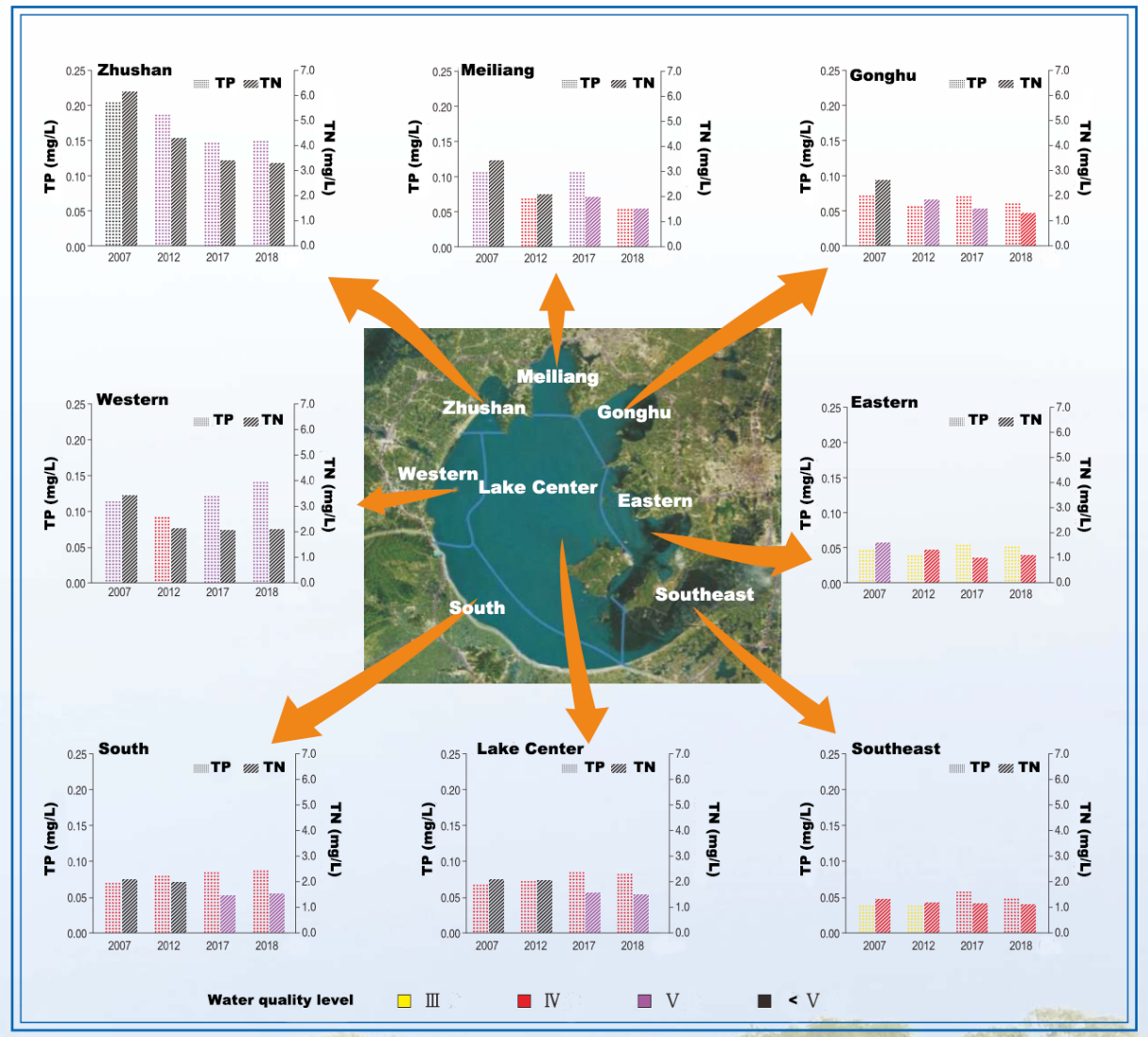


Figure 6 Changes of TN and TP distribution in recent years (2007, 2012, 2017, 2018). Adapted from The health status report of Taihu Lake (2019) in <http://www.tba.gov.cn/slbthlyglj/sj/sj.html>

The algal blooms in summer preferred to accumulate in northern bays (Fig.7), due to the dominated southeast wind (Qin, 2008). Regardless of the season, there is a weak counter-clockwise current in northern Meiliang Bay, which may explain why this area is favourable for concentrating algal blooms (Hu et al., 2011; Qin et al., 2007b).



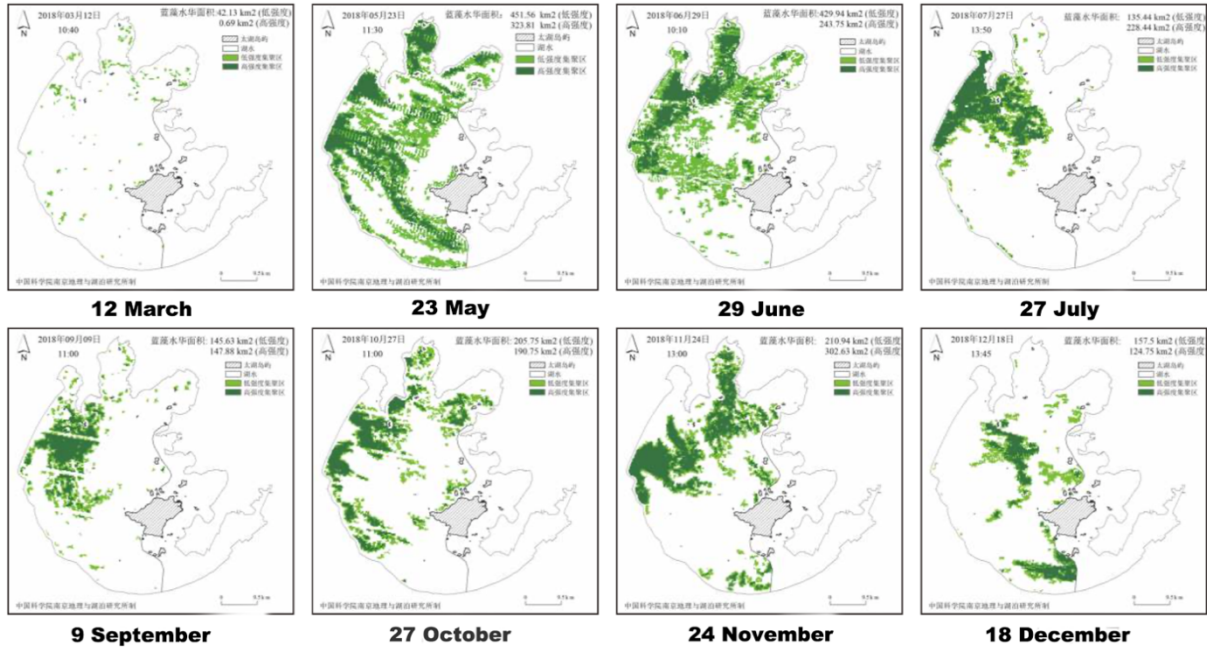


Figure 7 Algal bloom distribution in 2018 (the darker the colour, the greater the density). Adapted from The health status report of Taihu Lake (2019) in <http://www.tba.gov.cn/slbthlyglj/sj/sj.html>

Zhao et al. (2013) examined data on land use, pollution and the effects on the environment in the northwest Taihu basin, which is considered the most polluted area in the Taihu basin (Fig.8).

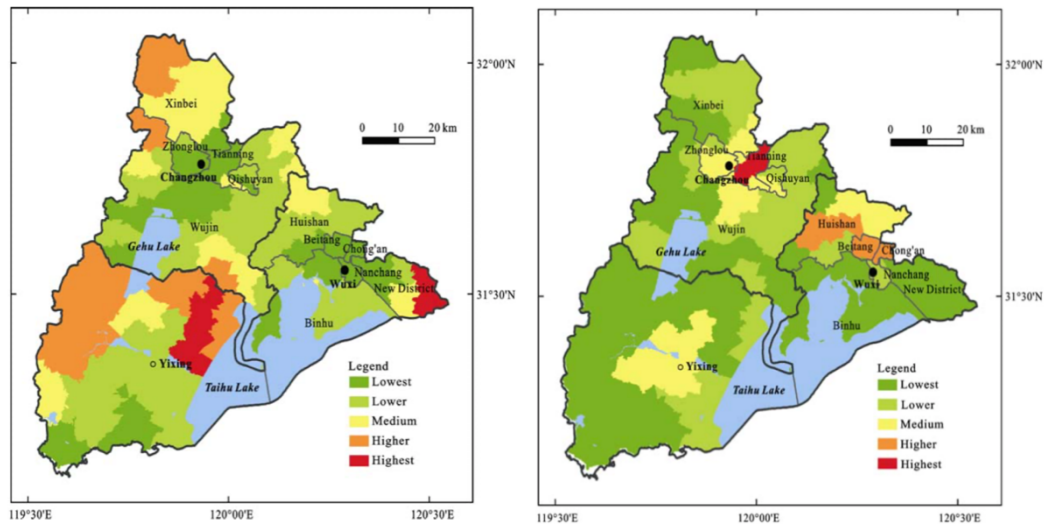


Figure 8 Spatial distribution of (left) agriculture and (right) industry pollution. Reprinted by permission from Zhao et al. (2013). © Springer Nature & Chinese Geographical Science.

## 1.5 Synoptic summary of field works and experiment methods

### 1.5.1 Stationary depth-profile multi-sensor system (BIOLIFT) for *in situ* water and meteorological parameter measurements

The BIOLIFT was the main monitoring and sampling device of this work, which can automatically measure the vertical water quality every 10 min. I installed it at a jetty, which reaches 250 m away from the shoreline in outer Meiliang Bay, where the Taihu Laboratory for Lake Ecosystem Research (TLLER) is located. The placement offered infrastructure and made it feasible to easily maintain the system, charge batteries and store required parts and tools. Each depth-profile of the BIOLIFT runs about 2 min with high-frequency data acquisition (getting 3 – 5 dataset per second and moving 2 – 3 cm per dataset, ca. 37000 data per day). The physicochemical sensors implemented in the BIOLIFT are pressure (water depth, [m]), water temperature [°C], pH-value, chlorophyll-a fluorescence [ $\mu\text{g/L}$ ], photosynthetically active radiation in the water in different depth (PAR, [ $\mu\text{mol}/(\text{m}^2 \cdot \text{s})$ ]), Oxygen saturation (Oxy-sat, [%]), turbidity (Turb, [FTU = Formazan Turbidity Unit]), colored dissolved organic matter (CDOM, [ $\mu\text{g/L}$ ]). A phycocyanin fluorescence sensor [ $\mu\text{g/L}$ ] has been added to the BIOLIFT multi-sensor system since 2018, which can represent the blue-green algae.

A weather station (Vaisala Weather Transmitter WXT520) was installed at around 5 m above the water surface and connected with the BIOLIFT. The measured parameters included wind direction [°], wind speed [m/s], rainfall [mm], air temperature [°C], and relative humidity [%], which were recorded in the same frequency as physicochemical parameters (10 min).

Moreover, a water pump was integrated into the BIOLIFT and next to the sensors (Fig.9). Water samples can be taken at any depth controlled manually by a control box. One aim of SIGN-DYNAQUA is to install and adapted the BIOLIFT system as a floating buoy. I have contributed to floating buoy and carrying frame optimization and instrument malfunctions minimization.

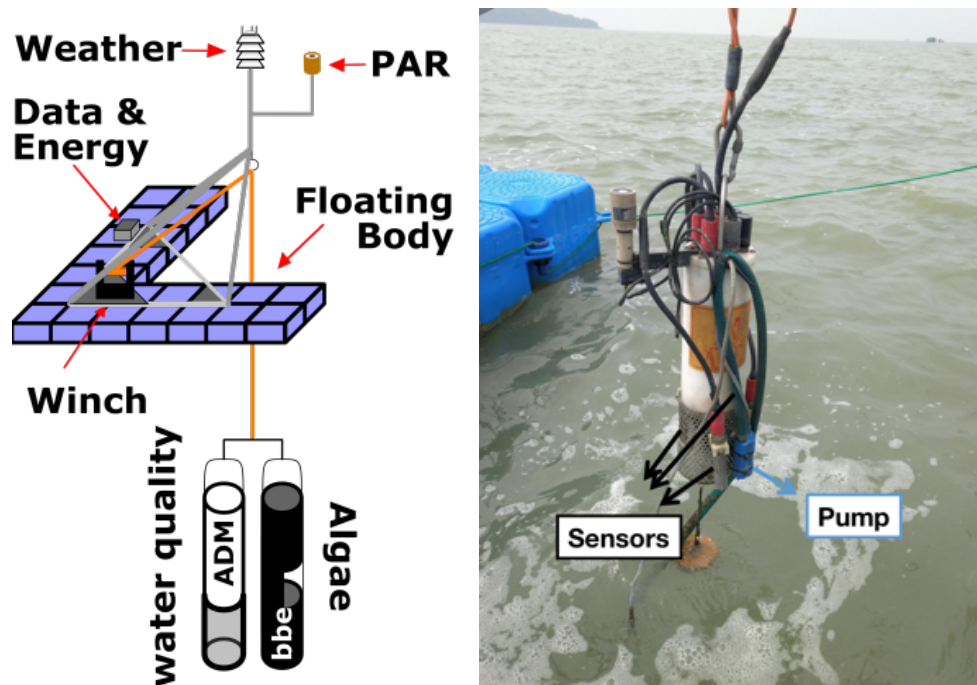


Figure 9 Structure of BIOLIFT-buoy system (left) and its application in Lake Taihu (right)

### 1.5.2 Spatial-temporal multi-sensor system (BIOFISH) for *in situ* water quality measurements at certain depth

A multi-sensor system (BIOFISH) equipped with similar state of the art sensors as the BIOLIFT was used to measure water quality spatially in northern Lake Taihu. The BIOFISH can be dragged behind a boat and is carrying a GPS system. Different from Holbach's Ph.D. work (Holbach, 2015), the typical spatial-temporal multi-sensor system with wings can not be used in shallow Lake Taihu. Because there is no safe distance (depth) for the instrument to move up and down. Therefore, Dr. Andreas Holbach and Prof. Dr. Stefan Norra (KIT, Germany) modified the BIOFISH by using a floating body on the top of the instrument (Fig.10). Then it can contentiously measure the spatial water quality at around about 1 m depth in Lake Taihu.

On 29th November and 2nd December 2015, BIOFISH was used to map the water quality at the junction of Meiliang Bay and Gonghu Bay on two days conducted by Dr. Andreas Holbach and Prof. Dr. Stefan Norra. After that, BIOFISH was only applied in the water body during sampling for collecting physicochemical data according to water samples.

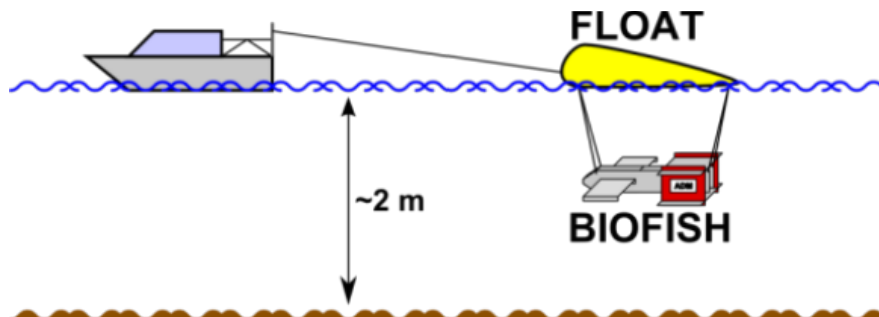


Figure 10 BIOFISH measuring spatial water quality at certain depth by using float body

### 1.5.3 Performed fieldwork and chemical analytics

In total, I attended nine field trips for sampling and monitoring in Lake Taihu (Fig. 11) from June 2016.

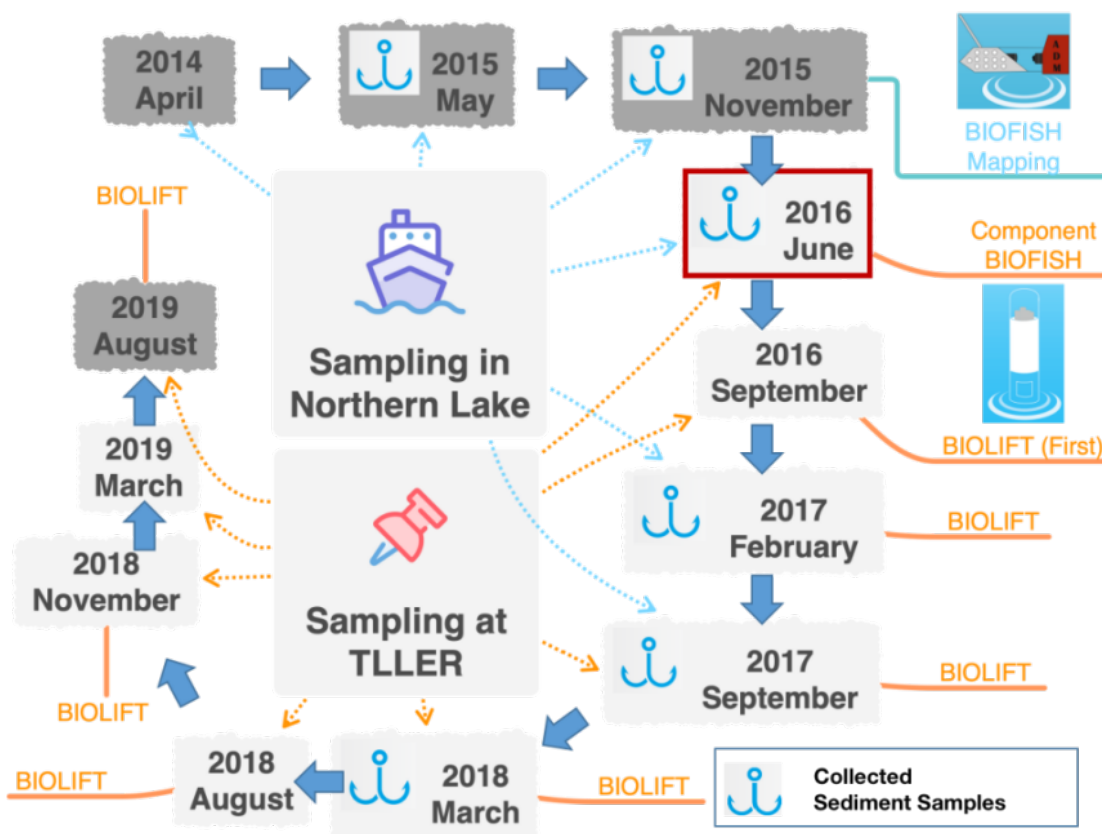


Figure 11 Timeline of fieldworks conducted within the SIGN project. Note: the campaigns conducted by other colleagues were with dark background (2014 April, 2015 May & November, 2019 August)

The BIOLIFT was implemented and first applied in Lake Taihu in September 2016 (Fig.12). After four months of troubleshooting, the BIOLIFT ran well in February 2017 and then the operational BIOLIFT was tried to be installed on a floating buoy one year later (2017 September). The following scientific journal publications are based on data from: 2014 April, 2015 May, 2015 November/December, 2016 June/July, 2016 September, 2017 February, 2017 September, 2018 March/April, 2018 August/September, 2018 November. Data from 2019 March and 2019 August was also used in my Ph.D. work. In the field, I contributed to instrument setup and maintenance, as well as sample taking and preparation. For all field trips from February 2017, I was responsible for the organizational and infrastructural arrangements within China and the prearrangements of sampling schedules.

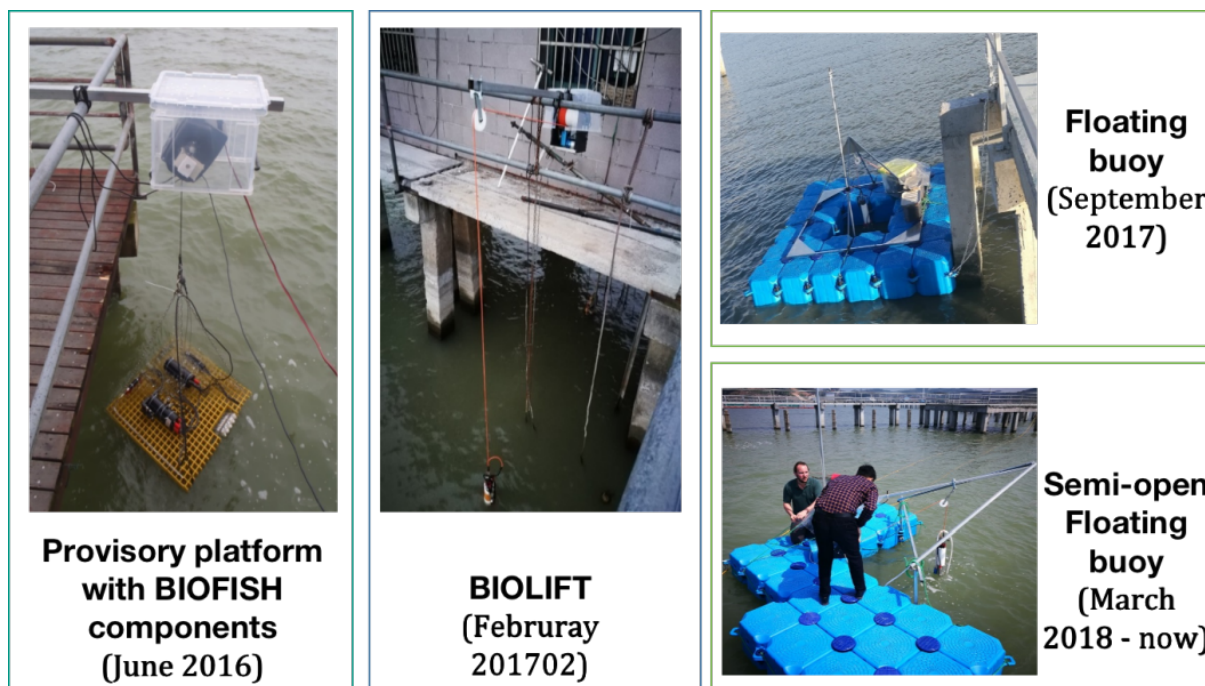


Figure 12 The developments of BIOLIFT-buoy system

#### 1.5.4 Sample collection and chemical analytics

Water samples were collected either by a pump connected to BIOLIFT winch at TLLER station at different water depths (surface (~0.2 m), intermediate (half of the depth), and bottom (depend on the depth)) or by organic glass water sampler to collect near-surface (0.2 m) water samples in

northern Lake Taihu. All in all, 566 water samples were taken in northern Lake Taihu from 2014 April to 2019 August. Sediment cores were taken by an Uwitec Corer (Uwitec, Mondsee, Austria) and surface sediments were collected by A Van Veen Grab Sampler (KC Denmark A/S, Silkeborg, Denmark). In total, I got 164 sediment samples in northern Lake Taihu.

The study contents, the applied techniques and instruments for analysing samples are introduced in Table 3:

**Table 3 The instruments and technologies used for sample analysis**

Parameters	Method	Instruments
TN NH <sub>4</sub> -N	Merck Quick Test: 2,6-dimethylphenol (DMP) Tetrasodium (1 - hydroxyethylidene) bisphosphona Method	NOVA 60 A Spectroquant (Merck Chemicals, Darmstadt, Germany)
Anion	ERS500 suppressor, AS14-2 anion column Na <sub>2</sub> CO <sub>3</sub> /NaHCO <sub>3</sub> eluent (flow rate: 1.2 mL/min)	Ion Chromatography (IC; ICS-1000, Thermo Fischer Scientific, Waltham, USA)
Cation	Atomizer conikal with peltier cooled spray chamber Collision gas (Helium/H <sub>2</sub> )	Inductively Coupled Plasma Mass Spectrometry (ICP-MS; X-Series 2, Thermo Fischer Scientific, Waltham, USA)
Filter digestion	Complete acid digestion (superpure 65 % HNO <sub>3</sub> , 40 % HF, 65 % HClO <sub>4</sub> )	Teflon beakers, heating plate Ceran 500, fume hood
Chlorophyll-a fluorescence concentration	Fluorescence with seven excitation illuminants (LEDs) and two detection photomultipliers (resolution: 0.01 µg/L)	Phycola (bbe moldaenke, Schwentental, Germany)
Total Chlorophyll-a concentration	Hot-ethanol extraction (90% ethanol)	UV-Visible Spectrophotometer (UV-1100; Mapada Instruments, Shanghai, China )
Main compounds (sediment)*	Tube: Rh X-ray Maximal energy: 50 keV	Wavelength Dispersive X-ray Fluorescence (WDX; S4 Explorer, Bruker, Billerica, USA)
Trace elements (sediment)**	Ge-semiconductor detector Tube: W/Sc X-ray tube with a Maximal energy: 80 keV	Energy Dispersive X-ray Fluorescence (EDX; Epsilon 5, Malvern Panalytical, Malvern, UK)
Mineral content (sediment)	Tube: Cu, Voltage: 40 kV Electric current: 40 mA, p Power: 1600 W	X-Ray Powder Diffraction (XRD; D8 Discover, Bruker, Billerica, USA)

\*SiO<sub>2</sub>, Al<sub>2</sub>O<sub>3</sub>, Fe<sub>2</sub>O<sub>3</sub>, K<sub>2</sub>O, Na<sub>2</sub>O, CaO, MgO, TiO<sub>2</sub>, P<sub>2</sub>O<sub>5</sub>, MnO and Co  
 \*\*Cr, Zn, Ni, Cu, Pb, As, Sr, Cd, Ag, S, V, Rb, Nb, Sn, U, Mo, Sb, Ga, Y, Ba, Zr, La, Ce, Th

I conducted Merck quick tests (TN and NH<sub>4</sub>-N) every day after sampling in the lab of Jiangnan University, China. At the KIT-AGW, I got help in the labs for filter digestions from the technician Mrs. Chantalle Kotschenreuther. Further, I performed IC analyses for dissolved anions assisted by the technician Mrs. Claudia Mößner, and I assisted Mrs. Claudia Mößner with the analyses of major, minor, and trace element contents using ICP-MS. For the sediment samples, I prepared the sediment samples with the help of technician Mr. Kristian Nikoloski. Moreover, I assisted Mrs. Beate Oetzel with measuring minerals and elements in the sediments by XRD, WDX, and EDX.

### 1.5.5 Statistical methods

I performed all the scientific data evaluation and interpretation of BIOLIFT and water/sediment chemistry datasets. The relevant statistic methods and performed software are shown in Table 4:

**Table 4 The software and statistic methods used in the study**

Method	Applied for	Software
Shapiro-Wilk test	Normal distribution test (elements/parameters)	OriginPro (Origin Professional 2016; OriginLab, Northampton, USA)
Hierarchical cluster; Pearson's/Spearman's correlation	Grouping elements; Correlation/regression	
Stepwise linear regression	Algal simulation models	SPSS (IBM SPSS Statistics 24.0)
Evaluating high frequency BIOLIFT data	Transferring data to a matrix (0.1 m * 3 hours) by calculating the average	MATLAB R2018a (MathWorks, Stuttgart, Germany)
Water quality spatial distribution	Kriging interpolation	ArcGIS 10.5.1 (Esri, California, USA)

The Ward method of hierarchical cluster analysis starts by placing its own cluster for each object and grouping different objects to a cluster, where the smallest difference is given (Ward, 1963). The minimal increase in the sum of squared errors and absolute correlation distance was used. Stepwise linear regression, used in algal simulation models (section 2.1.3), is a procedure for automatically selecting independent variables. During the process, variables added to the model were based solely on the t-statistics of their estimated coefficients and maximizing the squared multiple correlations coefficient ( $R^2$ ) of the model. The p-value ( $p$ ; 0.05) for each independent

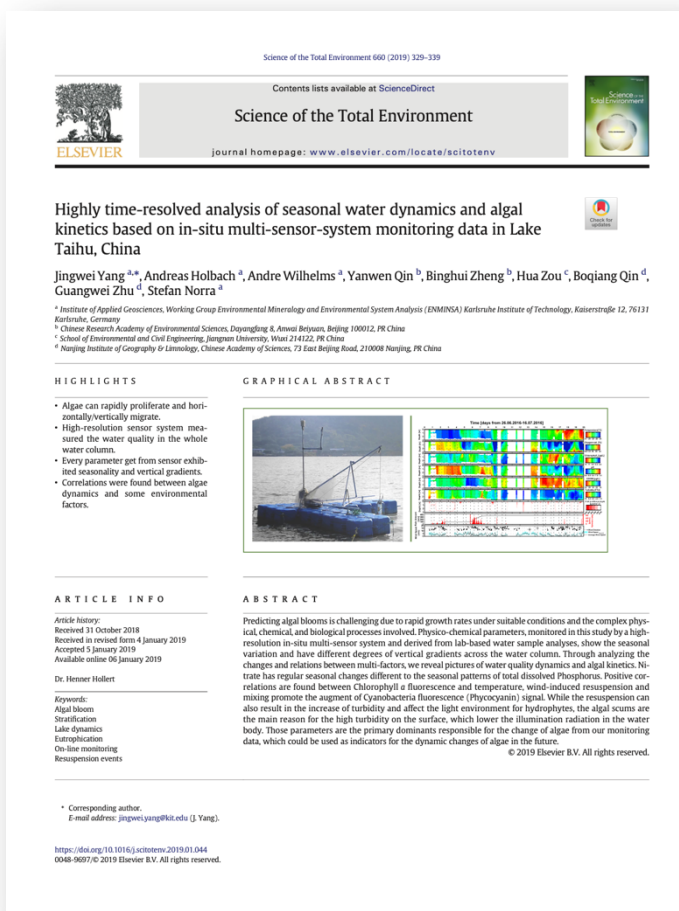
variable tests the null hypothesis to remove multicollinearity source variables. AICc (Akaike information criterion for the model with small sample size) was also used to estimate the relative amount of information lost by models, which provides a means for model selection (Cavanaugh, 1997).



## 2 Results

### 2.1 Published results and discussion

#### 2.1.1 Highly time-resolved analysis of seasonal water dynamics and algal kinetics based on in-situ multi-sensor-system monitoring data in Lake Taihu, China



**Authors:** Jingwei Yang, Andreas Holbach, Andre Wilhelms, Yanwen Qin, Binghui Zheng, Hua Zou, Boqiang Qin, Guangwei Zhu, Stefan Norra

**Journal:** Science of the Total Environment, 2019, 660, 329-339, DOI: 10.1016/j.scitotenv.2019.01.044

**Authorship statement:** This peer-reviewed scientific journal article was written by me, based on the data obtained from four monitoring and sampling fieldtrips, June/July 2016, February/March 2017, September 2017, March/April 2018. I participated all the fieldtrips and responsible for the fieldtrip preparation and coordinate work with Chinese colleagues from

February/March 2017 campaign. Further, I performed the corresponding analytics in the laboratories at KIT-AGW with the help of technicians Claudia Mößner for ICP-MS and IC from February/March 2017 campaign. Andre Wilhelms conducted the dissolved water quality analysis with technicians Claudia Mößner for the samples in June/July 2016 as the content of his master's

thesis. All scientific data evaluation in this article were performed by me. Yanwen Qin and Binghui Zheng were the responsible scientists and primary project partner from the Chinese Research Academy of Environmental Sciences (CRAES). Hua Zou from Jiangnan University and Boqiang Qin and Guangwei Zhu from Nanjing Institute of Geography and Limnology (NIGLAS) made the necessary arrangements for the fieldwork in Wuxi, China. Andre Wilhelms and/or Andreas Holbach installed BIOLIFT instrument and taken water samples with me in the field together. Stefan Norra designed and supervised the respective project and raised funds from the BMBF. All co-authors critically reviewed the manuscript and agreed to its publication.

**Abstract:** Predicting algal blooms is challenging due to rapid growth rates under suitable conditions and the complex physical, chemical, and biological processes involved. Physico-chemical parameters, monitored in this study by a high-resolution in-situ multi-sensor system and derived from lab-based water sample analyses, show the seasonal variation and have different degrees of vertical gradients across the water column. Through analyzing the changes and relations between multi-factors, we reveal pictures of water quality dynamics and algal kinetics. Nitrate has regular seasonal changes different to the seasonal patterns of total dissolved Phosphorus. Positive correlations are found between Chlorophyll a fluorescence and temperature, wind-induced resuspension and mixing promote the augment of Cyanobacteria fluorescence (Phycocyanin) signal. While the resuspension can also result in the increase of turbidity and affect the light environment for hydrophytes, the algal scums are the main reason for the high turbidity on the surface, which lower the illumination radiation in the water body. Those parameters are the primary dominants responsible for the change of algae from our monitoring data, which could be used as indicators for the dynamic changes of algae in the future.

© The full article is reprinted with kind permission from Elsevier B.V. (2019) and Science of the Total Environment in Appendix B.1.

## 2.1.2 Identifying spatio-temporal dynamics of trace metals in shallow eutrophic lakes on the basis of a case study in Lake Taihu, China



**Authors:** Jingwei Yang, Andreas Holbach, Andre Wilhelms, Julia Krieg, Yanwen Qin, Binghui Zheng, Hua Zou, Boqiang Qin, Guangwei Zhu, Tingfeng Wu, Stefan Norra

**Journal:** Environmental Pollution, 2020, 264, 114802, DOI: 10.1016/j.envpol.2020.114802

**Authorship statement:** This peer-reviewed scientific journal article was written by me and is based on seven fieldtrips, including April 2014, May 2015, November/December 2015, June/July 2016, February/March 2017, September 2017, March/April 2018. In April 2014 and May 2015, the water and sediment samples were taken by

Andreas Holbach and Stefan Norra. In November/December 2015, the sampling and BIOFISH were carried out by Andreas Holbach, Stefan Norra and Julia Krieg. I participated the fieldtrips from June/July 2016 and responsible for the fieldtrip preparation and coordinate work with Chinese colleagues from February/March 2017 campaign. The water chemical analysis (IC & ICP), filter digestion, and sediment element and mineral analysis (WDX & EDX & XRD & SEM) in campaign April 2014, May 2015, November/December 2015 were conducted by Julia Krieg with the help of technicians Claudia Mößner and Beate Oetzel as part of her master thesis's work. Andre Wilhelms conducted the dissolved water quality analysis with technician Claudia Mößner for the samples in June/July 2016 as the content of his master's thesis. Further, I performed the

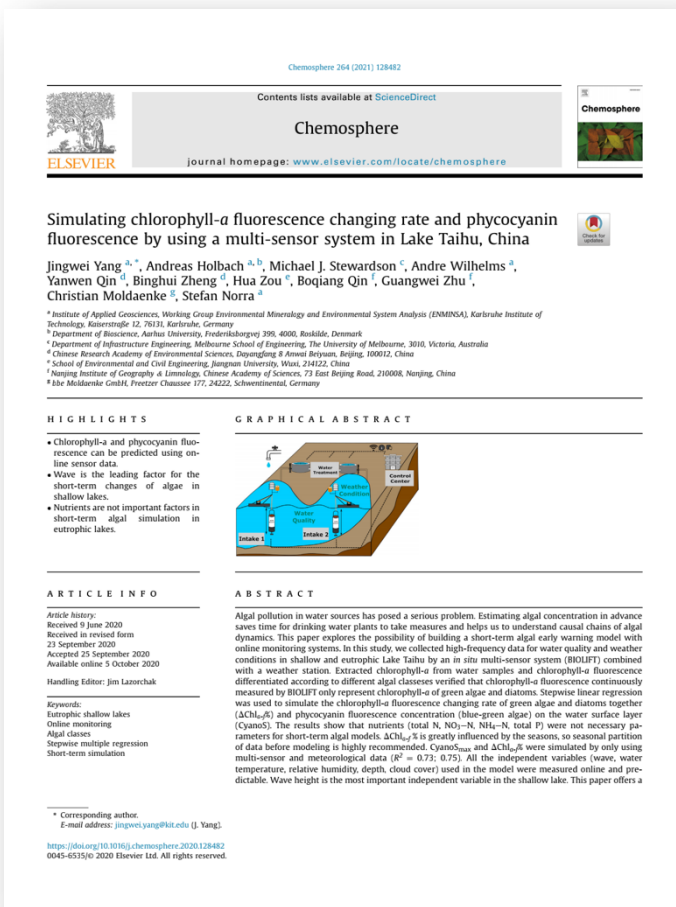
corresponding analytics (ICP-MS, IC, WDX, EDX, XRD, filter digestion) in the laboratories at KIT-AGW with the help of technicians from February/March 2017. All scientific data evaluation in this article were performed by me. Yanwen Qin and Binghui Zheng were the responsible scientists and primary project partner from the Chinese Research Academy of Environmental Sciences (CRAES). Hua Zou from Jiangnan University and Boqiang Qin and Guangwei Zhu from Nanjing Institute of Geography and Limnology (NIGLAS) made the necessary arrangements for the fieldwork in Wuxi, China. Tingfeng Wu from NIGLAS organized boat for us for dragging BIOFISH around Meiliang Bay and Gonghu Bay junction. Andre Wilhelms and/or Andreas Holbach installed BIOLIFT instrument and taken water samples with me in the field together. Stefan Norra designed and supervised the respective project and raised funds from the BMBF. All co-authors critically reviewed the manuscript and agreed to its publication.

**Abstract:** In shallow eutrophic lakes, metal remobilization is closely related to the resuspension and eutrophication. An improved understanding of metal dynamics by biogeochemical processes is essential for effective management strategies. We measured concentrations of nine metals (Cr, Cu, Zn, Ni, Pb, Fe, Al, Mg, and Mn) in water and sediments during seven periods from 2014 to 2018 in northern Lake Taihu, to investigate the metal pollution status, spatial distributions, mineral constituents, and their interactions with P. Moreover, an automatic weather station and online multi-sensor systems were used to measure meteorological and physicochemical parameters. Combining these measurements, we analyzed the controlling factors of metal dynamics. Shallow and eutrophic northern Lake Taihu presents more serious metal pollution in sediments than the average of lakes in Jiangsu Province. We found chronic and acute toxicity levels of dissolved Pb and Zn (respectively), compared with US-EPA “National Recommended Water Quality Criteria”. Suspended particles and sediment have been polluted in different degrees from uncontaminated to extremely contaminated according to German pollution grade by LAWA (Bund/Länder-Arbeitsgemeinschaft Wasser). Polluted particles might pose a risk due to high resuspension rate and intense algal activity in shallow eutrophic lakes. Suspended particles have similar mineral constituents to sediments and increased with increasing wind velocity. Al, Fe, Mg, and Mn in the sediment were rarely affected by anthropogenic pollution according to the geoaccumulation index. Among them, Mn dynamics is very likely associated with algae. Micronutrient uptake by algal will affect the migration of metals and intensifies their remobilization. Intensive pollutions of most particulate metals were in the industrialized and down-wind area, where algae form mats and

decompose. Moreover, algal decomposition induced low-oxygen might stimulate the release of metals from sediment. Improving the eutrophication status, dredging sediment, and salvaging cyanobacteria biomass are possible ways to remove or reduce metal contaminations.

© The full article is reprinted with kind permission from Elsevier Ltd. (2019) and Environmental Pollution in Appendix B.2.

## 2.1.3 Simulating chlorophyll-a fluorescence changing rate and phycocyanin fluorescence at one location by using a multi-sensor system in Lake Taihu, China



**Authors:** Jingwei Yang, Andreas Holbach, Michael J. Stewardson, Andre Wilhelms, Yanwen Qin, Binghui Zheng, Hua Zou, Boqiang Qin, Guangwei Zhu, Christian Moldaenke, Stefan Norra

**Journal:** Chemosphere, 2021, 264, 128482, DOI: 10.1016/j.chemosphere.2020.128482

**Authorship statement:** This peer-reviewed scientific journal article was written by me and is based on five fieldtrips, including June/July 2016, February/March 2017, March/April 2018, August/September 2018, and November 2018. I participated all the fieldtrips and responsible for the fieldtrip preparation and coordinate

work with Chinese colleagues from February/March 2017 campaign. Moreover, I conducted quick test (NH<sub>4</sub>-N and TN) and chlorophyll-a extraction experiments in the lab of Jiangnan University after fieldtrips of March/April 2018, August/September 2018, and November 2018. Further, I performed the corresponding analytics in the laboratories at KIT-AGW with the help of technicians Claudia Mößner for ICP-MS and IC from February/March 2017 campaign. Andre Wilhelms conducted the dissolved water quality analysis with technicians Claudia Mößner for the samples in June/July 2016 as the content of his master's thesis. All scientific data evaluation in this article were performed by me. Yanwen Qin and Binghui Zheng were the responsible scientists and

primary project partner from the Chinese Research Academy of Environmental Sciences (CRAES). Hua Zou from Jiangnan University and Boqiang Qin and Guangwei Zhu from Nanjing Institute of Geography and Limnology (NIGLAS) made the necessary arrangements for the fieldwork in Wuxi, China. Michael J. Stewardson provided good suggestions for the construction of the simulation model. Andre Wilhelms and/or Andreas Holbach installed BIOLIFT instrument and taken water samples with me in the field together. Christian Moldaenk offering the PhycoLA algal classes devices and gave technical support in the field. Stefan Norra designed and supervised the respective project and raised funds from the BMBF. All co-authors critically reviewed the manuscript and agreed to its publication.

**Abstract:** Algal pollution in water sources has posed a serious problem. Estimating algal concentration in advance saves time for drinking water plants to take measures and helps us to understand causal chains of algal dynamics. This paper explores the possibility of building a short-term algal early warning model with online monitoring systems. In this study, we collected high-frequency data for water quality and weather conditions in shallow and eutrophic Lake Taihu by an in situ multi-sensor system (BIOLIFT) combined with a weather station. Extracted chlorophyll-a from water samples and chlorophyll-a fluorescence differentiated according to different algal classes verified that chlorophyll-a fluorescence continuously measured by BIOLIFT only represent chlorophyll-a of green algae and diatoms. Stepwise linear regression was used to simulate the chlorophyll-a fluorescence changing rate of green algae and diatoms together ( $\Delta\text{Chl}_{a-f}\%$ ) and phycocyanin fluorescence concentration (blue-green algae) on the water surface layer (CyanoS). The results show that nutrients (total N,  $\text{NO}_3\text{-N}$ ,  $\text{NH}_4\text{-N}$ , total P) were not necessary parameters for short-term algal models.  $\text{Chl}_{a-f}\%$  is greatly influenced by the seasons, so seasonal partition of data before modeling is highly recommended.  $\text{CyanoS}_{\text{max}}$  and  $\Delta\text{Chl}_{a-f}\%$  were simulated by only using multi-sensor and meteorological data ( $R^2 = 0.73; 0.75$ ). All the independent variables (wave, water temperature, relative humidity, depth, cloud cover) used in the model were measured online and predictable. Wave height was the most important independent variable in the shallow lake. This paper offers a new approach to simulate and predict the algal dynamics, which also can be applied in other surface water.

© The full article is reprinted with kind permission from Elsevier Ltd. (2020) in Appendix B.3.

## 2.2 Further results and discussions

### 2.2.1 Water quality vertical distribution at different times and seasons

Thermal stratification is a stable state in lakes that circumscribes the vertical transport of oxygen and other dissolved gases, limiting the supply of nutrients for aquatic organisms. Shallow lakes show significant differences in diurnal variations compared to deep lakes. In shallow lakes, the heat storage is not large enough to maintain thermal stratification for more than 24 h, which leads to rapid diurnal changes in thermal structure (Yang et al., 2018). Moreover, the rapid internal response to wind also causes the vertical variation in shallow lakes (Kimura et al., 2016).

To get a deep understanding of the vertical distribution variation in the shallow lakes, a stationary depth profile (BIOLIFT) was applied for getting high-frequency online data. In this study, three campaigns in different seasons in 2018 were taken into account (1. March/April, 2. August/September, and 3. November).

In this section, water temperature (WTemp, °C), air temperature (ATemp, °C), chlorophyll-a ( $\text{Chl}_{a-f}$ ,  $\mu\text{g/L}$ ), phycocyanin ( $\mu\text{g/L}$ ), photosynthetically active radiation at different water depths (IRR,  $\mu\text{mol}/(\text{m}^2\cdot\text{s})$ ), wind speed (m/s), and wind direction (°) measured by BIOLIFT were considered and analyzed.  $\text{Chl}_{a-f}$  of blue-green algae, diatoms and green algae were measured by PhycoLA and used to discuss the algal classes changes.

### Result and discussion

WTemp distributions show dramatic differences in different seasons. In general, in campaign 2018 March/April, WTemp distributions showed little changes at different depths (Fig. 13a). On 4<sup>th</sup> April 2018 in campaign 2018 March/April, ATemp was lower than WTemp, which lead to the colder and more dense WTemp on the water surface layer than the deeper water. As can be seen from the graph, WTemp decreased from 9 am to 9 pm. The lake "turns" when the colder surface water sinks to the lake bottom. In summer (2018 August), the water body presents stronger thermal stratification with warmer water on the water surface. On 28<sup>th</sup> August 2018 at 9 pm (without sunlight), WTemp values were similar at different depths and were lower than that in the afternoon. In November 2018, slight stratification was found and normally happened at noon (12 pm). Similar



to 28<sup>th</sup> August in campaign 2018 August, ATemp was generally higher than WTemp and the highest WTemp was in the afternoon on day five in campaign 2018 November.

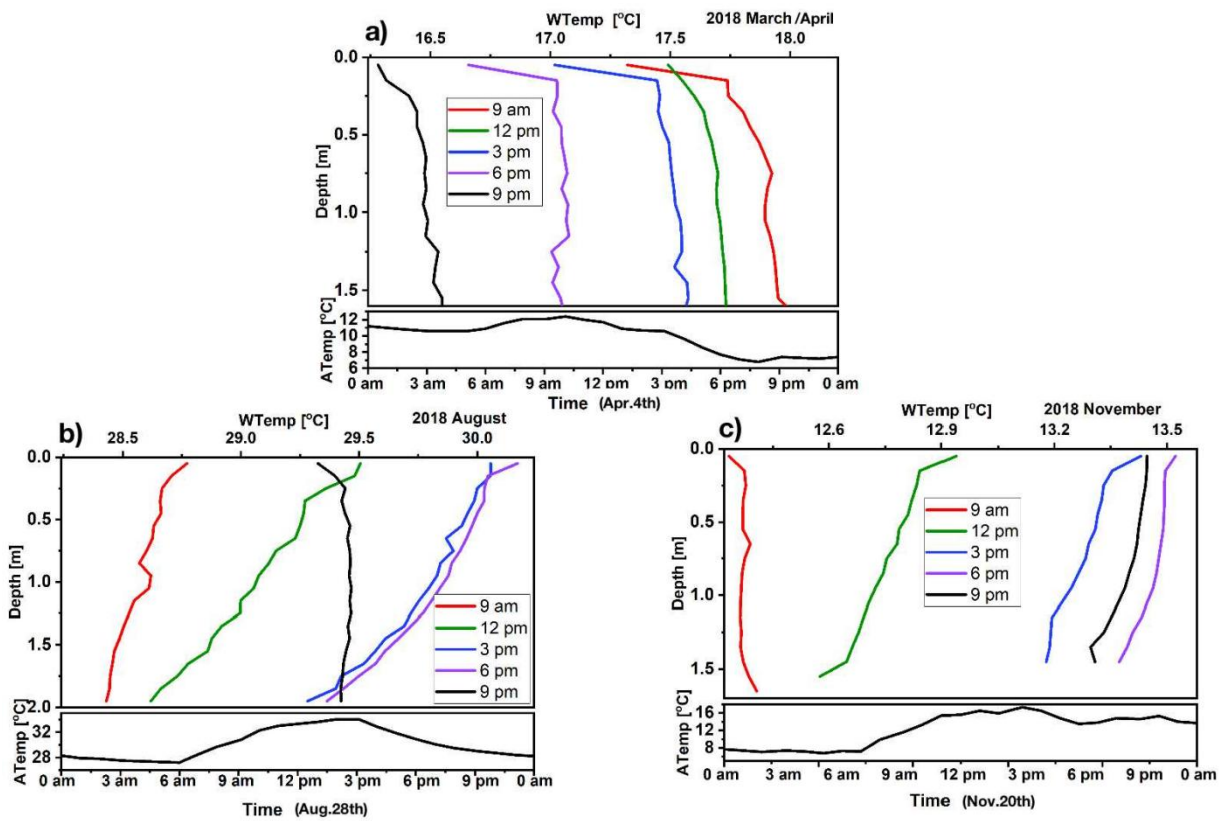


Figure 13 Depth-profile of water temperature and air temperature changes in three days in different campaigns in 2018

$Chl_{a-f}$  of green algae and diatoms had quite different vertical distributions in different algal species and seasons. From Fig. 14,  $Chl_{a-f}$  (green algae and diatoms) do not show dramatic changes within one day at different times. However,  $Chl_{a-f}$  was slightly higher in the middle layer in 2018 March/April and the upper layer in 2018 November. Algal species-specific depth distribution patterns of green algae and diatoms are related to the cell or colony density, which varies largely in different algal species (Miklasz and Denny, 2010, 2010; Peperzak et al., 2003).

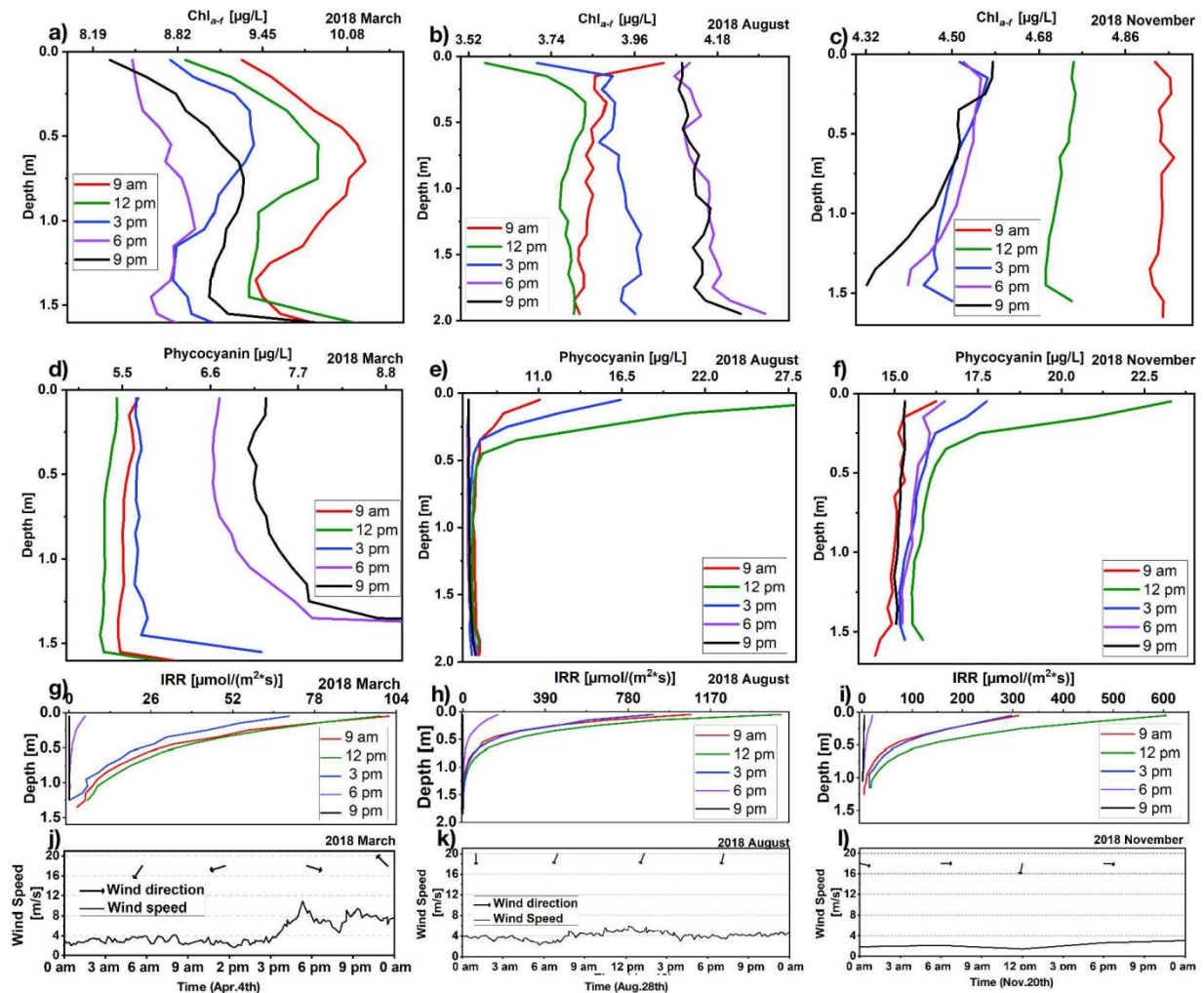


Figure 14 Vertical distributions of a) - c) Chl<sub>a-f</sub>, d) - f) Phycocyanin, g) - i) photosynthetically active radiation at different water depths (IRR), as well as j) - l) wind direction and speed in three days in three different campaigns in 2018

Algal species compositions are different in the three campaigns. As can be seen from Fig.15, green algae was the dominant algal class in most days of campaign 2018 March/April (Chl<sub>a-f</sub>: 46%-95%) compared to diatoms (0-54%) and blue-green algae (0-12%). The ratio of green algae was also high in 2018 November (27%-72%), but blue-green algae (17%-59%) was much more than diatoms (3-21%). The high concentration of Chl<sub>a-f</sub> and phycocyanin at the water bottom is related to the wind-induced resuspension (Fig.14j, wind speed > 6 m/s) (Qin et al., 2004a), which lead to thermocline movements of benthic algae (Cyr, 2016). On day 4<sup>th</sup> April in 2018 March/April, the continuous high wind speed (Fig.14j) mixed the water body to a certain degree. Algal vertical movements are influenced by wind speed, hydrodynamic and algal sinking rate or buoyancy. Especially for green algae and diatoms, because they have no means of locomotion, they sink

(Miklasz and Denny, 2010). Moreover, specific algal species composition structures vary in different seasons. For example, even though two species belong to diatoms, they have different sizes, densities and sinking rates.

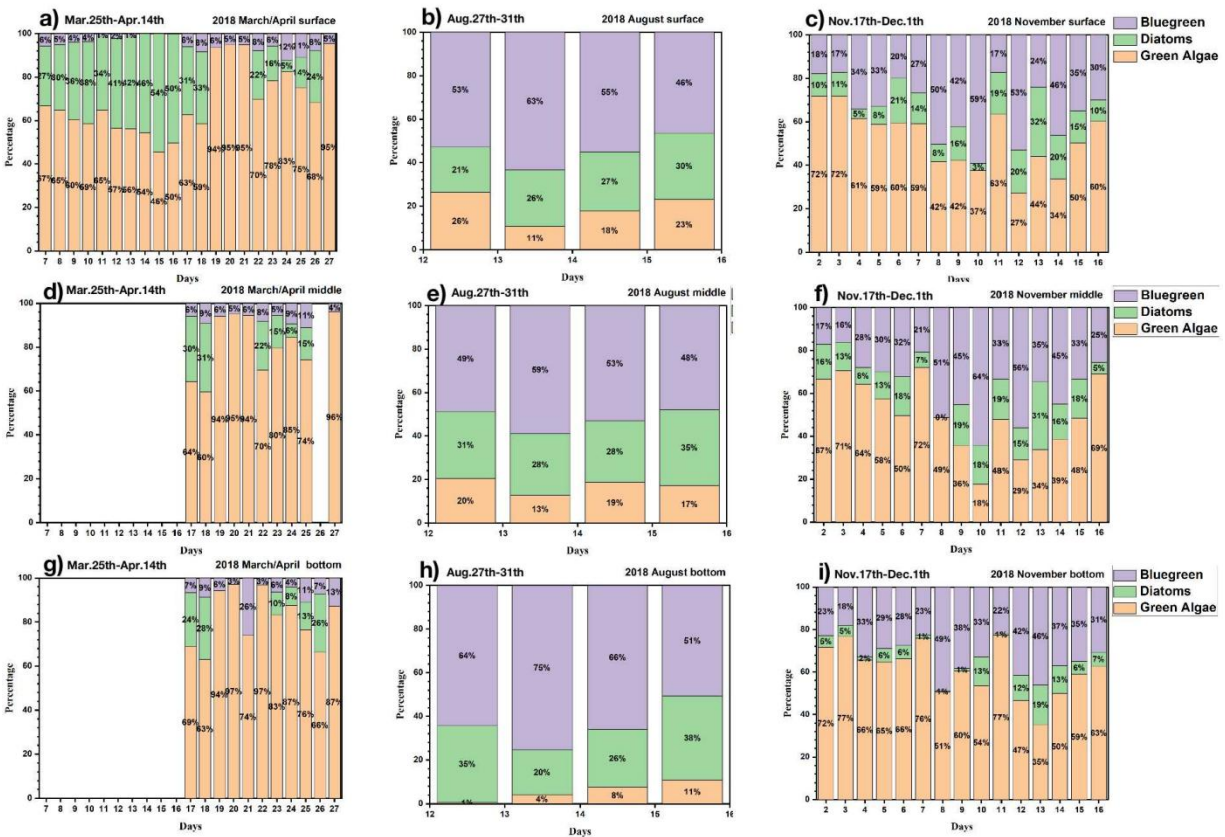


Figure 15 Percentage of Chl-a-f of blue-green algae, diatoms and green algae measured by PhycoLA in three campaigns in 2018.

Different from campaign 2018 August and 2018 November, phycocyanin concentrations were evenly distributed at different water depths in 2018 March/April, which is related to the cold weather and low irradiation. IRR on day 4<sup>th</sup> April of campaign 2018 March/April (maxima: 104  $\mu\text{mol}/(\text{m}^2 \cdot \text{s})$ ) was much lower than that day 28<sup>th</sup> August of 2018 August (maxima: 1502  $\mu\text{mol}/(\text{m}^2 \cdot \text{s})$ ) and 20<sup>th</sup> November of 2018 November (maxima: 600  $\mu\text{mol}/(\text{m}^2 \cdot \text{s})$ ). Phycocyanin concentrations were much higher in the upper layer in 2018 August and November, especially in the afternoon under stronger irradiation. Blue-green algal buoyancy can be altered in response to better living conditions by its gas vesicle (Brookes and Ganf, 2001).

In some cases, the  $\text{Chl}_{a-f}$  of green algae and diatoms, as well as phycocyanin, were higher at night when there is so sunlight (Fig 14 a, b, d). On 4<sup>th</sup> April in campaign 2018 March/April, the high concentration of  $\text{Chl}_{a-f}$  and phycocyanin at night was related to the strong wind with high concentration at the water bottom (mentioned above). On 28<sup>th</sup> August in campaign 2018 August/September, the high measured concentration of  $\text{Chl}_{a-f}$  at night was associated with the high irradiances during the daytime. Under strong irradiation, photoinhibition or fluorescence quenching can happen (Demmig-Adams et al., 2014; Marra, 1992). Photoinhibition will lead to light-induced irreversible damage to PSII, the system recovered over the following night hours (Collos et al., 1989; Marra, 1992). On 28<sup>th</sup> August, the  $\text{Chl}_{a-f}$  remained instead of decreased from 9 am to 3 pm. Therefore, the high measured  $\text{Chl}_{a-f}$  at night is more likely related to fluorescence quenching.

## **Conclusion**

In general, in shallow Lake Taihu, WTemp stratification can happen in summer under warmer ATemp and weak stratification can also occur in autumn, when ATemp is much higher than WTemp. WTemp and it changes, as well as wind characteristics, are very important factors for the vertical distribution of algae in shallow lakes. Blue-green algae can move and stay on the water surface layer by its gas vesicles under suitable conditions. Wind-induced resuspension can move settled algae from sediments to the lake surface and increase the algal biomass in the lake water. Algal class distribution varies largely across different seasons. Different algal species show different vertical distribution patterns in the lake. Moreover, the photoinhibition during daytime can lead to an increase of measured algal biomass at night.

### **2.2.2 Nutrients spatial distribution and temporal dynamics**

Nutrients are essential for plant growth, but the overabundance of nutrients in the water can have harmful health and environmental effects (eutrophication). Algal growth is usually limited by the available supply of either phosphate or nitrate (Munn et al., 2010). In the short-term, nutrients do not significantly influence the algal biomass (chlorophyll-a) in Lake Taihu because the nutrients are always sufficient for algal growth. Therefore, none of the nutrients were included in the simulation model (Yang et al., 2021). Moreover, algae need enough nutrients for fast growth and

will also consume nutrients during the growth process. Therefore, there is no clear correlation between nutrients and algal biomass from the result in the short-term. However, in the long-term and at large spatial scales, the correlation is proven in previous studies (Wurtsbaugh et al., 2019).

In this section, nutrients, chlorophyll-a, and phycocyanin concentrations measured at the TLLER station of Lake Taihu in different seasons were involved in discussing their correlations. Moreover, water samples in the inflow rivers and river mouths of Wuli Bay were taken in two days to compare the algae species differences in different inflow rivers as well as the changes of algal species and nutrients within two days.

Campaigns included in the nutrients analysis are 2014 April, 2015 May, 2015 November/December, 2016 June/July, 2017 February/March, 2017 September, 2018 March/April, 2018 August/September, 2018 November, and 2019 March. Sample collection, preparation, and measurement procedures of anion concentration ( $\text{NO}_3^-$ ), dissolved/particulate element concentration (dissolved and particulate P),  $\text{NH}_4\text{-N}$  and TN at the TLLER station were the same as those described in my publications (Yang et al., 2021, 2020). The campaign information and measured parameters at the TLLER station were shown in Table 5.

**Table 5 Campaign information and measured parameters at TLLER station**

Campaigns	Start	End	Dissolved	Particulate	$\text{NH}_4\text{-N/TN}$
June/July 2016	27.06.2016	15.07.2016	√	√	-
February/March 2017	24.02.2017	06.03.2017	√	√	-
September 2017	15.09.2017	23.09.2017	√	√	-
March/April 2018	19.03.2018	16.04.2018	√	√	√
August/September 2018	16.08.2018	09.09.2018	√	-	√
November 2018	16.11.2018	30.11.2018	√	-	√
March 2019	21.03.2019	31.03.2019	√	-	√

Water samples were also taken in Wuli Bay and from two of its inflow rivers, which are River Ludianqiaobang (LD) and River Xinhuzhuangtianbin (XH), in two days. Only surface water samples were taken by a plastic bucket on 30<sup>th</sup> March 2019. On 1<sup>st</sup> April 2019, a sediment core sampler was applied to collect overlying water above the sediment.

## Result and discussion

**Nutrients and algae at the TLLER station.** In Fig.16a, TN was much higher in 2018 November than in 2018 March/April, 2018 August/September and 2019 March, with a mean of 5.2 mg/L and a maximum of 20.0 mg/L, which is not the case of  $\text{NO}_3\text{-N}$  and  $\text{NH}_4\text{-N}$ . Li et al. (2013) also found high TN in the littoral areas of Meliang Bay in November. This is likely related to the exogenous pollution of N from agriculture in November.

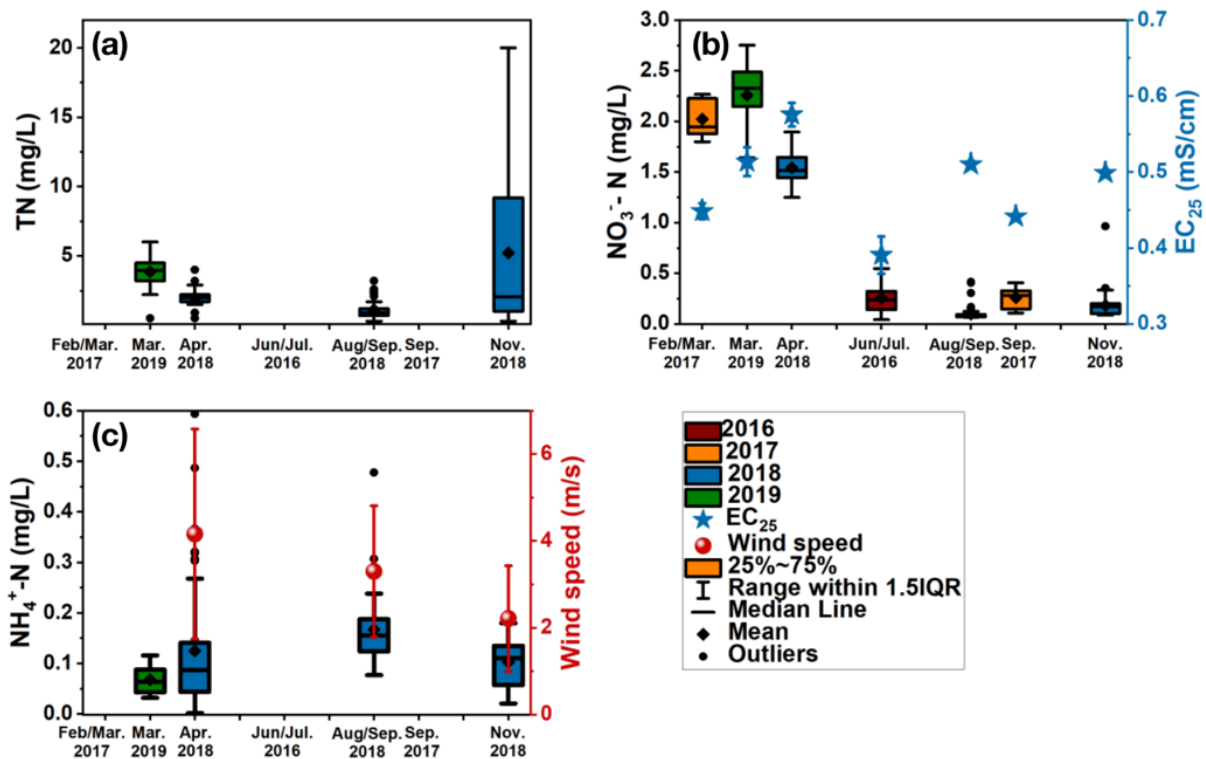


Figure 16 Seasonal changes of a) TN, b)  $\text{NO}_3\text{-N}$  and  $\text{EC}_{25}$ , c)  $\text{NH}_4\text{-N}$  and wind speed

As can be seen from Fig. 17, TN had two times increase in campaign 2018 November, which is day seven and day 14. On day 7, over 4 m/s wind speed was observed, at the same time, the turbidity increased from the lake bottom. Moreover, TN in the water bottom was higher than in the water surface. Therefore, the increase of TN on day seven was related to the wind-induced resuspension, which rolled up the settled algae and biomass. Unlike day seven, higher TN was found on the water surface instead of water bottom on day 14, in which period algae accumulated on the water surface. Nitrogen in algal cells is very likely the major form of TN on day 14.

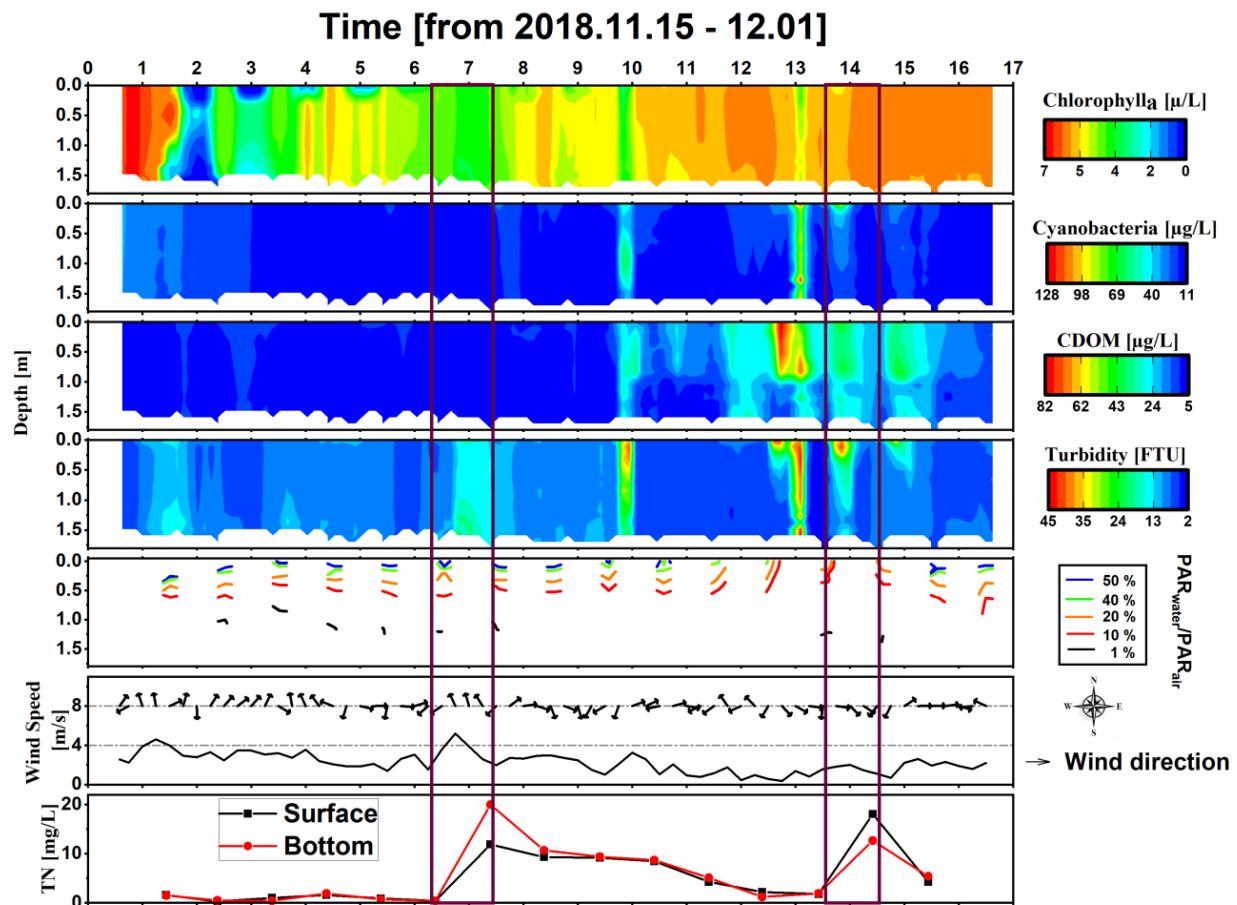


Figure 17 Time series of chlorophyll-a fluorescence, phycocyanin fluorescence (blue-green algae), CDOM, turbidity,  $PAR_{water}/PAR_{air}$ , wind speed, wind direction and TN in 2018 November

$EC_{25}$  measured by BIOLIFT can represent dissolved ionic components (Reluy et al., 2004). In general,  $EC_{25}$  had maxima in spring and minima in summer (Fig. 16b), which related to rainfall dilution in June/July (East Asian summer monsoon) (Yang et al., 2020). The seasonal change of  $NO_3-N$  was inconsistent with major ions at the TLLER station (Fig. 16b). The  $NO_3-N$  was the highest in February and March (winter-spring period) and the lowest in August. The highest concentration of  $NO_3-N$  was measured in wheat-season, especially in months of second top dressing in February/March (Zhao et al., 2011). In the Lake Taihu region, rice is planted in mid-June and harvested in late October, while wheat is grown from early November to late May (Yu et al., 2018). Even though more rain and flooding appeared during rice-season (June-October) related to the summer monsoon, the runoff was higher in wheat-season (November-May). Because the ridges of rice fields can help to prevent water overflow (Yu et al., 2018) and fields act as flood

retention basins. The low concentration of  $\text{NO}_3\text{-N}$  in 2018 August is very likely due to the algal uptake.  $\text{NO}_3\text{-N}$ , the same as  $\text{EC}_{25}$ , was diluted by the strong rainfall in 2016 June, influenced by the monsoon season.

The wind speed (Fig.16c) is based on the hourly wind speed data measured in different months. The fastest wind speed was in 2018 March/April, with an average of 4.2 m/s and a maximum of 12.1 m/s. During this period,  $\text{NH}_4\text{-N}$  concentration varied largely and the highest  $\text{NH}_4\text{-N}$  was 0.6 mg/L. The peak of mean  $\text{NH}_4\text{-N}$  was in 2018 August/September (0.2 mg/L), during which time increased biological activity is to be expected due to warm weather. Moreover, under anaerobic conditions (Fig.18a), nitrification of ammonia to nitrate is limited and ammonia accumulates.

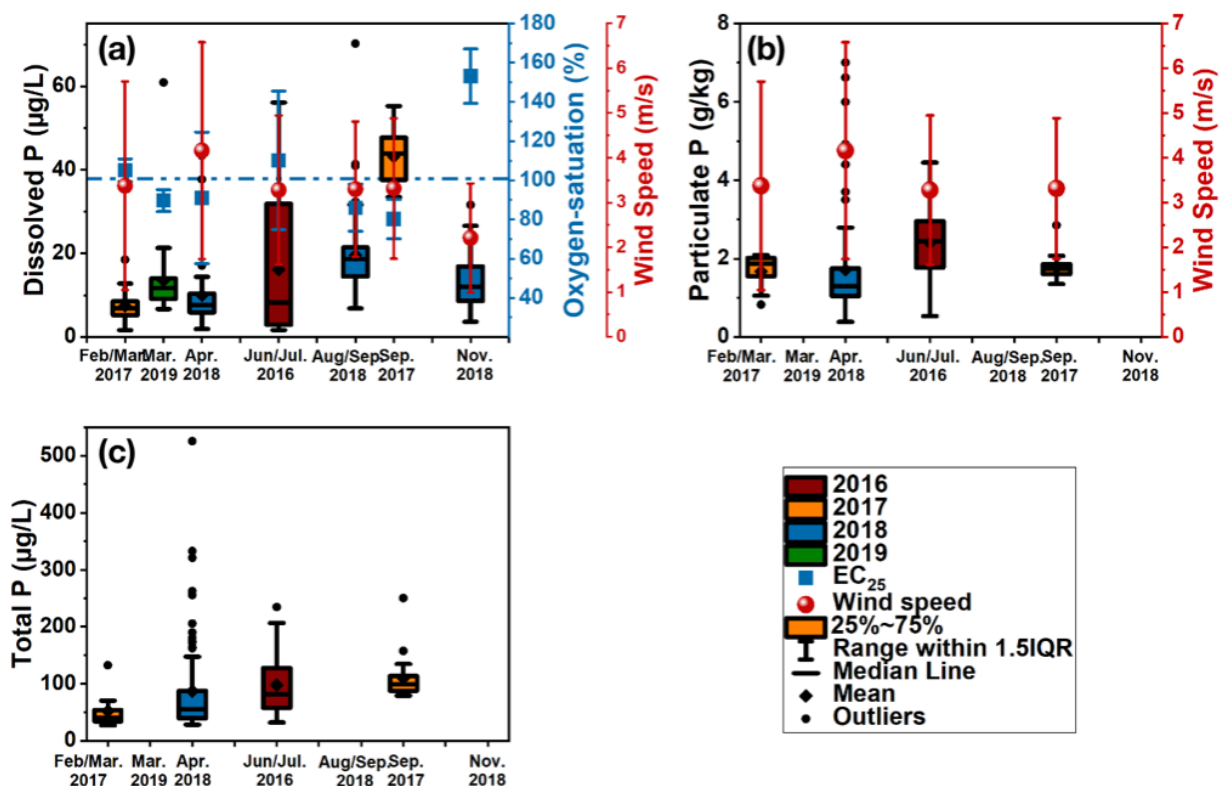


Figure 18 Seasonal changes of a) dissolved P, Oxygen-sat., wind speed, b) particulate P and wind speed, c) total P at TLLER station

During the monitoring time, the seasonal variation tendency of dissolved P was different from  $\text{EC}_{25}$ . Dissolved P was low ( $9.9 \mu\text{g/L}$ ) in 2018 March/April and extremely high ( $43.2 \mu\text{g/L}$ ) in 2017 September. Oxygen-sat. was the highest in 2018 November, the average value was 153%. Oxygen-sat. in 2019 March, 2018 August/September, 2017 September and most of 2018



March/April were below 100% (Fig.18a). Dissolved P was high in both 2018 August/September and 2017 September, during which times the Oxy-sat. were low and at the mean time wind speed was slow. The dissolved P desorption from the sediment prefer to happen under calm (less wind) and oxygen-poor condition (Kowalczywska-Madura et al., 2017). In 2016 June/July, the dissolved and particulate P fraction was high (Fig.20a and 20b), which was very likely coming from soil runoff due to the heavy rainfall. Moreover, the high concentration and variance of particulate P in 2016 June/July was also related to algal dynamics. Some of the dissolved P might be taken up by algae and stored as particulate P (Wetzel, 2001). Same with  $\text{NH}_4\text{-N}$ , the highest particulate P (7 g/kg) was measured in 2018 March/April under the highest wind speed. The strong turbulence induced by strong wind can easily resuspend the fine particles from surface sediments into the water column (Qin et al., 2004b), which can happen in 2018 March/April with high wind speed (Fig.18b). Total P, mainly composed of particulate P, had the highest mean value of 109.5  $\mu\text{g/L}$  in 2016 June/July and the highest value in 2018 March/April (525.5  $\mu\text{g/L}$ ).

In the surface sediments, the concentrations of P in Zhushan Bay were approximately two times higher than that in Meiliang Bay and Gonghu Bay. The higher concentrations were close to the river mouth (Fig. 19a). A consistent result can be seen from the dissolved P (Fig. 19b), which had higher concentrations near the river mouth in Zhushan Bay during all campaigns. Dissolved P in Zhushan Bay were all over 56  $\mu\text{g/L}$  and the highest values reached 161  $\mu\text{g/L}$ . These might be due to the pollution of P from the river around Zhushan Bay and its direct influence on the water column and sediment concentrations. Dissolved P is probably coming from external inputs or released from surface sediment. Furthermore, the dominated southeast wind in summer makes the down-wind location of Zhushan Bay to be a favourable area for serious cyanobacteria accumulation. After algae death, the bio-accumulated P will be returned to the local sediments. The sediments, as a nutrient sink and source, are essential for the re-introduction of mobile phosphate species into the water column, especially in shallow lakes like Lake Taihu.

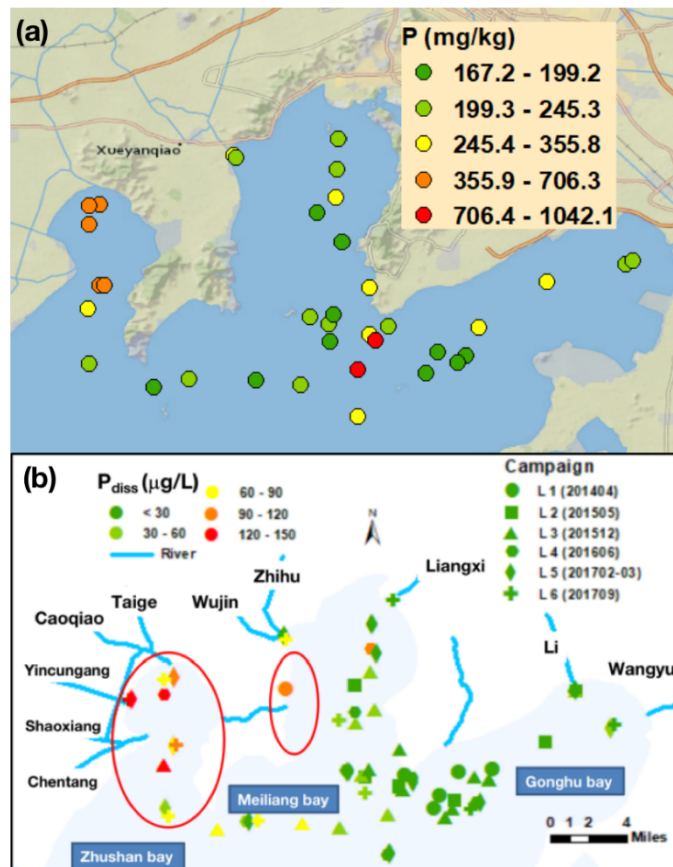


**Figure 19** Spatial distribution of a) P in the surface sediment; b) dissolved P in the surface water samples in northern Lake Taihu

In Meiliang Bay, the dissolved P close to river mouths were higher. The highest value was 136 µg/L measured in 2016 June/July. In this period, dissolved P had more than 100 times difference in different regions. The highest concentration of P occurred at the junction of Meiliang Bay and Gonghu Bay, measured in 2015 November/December where there are fish farms nearby.

Even though from the perspective of laboratory research, increased nutrients can stimulate the increase of algae (Heisler et al., 2008), I did not observe clear correlations between algae (chlorophyll-a and phycocyanin) and nutrients (dissolved P, NO<sub>3</sub>-N, NH<sub>4</sub>-N, TN, and TP) on a daily basis. This is because the nutrient changes in the natural water body are influenced by many factors, including external pollution, algal uptake, and resuspension. A time-series graph of nutrients (dissolved P, NO<sub>3</sub>-N, NH<sub>4</sub>-N, TN) and total chlorophyll-a fluorescence measured by

PhycoLA ( $Chl_{a-f}$ \_PhycoLA; bbe moldaenke, Schwentinal, Germany) is shown in Fig.20 and Fig.21.

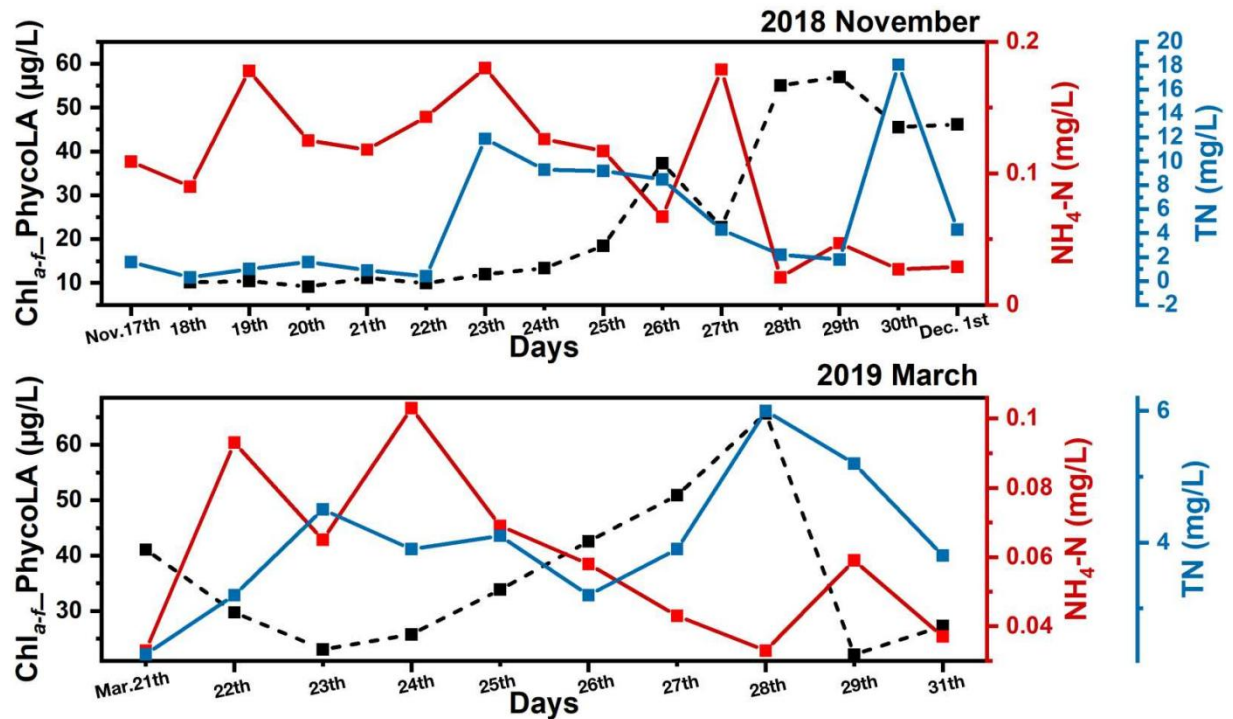


Figure 20 Time series of  $Chl_{a-f}$ \_PhycoLA, TN and  $NH_4-N$  changes in a) 2018 November; b) 2019 March

From the result, the peak of nutrients and  $Chl_{a-f}$ \_PhycoLA are not consistent. In general, the changes of dissolved P,  $NH_4-N$ ,  $NO_3-N$  and  $Chl_{a-f}$ \_PhycoLA with time in 2018 November and 2019 March shown relationship patterns like Fig.21d. On the one hand,  $Chl_{a-f}$  increased with the increase of dissolved P,  $NO_3-N$  and  $NH_4-N$ . On the other hand, the growth of algae will decrease the nutrients concentration, especially  $NO_3-N$ ,  $NH_4-N$  and dissolved inorganic P, which can be taken up by algae directly (Ji, 2017). The changes of dissolved P,  $NO_3-N$  and  $Chl_{a-f}$ \_PhycoLA in 2018 March/April did not fit well with the curves in Fig. 21d. The variation of dissolved P was very likely related to the strong wind by release from sediment. Moreover, the different changing trends of  $NO_3-N$  are likely due to potential external pollution from fertilization in February/March.

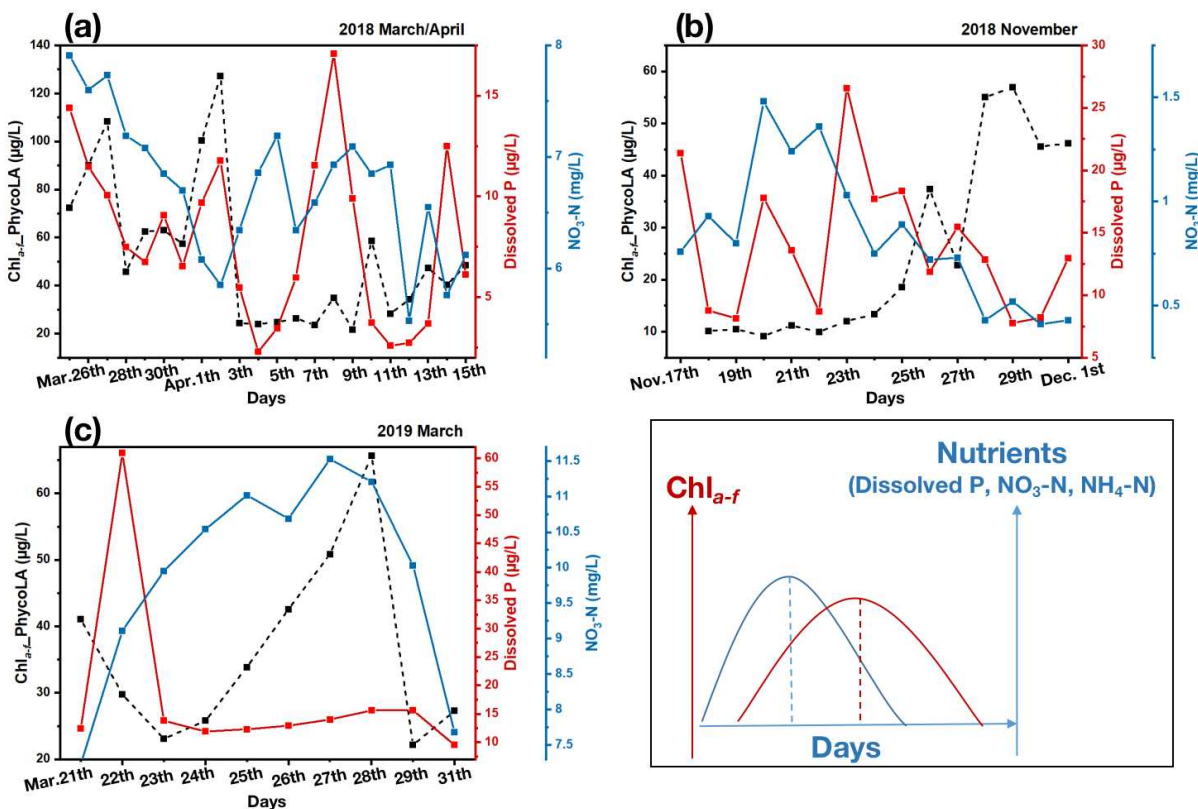


Figure 21 a)-c) Time series of Chl<sub>a-f</sub> PhycoLA, dissolved P and NO<sub>3</sub>-N changes in 2018 March/April, 2018 November and 2019 March; d) summarized variation curve of Chl<sub>a-f</sub> and nutrients

**Nutrients and algae in Wuli Bay and inflow river.** Wuli Bay is a small lagoon located in the north part of Lake Taihu, which is connected to Meiliang Bay. Wuli Bay receives millions of tons of domestic and industrial sewage water each day via rivers from Wuxi city (Qin et al., 2007a). Wuli Bay is 6 km from east to west, 0.3 - 1.5 km from south to north and has approximately 6.4 km<sup>2</sup> of surface area. Wuli Bay has an annual water level of 3.07 m and its mean depth is 1.60 m, with water level fluctuation of 1.3 - 2.0 m (Ye et al., 2011). River Ludianqiaobang (LD) is located in northern Wuli Bay and River Xinhuzhuangtianbang (XH) is located in eastern Wuli Bay (Fig. 22). These two rivers have long been polluted by industrial and domestic sewage water. Because the construction of the sewage pipe network in this area is not perfect and the rainwater and sewage diversion is not implemented, which leads to the direct discharge of domestic sewage into the river.

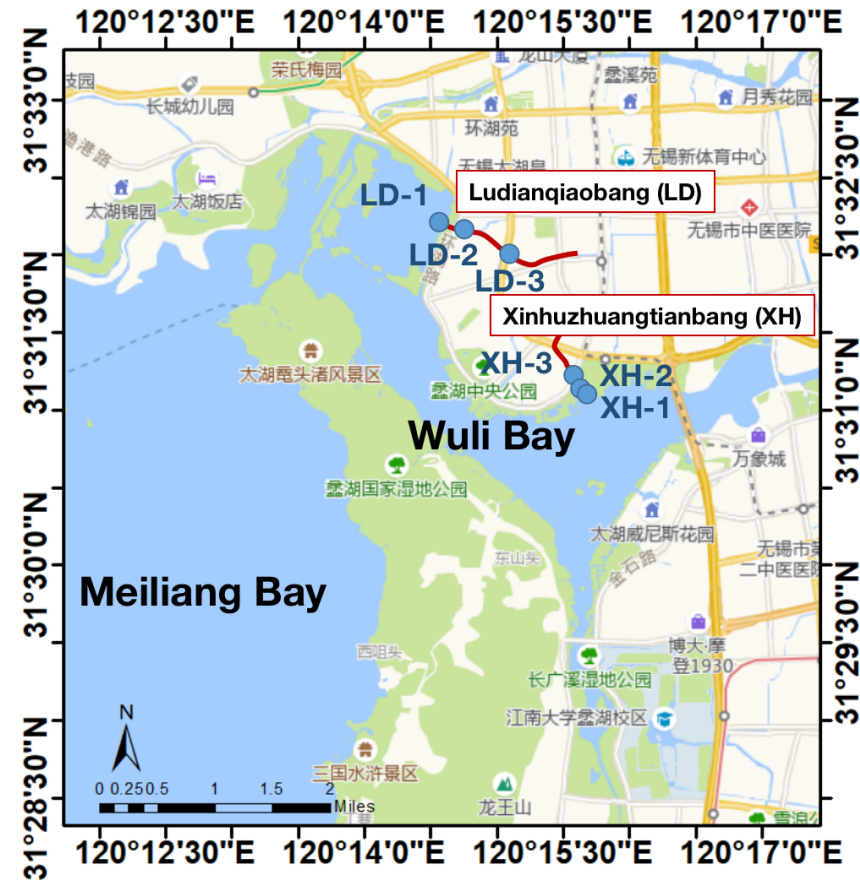


Figure 22 Location of River Ludianqiaobang (LD) and River Xinhuzhuangtianbang (XH)

In general, the nutrient concentrations ( $\text{NO}_3\text{-N}$ ,  $\text{NH}_4\text{-N}$ , TN and dissolved P) were higher in River XH than that in River LD (Fig.23).  $\text{NO}_3\text{-N}$  in River XH was much higher than that in the lake (Wuli bay). Moreover,  $\text{NO}_3\text{-N}$  concentration was much higher in the overlaying water than in the surface water on 1<sup>st</sup> April 2018.  $\text{NH}_4\text{-N}$  concentration was much higher in Wuli Bay, River LD and River XH than at the TLLER station during the same measuring time. TN varies quite a lot from the lake to river and within two days. Dissolved P was also much higher in the River XH than that at the TLLER station.

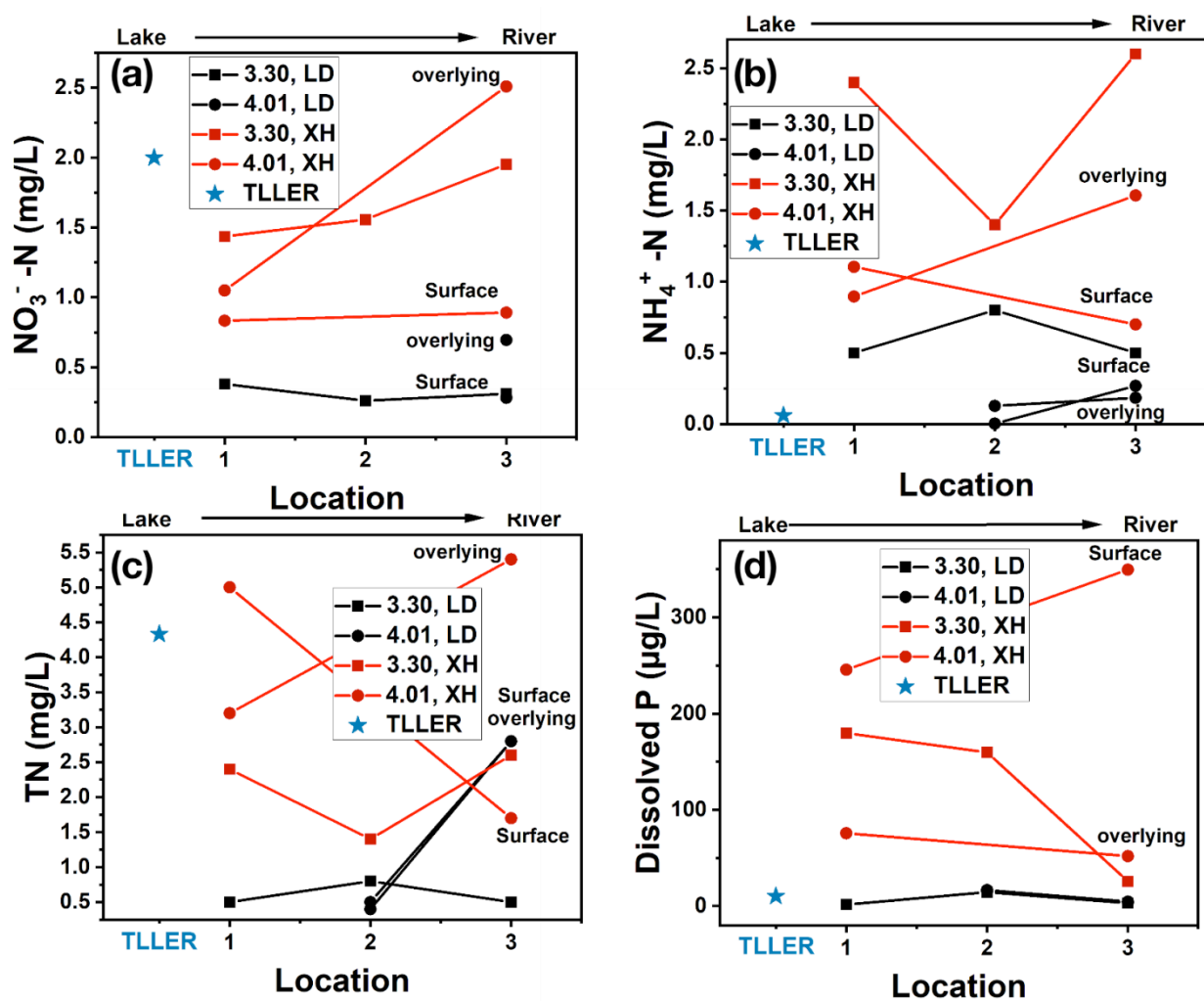


Figure 23 Concentration of NO<sub>3</sub><sup>-</sup>-N, NH<sub>4</sub><sup>+</sup>-N, TN and dissolved P in different locations and two different days (30<sup>th</sup> March and 1<sup>st</sup> April)

Total chlorophyll-a measured by PhycoLA (Chl<sub>a-f</sub>\_PhycoLA) on the water surface layer at the TLLER station on 29<sup>th</sup> and 31<sup>th</sup> March were 28.3 µg/L and 19.7 µg/L, respectively (Fig.24). The ratio of algae classes does not have dramatic changes within two days.

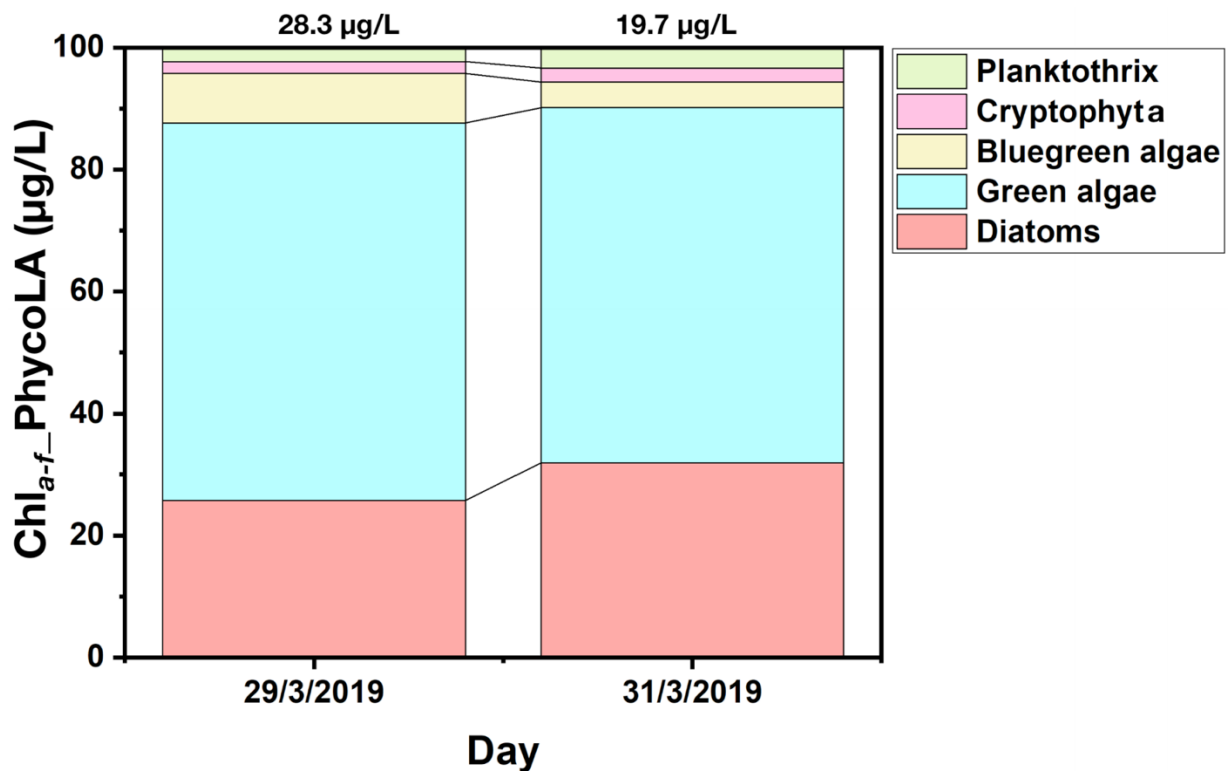


Figure 24 Ratio changes of algal classes within two days at the TLLER station

Chl<sub>a-f</sub>PhycoLA was 28.3 μg/L and 19.7 μg/L in the river mouth of LD and XH river on 30<sup>th</sup> March (Fig.25). Chl<sub>a-f</sub>PhycoLA in River LD was generally higher than the river mouth and nearby lake. However, the Chl<sub>a-f</sub>PhycoLA was lower in River XH than the nearby river mouth and lake. From the result, even though the nutrient concentrations in River XH were much higher than River LD, the Chl<sub>a-f</sub>PhycoLA concentrations were higher in River LD. Moreover, the algal classes and Chl<sub>a-f</sub>PhycoLA concentrations varied more largely in River XH than that in River LD. In terms of proportion, River XH contained more blue-green algae than River LD. It is supposed that blue-green algae prefer to grow under high nutrient conditions at spatial scales. Nutrient concentration is an important factor for algal class changes instead of algal biomass.

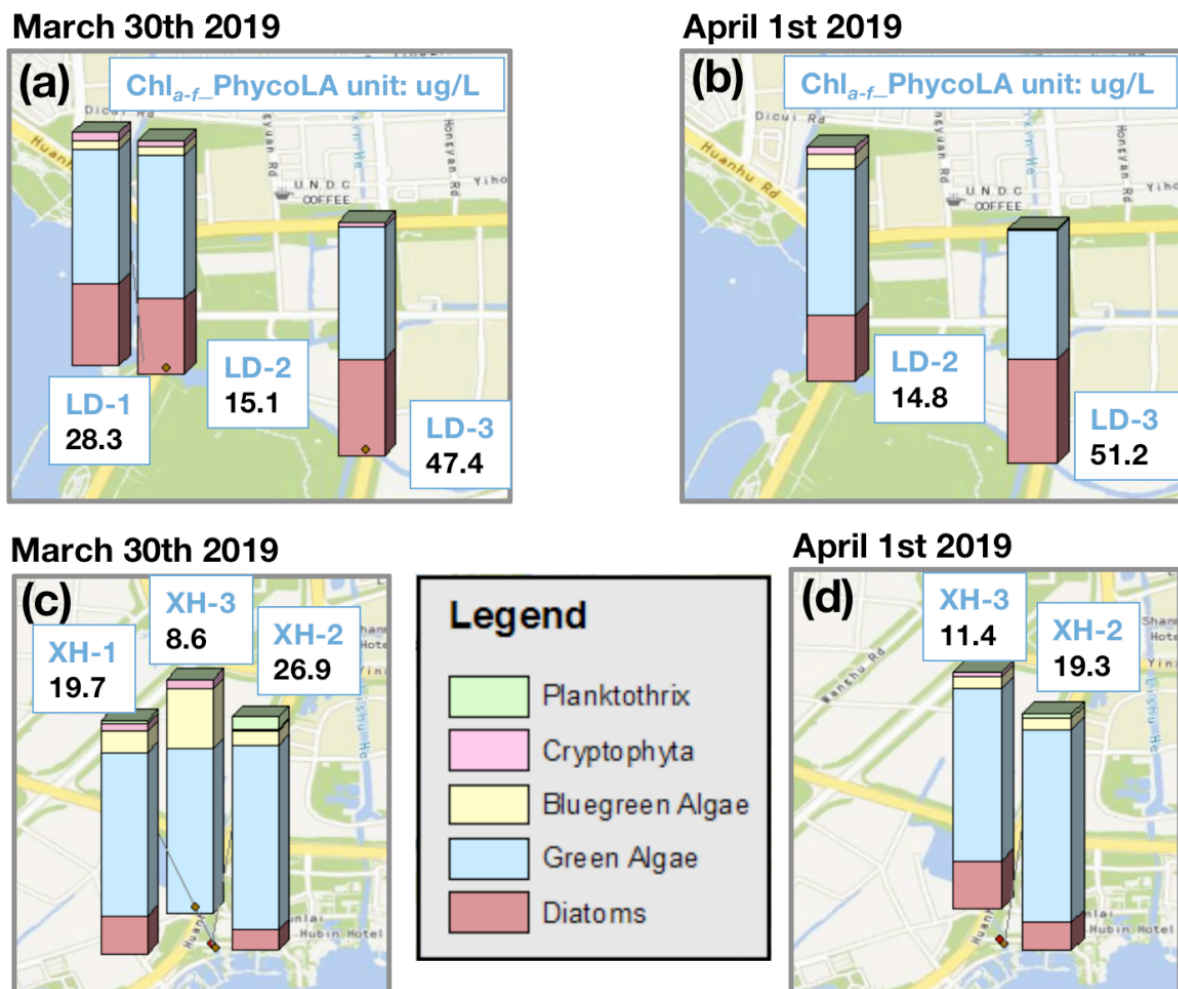


Figure 25 Ratio changes of algal classes in different location along River LD and XH

## Conclusion

Wind-induced resuspension can easily happen in shallow Lake Taihu, which can roll up sediment and settled algae to the water body and promote the release of nutrients from sediment. In summer, the particulate N taken up by algae is very likely the major component of TN. High NO<sub>3</sub>-N was observed in February/March, which is related to the fertilization in wheat season. High NH<sub>4</sub>-N was observed in August/September, which is because of the strong biological activity and anaerobic condition. Low Oxygen-sat. can limit nitrification and stimulate the release of dissolved matter. Higher P in the sediment was found in Zhushan Bay and at the junction of Meiliang Bay and Gonghu Bay. Zhushan Bay is located near an industrial area and down-wind location in summer,



where pollution and blue-green algae accumulated and settled in the sediment. The junction of Meiliang Bay and Gonghu Bay is polluted by fish farms nearby. The local government should pay more attention to the pollution, especially the industrial discharge and fish farm, in the Zhushan Bay area as well as the junction of Meiliang Bay and Gonghu Bay. No clear correlations were found between nutrients and  $\text{Chl}_{a-f}$ . Algal biomass is not necessarily higher in water with high nutrients. The increase in nutrients does not lead to the rapid growth of algae. However, the algal growth consumes nutrients and will lead to the decrease of nutrients, if no external or internal nutrients are input into the lake water. Blue-green algae concentration is higher in the high nutrients river.

### **2.2.3 Water quality comparison of Lake Westensee in Germany and Lake Taihu in China**

In this section, hypertrophic Lake Taihu, China and eutrophic Lake Westensee, Germany (Berger, 2005) were compared in geographic location, local climate, land use and water quality. High-frequency data of water quality and weather conditions in Lake Taihu and Lake Westensee were simultaneously measured by two equally configured BIOLIFT on 23-24<sup>th</sup> August 2019. The application of the BIOLIFT buoy system in Lake Westensee is based on the WAQUAVID project, which aims for “Development of an Advanced Depth Profiling Monitoring System for Water Quality, Algae-Vitality, and -Diversity”. This project is funded by the Federal Ministry of Education and Research of Germany (BMBF grant no. 02WQ1375A).

Lake Westensee is the third largest lake in Schleswig-Holstein and lies between the cities of Kiel and Rendsburg. It covers an area of 720 hectares and is the center of the Westensee Nature Park. Lake Westensee has formed at the end of the last ice age, the Vistula Ice Age. Schleswig-Holstein's largest river, the Eider, flows through the Westensee. Lake Westensee is one of the carbonate-rich lowland lakes. From Werner and Dreßler's study (2007), Lake Westensee inferred good ecological status, according to Schaumburg et al. (2006).

The geographic location of Lake Westensee and Lake Taihu is shown in Fig.26. The latitude and longitude differences between the two lakes are round about 110° and 25°, respectively. The land use of the Lake Westensee area is dominated by agriculture and forestry of different intensity and dimensions, which has an increased but weak human impact (Sadovnik et al., 2014). The lake area is characterized by forest areas in the east, agricultural land in the south and west, also loosened settlement areas from Felde on the north-west bank (Biota, 2017). Several smaller water bodies such as rivers, streams and little lakes are connected to the lake. These lakes, ponds, streams and rivers are, to a certain extent, embedded in woodland patches, meadows, and pasture, often lined by riverine groves (Nissen et al., 2013). In comparison, the Lake Taihu area (section 1.4) is more urbanized and industrialized than the Lake Westensee area.

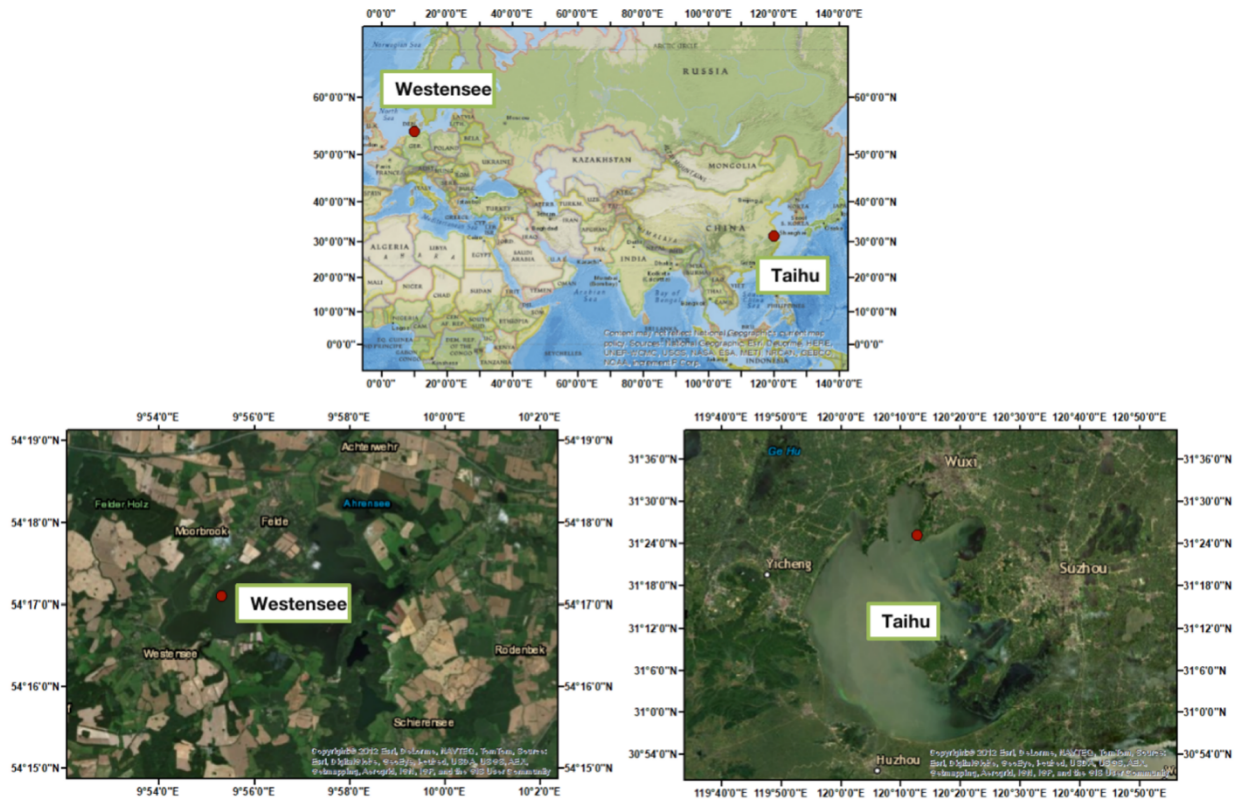


Figure 26 Geographic location of Lake Westensee and Lake Taihu

Basic lake and local climate information of Lake Taihu and Lake Westensee are shown in Table 6. The water area of Lake Taihu (2, 338.1 km<sup>2</sup>) is much larger than Lake Westensee (6.8 km<sup>2</sup>). Moreover, Lake Taihu (maximum water depth: 2.6 m) is much shallower than Lake Westensee (maximum water depth: 17.5 m) (Umweltbericht des Landes Schleswig-Holstein zum Westensee, 2020).

Table 6 Basic information and annual air temperature, wind speed, wind direction, rainfall in Lake Westensee and Lake Taihu

	Water area (km <sup>2</sup> )	Mean depth (m)	Climate	Air Temp (°)	Wind speed (m/s)	Wind direction (°)	Rainfall (mm)
Westensee*	6.8	6.1	Oceanic	8	4 - 5	West Southwest	750
Taihu **	2338.1	1.9	Monsoon	15 - 16	3 - 4	Southwest Southeast	1177

\*(LBP, 2015; LLUR, 2018)

\*\* (Qin et al., 2010)

Lake Westensee area belongs to the oceanic climate. The monthly mean temperature in the warmest month is below 22 °C, which is much cooler than Lake Taihu. Annual average wind speed

is slightly higher in the Lake Westensee area than that in the Lake Taihu area. Moreover, different from the summer monsoon in the Lake Taihu area, the precipitation in the Lake Westensee area is more evenly dispersed throughout the year.

Data from literature and the government's water quality report were collected to compare TP, TN and chlorophyll-a of Lake Westensee and Taihu in 2017 (Table 7). From the Table, Lake Taihu was more polluted by nutrients than Lake Westensee. According to the trophic status (Table 1), Lake Westensee belongs to the eutrophic status and Lake Taihu was hypertrophic. Same with Lake Taihu, diffuse pollution loads from agriculture is recognized as the primary source of phosphorus in Lake Westensee (MELUND SH, 2020).

**Table 7 Comparison of annual TP, TN and chlorophyll-a concentraton in Lake Taihu and Lake Westensee in 2017**

	TP (mg/L)	TN (mg/L)	Chl <sub>a</sub> (µg/L)
Westensee (LLUR, 2018)	0.072	1.42	14.9
Taihu (Qin et al., 2019)	0.136	2.37	40.5

## Result and discussion

Two BIOLIFTs were installed in Lake Taihu and Lake Westensee, respectively, on the same day (23<sup>th</sup> - 24<sup>th</sup> August 2019). In general, the water temperature was higher in Lake Taihu (29 - 33 °C) than that of Lake Westensee (16 - 20 °C) in the one-day measurement (Fig.27). Moreover, the maxima PAR was higher in Lake Taihu (1739 µmol/(m<sup>2</sup>\*s) ) than in Lake Westensee as well. The high temperature and PAR play a part in the higher phycocyanin concentration (blue-green algae) in Lake Taihu (8 - 17 µg/L) compared with that in Lake Westensee (1 - 9 µg/L). Chlorophyll-a fluorescence (Chl<sub>a-f</sub>) of green algae and diatoms varied largely from 2 to 13 µg/L within 10 m depth and had clear delamination in Lake Westensee. However, Chl<sub>a-f</sub> of green algae and diatoms only slightly differed in different layers (6 - 10 µg/L) in Lake Taihu. This is due to the shallowness of Lake Taihu, where the water is easy to be well mixed by the wind and turbulence. Even though the wind speed was much higher in the Lake Westensee area during the measuring time, the turbidity was much higher in the shallow Lake Taihu. pH and EC<sub>25</sub> were on the same scale (7.6 - 8.9; 422 - 465 µS/cm) in the two lakes. Moreover, CDOM in Lake Westensee was round about eight times higher than that in Lake Taihu. This is very likely related to the decomposition process corresponding to extremely low oxygen saturation on the bottom of Lake Westensee (lowest: 12 %). The increasing density of the phytoplankton in the lake is due to the nutrients present in

excess. The result is low light penetration, which leads to the plant and bottom algae die and decomposition at the bottom of the water, depleting a lot of oxygen.

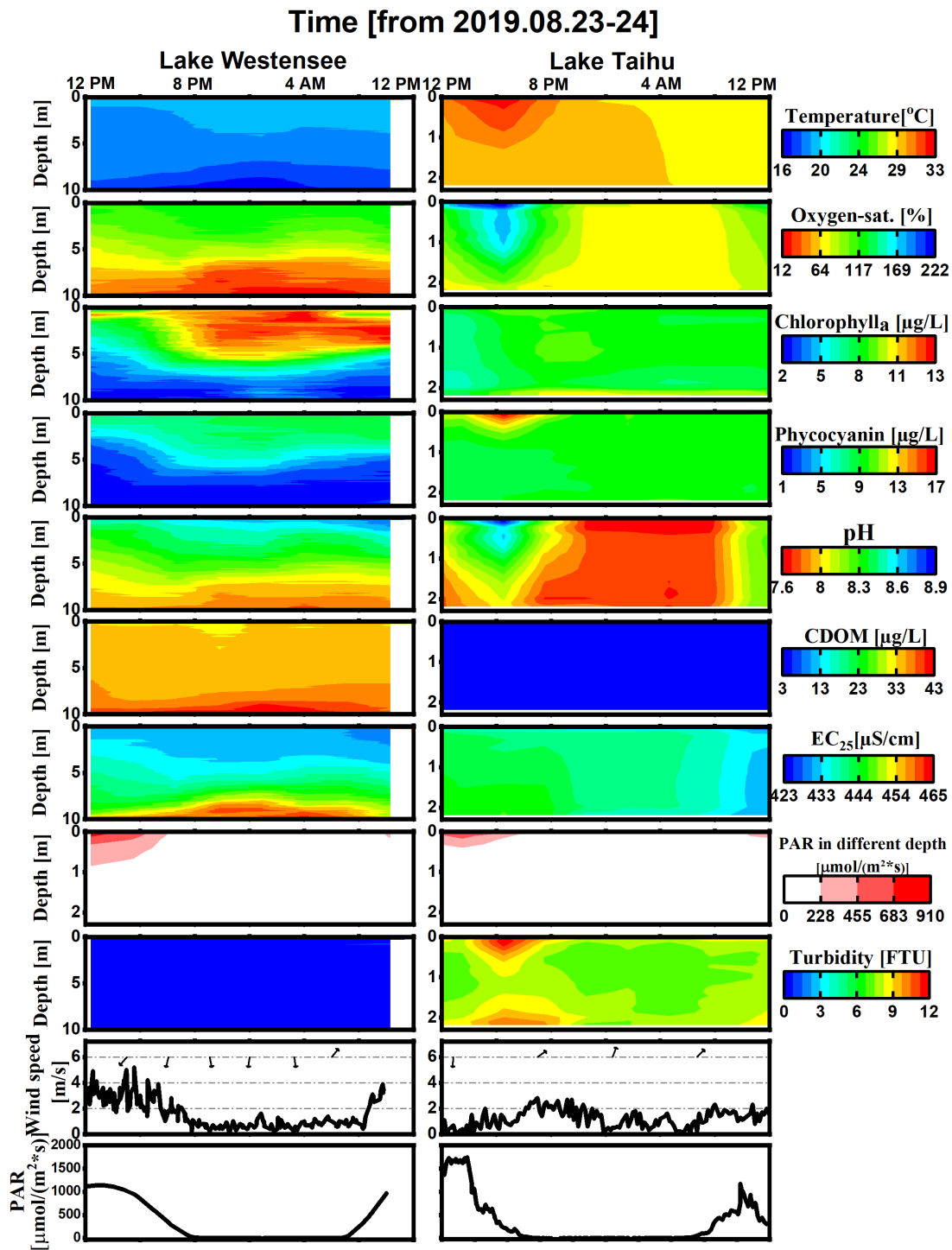


Figure 27 Color map and time series of parameters measured by BIOLIFT in Lake Westensee and Lake Taihu

## **Conclusion**

In general, in the summertime,  $\text{Chl}_{a-f}$  of green algae and diatoms was at a similar level in the two lakes. However, more blue-green algae were observed in Lake Taihu, which is related to the warmer water temperature and higher PAR. Turbidity is much higher in the shallow Lake Taihu, even under lower wind speed than Lake Westensee. The delamination phenomenon is much stronger and  $\text{EC}_{25}$ ,  $\text{Chl}_{a-f}$  (diatoms & green algae), CDOM concentrations were higher in deeper Lake Westensee. The eutrophication induced by extremely low Oxy-sat. on the water bottom will be harmful to the aquatic life (especially in Lake Westensee), which needs to be solved urgently.

### **3 Synoptic discussion**

Traditional laboratory methods can only get delayed data, which can not reflect real-time and fast algal and water quality dynamics. Therefore, a high-frequency online multi-sensor system (BIOLIFT) was adapted and installed in shallow and eutrophic Lake Taihu (section 2.1.1). From the result, the BIOLIFT multi-sensor system is necessary to be used in Lake Taihu, which can virtually show the daily, seasonal, and vertical water quality dynamics (section 2.1.1, 2.2.1). Stepwise linear regression models were successfully created for chlorophyll-a fluorescence changing rate ( $\Delta\text{Chl}_{a-f}\%$ ) of green algae and diatoms as well as phycocyanin fluorescence on the water surface layer (CyanoS) by only using the BIOLIFT multi-sensor data (section 2.1.3). Nutrients are not involved in the short-term algal simulation models because, in eutrophic lakes, nutrients will not have a fast response to the algal growths (section 2.1.3, 2.2.2). However, the nutrients impact algal growth in the long-term and at large spatial scales (section 2.2.2). The improvement of eutrophication status can also alleviate the trace metal pollution in the lake because the algal dynamics will influence the trace metal dynamics by algal uptake (section 2.1.2). The lake shallowness also makes nutrients and trace metals easily returned to the water column from sediment by resuspension (section 2.1.1, 2.1.2). The multi-sensor system was also applied in Lake Westensee to compare its water quality and weather conditions with shallow eutrophic Lake Taihu (section 2.2.3). The driving factors for algal biomass dynamics and algal species changes, as well as the influence of algal dynamic, lake eutrophication and shallowness to the water quality and aquatic life were discussed in this chapter.

#### **3.1 Algal biomass dynamics**

From the result, lake water quality and algae show obvious seasonal dynamics, which are related to the climate (section 2.1.1, 2.1.2, 2.2.1, 2.2.2). From the literature, the possible factors that might influence the algal dynamic including temperature, wind, irradiation, nutrients (James et al., 2013; Qin et al., 2018; Schmidt and Kannenberg, 1998; Singh and Singh, 2015). A conceptual model was established based on the literature review and the monitoring data together (Fig. 28).

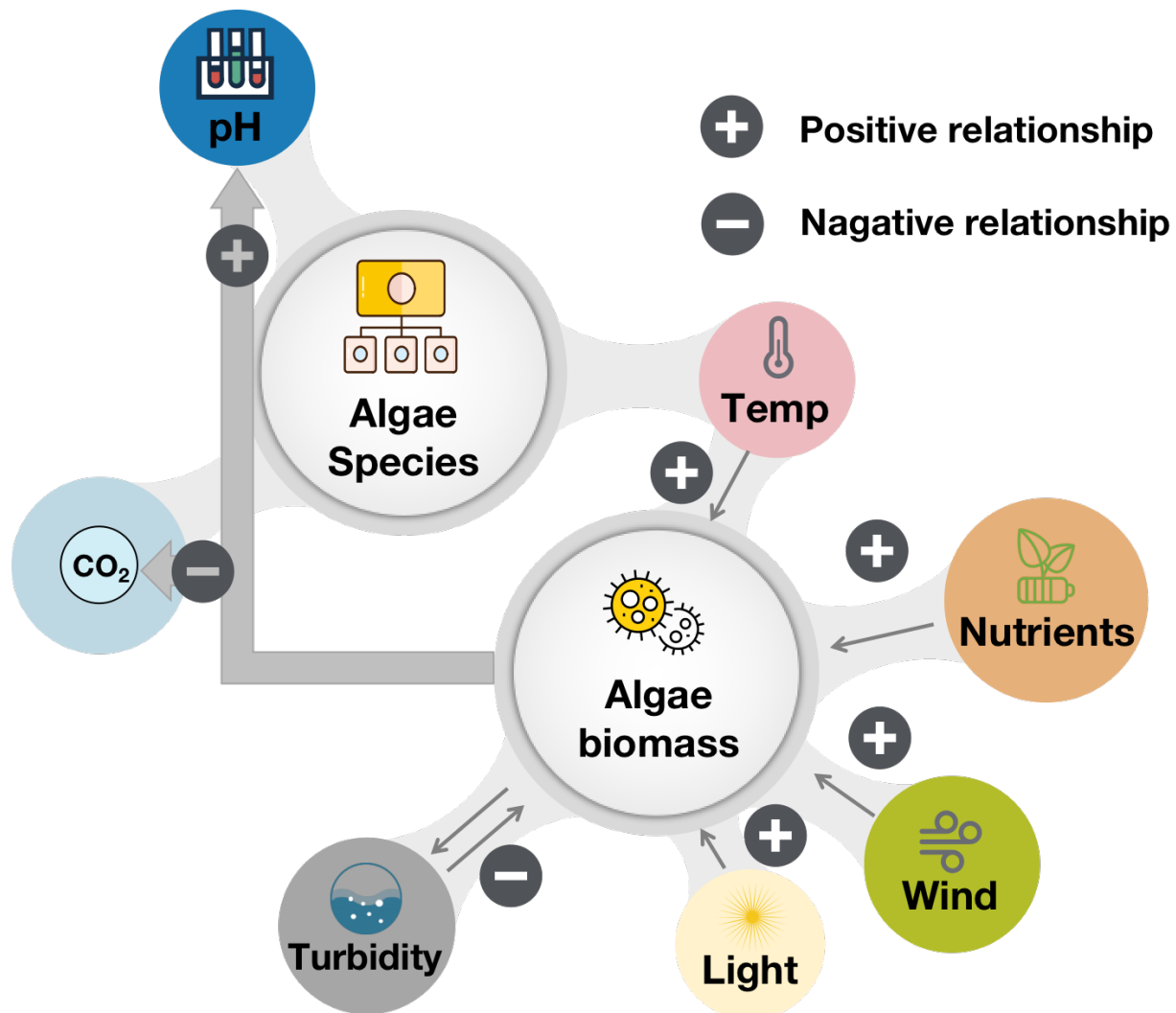


Figure 28 Conceptual model of algal biomass and species changes

In general, water temperature, sunlight, nutrients, and wind have positive relations with algal growth. Light, temperature, and nutrients are the essential conditions for algal growth (Singh and Singh, 2015). Sunlight is the major driving force for photosynthesis. As a result, the geographic location, the seasonality, and the hour of the day, which affect incident sunlight, are all important factors to the eutrophication process in natural waters. The optimum PAR varies for different algal species (section 2.1.1). The relationship between absorbed light and algal photosynthetic rates is non-linear, excessive sunlight will cause photoinhibition or fluorescence quenching during the daytime (Grobbelaar, 2013), and measured biomass can increase at night due to recovery overnight (section 2.2.1) (Collos et al., 1989; Marra, 1992). Light levels and water turbidity in the water



determine the maximum depth at which algae can grow. Algal biomass and turbidity interact with each other. The increase of algal growth, especially the blue-green algae scums, increased the turbidity and reduced underwater light availability (section 2.1.1). Without algal scums, a better light condition in the water body is offered, which is good for the growth of non-buoyant algae (e.g., green algae and diatoms). In general, shallow lakes have better light availability (section 2.1.1, 2.2.3). However, wind-induced resuspension and resulting turbidity can easily reduce light transmission in shallow water (section 2.1.1, 2.2.3).

Chlorophyll-a changing rate ( $\Delta\text{Chl}_{a-f}\%$ ) is raised with increasing temperature up to a certain limit (Fig. 29a). The optimum temperature is widely variable for different algal species. Stratification can also happen in shallow lakes in summer under high air temperature (section 2.1.1, 2.2.1). In shallow lakes, water temperature and wind have strong influences on the vertical water quality distribution (section 2.2.1). Wind-induced resuspension can stimulate settled nutrients and trace metals (in the surface sediment) back to the water body (section 2.1.1, 2.1.2). Wind can promote the increase of algae by wind-induced mixing (section 2.1.3). For instance, it can increase  $\text{Chl}_{a-f}$  at the water bottom by bringing the benthic (diatoms and green algae) or dead algae to the upper layer to get better light conditions (section 2.1.1, 2.2.1) and push the water surface blue-green algae to the deep layer (section 2.1.1) (Qin et al., 2004b; Zhang et al., 2006).

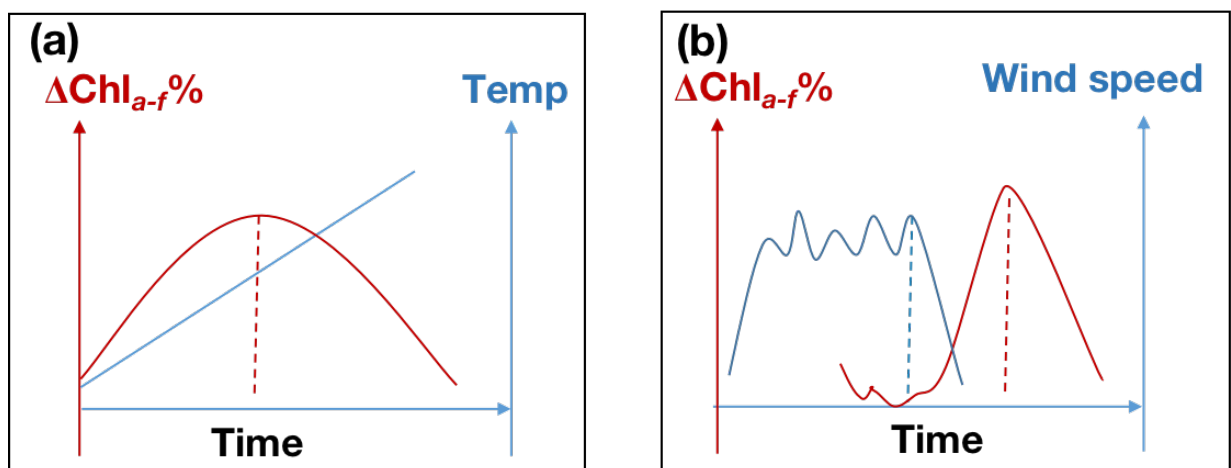


Figure 29 Variation curve of  $\text{Chl}_{a-f}$  changing rate and a) temperature, b) wind speed

Nitrogen and phosphorus seasonal dynamics are affected by seasonal pollution (agriculture), wind patterns, and algal dynamics. Wind can lead to resuspension as a nutrient source. Nutrients do not

have direct short-term and small-scale correlations with algal dynamics in eutrophic lakes (Zhang et al., 2018), therefore, they were not included in the algal simulation models (section 2.1.3). Nutrients are the essential elements for the algal growth, in turn, they will be taken up by algae (Ji, 2017). Therefore, from the result,  $Chl_{a-f}$  increased with the increase of nutrients (dissolved P,  $NO_3-N$  and  $NH_4-N$ ) in long-term scales (Fig.21d). Then, the growth of algae will decrease the concentration of nutrients (section 2.2.2). In general, once the nutrients are exceeded, the water temperature and wave is an indispensable factor for the growth of algal in freshwater (Sahoo and Seckbach, 2015) (section 2.1.3). The changes of those factors are responsible for the algal dynamic and become potential indicators for predicting algal blooms.

### 3.2 Algal species changes

In natural waters, some algal species bloom for a period of time and then give way to other species that are more compatible with changed conditions. Typically, the first algae to increase in early spring are frequently the diatoms (Fig. 30), followed by green algae, and then blue-green algae (Ji, 2017).

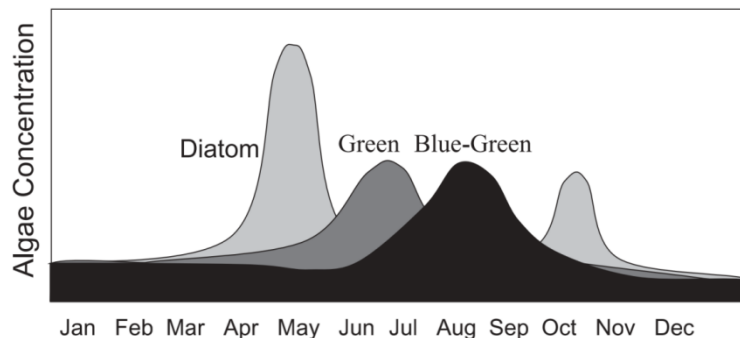


**Figure 30** Typical seasonal variations of algal concentration. Reprinted from Fig.5.1.2 in Ji (2017). © John Wiley and Sons & Wiley Books.

The algal species seasonal variation also follows this pattern in Lake Taihu. Blue-green algal biomass peak was found between June to September (section 2.1.1, 2.2.1) (M. Li et al., 2013; Q. Xu et al., 2008). It is examined that eukaryotic algal taxa (green algae and diatoms) will be actively growing when the water temperature is above 15°C. Blue-green algae can tolerate and grow under higher temperatures, from 0 °C to 26–35 °C (Paerl et al., 2014; Sahoo and Seckbach, 2015; Schmidt and Kannenberg, 1998). This is one of the reasons that blue-green algae dominate in summer.

In general, from the results, blue-green algae prefer calm and warm conditions and can tolerate high pH (section 2.1.1, 2.1.3, 2.2.3). Combined with observations, the blue-green algae blooms normally happen under calm and sunny days straight after days with strong windy, related to the well-mixed lake by strong winds (Fig.29b) (section 2.1.1). From Fig.31a, the relatively high concentration of  $Chl_{a-f}$ \_PhycoLA of blue-green algae all happened under high pH.

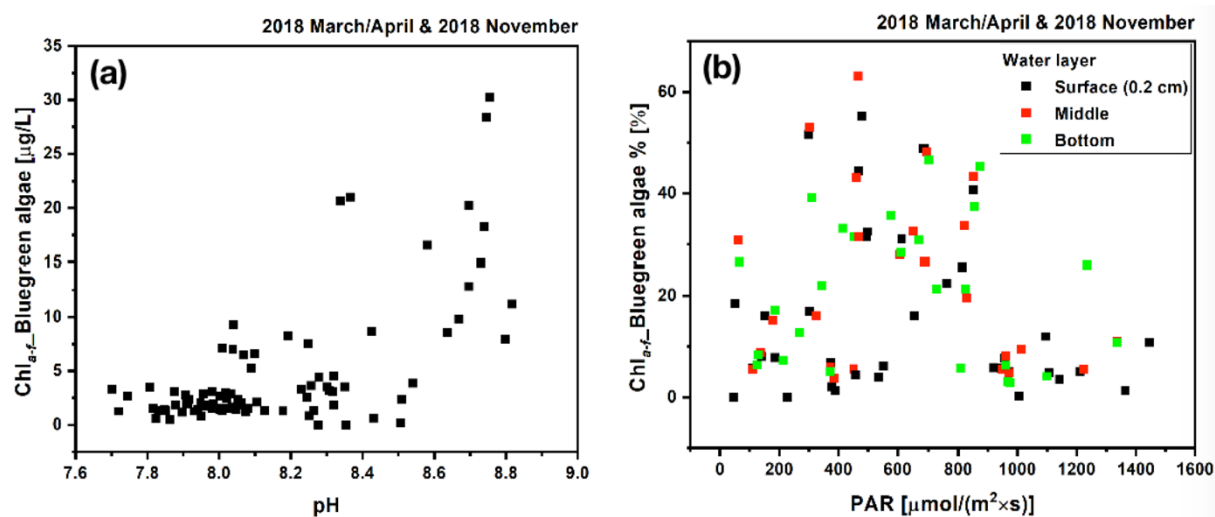


Figure 31 Correlation between a) pH and  $Chl_{a-f}$  of blue-green algae, b) PAR and ratio of  $Chl_{a-f}$  of blue-green algae

Similarly, in other studies, the blue-green algae bloom usually coincides with either high pH and/or low  $CO_2$  concentrations, and the photosynthetic rate of green algal decreased with pH from 7 to 10 (National Rivers Authority, 1990; van der Westhuizen and Eloff, 1983). The increase of algal biomass in late winter and spring will increase pH and Oxygen (section 2.1.1, 2.2.3). Therefore, in the long-term, the algae species change from diatoms/green algae dominated (spring) to blue-green algae dominated (summer) in the end. Although this general pattern is often observed, it can also have variations (USEPA, 2000b). In Lake Taihu, due to the water and meteorological condition difference, the blue-green algae dominated time might shift every year. Climate changes will also influence the algae species changes due to increased air temperature and alternated rainfall patterns (section: 2.1.3).

Blue-green algae are easier to survive under low-light conditions by floating at the water surface (Hajdu et al., 2007). As can be seen from Fig.31b, the days with over 40% of the  $Chl_{a-f}$  of blue-

green algae were under the PAR from 400 to 600  $\mu\text{mol}/(\text{m}^2\cdot\text{s})$  in 2018 March/April and 2018 November. Similar phenomena were not observed for other algal species in the same period.

From literature, light fluctuation affected the phytoplankton community structure and diversity (Singh and Singh, 2015). However, no accurate numbers have been reported yet. Because the algal growth is affected by many different factors and the optimum light intensity would be different under different water conditions (nutrients, temperature, etc.). Daily fluctuations of  $\Delta\text{Chl}_{a-f}\%$  (green algae and diatoms) were observed in both winter and summer (Fig.32).  $\Delta\text{Chl}_{a-f}\%$  decreased during the night and increased in the afternoon.

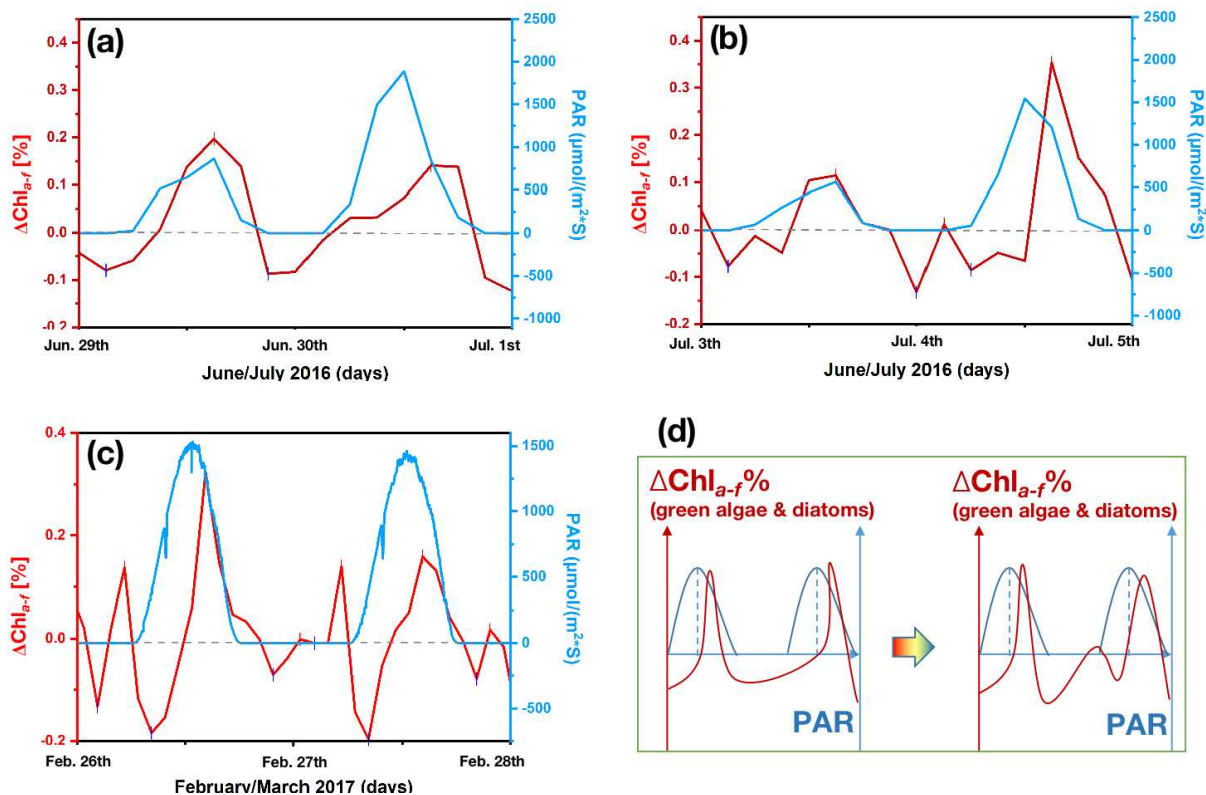


Figure 32 Diurnal changes of  $\Delta\text{Chl}_{a-f}\%$  and PAR in a) 2016 June/July; June 29<sup>th</sup> - July 1<sup>st</sup>, b) 2016 June/July; July 3<sup>th</sup>-5<sup>th</sup>, c) 2017 February/March; February 26<sup>th</sup> - 28<sup>th</sup>, d) summarized diurnal variation curve of  $\Delta\text{Chl}_{a-f}\%$  and PAR.

From the result, chlorophyll-a fluorescence changing rate ( $\Delta\text{Chl}_{a-f}\%$ ) of green algae and diatoms as well as phycocyanin fluorescence on the water surface layer (CyanoS) can be simulated and have the potential to be short-term predicted (2 - 3 days) by only using high-frequency multi-sensor data and weather forecast data (section: 2.1.3). In the simulation model (linear regression), waves

were the most important factor because the wind-induced mixing and resuspension easily happen in shallow Lake Taihu. The subdominant parameter is water temperature for  $\Delta\text{Chl}_{a-f}\%$  and cloud cover for CyanoS. The knowledge and model can be used in other shallow and eutrophic lakes as well.

### **3.3 Influence of algal dynamic, lake eutrophication and shallowness to the water quality and aquatic life**

As discussed above, eutrophication and lake shallowness create better conditions for algal growth (section 2.1.1, 2.1.3, 2.2). However, eutrophication, lake shallowness and algal dynamic will also influence the water quality and aquatic life (section: 2.1.1, 2.1.2).

Firstly, algal photosynthesis increases the pH and Oxygen saturation in the lake. Moreover, decomposition process of algal biomass consumes oxygen and easily leads to anaerobic conditions at the bottom, which will kill aquatic animals and reduce biodiversity (Ji, 2017; Sahoo and Seckbach, 2015) (section 2.1.1, 2.2.3). In addition, surface algal blooms block sunlight from reaching other organisms (Benayache et al., 2019; Heisler et al., 2008) (section 2.1.1).

Moreover, lake shallowness and eutrophication will aggravate the remobilization of trace metals. Wind-induced resuspension can easily lead to an increase of suspended metals in shallow lakes (section 2.1.2). In the eutrophic lakes, algal uptake has a great impact on the metal cycles and distributions (Duan et al., 2009). Sediment pollution in the down-wind location of blooms is found to be the worst (section 2.1.2). Moreover, the algal decomposition might lower Oxy-sat. and accelerate the release of metals from sediment (Atkinson et al., 2007; Zhu et al., 2013) (section 2.1.2).

In general, algal growth is harmful to the ecosystem by consuming the nutrients needed by other aquatic animals and plants, consuming the oxygen on the lake bottom, reducing the light availability, and accelerating the nutrients and trace metal vertical and spatial dynamics. The frequent resuspension caused by the lake shallowness increased turbidity as well as the concentration of nutrients and particulate trace metals.

## **4. Conclusions and outlook**

### **4.1 Conclusions**

Algal pollution has been plagued worldwide for decades. However, the algae are very dynamic under different conditions and can change very fast, making it difficult to monitor and predict. Therefore, in this study, an online weather station combined multi-sensor system was used to observe as much information as possible for the vertical water quality and meteorological changes accompanying the algal dynamics in a shallow and eutrophic lake (Lake Taihu, China). By integrating the real-time high-frequency data, leading factors for the algal growth as well as algal vertical and diurnal distribution patterns were found. In shallow and eutrophic lakes, wind-induced mixing/resuspension and water temperature are the most important factors for algal growth. Moreover, wind-induced resuspension is an internal pollution source of nutrients, as it stimulates the release of nutrients from sediment. Light is also an important factor for blue-green algae, which are able to buoyant to the water surface. Stratification can occur in Lake Taihu in summer and possibly in autumn. Algal growth shows diurnal changes and is mostly negative during night time, unless there is photoinhibition or fluorescence quenching during the daytime. In general, blue-green algal bloom normally appears quickly on warm, calm, and sunny days, especially after days with strong wind. Blue-green algae can tolerate extreme conditions, and after these rapidly become the dominant species. Therefore, strong winds can be an early warning factor for blue-green algal blooms.

Data-based algal simulation models and conceptual models were created to get a deep understanding of the algal dynamics and explore the potential of predicting short-term algal dynamics by only using multi-sensor data. Algal species seasonal changes and blue-green algae bloom mainly happened in late spring to summer because blue-green algae prefer warmer conditions than green algae and diatoms. Moreover, the rapid algal growth of green algae and diatoms in spring happens under sufficient nutrients, warmth, enough sunlight conditions, which increased pH and decreased CO<sub>2</sub>. These create suitable conditions for blue-green algae growth in summer. However, the warmer winter due to the climate changes leads to early blue-green algae bloom (late-spring) in recent years. Based on these results, preventive work can be done beforehand according to water and weather conditions. For example, arranging blue-green algae

salvage work beforehand and adjusting the water treatment procedure for drinking water plants. Meteorological parameters (wind-induced wave, water temperature, cloud cover) are the most important factors for short-term algal biomass changes. There is potential to predict algal growth 2-3 days in advance by using a high-frequency multi-sensor system and weather forecast data.

Moreover, in an aquatic system, the algal problem does not solely exist. Algal blooms reduce light availability and biomass decomposition leads to oxygen depletion, which is harmful to other aquatic animals. Moreover, the algal dynamics might also impact the dynamics of other compounds, for example, trace metals. In general, in shallow eutrophic lakes, the improvement of the eutrophic state can alleviate the metal pollution problem. Controlling excessive fertilization can reduce nutrient and also metal inputs due to fertilizer impurities. Blue-green algae salvaging and sediment dredging in down-wind areas might mitigate metal pollution by removing metals from aquatic systems. Warmer water temperature, higher irradiation and shallower water depths are the reason for the higher concentration of blue-green algae and turbidity in Lake Taihu compared with Lake Westensee.

## **4.2 Outlook**

### **4.2.1 Early-warning system for drinking water plants**

Fig. 33 presents the ideal prediction platform for drinking water plants. The BIOLIFT multi-sensor system can offer high-frequency water and meteorological data in each intake area. BIOLIFT data has proven to have the potential to predict the chlorophyll-a changing rate of diatoms and green algae and surface-layer blue-green algae (section 2.1.3). The data can be transferred to the control center of drinking water plants for further decision-making, either with respect to controlling the amount of water pumped from each intake area, or adapted/additional water treatment procedures.

After collecting long-term high-frequency data in different seasons, methods of machine learning can be used to create a short-term (2-3 days) algal prediction model based on *in situ* sensor data and weather forecast data.

A boat dragged BIOFISH can be applied to measure the spatial water quality between BIOLIFTS to overview the water quality status and changes in the whole lake. A 3D hydrodynamic lake model can then be established for simulating the water quality in the entire lake.

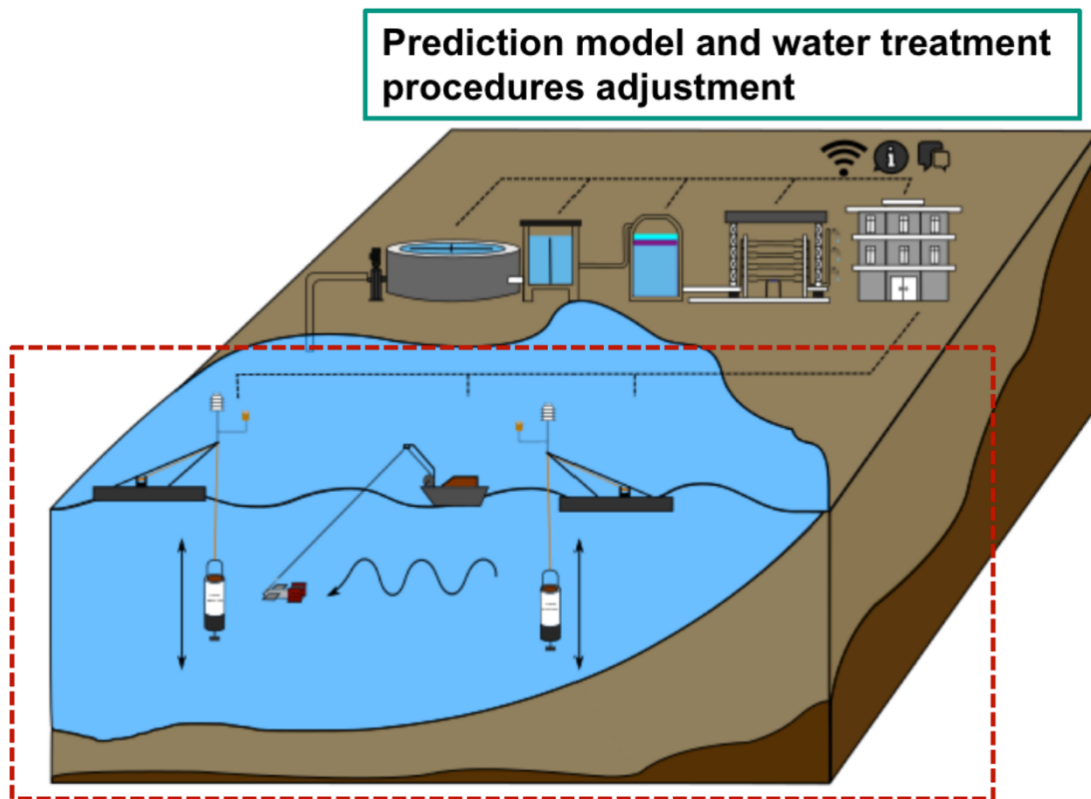


Figure 33 Structure diagram of algal early warning system for drinking water plants

#### 4.2.2 Transferred the knowledge and technology to other aquatic systems

Except for Lake Taihu, the BIOLIFT multi-sensor system has also been successfully applied in the deeper Lake Westensee (section 2.2.3). Similar sensor technologies and data processing methods can also be used in other aquatic systems for getting long-term high-frequency vertical profile data.

From the study, even lakes as shallow as Lake Taihu (mean: 1.9 m) can have stratification in the summer time. Therefore, vertical water quality profiling and water sampling at different water depths are necessary for all the lakes, as it helps to understand water quality dynamics in detail.

The knowledge about the water and algal dynamics (section 2.1.1, 2.1.2, 2.2.1, 2.2.2, 2.2.3) should also be suitable in other eutrophic lakes. The algal dynamic simulation and potential prediction model (section 2.1.3) can also be used in other lakes. However, selected parameters and equations of the models should be modified based on the different water quality and weather conditions.



## References

- Ahn, C.Y., Joung, S.H., Yoon, S.K., Oh, H.M., 2007. Alternative alert system for cyanobacterial bloom, using phycocyanin as a level determinant. *J. Microbiol.* 45, 98–104.
- Ansari, A.A., Gill, S.S., Lanza, G.R., Rast, W., 2010. *Eutrophication: Causes, Consequences and Control*. Springer Science & Business Media, Dordrecht. <https://doi.org/10.1007/978-90-481-9625-8>
- Atkinson, C.A., Jolley, D.F., Simpson, S.L., 2007. Effect of overlying water pH, dissolved oxygen, salinity and sediment disturbances on metal release and sequestration from metal contaminated marine sediments. *Chemosphere* 69, 1428–1437. <https://doi.org/10.1016/j.chemosphere.2007.04.068>
- Benayache, N.-Y., Nguyen-Quang, T., Hushchyna, K., McLellan, K., Afri-Mehennaoui, F.-Z., Bouaïcha, N., 2019. An Overview of Cyanobacteria Harmful Algal Bloom (CyanoHAB) Issues in Freshwater Ecosystems. *Limnol. New Asp. Inl. Water Ecol.* <https://doi.org/10.5772/intechopen.84155>
- Bennett, E.M., Carpenter, S.R., Caraco, N.F., 2001. Human impact on erodable phosphorus and eutrophication. *Bioscience* 51, 227–234.
- Berger, S.A., 2005. Environmental variable and plankton communities in the pelagic of lakes: enclosure experiment and comparative lake survey. Ludwig-Maximilians-Universität München.
- Bhagowati, B., Ahamad, K.U., 2019. A review on lake eutrophication dynamics and recent developments in lake modeling. *Ecohydrol. Hydrobiol.* 19, 155–166. <https://doi.org/10.1016/j.ecohyd.2018.03.002>
- Biota, 2017. Monitoring der Qualitätskomponente Makrophyten/Phytobenthos für WRRL und FFH-RL in schleswig-holsteinischen Seen 2017.
- Boyd, C.E., 2015. *Water Quality*. Springer, Auburn.
- Brookes, J.D., Ganf, G.G., 2001. Variations in the buoyancy response of *microcystis aeruginosa* to nitrogen, phosphorus and light. *J. Plankton Res.* 23, 1399–1411. <https://doi.org/10.1093/plankt/23.12.1399>

- Çamdevýren, H., Demýr, N., Kanik, A., Keskýn, S., 2005. Use of principal component scores in multiple linear regression models for prediction of Chlorophyll-a in reservoirs. *Ecol. Modell.* 181, 581–589. <https://doi.org/10.1016/j.ecolmodel.2004.06.043>
- Carlson, R.E., 1977. A trophic state index for lakes. *Limnol. Oceanogr.* 22, 361–369. <https://doi.org/10.4319/lo.1977.22.2.0361>
- Cavanaugh, J.E., 1997. Unifying the derivations for the Akaike and corrected Akaike information criteria. *Stat. Probab. Lett.* 33, 201–208. [https://doi.org/10.1016/s0167-7152\(96\)00128-9](https://doi.org/10.1016/s0167-7152(96)00128-9)
- Collos, Y., Maestrini, S.Y., Robert, J.M., 1989. Nocturnal synthesis and diurnal degradation of phytoplankton biomass in surface waters. *Mar. Biol.* 101, 457–462. <https://doi.org/10.1007/BF00541647>
- Cyr, H., 2016. Wind-driven thermocline movements affect the colonisation and growth of *Achnanthisidium minutissimum*, a ubiquitous benthic diatom in lakes. *Freshw. Biol.* 61, 1655–1670. <https://doi.org/10.1111/fwb.12806>
- Dai, L., 2014. Exploring China’s approach to implementing ‘eco-compensation’ schemes: the Lake Tai watershed as case study considered through a legal lens. *Water Int.* 39, 755–773. <https://doi.org/10.1080/02508060.2014.950860>
- Demmig-Adams, B., Garab, G., Adams Iii, W., 2014. *Non-Photochemical Quenching and Energy Dissipation in Plants, Algae and Cyanobacteria*. Springer Netherlands, Dordrecht. [https://doi.org/10.1007/978-94-017-9032-1\\_1](https://doi.org/10.1007/978-94-017-9032-1_1)
- Duan, H., Ma, R., Xu, X., Kong, F., Zhang, S., Kong, W., Hao, J., Shang, L., 2009. Two-Decade Reconstruction of Algal Blooms in China’s Lake Taihu. *Environ. Sci. Technol.* 43, 3522–3528. <https://doi.org/10.1021/es8031852>
- Environmental Protection Department of Jiangsu Province, 2016. Outline of the construction plan of environmental protection credit system in Jiangsu province (2016-2020).
- Glibert, P.M., 2016. Margalef revisited: A new phytoplankton mandala incorporating twelve dimensions, including nutritional physiology. *Harmful Algae* 55, 25–30. <https://doi.org/10.1016/j.hal.2016.01.008>
- Glibert, P.M., Berdalet, E., Burford, M.A., Pitcher, G.C., Zhou, M., 2006. Global Ecology and Oceanography of Harmful Algal Blooms, *Harmful Algal Blooms in Eutrophic Systems.*, in:

- Paris and Baltimore: Scientific Committee on Oceanic Research (SCOR) and Intergovernmental Oceanographic Commission (IOC), UNESCO. p. 74.
- Grobbelaar, J.U., 2013. Mass Production of Microalgae at Optimal Photosynthetic Rates, InTech. Rijeka. <https://doi.org/10.5772/55193>
- Guzel, H.O., 2019. Prediction of Freshwater Harmful Algal Blooms in Western Lake Erie Using Artificial Neural Network Modeling Techniques. North Dakota State University.
- Hajdu, S., Högländer, H., Larsson, U., 2007. Phytoplankton vertical distributions and composition in Baltic Sea cyanobacterial blooms. *Harmful Algae* 6, 189–205. <https://doi.org/10.1016/j.hal.2006.07.006>
- Heisler, J., P. Glibert, Burkholder, J., Anderson, D., Cochlan, W., Dennison, W., Gobler, C., Dortch, Q., Heil, C., Humphries, E., Lewitus, A., Magnien, R., H.Marshall, Sellner, K., Stockwell, D., Stoecker, D., Suddleson, M., 2008. Eutrophication and harmful algal blooms: A scientific consensus. *Harmful Algae* 8, 3–13. <https://doi.org/10.1016/j.hal.2008.08.006>
- Ho, L., Goethals, P., 2020. Research hotspots and current challenges of lakes and reservoirs: a bibliometric analysis. *Scientometrics*. <https://doi.org/10.1007/s11192-020-03453-1>
- Holbach, A., 2015. Water quality and pollutant dynamics in the Three Gorges Reservoir on the Yangtze River, China. Karlsruhe Institute of Technology.
- Hu, J., Liu, M., Zhou, W., Xu, C., Yang, X., Zhang, S., Wang, L., 2011. Correlations between water quality and land use pattern in Taihu Lake basin (Chinese). *Chinese J. Ecol.* 30, 1190–1197.
- Hunter, P.D., Tyler, A.N., Willby, N.J., Gilvear, D.J., 2008. The spatial dynamics of vertical migration by *Microcystis aeruginosa* in a eutrophic shallow lake: A case study using high spatial resolution time-series airborne remote sensing. *Limnol. Oceanogr.* 53, 2391–2406. <https://doi.org/10.4319/lo.2008.53.6.2391>
- Izmailova, A. V., Rummyantsev, V.A., 2016. Trophic status of the largest freshwater lakes in the world. *Lakes Reserv. Res. Manag.* 21, 20–30. <https://doi.org/10.1111/lre.12123>
- Izydorczyk, K., Tarczynska, M., Jurczak, T., Mrowczynski, J., Zalewski, M., 2005. Measurement of phycocyanin fluorescence as an online early warning system for cyanobacteria in reservoir intake water. *Environ. Toxicol.* 20, 425–430. <https://doi.org/10.1002/tox.20128>

- James, S.C., Janardhanam, V., Hanson, D.T., 2013. Simulating pH effects in an algal-growth hydrodynamics model. *J. Phycol.* 49, 608–615. <https://doi.org/10.1111/jpy.12071>
- Janssen, A.B.G., Teurlinx, S., An, S., Janse, J.H., Paerl, H.W., Mooij, W.M., 2014. Alternative stable states in large shallow lakes? *J. Great Lakes Res.* 40, 813–826. <https://doi.org/10.1016/j.jglr.2014.09.019>
- Ji, Z., 2017. *Hydrodynamics and water quality: modeling rivers, lakes, and estuaries*. John Wiley & Sons, Hoboken.
- Kimura, N., Wu, C.H., Hoopes, J.A., Tai, A., 2016. Diurnal dynamics in a small shallow lake under spatially nonuniform wind and weak stratification. *J. Hydraul. Eng.* 142, 1–21. [https://doi.org/10.1061/\(ASCE\)HY.1943-7900.0001190](https://doi.org/10.1061/(ASCE)HY.1943-7900.0001190)
- Klemas, V., 2012. Remote sensing of algal blooms: An overview with case studies. *J. Coast. Res.* 278, 34–43. <https://doi.org/10.2112/jcoastres-d-11-00051.1>
- Köster, S., 2019. *Urban Water Management for Future Cities*. Springer, Basel.
- Kowalczywska-Madura, K., Dondajewska, R., Gołdyn, R., Podsiadłowski, S., 2017. The influence of restoration measures on phosphorus internal loading from the sediments of a hypereutrophic lake. *Environ. Sci. Pollut. Res.* 24, 14417–14429. <https://doi.org/10.1007/s11356-017-8997-2>
- Kown, Y.S., Baek, S.H., Lim, Y.K., Pyo, J.C., Ligaray, M., Park, Y., Cho, K.H., 2018. Monitoring coastal chlorophyll-a concentrations in coastal areas using machine learning models. *Water (Switzerland)* 10, 1–17. <https://doi.org/10.3390/w10081020>
- Lamon, E.C., 1995. A regression model for the prediction of chlorophyll a in lake okeechobee, florida. *Lake Reserv. Manag.* 11, 283–290. <https://doi.org/10.1080/07438149509354209>
- LBP, 2015. *Planfeststellungsverfahren Ersatzneubau der alten Levensauer Hochbrücke und Ausbau des Nord-Ostsee-Kanals NOK-Km 93,2 – 94,2*.
- Lee, R.E., 2008. *Phycology*, 4th edn. ed. Cambridge University Press, London.
- Li, L., Li, Y., Biswas, D.K., Nian, Y., Jiang, G., 2008. Potential of constructed wetlands in treating the eutrophic water: Evidence from Taihu Lake of China. *Bioresour. Technol.* 99, 1656–1663. <https://doi.org/10.1016/j.biortech.2007.04.001>

- Li, M., Zhu, W., Gao, L., Huang, J., Li, N., 2013. Seasonal variations of morphospecies composition and colony size of microcystis in a shallow hypertrophic lake (Lake Taihu, China). *Fresenius Environ. Bull.* 22, 3474–3483.
- Li, Y., Acharya, K., Stone, M.C., Yu, Z., Young, M.H., Shafer, D.S., Zhu, J., Gray, K., Stone, A., Fan, L., Tang, C., Warwick, J., 2011. Spatiotemporal patterns in nutrient loads, nutrient concentrations, and algal biomass in Lake Taihu, China. *Lake Reserv. Manag.* 27, 298–309. <https://doi.org/10.1080/07438141.2011.610560>
- Li, Y., Guo, Y., Yu, G., 2013. An analysis of extreme flood events during the past 400 years at Taihu Lake, China. *J. Hydrol.* 500, 217–225. <https://doi.org/10.1016/j.jhydrol.2013.02.028>
- Lian, H., Qiuliang, L., Xinyu, Z., Haw, Y., Hongyuan, W., Limei, Z., Hongbin, L., Huang, J.-C., Tianzhi, R., Jiaogen, Z., Weiwen, Q., 2018. Effects of anthropogenic activities on long-term changes of nitrogen budget in a plain river network region: A case study in the Taihu Basin. *Sci. Total Environ.* 645, 1212–1220. <https://doi.org/10.1016/J.SCITOTENV.2018.06.354>
- LLUR, 2018. Untersuchungen des Phyto- und Zooplanktons schleswig-holsteinischer Seen 2017.
- Mao, J., Chen, Q., Chen, Y., 2008. Three-dimensional eutrophication model and application to Taihu Lake, China. *J. Environ. Sci.* 20, 278–284. [https://doi.org/https://doi.org/10.1016/S1001-0742\(08\)60044-3](https://doi.org/https://doi.org/10.1016/S1001-0742(08)60044-3)
- Margalef, R., Estrada, M., Blasco, D., 1979. Functional morphology of organisms involved in red tides, as adapted to decaying turbulence, in: Taylor DL, Seliger HH (Eds) *Toxic Dinoflagellate Blooms*. Elsevier, North Holland, pp. 89–94.
- Marra, J., 1992. Diurnal variability in chlorophyll fluorescence: observations and modeling. *Ocean Opt.* XI 1750, 233–244. <https://doi.org/10.1117/12.140654>
- MELUND SH, 2020. Westensee [WWW Document]. Schleswig-Holstein Minist. für energiewende, landwirtschaft, umwelt, natur und Digit.
- Miklasz, K.A., Denny, M.W., 2010. Diatom sinking speeds: Improved predictions and insight from a modified Stoke's law. *Limnol. Oceanogr.* 55, 2513–2525. <https://doi.org/10.4319/lo.2010.55.6.2513>

- Munn, M., Frey, J., Tesoriero, A., 2010. The influence of nutrients and physical habitat in regulating algal biomass in agricultural streams. *Environ. Manage.* 45, 603–615. <https://doi.org/10.1007/s00267-010-9435-0>
- National Bureau of Statistics of China, 2018. Annual Statistics of Jiangsu Province [WWW Document]. Natl. Bur. Stat. China. URL <http://data.stats.gov.cn/easyquery.htm?cn=C01>
- National Rivers Authority, 1990. Toxic Blue-green Algae. National Rivers Authority, England.
- Nazeer, M., Wong, M.S., Nichol, J.E., 2017. A new approach for the estimation of phytoplankton cell counts associated with algal blooms. *Sci. Total Environ.* 590–591, 125–138. <https://doi.org/10.1016/j.scitotenv.2017.02.182>
- Nissen, H., Krüger, F., Fichtner, A., Sommer, R.S., 2013. Local variability in the diet of daubenton's bat (*myotis daubentonii*) in a lake landscape of Northern Germany. *Folia Zool.* 62, 36–41. <https://doi.org/10.25225/fozo.v62.i1.a5.2013>
- O'Boyle, S., Wilkes, R., McDermott, G., Ní Longphuirt, S., Murray, C., 2015. Factors affecting the accumulation of phytoplankton biomass in Irish estuaries and nearshore coastal waters: A conceptual model. *Estuar. Coast. Shelf Sci.* 155, 75–88. <https://doi.org/10.1016/j.ecss.2015.01.007>
- Ogashawara, I., 2019. Advances and limitations of using satellites to monitor cyanobacterial harmful algal blooms. *Acta Limnol. Bras.* 31. <https://doi.org/10.1590/s2179-975x0619>
- Paerl, H.W., Xu, H., Hall, N.S., Zhu, G., Qin, B., Wu, Y., Rossignol, K.L., Dong, L., McCarthy, M.J., Joyner, A.R., 2014. Controlling cyanobacterial blooms in hypertrophic Lake Taihu, China: Will nitrogen reductions cause replacement of non-N<sub>2</sub> Fixing by N<sub>2</sub> fixing taxa? *PLoS One* 9. <https://doi.org/10.1371/journal.pone.0113123>
- Peperzak, L., Colijn, F., Koeman, R., Gieskes, W.W.C., Joordens, J.C.A., 2003. Phytoplankton sinking rates in the rhine region of freshwater influence. *J. Plankton Res.* 25, 365–383. <https://doi.org/10.1093/plankt/25.4.365>
- Prepas, E.E., Charette, T., 2003. Worldwide eutrophication of water bodies: causes, concerns, controls. *Treatise on Geochemistry* 9–9, 311–331. <https://doi.org/10.1016/B0-08-043751-6/09169-6>

- Principles, G., 2017. *Advances in Monitoring and Modelling Algal Blooms in Freshwater Reservoirs*, Springer. New York. <https://doi.org/10.1007/978-94-024-0933-8>
- Qin, B., 2008. *Lake Taihu, China: Dynamics and Environmental Change*. Springer Science & Business Media, Berlin.
- Qin, B., Hu, W., Gao, G., Luo, L., Zhang, J., 2004a. Dynamics of sediment resuspension and the conceptual schema of nutrient release in the large shallow Lake Taihu, China. *Chinese Sci. Bull.* 49, 54–64. <https://doi.org/10.1360/03wd0174>
- Qin, B., Hu, W., Gao, G., Luo, L., Zhang, J., 2004b. Dynamics of sediment resuspension and the conceptual schema of nutrient release in the large shallow Lake Taihu, China. *Chinese Sci. Bull.* 49, 54–64. <https://doi.org/10.1007/BF02901743>
- Qin, B., Liu, Z., Havens, K., 2007a. *Eutrophication of shallow lakes with special reference to Lake Taihu, China*. Springer Science & Business Media, Dordrecht.
- Qin, B., Paerl, H.W., Brookes, J.D., Liu, J., Jeppesen, E., Zhu, G., Zhang, Y., Xu, H., Shi, K., Deng, J., 2019. Why Lake Taihu continues to be plagued with cyanobacterial blooms through 10 years (2007–2017) efforts. *Sci. Bull.* 64, 354–356. <https://doi.org/10.1016/j.scib.2019.02.008>
- Qin, B., Xu, P., Wu, Q., Luo, L., Zhang, Y., 2007b. Environmental issues of Lake Taihu, China. *Hydrobiologia* 581, 2–14. <https://doi.org/10.1007/978-1-4020-6158-5>
- Qin, B., Yang, G., Ma, J., Wu, T., Li, W., Liu, L., Deng, J., Zhou, J., 2018. Spatiotemporal changes of cyanobacterial bloom in large shallow eutrophic lake Taihu, China. *Front. Microbiol.* 9, 1–13. <https://doi.org/10.3389/fmicb.2018.00451>
- Qin, B., Zhu, G., Gao, G., Zhang, Y., Li, W., Paerl, H.W., Carmichael, W.W., 2010. A drinking water crisis in Lake Taihu, China: Linkage to climatic variability and lake management. *Environ. Manage.* 45, 105–112. <https://doi.org/10.1007/s00267-009-9393-6>
- Reluy, F.V., Bécáres, J.M. de P., Hernández, R.D.Z., Díaz, J.S., 2004. Development of an equation to relate electrical conductivity to soil and water salinity in a Mediterranean agricultural environment. *Aust. J. Soil Res.* 42, 381–388. <https://doi.org/10.1071/SR03155>

- Sadovnik, M., Robin, V., Nadeau, M.J., Bork, H.R., Nelle, O., 2014. Neolithic human impact on landscapes related to megalithic structures: Palaeoecological evidence from the Krähenberg, northern Germany. *J. Archaeol. Sci.* 51, 164–173. <https://doi.org/10.1016/j.jas.2012.05.043>
- Sahoo, D., Seckbach, J., 2015. *The Algae World*. Springer, London. [https://doi.org/10.1007/978-94-017-7321-8\\_8](https://doi.org/10.1007/978-94-017-7321-8_8)
- Schaumburg, J., Schranz, C., Stelzer, D., Hofmann, G., 2006. Handlungsanweisung für die ökologische Bewertung von Seen zur Umsetzung der EU-Wasserrahmenrichtlinie: Makrophyten und Phytobenthos.
- Scheffer, M., Van Nes, E.H., 2007. Shallow lakes theory revisited: Various alternative regimes driven by climate, nutrients, depth and lake size. *Hydrobiologia* 584, 455–466. <https://doi.org/10.1007/s10750-007-0616-7>
- Schindler, D.W., Hecky, R.E., Findlay, D.L., Stainton, M.P., Parker, B.R., Paterson, M.J., Beaty, K.G., Lyng, M., Kasian, S.E.M., 2008. Eutrophication of lakes cannot be controlled by reducing nitrogen input: results of a 37-year whole-ecosystem experiment. *Proc. Natl. Acad. Sci.* 105, 11254–11258. <https://doi.org/https://doi.org/10.1073/pnas.0805108105>
- Schmidt, J.C., Kannenberg, J.R., 1998. *How to Identify and Control Water Weeds and Algae*. Applied Biochemists, New York.
- Selig, U., 2003. Particle size-related phosphate binding and P-release at the sediment-water interface in a shallow German lake. *Hydrobiologia* 492, 107–118.
- Singh, S.P., Singh, P., 2015. Effect of temperature and light on the growth of algae species: A review. *Renew. Sustain. Energy Rev.* 50, 431–444. <https://doi.org/10.1016/j.rser.2015.05.024>
- Smith, D.R., King, K.W., Williams, M.R., 2015. What is causing the harmful algal blooms in Lake Erie? *J. Soil Water Conserv.* 70, 27A-29A. <https://doi.org/10.2489/jswc.70.2.27A>
- Smith, V.H., Tilman, G.D., Nekola, J.C., 1998. Eutrophication: Impacts of excess nutrient inputs on freshwater, marine, and terrestrial ecosystems. *Environ. Pollut.* 100, 179–196. [https://doi.org/10.1016/S0269-7491\(99\)00091-3](https://doi.org/10.1016/S0269-7491(99)00091-3)
- Tao, Y., Zhang, Y., Meng, W., Hu, X., 2012. Characterization of heavy metals in water and sediments in Taihu Lake, China. *Environ. Monit. Assess.* 184, 4367–4382. <https://doi.org/10.1007/s10661-011-2270-9>



- Tian, W., Liao, Z., Zhang, J., 2017. An optimization of artificial neural network model for predicting chlorophyll dynamics. *Ecol. Modell.* 364, 42–52. <https://doi.org/10.1016/j.ecolmodel.2017.09.013>
- Umweltbericht des Landes Schleswig-Holstein zum Westensee, 2020. Westensee [WWW Document]. URL <http://www.umweltdaten.landsh.de/nuis/wafis/seen/seenanzeige.php?iseenr=0443&smodus=long> (accessed 5.22.20).
- van der Westhuizen, A.J., Eloff, J.N., 1983. Effect of Culture Age and pH of Culture Medium on the Growth and Toxicity of the Blue-green Alga *Microcystis aeruginosa*. *Zeitschrift für Pflanzenphysiologie* 110, 157–163. [https://doi.org/10.1016/s0044-328x\(83\)80162-7](https://doi.org/10.1016/s0044-328x(83)80162-7)
- Vinçon-Leite, B., Casenave, C., 2019. Modelling eutrophication in lake ecosystems: A review. *Sci. Total Environ.* 651, 2985–3001. <https://doi.org/10.1016/j.scitotenv.2018.09.320>
- Wang, H., Wang, H., 2009. Mitigation of lake eutrophication: Loosen nitrogen control and focus on phosphorus abatement. *Prog. Nat. Sci.* 19, 1445–1451. <https://doi.org/10.1016/j.pnsc.2009.03.009>
- Wang, J., Chen, X., Zhu, X. hua, Liu, J. ling, Chang, W.Y.B., 2001. Taihu Lake, lower Yangze drainage basin: Evolution, sedimentation rate the sea level. *Geomorphology* 41, 183–193. [https://doi.org/10.1016/S0169-555X\(01\)00115-5](https://doi.org/10.1016/S0169-555X(01)00115-5)
- Wang, L., Cai, Y., Fang, L., 2009. Pollution in Taihu Lake China: Causal chain and policy options analyses. *Front. Earth Sci. China* 3, 437–444. <https://doi.org/10.1007/s11707-009-0043-3>
- Wang, S., Li, J., Zhang, B., Spyrakos, E., Tyler, A.N., Shen, Q., Zhang, F., Kuster, T., Lehmann, M.K., Wu, Y., Peng, D., 2018. Trophic state assessment of global inland waters using a MODIS-derived Forel-Ule index. *Remote Sens. Environ.* 217, 444–460. <https://doi.org/10.1016/j.rse.2018.08.026>
- Wang, Y., Xie, Z., Lou, I., Ung, W., Mok, K., 2017. Algal bloom prediction by support vector machine and relevance vector machine with genetic algorithm optimization in freshwater reservoirs Yanjie. *Eng. Comput.* 34, 664–679.
- Wang, Yu, Zhao, X., Wang, L., Wang, Yujun, Li, W., Wang, S., Xing, G., 2015. The regime and P availability of omitting P fertilizer application for rice in rice/wheat rotation in the Taihu

- Lake region of southern China. *J. Soils Sediments* 15, 844–853. <https://doi.org/10.1007/s11368-014-1047-5>
- Ward, J.J.H., 1963. Hierarchical grouping to optimize an objective function. *J. Am. Stat. Assoc.* 58, 236–244. <https://doi.org/10.1198/016214503000000468>
- Weihrauch, C., Opp, C., 2018. Ecologically relevant phosphorus pools in soils and their dynamics: The story so far. *Geoderma* 325, 183–194. <https://doi.org/10.1016/j.geoderma.2018.02.047>
- Werner, P., Dreßler, M., 2007. Assessment of the ecological status of eight lakes from northern Germany according to the Water Framework Directive (WFD) using benthic diatoms: problems and achievements of the newest German WFD guideline, in: 1st Central European Diatom Meeting. pp. 173–178. <https://doi.org/10.3372/cediatom.136>
- Wetzel, R.G., 2001. The Phosphorus Cycle, in: *Limnology: Lake and River Ecosystems*. Elsevier Science, Amsterdam, pp. 239–288. <https://doi.org/10.1016/B978-0-08-057439-4.50017-4>
- Wilhelm, S.W., Farnsley, S.E., LeClerc, G.R., Layton, A.C., Satchwell, M.F., DeBruyn, J.M., Boyer, G.L., Zhu, G., Paerl, H.W., 2011. The relationships between nutrients, cyanobacterial toxins and the microbial community in Taihu (Lake Tai), China. *Harmful Algae* 10, 207–215. <https://doi.org/10.1016/j.hal.2010.10.001>
- Wurtsbaugh, W.A., Paerl, H.W., Dodds, W.K., 2019. Nutrients, eutrophication and harmful algal blooms along the freshwater to marine continuum. *Wiley Interdiscip. Rev. Water* 6, 1–27. <https://doi.org/10.1002/wat2.1373>
- Xu, H., Liu, Z., Jiao, J., Yang, L., 2008. Nitrogen pollution status of various types of passing-by water bodies in upper reaches of Taihu Lake (in Chinese). *Chinese J. Ecol.* 27, 43–49.
- Xu, H., Yang, L., Zhao, G., Jiao, J., Yin, S., Liu, Z., 2009. Anthropogenic impact on surface water quality in Taihu Lake region, China. *Pedosphere* 19, 765–778. [https://doi.org/10.1016/S1002-0160\(09\)60172-7](https://doi.org/10.1016/S1002-0160(09)60172-7)
- Xu, J., Zhang, Y., Zhou, C., Guo, C., Wang, D., Du, P., Luo, Y., Wan, J., Meng, W., 2014. Distribution, sources and composition of antibiotics in sediment, overlying water and pore water from Taihu Lake, China. *Sci. Total Environ.* 497–498, 267–273. <https://doi.org/10.1016/j.scitotenv.2014.07.114>

- Xu, Q., Chen, W., Gao, G., 2008. Seasonal variations in microcystin concentrations in Lake Taihu, China. *Environ. Monit. Assess.* 145, 75–79. <https://doi.org/10.1007/s10661-007-0016-5>
- Xu, Y., Wu, Y., Han, J., Li, P., 2017. The current status of heavy metal in lake sediments from China: Pollution and ecological risk assessment. *Ecol. Evol.* 7, 5454–5466. <https://doi.org/10.1002/ece3.3124>
- Yang, J., Holbach, A., Stewardson, M.J., Wilhelms, A., Qin, Y., Zheng, B., Zou, H., Qin, B., Zhu, G., Moldaenke, C., Norra, S., 2021. Simulating chlorophyll-a fluorescence changing rate and phycocyanin fluorescence by using a multi-sensor system in Lake Taihu, China. *Chemosphere* 264, 128482. <https://doi.org/10.1016/j.chemosphere.2020.128482>
- Yang, J., Holbach, A., Wilhelms, A., Krieg, J., Qin, Y., Zheng, B., Zou, H., Qin, B., Zhu, G., Wu, T., Norra, S., 2020. Identifying spatio-temporal dynamics of trace metals in shallow eutrophic lakes on the basis of a case study in Lake Taihu, China. *Environ. Pollut.* 264, 114802. <https://doi.org/10.1016/j.envpol.2020.114802>
- Yang, J., Holbach, A., Wilhelms, A., Qin, Y., Zheng, B., Zou, H., Qin, B., Zhu, G., Norra, S., 2019. Highly time-resolved analysis of seasonal water dynamics and algal kinetics based on in-situ multi-sensor-system monitoring data in Lake Taihu, China. *Sci. Total Environ.* 660, 329–339. <https://doi.org/10.1016/j.scitotenv.2019.01.044>
- Yang, S.Q., Liu, P.W., 2010. Strategy of water pollution prevention in Taihu Lake and its effects analysis. *J. Great Lakes Res.* 36, 150–158. <https://doi.org/10.1016/j.jglr.2009.12.010>
- Yang, Y., Wang, Y., Zhang, Z., Wang, W., Ren, X., Gao, Y., Liu, S., Lee, X., 2018. Diurnal and Seasonal Variations of Thermal Stratification and Vertical Mixing in a Shallow Fresh Water Lake. *J. Meteorol. Res.* 32, 219–232. <https://doi.org/10.1007/s13351-018-7099-5>
- Ye, C., Li, C.H., Yu, H.C., Song, X.F., Zou, G.Y., Liu, J., 2011. Study on ecological restoration in near-shore zone of a eutrophic lake, Wuli Bay, Taihu Lake. *Ecol. Eng.* 37, 1434–1437. <https://doi.org/10.1016/j.ecoleng.2011.03.028>
- Yi, H.S., Lee, B., Park, S., Kwak, K.C., An, K.G., 2019. Prediction of short-term algal bloom using the M5P model-tree and extreme learning machine. *Environ. Eng. Res.* 24, 404–411. <https://doi.org/10.4491/EER.2018.245>

- Yu, Y., Yang, L., Hou, P., Xue, L., Odindo, A.O., 2018. Nitrogen Management in the Rice-wheat System of China and South Asia, in: Sustainable Agriculture Reviews 32. Springer, Cham, Basel, pp. 135–167. <https://doi.org/10.1007/978-94-007-5961-9>
- Zhang, H., Shi, Y., Xu, Z., Ni, G., Li, J., 2019. The Health Status Report of Taihu Lake in 2018 [WWW Document]. Taihu Basin Auth. Minist. Water Resour. URL <http://www.tba.gov.cn//tba/content/TBA/lygb/thjkzkgb/0000000000013895.html> (accessed 9.11.17).
- Zhang, H.C., Cao, Z.H., Shen, Q.R., Wong, M.H., 2003. Effect of phosphate fertilizer application on phosphorus (P) losses from paddy soils in Taihu Lake Region: I. Effect of phosphate fertilizer rate on P losses from paddy soil. *Chemosphere* 50, 695–701. [https://doi.org/10.1016/S0045-6535\(02\)00207-2](https://doi.org/10.1016/S0045-6535(02)00207-2)
- Zhang, Limin, Xia, M., Zhang, Lei, Wang, C., Lu, J., 2008. Eutrophication status and control strategy of Taihu Lake. *Front. Environ. Sci. Eng. China* 2, 280–290. <https://doi.org/10.1007/s11783-008-0062-4>
- Zhang, M., Shi, X., Yang, Z., Yu, Y., Shi, L., Qin, B., 2018. Long-term dynamics and drivers of phytoplankton biomass in eutrophic Lake Taihu. *Sci. Total Environ.* 645, 876–886. <https://doi.org/10.1016/J.SCITOTENV.2018.07.220>
- Zhang, Y., Qin, B., Zhu, G., Gao, G., Luo, L., Chen, W., 2006. Effect of sediment resuspension on underwater light field in shallow lakes in the middle and lower reaches of the Yangtze River: A case study in Longgan Lake and Taihu Lake. *Sci. China, Ser. D Earth Sci.* 49, 114–125. <https://doi.org/10.1007/s11430-006-8111-y>
- Zhao, H., You, B., Duan, X., Becky, S., Jiang, X., 2013. Industrial and agricultural effects on water environment and its optimization in heavily polluted area in Taihu Lake Basin, China. *Chinese Geogr. Sci.* 23, 203–215. <https://doi.org/10.1007/s11769-013-0593-x>
- Zhao, X., 2013. Satellite data application for the assessment of water balance in the Taihu watershed, China. *J. Appl. Remote Sens.* 7, 073482. <https://doi.org/10.1117/1.jrs.7.073482>
- Zhao, X., Min, J., Wang, S., Shi, W., Xing, G., 2011. Further understanding of nitrous oxide emission from paddy fields under rice / wheat rotation in south China. *J. Geophys. Res.* 116, 1–7. <https://doi.org/10.1029/2010JG001528>

- Zhao, X., Zhou, Y., Min, J., Wang, S., Shi, W., Xing, G., 2012. Nitrogen runoff dominates water nitrogen pollution from rice-wheat rotation in the Taihu Lake region of China. *Agric. Ecosyst. Environ.* 156, 1–11. <https://doi.org/10.1016/j.agee.2012.04.024>
- Zhu, M., Zhu, G., Nurminen, L., Wu, T., Deng, J., Zhang, Y., Qin, B., Ventelä, A.M., 2015. The influence of macrophytes on sediment resuspension and the effect of associated nutrients in a shallow and Large Lake (Lake Taihu, China). *PLoS One* 10, 1–20. <https://doi.org/10.1371/journal.pone.0127915>
- Zhu, M., Zhu, G., Zhao, L., Yao, X., Zhang, Y., Gao, G., Qin, B., 2013. Influence of algal bloom degradation on nutrient release at the sediment-water interface in Lake Taihu, China. *Environ. Sci. Pollut. Res.* 20, 1803–1811. <https://doi.org/10.1007/s11356-012-1084-9>

## **Appendix A-List of publications during my Ph.D. study as first author**

**Jingwei Yang**, Andreas Holbach, Andre Wilhelms, Yanwen Qin, Binghui Zheng, Hua Zou, Boqiang Qin, Guangwei Zhu, and Stefan Norra. "Highly time-resolved analysis of seasonal water dynamics and algal kinetics based on in-situ multi-sensor-system monitoring data in Lake Taihu, China." *Science of The Total Environment* 660 (2019): 329-339.

**Jingwei Yang**, Andreas Holbach, Andre Wilhelms, Julia Krieg, Yanwen Qin, Binghui Zheng, Hua Zou, Boqiang Qin, Guangwei Zhu, and Stefan Norra. "Identifying spatio-temporal dynamics of trace metals in shallow eutrophic lakes on the basis of a case study in Lake Taihu, China." *Environmental Pollution* (2020): 114802.

**Jingwei Yang**, Andreas Holbach, Michael J. Stewardson, Andre Wilhelms, Yanwen Qin, Binghui Zheng, Hua Zou, Boqiang Qin, Guangwei Zhu, Christian Moldaenke, StefanNorra. "Simulating chlorophyll-a fluorescence changing rate and phycocyanin fluorescence by using a multi-sensor system in Lake Taihu, China." *Chemosphere* (2020): 128482.

## **Appendix B-Full articles of scientific publications as first author**

Appendix B.1 Highly time-resolved analysis of seasonal water dynamics and algal kinetics based on in-situ multi-sensor-system monitoring data in Lake Taihu, China



ELSEVIER

Contents lists available at ScienceDirect

Science of the Total Environment

journal homepage: [www.elsevier.com/locate/scitotenv](http://www.elsevier.com/locate/scitotenv)



## Highly time-resolved analysis of seasonal water dynamics and algal kinetics based on in-situ multi-sensor-system monitoring data in Lake Taihu, China



Jingwei Yang<sup>a,\*</sup>, Andreas Holbach<sup>a</sup>, Andre Wilhelms<sup>a</sup>, Yanwen Qin<sup>b</sup>, Binghui Zheng<sup>b</sup>, Hua Zou<sup>c</sup>, Boqiang Qin<sup>d</sup>, Guangwei Zhu<sup>d</sup>, Stefan Norra<sup>a</sup>

<sup>a</sup> Institute of Applied Geosciences, Working Group Environmental Mineralogy and Environmental System Analysis (ENMINSA) Karlsruhe Institute of Technology, Kaiserstraße 12, 76131 Karlsruhe, Germany

<sup>b</sup> Chinese Research Academy of Environmental Sciences, Dayangfang 8, Anwai Beiyuan, Beijing 100012, PR China

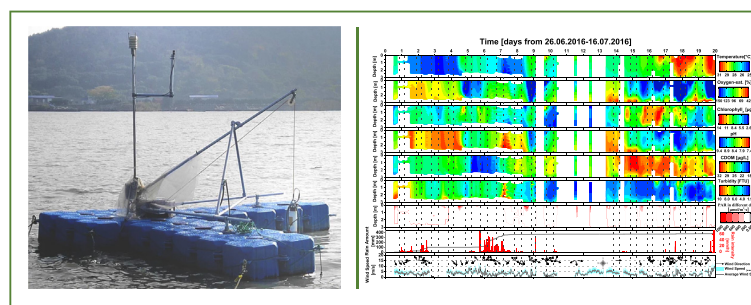
<sup>c</sup> School of Environmental and Civil Engineering, Jiangnan University, Wuxi 214122, PR China

<sup>d</sup> Nanjing Institute of Geography & Limnology, Chinese Academy of Sciences, 73 East Beijing Road, 210008 Nanjing, PR China

### HIGHLIGHTS

- Algae can rapidly proliferate and horizontally/vertically migrate.
- High-resolution sensor system measured the water quality in the whole water column.
- Every parameter get from sensor exhibited seasonality and vertical gradients.
- Correlations were found between algae dynamics and some environmental factors.

### GRAPHICAL ABSTRACT



### ARTICLE INFO

#### Article history:

Received 31 October 2018  
Received in revised form 4 January 2019  
Accepted 5 January 2019  
Available online 06 January 2019

Dr. Henner Hollert

#### Keywords:

Algal bloom  
Stratification  
Lake dynamics  
Eutrophication  
On-line monitoring  
Resuspension events

### ABSTRACT

Predicting algal blooms is challenging due to rapid growth rates under suitable conditions and the complex physical, chemical, and biological processes involved. Physico-chemical parameters, monitored in this study by a high-resolution in-situ multi-sensor system and derived from lab-based water sample analyses, show the seasonal variation and have different degrees of vertical gradients across the water column. Through analyzing the changes and relations between multi-factors, we reveal pictures of water quality dynamics and algal kinetics. Nitrate has regular seasonal changes different to the seasonal patterns of total dissolved Phosphorus. Positive correlations are found between Chlorophyll *a* fluorescence and temperature, wind-induced resuspension and mixing promote the augment of Cyanobacteria fluorescence (Phycocyanin) signal. While the resuspension can also result in the increase of turbidity and affect the light environment for hydrophytes, the algal scums are the main reason for the high turbidity on the surface, which lower the illumination radiation in the water body. Those parameters are the primary dominants responsible for the change of algae from our monitoring data, which could be used as indicators for the dynamic changes of algae in the future.

© 2019 Elsevier B.V. All rights reserved.

\* Corresponding author.

E-mail address: [jingwei.yang@kit.edu](mailto:jingwei.yang@kit.edu) (J. Yang).



## 1. Introduction

Since the massive Cyanobacteria dominated algal bloom, which occurred in early June 2007 and was a reason to shut down drinking water plants, the water quality of Lake Taihu has aroused extraordinary concerns from all stakeholders, including government, researchers, and the public (Guo, 2007). Since some measures have been done for pollution control and treatment over the last decades, the water qualification rate (based on China's environmental quality standards for surface water) of Lake Taihu itself and its tributaries generally improved in recent five years (Zhang et al., 2017). Nevertheless, it still has not met expectations, and the algal biomass moderate increase despite the decrease of the nutrient level. The influence of climate-related variables, like the temperature, wind and light, cannot afford to neglect (Zhang et al., 2018). An algal bloom started again in mid-March 2017, which is more than ten days earlier than the year before. Moreover, in the first quarter of 2017, the density of algae in Lake Taihu increased by 38.7% compared to the same period of 2016 (Ma, 2017). This is attributed to warmer weather conditions in spring 2017 (Deng et al., 2014) and elevated nutrient input by massive monsoon rain events in 2016 (Zhang et al., 2017).

Some types of cyanobacteria, also called blue-green algae, can use their cells to form oxygen-filled cavities, which help them to move vertically through the water column to access optimal levels of light and nutrients (Fogg and Walsby, 1971). Dominant algal species can differ among regions and seasons because of their different optimum growth conditions relative to water quality, meteorological, hydrological and hydrodynamic conditions (Ji, 2017). Consequently, the timing of an algae bloom outbreak, as well as its intensity, duration and the dominating algae species vary from year to year that makes it hard to predict or control.

When algae, and in particular cyanobacteria, accumulate at the water surface, typical visible 'algal scums' appear (Paerl and Ustach, 1982). Remote sensing applications by using multi-spectral satellite imagery can be used to estimate accumulation of phytoplankton at the water surface for a whole water body (Allee and Johnson, 1999), but algae may also be present in the deeper water layers. New research is needed to better understand why and when algae accumulate in large numbers in specific depths. Either algae are very fast growing due to suitable environmental conditions or they spatially migrate through vertical buoyancy or horizontal shift.

In this challenging environmental context, the "Sino-German Network" (SIGN) formed to investigate the water cycle of Lake Taihu from the source to the tap (Schmidt et al., 2016). Therein, the sub-project "Dynamics of Water Quality" (DYNAQUA) aims at developing the new in situ and on-line monitoring platform "BIOLIFT" to record depth- and time-resolved water quality profiles (nine physicochemical parameters) directly combined with meteorological data and corresponding frequent water samples. Such datasets provide highly time-resolved insights into lake processes that are related to dynamic conditions in the vertical structure of the water column of Lake Taihu.

This study evaluates data from four monitoring and sampling campaigns at Lake Taihu, one from 26th June to 16th July 2016, referred to as "2016-Summer"; one from 23rd February to 07th March 2017, referred to as "2017-Winter"; one from 13rd to 24th September 2017, referred to as "2017-Autumn"; one from 19th March to 16th April 2018, referred to as "2018-Spring".

## 2. Materials and methods

### 2.1. Study area

Lake Taihu is a shallow lake with the mean water level of 3.0 m above sea level and located in the Yangtze River delta in southeastern China. The Lake Taihu region belongs to the administrative divisions of Jiangsu and Zhejiang. The study was conducted at the end of a jetty with a length of about 250 m (N 31.418903, E 120.213293), which is located in outer Meiliang Bay of northern Lake Taihu and belongs to the

Taihu Laboratory for Lake Ecosystem Research (TLER) of the Nanjing Institute of Geography and Limnology (NIGLAS). In Lake Taihu region, the yearly heavy rainfall period is related to the East-Asian summer monsoon climate from June to July. The study area and operation location are shown in Fig. 1.

### 2.2. Method for water quality monitoring

#### 2.2.1. Physicochemical parameters measured by BIOLIFT

Physicochemical parameters of the lake water were continuously measured by the newly developed multi-sensor-system 'BIOLIFT' (ADM Elektronik Germany; ENMINSA) during the profiling process at the jetty of TLLER. These parameters include Electrical Conductivity at 25 °C ( $EC_{25}$ ) [ $\mu\text{S}/\text{cm}$ ], Temperature (Temp) [ $^{\circ}\text{C}$ ], pH-value, Oxygen Saturation (Oxy-sat) [%], Turbidity (Turb) [FTU = Formazin Turbidity Unit], Colored Dissolved Organic Matter (CDOM) [ppbQS (Quinine Sulfate)], Chlorophyll *a* Fluorescence ( $Chl_{a-f}$ ) [ $\mu\text{g}/\text{L}$ ], Cyanobacteria Fluorescence ( $Cyano_{FC}$ ) [ $\mu\text{g}/\text{L}$  (Phycocyanin pigment)], Pressure [dBar] (for depth information [m]). Also, Photosynthetically Active Radiation ca. 2 m above water (PAR) and in the water in different depths ( $PAR_{\text{water}}$ ) for getting information about depths of light penetration into the water body (sensor details are in supporting information Table A.1).

CDOM fluorescence is an indicator of dissolved humic substances, which are produced by the decay of organic matter, excretion from living organisms, or introduced from exogenous sources of dissolved organic matter (Kalbitz and Geyer, 2001; Peuravuori et al., 2002; Rochelle-Newall and Fisher, 2002a). The organic matter, respective biomass, produced by photosynthesis does not have fluorescent responses (Rochelle-Newall and Fisher, 2002b).  $Chl_{a-f}$  is a sensitive and rapid parameter to determine Chlorophyll *a* concentrations ( $Chl_a$ ) and dynamics in water. The  $Chl_{a-f}$  installed on the continuous water column profiling BIOLIFT, allows collecting high-frequency  $Chl_a$  data of the spectral group of green, red and mixed (except for blue group, i.e. Cyanobacteria) (Beutler, 2003). Since  $Chl_{a-f}$  cannot accurately determine the cyanobacteria and its dynamics, we add another sensor to detect and quantify phycocyanin concentration, which is the marker pigment of Cyanobacteria (Asai et al., 2001).

#### 2.2.2. Weather station

In addition to the measurement of physicochemical water parameters, a weather station (Vaisala Weather Transmitter WXT520) was installed at around 5 m above the water surface on the jetty and the application integrated on BIOLIFT. The measured parameters included wind direction [ $^{\circ}$ ], wind speed [m/s], precipitation [mm], and were recorded as average values for every 10 min interval (parameter details are in supporting information Table A.2).

#### 2.2.3. The monitoring process of BIOLIFT system

In "2016-Summer", the BIOLIFT was set to record continuously vertical profiles from the water surface to just above the lake bottom in 30 cm per steps. At each depth, it remained for 10 min. From "2017-Winter", the monitoring setup was slightly adapted. Every 10 min, the sensor probe was lowered in the water column ( $EC_{25}$  is the detector). And then it remained at the water surface (ca. 0.1 m) for 10 s to allow stable sensor readings. Subsequently, it slowly moved down to just above the lake bottom, stayed there for 15 s and then slowly moved up again to just above the water surface. The improved system could get a larger range of data for every parameter in short time for the whole water column, and the higher frequency of monitoring data improves accuracy when calculating the average value across a depth-time matrix. Calibration of every sensor in the BIOLIFT was conducted before field monitoring.

### 2.3. Method for water samples collection and treatment

Water samples were taken once every day at three depths (water bottom, intermediate, surface) in "2016-Summer", "2017-Autumn" and

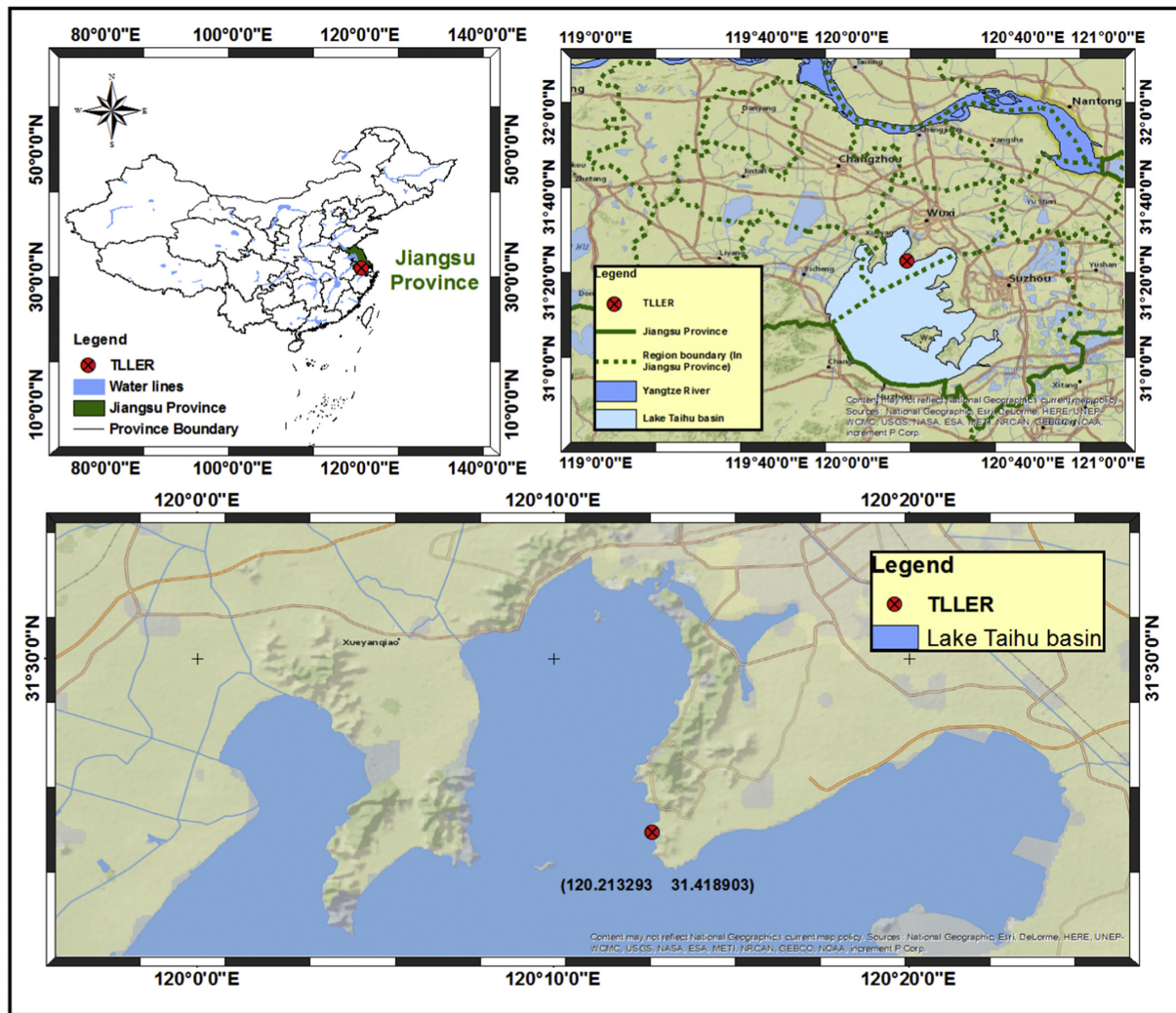


Fig. 1. Outline of the Lake Taihu, its location within China, and our sampling location in outer Meiliang bay.

“2018-Spring”, and two depths in “2017-Winter”, during the continuous profiling measurement periods.

All samples were filtered through cellulose-acetate filters (Sartorius) with a porosity of 0.45  $\mu\text{m}$  to separate suspended particulate matter and the dissolved phase. Two dissolved water samples per depth were bottled in 20 mL polyethylene vials and stored in a fridge at about 4  $^{\circ}\text{C}$ . One aliquot of the dissolved water samples were stabilized with 50  $\mu\text{L}$  of concentrated (65%) double distilled nitric acid ( $\text{HNO}_3$ ) to prevent precipitation of metals. This sample was used for Inductively Coupled Plasma Mass Spectrometry (ICP-MS) analyses to detect major, minor, and trace elements. The other aliquot was treated with 50  $\mu\text{L}$  of 1 g/L pure sodium azide solution ( $\text{NaN}_3$ ) to prevent biological activity in the sample. This sample was used for Ion Chromatography (IC) to detect the major anions.

#### 2.4. Data processing and analysis

##### 2.4.1. Vertical-temporal statistical data evaluation

For the evaluation of the measured physicochemical parameters ( $i$ ) from BIOLIFT (except PAR above water), an algorithm was written in the software MATLAB R2018a, which transfers the punctiform

measured values to a matrix (0.1 m \* 3 h) by calculating the average in the coordinates depth and time. Then, the depth profile time series could be plotted visually using the OriginPro software (Origin Professional 2016), in conjunction with the ten minute recorded meteorological data from the integrated Vaisala monitoring station (supporting information Figs. E.1–4).

##### 2.4.2. Daily vertical gradients of parameters

All physicochemical parameters ( $i$ ) are normalized by min-max normalization technique before using them for vertical gradients calculation and seasonal comparison, the data after normalization and at a depth of  $d$  named  $i_{\text{norm}(d)}$ . The daily vertical gradients of every parameter ( $\delta_i$ ) were calculated using Eq. (1) (Holbach et al., 2015) for every 0.5 m.

$$\delta_i = \frac{i_{\text{norm}(d)}}{i_{\text{norm}(d-0.5\text{m})}} \quad (1)$$

##### 2.4.3. Rainfall rate

Rainfall rate ( $\text{Rainfall}_{\text{rate}}$ ) here calculated by the rainfall hours ( $\text{Rainfall}_{\text{hours}}$ ) divided measuring hours ( $\text{Measuring}_{\text{hours}}$ ) in each

campaign, it is important to describe the proportion of rainfall time in each campaign since the total measuring time is different. The equation is as follows.

$$\text{Rainfall}_{\text{rate}} = \frac{\text{Rainfall}_{\text{hours}}}{\text{Measuring}_{\text{hours}}} \quad (2)$$

### 3. Results

#### 3.1. Basic sampling information and meteorological data of four field trips under different seasonal conditions

As can be seen from the table below, more rainfall events happened (Rainfall<sub>rate</sub>, 20.3%) during our monitoring period “2016-Summer”, and the rain accumulation in our measuring time (375 h) reached to 382.76 mm. The least Rainfall<sub>rate</sub> (0.1%) were recorded in “2017-Winter”. Followed by scenarios of “2018-Spring” and “2017-Autumn”, the Rainfall<sub>rate</sub> were 2.6% and 4.1%. We compared the wind characteristics during the monitoring periods in the different seasons. Some data gaps due to technical issues are present (Fig. 2). In “2017-Autumn” there were mainly northerly, northeasterly, and easterly winds. The other three periods were all dominated by easterly and southeasterly winds. The wind speed in “2018-Spring” was faster than the others, with an average wind speed of 4.2 m/s (ca. 0.8 m/s faster) and >4 m/s wind speed appeared during 38.2% of monitoring time. Even though in the three other scenarios the average wind speeds were similar, the maximal wind speed was much higher in “2017-Winter” (13.1 m/s) and “2018-Spring” (12.1 m/s).

#### 3.2. Comparison of in-situ physicochemical parameters of four field trips

The water quality exhibited strong seasonality for each parameter. Some data gaps exist across all campaigns. More specifically, pH-values were not available for “2017-Winter” due to malfunction of the pH-meter. Moreover, the absence of Chl<sub>a-f</sub> in “2017-Autumn” and Cyano<sub>PC</sub> in “2016-Summer” and “2017-Winter” were due to unavailable sensors at these times.

As expected the water was warmer in “2016-Summer” (24.6–30.6 °C) than that in “2017-Winter” (5.5–13.1 °C), “2017-Autumn” (22.9–27.8 °C) and “2018-Spring” (10.8–24.0 °C) (Fig. 3). Oxy-sat ranged from 42 to 205% in “2016-Summer” (with an oversaturated mean value of 108%), 75 to 122% in “2017-Winter”, 52 to 182% in “2017-Autumn” and 49 to 243% in “2018-Spring”. The accuracy is uncertain when values exceed the specified measuring range of 150% (supporting information Table A.1). The pH in “2016-Summer” (7.4–9.4), “2017-Autumn” (6.5–9.5), and “2018-Spring” (7.6–9.3) were all in the range of 6.5 to 9.5, which were slightly outside the Environmental quality standards for surface water of China (GB3838–2002) (range from 6 to 9).

Chl<sub>a-f</sub> available in three time-series showed very different ranges. It is evident that the highest Chl<sub>a-f</sub> signals (0.8–48.6 µg/L, mean: 15.6 µg/L) and standard deviation (8.7 µg/L) have been observed in “2018-Spring”. In general, more cyanobacteria (Cyano<sub>PC</sub>) were detected in “2018-Spring” (4.4–166.2 µg/L) than that in “2017-Autumn” (5.0–35.3 µg/L).

EC<sub>25</sub> represents the concentration of dissolved ionic components. The minimum values were increasing gradually from “2016-Summer”

to “2018-Spring”. The mean values ranked from largest to smallest: “2018-Spring” (578.4 µS/cm) > “2017-Winter” (447.8 µS/cm) > “2017-Autumn” (440.8 µS/cm) > “2016-Summer” (394.4 µS/cm). The EC<sub>25</sub> value in “2016-Summer” had the widest range (supporting information Table C.1). Total dissolved phosphorus (TDP) and NO<sub>3</sub><sup>-</sup>, as nutrients of algal growth, show an opposite trend, we found the highest NO<sub>3</sub><sup>-</sup> concentration in “2017-Winter”, but the TDP was the lowest in this scenario. A similar seasonal trend is presented in literature (Xu et al., 2015, 2010) where NO<sub>3</sub><sup>-</sup> peaks were found to always appear in the winter-spring period. The CDOM shows a reversed pattern compared to EC<sub>25</sub>. Lowest concentrations were found in “2018-Spring” (1.9–14.8 µg/L) whereas highest concentrations and standard deviations appeared in “2016-Summer” (18.4–32.2 µg/L).

For Turb, in “2016-Summer” and “2017-Autumn” the values were relatively stable and ranged from 1.9 to 10.0 FTU and 7.5 to 48.6 FTU, with a standard deviation of 1.6 and 2.6. However, in “2017-Winter” and “2018-Spring” there have been more substantial variations in the Turb, and values were ranging from 3.6 to 75.8 FTU and 1.4 to 50.0 FTU, with a higher standard deviation of 12.8 and 10.0, which was mainly related to the stronger wind in these two scenarios.

### 4. Discussion

#### 4.1. Water depth dynamics

The water depth at our monitoring location in “2016-Summer” (2.3–3 m) was much deeper than that in “2017-Winter” (1.2–1.5 m), “2017-Autumn” (1.6–1.9 m) and “2018-Spring” (1.6–1.9 m). An outstanding monsoon rain event happened during the “2016-Summer” campaign (Table 1), which was likely triggered by the pronounced “El Nino” event (World Water Council, 2018) in this year. Even though the Ministry of Water Resources managed to lower the water level by controlling the watergates, the continuous heavy rainfall caused the most massive flooding since 1999 on 08th July 2016 and the mean water level in the whole lake reached to 4.87 m above sea level (a.s.l.) (Zhang et al., 2017).

#### 4.2. Stratification and the relationship between parameters in four seasons

Every parameter shows different degrees of vertical gradients across the water column, as can be seen from the daily vertical gradients graph (Fig. 4). The observation of clear vertical structures in physicochemical parameter profiles points out the necessity of vertically profiling to capture relevant dynamic processes in Lake Taihu.

##### 4.2.1. Temp and Chl<sub>a-f</sub>

The δ<sub>i</sub> of Temp and Chl<sub>a-f</sub> is higher in “2016-Summer”, due to the deeper water level and slower wind speed compared to the other three campaigns. The water depths in the other three campaigns were low enough for the wind to mix the water from the top to bottom (Spigel R, 1980).

Fig. 5a shows the daily average value of Temp and Chl<sub>a-f</sub> across the whole water depth, the days with incomplete data were excluded from the calculation. A positive correlation is found between Temp and Chl<sub>a-f</sub> (Fig. 5a), the Pearson correlation coefficient (r) is 0.42 (P <

**Table 1**  
 Rainfall during four campaigns.

		2016 Summer	2017 Winter	2017 Autumn	2018 Spring
Basic information	Time period	26th June–16th July, 2016	23rd February–07th March, 2017	13th–24th September, 2017	19th March–16th April, 2018
	Measuring hours (M <sub>h</sub> )	375.0	181.7	142.8	450.0
Rain <sup>a</sup>	Rainfall hours (R <sub>h</sub> )	76.0	0.2	5.9	11.7
	Rainfall rate (R)	0.203	0.001	0.041	0.026
	Total rainfall (mm)	382.8	0.8	3.6	33.4

<sup>a</sup> The Rainfall data measured by Vaisala weather station (some data were missing during measuring).

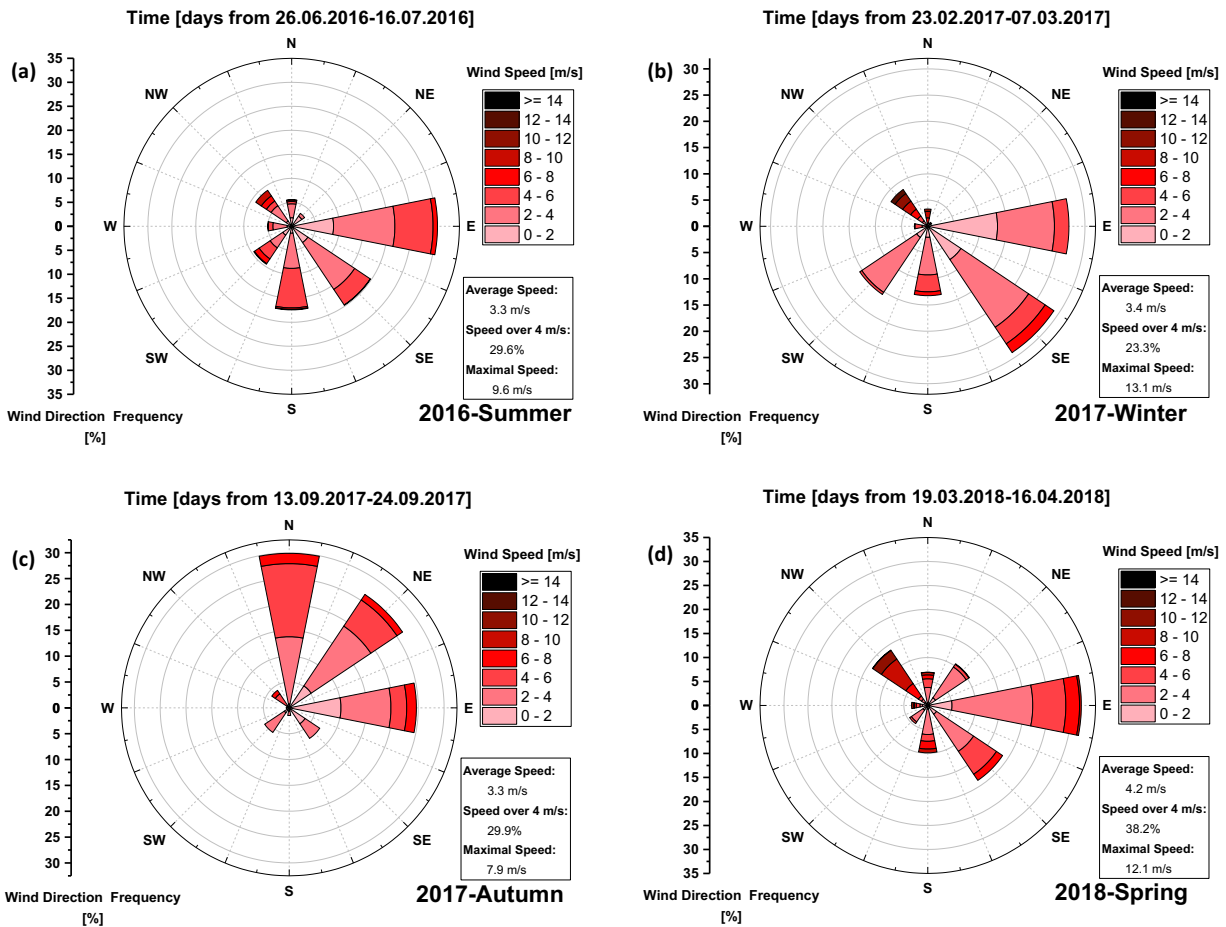


Fig. 2. Wind rose diagram in (a) 2016-Summer (observation time 375.0 h), (b) 2017-Winter (181.7 h), (c) 2017-Autumn (142.8 h), (d) 2018-Spring (450.0 h).

0.05), which indicates a prominent effect of Temp on the increase of  $Chl_{a-f}$  in most of the days.

#### 4.2.2. Oxy-sat and pH

Oxy-sat and pH are the parameters that reflect the photosynthesis, respiration and the decomposition. In the photosynthesis process, carbon dioxide is transformed into organic matter ( $C_6H_{12}O_6$ ) and oxygen (Formula (3)). In turn, aquatic respiration consumes organic matter, resulting in the production of carbon dioxide (Formula (4)). Photosynthesis, respiration and decomposition all contribute to pH fluctuations due to their influence on  $CO_2$  levels and trigger a shift in the carbonic acid equilibrium.



The Pearson's  $r$  of daily pH and Oxy-sat is 0.79 ( $P < 0.05$ ) (Fig. 5b), indicating that the changes of pH and Oxy-sat are dominated by the bio-activity process (Kairesalo, 1980).

From Fig. 4d, it is concluded that usually the upper layer has a higher value of Oxy-sat. Moreover, the Oxygen was frequently strongly depleted near the bottom in "2016-Summer", because the decomposition rate of biomass during summer was higher. This corresponds with similarly lower pH-values at the same times. In addition, since more illumination is available and more active algae can exist in the upper layer, the

photosynthesis process will be stronger in upper water, which produces more Oxygen and results in a high value of pH. Furthermore, the strong thermal gradient in "2016-Summer" inhibited the vertical mixing, this is why the oxygen depletion at the bottom and the oxygen oversaturation at the surface appeared quite stable (supporting information Fig. E.1).

#### 4.2.3. CDOM

In our observations, the CDOM is usually highest in the middle layer of the water column (Fig. 4h). The decay of biomass will be more effective under higher temperatures and cause the release of dissolved organic matter into the water, that is the reason for the high CDOM value and range in "2016-Summer" (Ji, 2017). Algae tend to proliferate under suitable condition, but every single alga cell is short-lived, and the result is a high concentration of detritus, which starts to decay resulting in a higher CDOM fluorescence signal. Moreover, some organic pollution in the water body from anthropogenic sources (industry, fishing farming, and agriculture) or wash out from soils into Lake Taihu by the rain during monsoon season in summer also contribute to the CDOM concentration.

#### 4.2.4. Turb, wind and $Cyano_{PC}$

The vertical gradient of Turb was higher near the bottom (Fig. 4e). This is due to wind-induced resuspension that resuspends particles from the sediment. For whole Lake Taihu, a critical wind speed of  $>4$  m/s was found to lead to extensive sediment resuspension, and when it reaches  $>6.5$  m/s massive sediment resuspension occurs (Qin

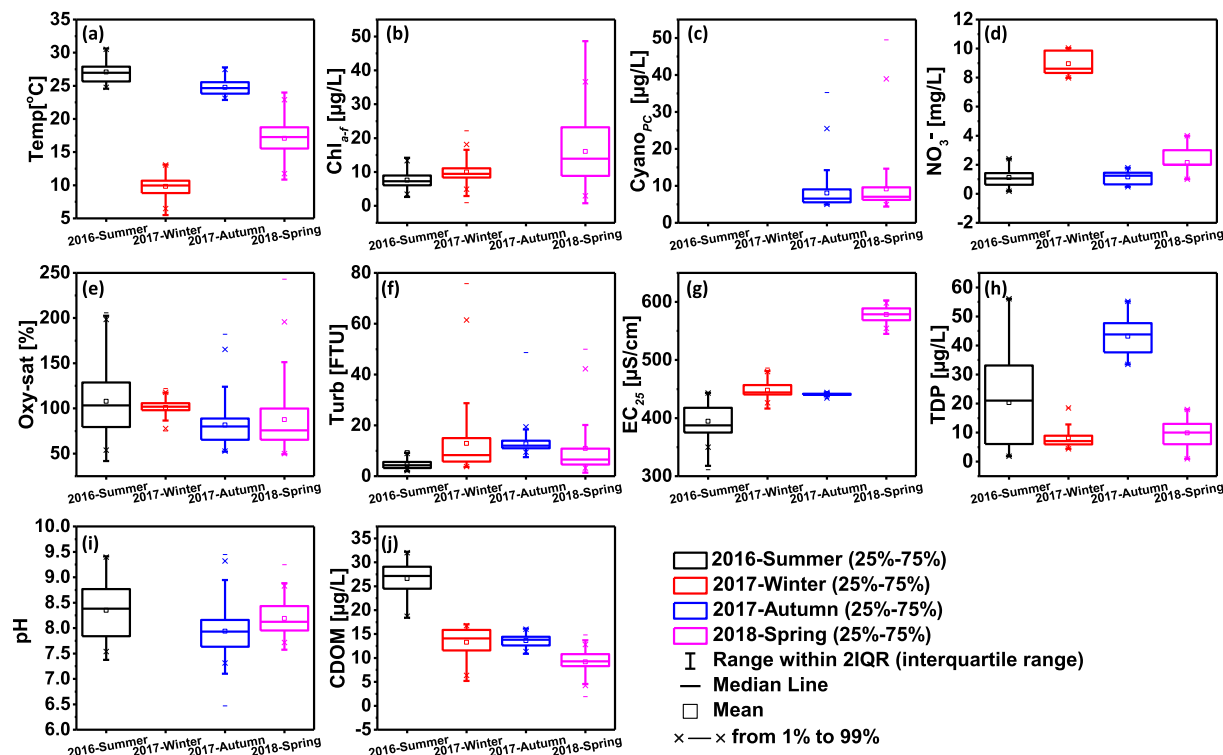


Fig. 3. Seasonal distribution graph of ten physicochemical parameters measured by multi-sensor-system (BIOLIFT) and derived from water samples. (a) Temperature [°C], (b) Chlorophyll a fluorescence [µg/L], (c) Cyanobacteria fluorescence [µg/L], (d) NO<sub>3</sub><sup>-</sup> concentration [mg/L], (e) Oxygen saturation [%], (f) Turbidity [FTU], (g) Electrical conductivity at 25 °C [µS/cm], (h) Total dissolved phosphorus [µg/L], (i) pH, (j) Colored dissolved organic matter (CDOM) [µg/L].

et al., 2004). Wind speeds >4 m/s happened within all four campaigns, and we observed visible resuspension events in all monitored time-series (Fig. 6). For instance, an increase of Turb from bottom to top happened on day seven in “2016-Summer” and “2017-Winter”, day 18 to 20 and day 26 in “2018-Spring”. However, this simple relationship could not always be verified, but wind direction also needs to be taken into account when only focusing on one small area (TLLER) in the Lake Taihu. According to the specific location of our monitoring point, easterly, northeasterly, and southeasterly winds cannot generate huge waves and shear stress because of the small fetch area before the monitoring location. For example, on day one in “2017-Autumn” and day 11 in “2018-Spring” no resuspension could be observed despite sufficient wind speeds >4 m/s.

The Turb on the surface (<0.5 m) in “2017-Winter” was quite exceptional. It is reasonable that in diatom-dominated winter the Turb on the upper layer was less than that on the deeper layer, because diatom cannot move to the surface by themselves as cyanobacteria can. In “2017-Autumn”, the changes of Turb under depth < 0.2 m were mainly affected by the Cyanobacteria (Pearson’s  $r = 0.92$ ,  $P < 0.05$ ) in the same depth (Fig. 7a), namely the accumulated algae. However, in “2018-Spring”, Cyano<sub>PC</sub> was not the predominant factor for the change of Turb anymore, because strong winds mixed the water column well. Also, strong wind-induced resuspension had a conclusive rapid effect on Turb. As can be seen from Fig. 7b, usually Turb increased with the increase of wind speed across all four seasons (days with incomplete data were excluded). This is either because wind forces cause resuspension of sediment or wind mixes algal scums back into the water column and then increase the detected Turb. The rate of Turb change is not exactly the same in different seasons, because different types of particles have varying effects on Turb readings. It is very likely that particle composition (incl. clay, silt, finely divided inorganic and organic matter, algae,

plankton and other microscopic organisms in the water column) was very different among seasons. In general, however, a good relationship between wind speed and Turb on a daily basis was found in all four campaigns (Pearson’s  $r = 0.75$ ,  $P < 0.05$ ).

No straightforward relationship of wind speed and Chl<sub>a-f</sub> can be seen from Fig. 7c, this is because of the different algal species in different seasons. The wind mixing is important to the unfloatable algae (as diatom) to move to the upper layer and benefit from better light conditions (in “2017-Winter”). If the nutrients are sufficient for the algal growth, the enrichment of nutrients from sediment will not make a significant change to the algal concentration; on the contrary, the increase of Turb related to the wind will decrease the amount of light penetration, which apparently has a negative effect on algal growth. Interestingly, a relationship exists between wind speed and Cyano<sub>PC</sub> (Fig. 7d), the reason would be that the stronger wind speed can generate greater force to the water body, which induces the blooms to accumulate on a down-wind shoreline or bring more surface accumulated cyanobacteria to the water body. This is a benefit for the in-situ detection by the fluorescence sensor and increases the sensor readings to the same extent.

#### 4.2.5. PAR and PAR<sub>water</sub>

The PAR values above water were all below 2000 µmol/(s·m<sup>2</sup>). The PAR<sub>water</sub> is not only related to the irradiation on that day but also to the light attenuation in the water. For example, in “2017-Winter”, even though the PAR values on days from one to five and seven to nine were similar, but the PAR<sub>water</sub> were much lower. This phenomenon corresponded to the high Turb in the water on the days from seven to nine. It was the same to that of “2018-Spring”, the low PAR<sub>water</sub> on days 18–22 were related to the high Turb in the water caused by the resuspension. Suspended particles, algae (in particular scums), but also light absorbing dissolved substances can absorb a large portion of the

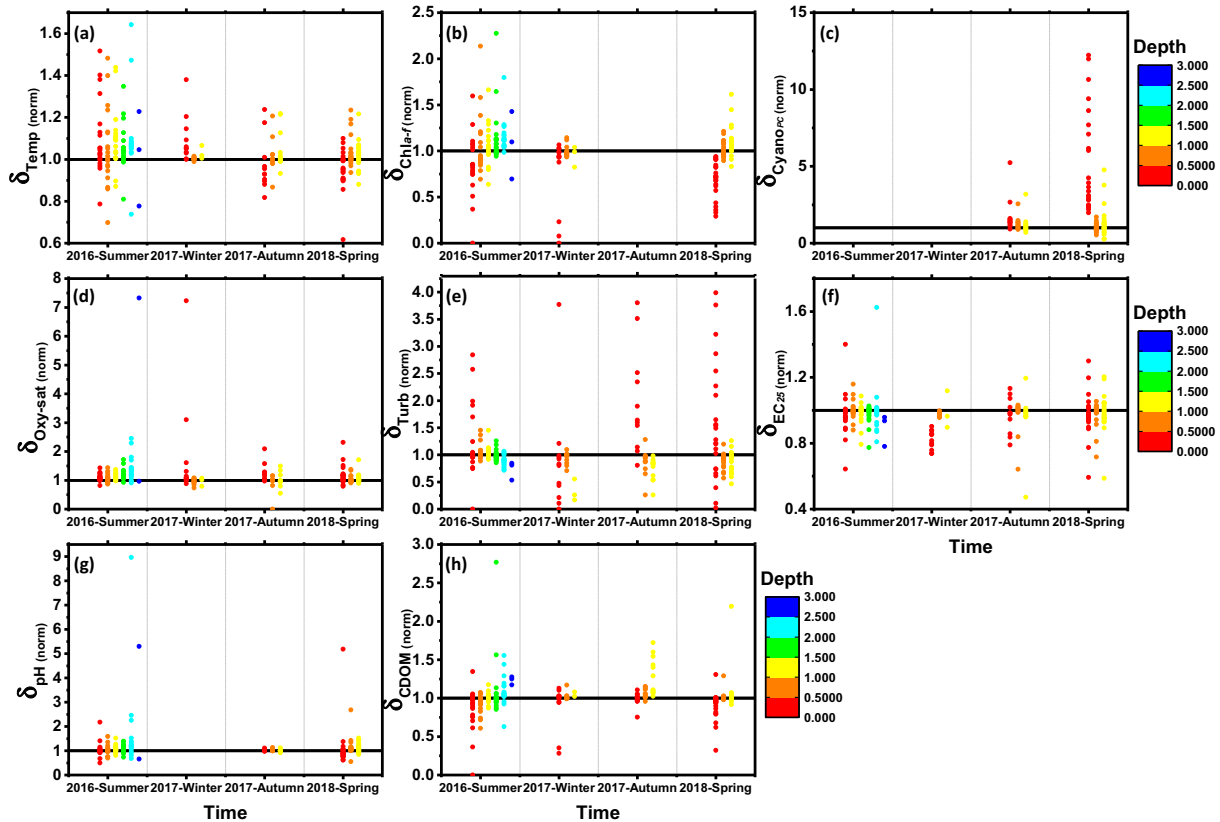


Fig. 4. Vertical gradient of eight parameters measured by multi-sensor-system (BIOLIFT) in every 0.5 m. (a) Temperature [°C], (b) Chlorophyll *a* fluorescence [µg/L], (c) Cyanobacteria fluorescence [µg/L], (d) Oxygen saturation [%], (e) Turbidity [FTU], (f) Electrical conductivity at 25 °C [µS/cm], (g) pH, (h) Colored dissolved organic matter (CDOM) [µg/L].

light and reduce light availability in the deeper layer. This leads to disadvantages for planktonic algae and benthic macrophytes underneath.

In “2017-Winter” and “2018-Spring”, during which time observable fluorescence quenching effects were found (Fig. 6). Fluorescence quenching (Demmig-Adams et al., 2014) is the depression of the fluorescence signal in surface waters during daylight and especially at noon. The  $Chl_{a-f}$  signals were much stronger at night than the daytime on days from one to five in “2017-Winter” and days from seven to 14 in “2018-Spring”. The common conditions on these days were the

continues high PAR values (daily PAR peak over or close to 1500  $\mu\text{mol}/\text{m}^2 \cdot \text{s}$ ) and low Turb (<10 FTU) which offered high  $PAR_{\text{water}}$  and the broader vertical illuminating area time. But from our data, pH and Oxy-sat were still higher in the daytime than at night (supporting information Figs. E.2, 4), which means the photosynthetic activity was not notably affected by the continuous  $PAR_{\text{water}}$  of under 2000  $\mu\text{mol}/\text{m}^2 \cdot \text{s}$  in the water. The exciting light from  $Chl_{a-f}$  sensor dissipated to heat, because the ambient sunlight is too strong and the photosynthetic reaction centers saturated.

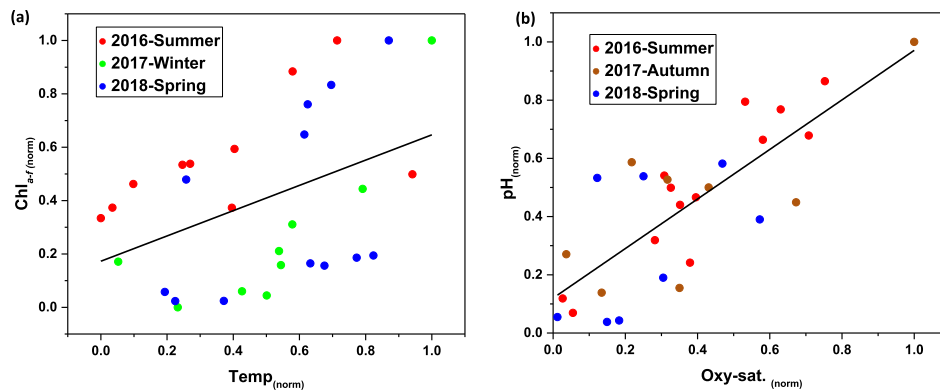


Fig. 5. (a) The scatter plot of normalized daily Temperature and Chlorophyll *a* fluorescence value in three campaigns, (b) The scatter plot of normalized Oxygen-saturation and pH in three campaigns.

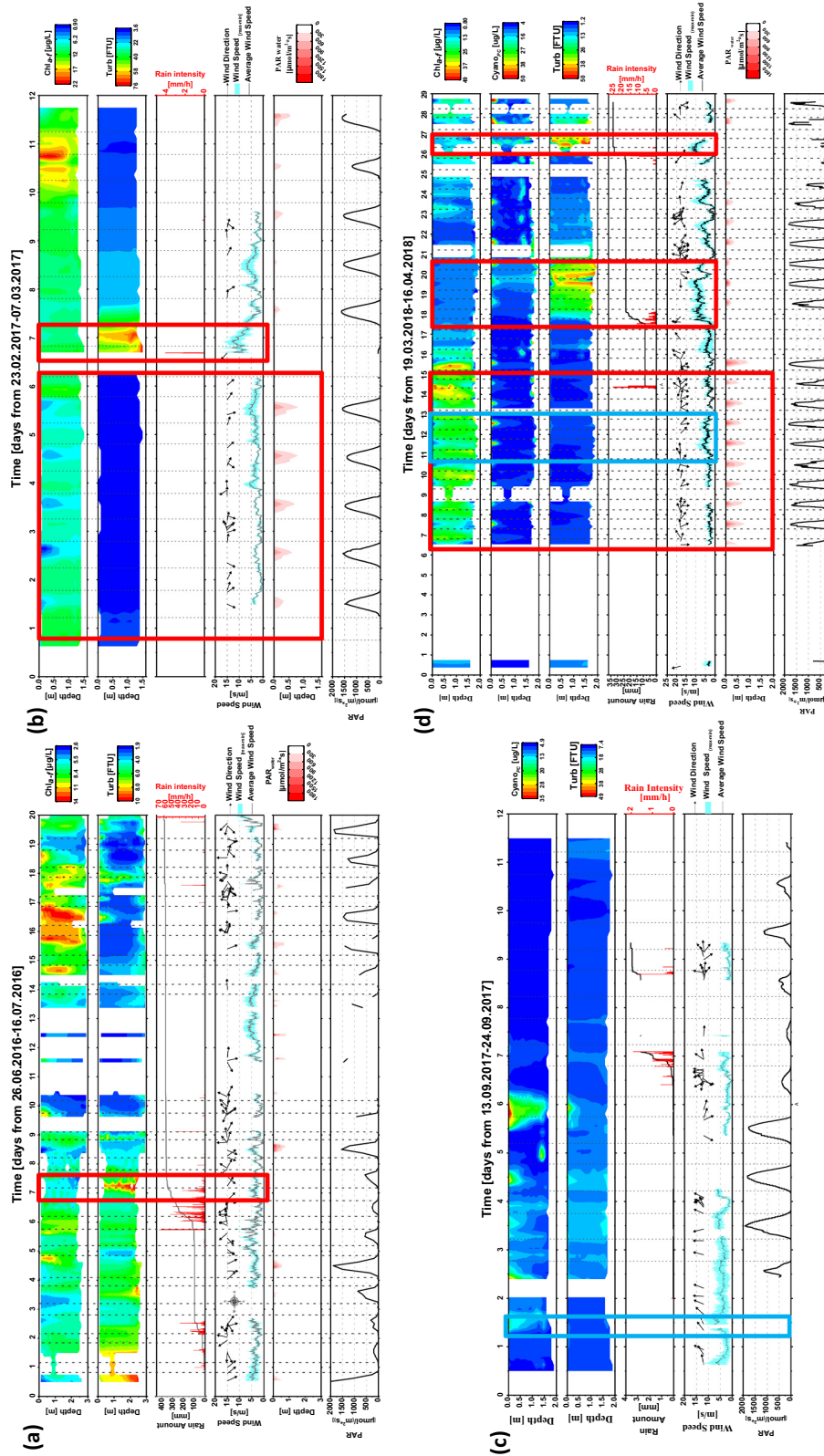


Fig. 6. Vertical-temporal data of Chlorophyll *a* fluorescence [ $\mu\text{g/L}$ ], Cyanobacteria fluorescence [ $\mu\text{g/L}$ ], Turbidity [FTU], PAR in the water (PAR<sub>water</sub>) [ $\mu\text{mol/m}^2\cdot\text{s}$ ], and Wind direction (arrows shows the direction of wind come from), Wind speed [m/s], Rain amount [mm], Rain intensity [mm/h], PAR above the water (PAR) [ $\mu\text{mol/m}^2\cdot\text{s}$ ]. (a) "2016-Summer", (b) "2017-Summer", (c) "2017-Winter", (d) "2018-Spring".

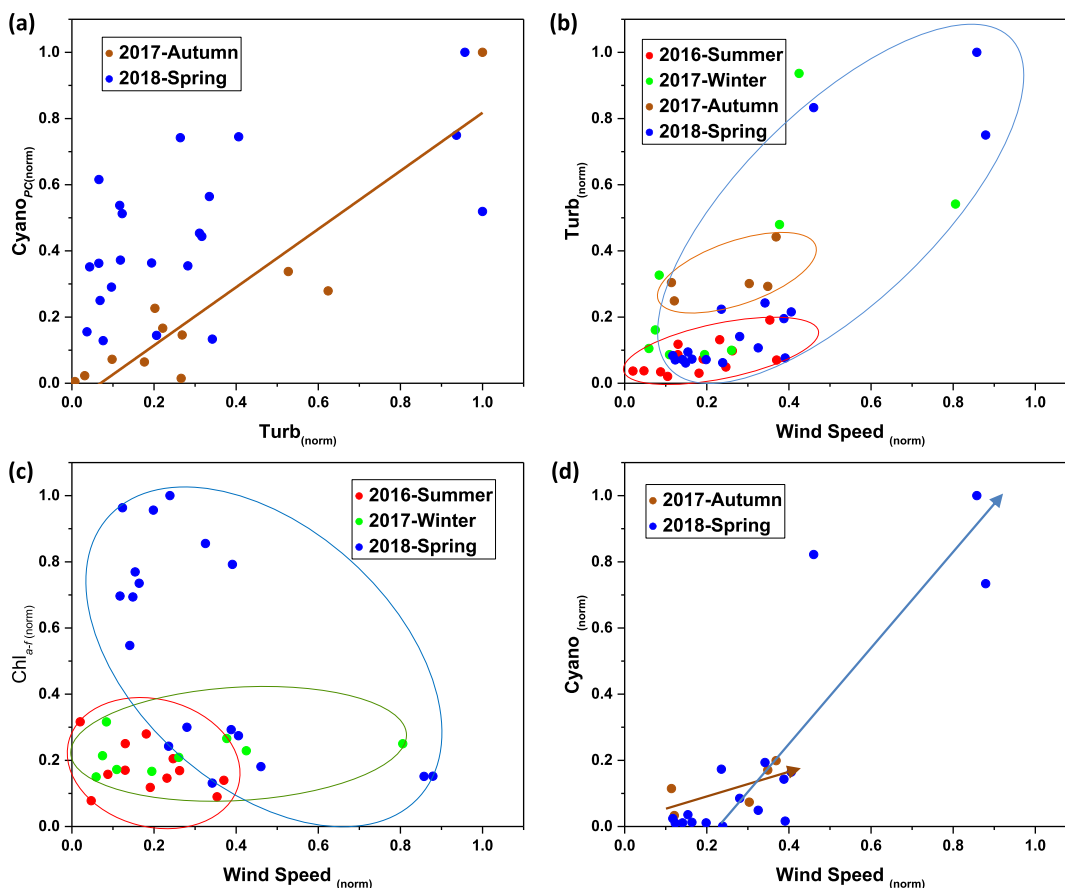


Fig. 7. The scatter plots of the normalized daily value of (a) Turbidity and Cyanobacteria fluorescence, (b) Wind speed and Turbidity, (c) Wind speed and Chlorophyll *a* fluorescence, (d) Wind speed and Cyanobacteria fluorescence.

#### 4.3. Water chemistry changes in four seasons

During spring inflow rivers carry a larger amount of nitrogen into Lake Taihu, due to the increased application of fertilizers in spring (main N source) (Xu et al., 2013; Ye et al., 2014). The fertilizer applications were still the main source of N input over the past three decades, even though overall the application decreased (Zhang et al., 2018). Moreover, the large numbers of hydrophyte deaths in winter return nutrients to the water. After winter, the growth condition improves, the algal growth rapidly consumes  $\text{NO}_3^-$ . However, unlike the nitrogen, phosphate is often strongly sorbed to sediment (Ji, 2017). As shown in the graph (Fig. 3), the TDP exhibited a similar seasonal pattern to Temp, which due to the microbial processes that release phosphorus by mineralization of organic matter. Also, Temp has a significant effect on the adsorption/desorption equilibrium, the elevated Temp in summer can enhance TDP release from the sediments (Jin et al., 2008; Xu et al., 2013).

The dynamics of anion concentrations (mainly  $\text{SO}_4^{2-}$  and  $\text{Cl}^-$ ) contribute a lot to the significant changes of  $\text{EC}_{25}$  during all four campaigns. Pearson's  $r$  of  $\text{EC}_{25}$  and  $\text{SO}_4^{2-}$  was 0.99 and was 0.96 for  $\text{EC}_{25}$  and  $\text{Cl}^-$  ( $P < 0.05$ , the solid line in Fig. 8), with 176 reference water samples.  $\text{Ca}^{2+}$  and  $\text{Na}^+$  are the principal dissolved cations in four campaign times, followed by  $\text{Mg}^{2+}$ . It was shown in Fig. 8b, that the change of  $\text{EC}_{25}$  is closely related to  $\text{Na}^+$  (Pearson's  $r = 0.99$ ,  $P < 0.05$ ),  $\text{Mg}^{2+}$  (Pearson's  $r = 0.96$ ,  $P < 0.05$ ) and to  $\text{Ca}^{2+}$  (Pearson's  $r = 0.89$ ,  $P < 0.05$ ). The highest concentration of  $\text{SO}_4^{2-}$ ,  $\text{Cl}^-$ ,  $\text{Ca}^{2+}$ ,  $\text{Na}^+$  and  $\text{Mg}^{2+}$  were found in “2018-

Spring” corresponding with the highest  $\text{EC}_{25}$ . The seasonal variation of  $\text{EC}_{25}$  is mainly related to the annual rainfall pattern.

In “2016-Summer”, the rapid and basically synchronous drop (dotted line as trendline) of  $\text{EC}_{25}$  with  $\text{SO}_4^{2-}$  and  $\text{EC}_{25}$  with  $\text{Cl}^-$  happened from day five with the onset of long-last heavy rainfall, it was the same situation for principal dissolved cations. We can draw the conclusion that the decrease of  $\text{EC}_{25}$  is largely related to the rain dilution due to the special rainfall event in this scenario.

#### 4.4. The $\text{Chl}_{a-f}$ and $\text{Cyanop}_c$ changes in different scenarios

The least  $\text{Chl}_{a-f}$  was detected by BIOLIFT in “2016-Summer” among three campaigns, even though according to our personal visual observations in the field, the formation of cyanobacteria scums happened in the last few days during our monitoring time in “2016-Summer”. One probable reason is that the growth of algae was influenced by the heavy rain and flood event in the first seven days (Kristiansen, 1996). Moreover, the sustained rainfall mentioned above strongly diluted the lake and lowered the concentration of  $\text{Chl}_a$ . The algal species vary from season to season is another important reason for the low  $\text{Chl}_{a-f}$  in “2016-Summer”. As mentioned in Section 2.2.1, in principle, the  $\text{Chl}_{a-f}$  cannot well represent the  $\text{Chl}_a$  of Cyanobacteria. From the literature, in winter in Meiliang Bay, *Cyclotella meneghiniana* (diatom) is the dominated species (Ying et al., 2015). While summer blooms in Lake Taihu are dominated by the buoyant *Microcystis* spp. (cyanobacteria), which is not as sensitive as diatom and green algae to the used  $\text{Chl}_{a-f}$  sensor and can



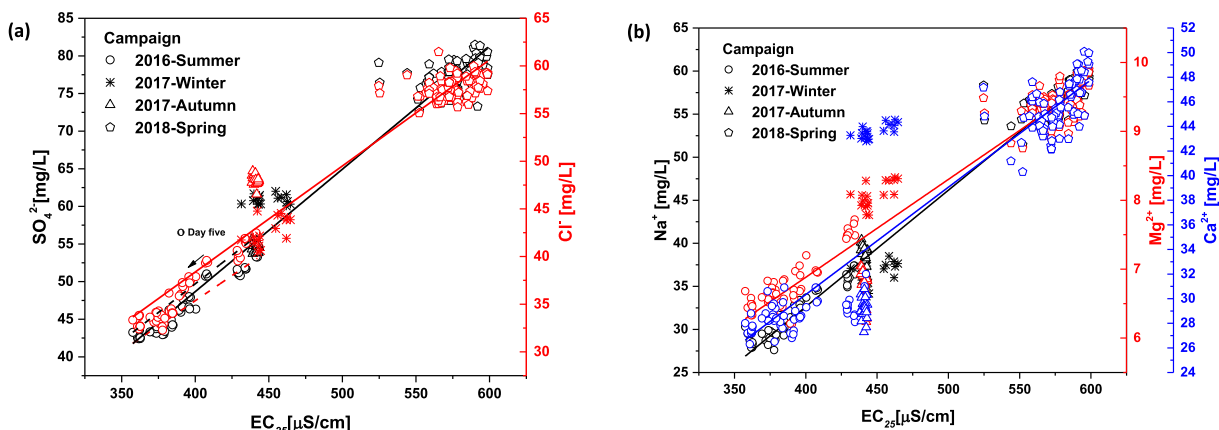


Fig. 8. The scatter plots of (a) Electrical conductivity at 25 °C and anions ( $\text{SO}_4^{2-}$ ,  $\text{Cl}^-$ ), (b) Electrical conductivity at 25 °C and cations ( $\text{Na}^+$ ,  $\text{Mg}^{2+}$ ,  $\text{Ca}^{2+}$ ).

cause much lower sensor readings. For this reason, we applied the phycoyanin fluorescence sensor to complement the analyses of cyanobacterial presence and dynamics. Besides Temperature and pH, nutrients (TDP and  $\text{NO}_3^-$ ) have an important impact on the structures of phytoplankton communities in different seasons (Li et al., 2018). The notable seasonal diversity of those parameters (Fig. 3) contribute to the algal species changes and the  $\text{Chl}_{a-f}$  signal difference.

The highest  $\text{Chl}_{a-f}$  signals and standard deviations were found in “2018-Spring”, during which time much stronger winds occurred. The wind-induced mixing can also lead to an increase of  $\text{Chl}_{a-f}$  by homogeneously mixing algae scums from the water surface into the whole water column and bring unbuoyant algae from bottom to surface to reach better living condition. The increase of N during the winter-spring transitional period and P supplement on exogenous and endogenous to water bodies will help to support and promote the growth of algae. From day 16, the  $\text{PAR}_{\text{water}}$  were very less and only arrived on the upper 0.5 m layer due to the low PAR and the high Turb. The immediate result was a decrease in monitored  $\text{Chl}_{a-f}$ . The highest concentrations of  $\text{Chl}_{a-f}$  in this scenario are on days from six to 16 correspond to the days when  $\text{PAR}_{\text{water}}$  are the highest. Under low  $\text{PAR}_{\text{water}}$ , the Cyanobacteria can migrate to the water surface to fight more illumination for themselves and will face less competition due to the growth limit of unfloatable algae, which is one of the reasons for the increase of  $\text{Cyano}_{\text{PC}}$  in the last 12 days.

The  $\text{Cyano}_{\text{PC}}$  varied greatly, which was attributed to gliding motility of cyanobacteria. As can be seen from Fig. 4b, usually higher  $\text{Chl}_{a-f}$  values were present in the middle layer (0.5–1 m) instead of in the surface layer (<0.5 m). This was different from  $\text{Cyano}_{\text{PC}}$  (Fig. 4c), which showed much higher readings in the upper water column. This also indicates the different sensitivities of the  $\text{Chl}_{a-f}$  sensor to different algal species (especially the cyanobacteria) and that different algal species can dominate in different water layers.

## 5. Conclusions

In summary, the high-resolution vertical-temporal data from BIOLIFT and the accompanying meteorological data can be used to describe dynamics in water quality depth-profiles of Lake Taihu visually, the reason for algal bloom and have the possibility to apply in other water bodies. In this study, we focused on the environmental variables in one location to compare the water quality changes among the four seasons and the determinants of seasonal algal varieties by  $\text{Chl}_{a-f}$  and  $\text{Cyano}_{\text{PC}}$  signals.

The physicochemical parameters show obvious seasonal dynamics. The continuous heavy rainfall in the monsoon season contributed to the 1.5 times deeper water column in “2016-Summer” compared to

the other three campaigns. The seasonal variation of  $\text{EC}_{25}$  is mainly related to the annual rainfall pattern. The rain cannot only act as a diluent but also wash pollutants into the lake, which is likely one of the contributions to the outstandingly high CDOM concentrations in “2016-Summer”. Furthermore, suitable conditions for biomass decay in the summertime can return large amounts of dissolved organic substances into the water column. The strong seasonal variation of  $\text{NO}_3^-$  is mainly because of external pollution, decomposition and nitrification processes after the death of phytoplankton and hydrophytes in the winter-spring period, and the high inorganic nitrogen consumption rate in algal growth season. On the contrary, the release of phosphorus from sediment contributes the high concentration of TDP in summer.

The highest daily thermal vertical gradients ( $\delta_{\text{Temp}}$ ) and  $\delta_{\text{Chl}_{a-f}}$  were observed in “2016-Summer” on the common role of deeper water depth and slower wind speed. Wind-induced resuspension will happen under strong wind speed (>4 m/s) but in an effective direction (avoid shore hinder), which rise the Turb from the bottom to top. Except for the resuspension, the algae scums will also reduce the water transmittance and increase the Turb on the surface. Continuously high PAR values and low Turb in the water are the main causes of fluorescence quenching. However, the photosynthetic process was not conspicuously inhibited during all our monitoring time.

Vertical and temporal algal kinetics occurred in all the scenarios. In general, once the nutrients exceeded, the Temp is an indispensable factor to the increase of algal biomass and controls the phytoplankton communities in fresh water. Wind can lead to resuspension as a nutrient source, and the wind-induced mixing can help the unfloatable algae to get better living conditions and bring the surface cyanobacteria back to the water column. Light is the necessity for algal growth and photosynthesis. The Cyanobacteria are easier to survive under low  $\text{PAR}_{\text{water}}$  condition by floating to the water surface. Without the algal scums, the better light condition in the water body is offered, which is good for the growth of unfloatable algae. Combine with our observation, the cyanobacteria bloom normally happened under calm and sunny days straight after the strong windy days (bring nutrients). The changes of those factors responsible for the variability the  $\text{Chl}_{a-f}$  and  $\text{Cyano}_{\text{PC}}$  and become potential indicators for the prediction of  $\text{Chl}_{a-f}$  and cyanobacterial blooms. The ethanol extraction method will be used to determine the  $\text{Chl}_a$  concentration and calibrate the  $\text{Chl}_{a-f}$  in the future.

## Acknowledgments

This work was supported by the Federal Ministry of Education and Research of Germany (BMBF, grant.-no.: 02WCL1336B). The first author was supported by the China Scholarship Council.

### Appendix A. Supplementary data

Supplementary data to this article can be found online at <https://doi.org/10.1016/j.scitotenv.2019.01.044>.

### References

- Allee, R.J., Johnson, J.E., 1999. Use of satellite imagery to estimate surface chlorophyll a and Secchi disc depth of Bull Shoals Reservoir, Arkansas, USA. *Int. J. Remote Sens.* 20(6), 143–1161. <https://doi.org/10.1080/014311699212849>.
- Asai, R., Horiguchi, Y., Yoshida, A., McNiven, S., Tahira, P., Ikebukuro, K., Uchiyama, S., Masuda, Y., Karube, I., 2001. Detection of phycobilin pigments and their seasonal change in Lake Kasumigaura using a sensitive in situ fluorometric sensor. *Anal. Lett.* 34, 2521–2533. <https://doi.org/10.1081/AL-100107533>.
- Beutler, M., 2003. Spectral Fluorescence of Chlorophyll and Phycobilins as an In-Situ Tool of Phytoplankton Analysis - Models, Algorithms and Instruments. PhD Thesis. Christian-Albrechts-Universität, Kiel.
- Demmig-Adams, B., Garab, G., Adams III, W., 2014. Advances in photosynthesis and respiration including bioenergy and related processes non-photochemical quenching and energy dissipation in plants, algae and cyanobacteria. *Non-Photochemical Quenching and Energy Dissipation in Plants, Algae and Cyanobacteria* [https://doi.org/10.1007/978-94-017-9032-1\\_1](https://doi.org/10.1007/978-94-017-9032-1_1).
- Deng, J., Qin, B., Paerl, H.W., Zhang, Y., Ma, J., Chen, Y., 2014. Earlier and warmer springs increase cyanobacterial (*Microcystis* spp.) blooms in subtropical Lake Taihu, China. *Freshw. Biol.* 59, 1076–1085. <https://doi.org/10.1111/fwb.12330>.
- Fogg, G.E., Walsby, A.E., 1971. Buoyancy regulation and the growth of planktonic blue-green algae. *Int. Ver. Theor. Angew. Limnol. Mitt.* 19, 182–188.
- Guo, L., 2007. Doing battle with the green monster of Taihu Lake. *Science* (80-) 317, 1166. <https://doi.org/10.1126/science.317.5842.1166>.
- Holbach, A., Bi, Y., Yuan, Y., Wang, L., Zheng, B., Norra, S., 2015. Environmental water body characteristics in a major tributary backwater of the unique and strongly seasonal Three Gorges Reservoir, China. *Environ. Sci. Process. Impacts* 17, 1641–1683. <https://doi.org/10.1039/c5em00201j>.
- Ji, Z., 2017. *Hydrodynamics and Water Quality: Modeling Rivers, Lakes, and Estuaries*. John Wiley & Sons.
- Jin, X., Jiang, X., Wang, Q., Liu, D., 2008. Seasonal changes of P adsorption-desorption characteristics at the water-sediment interface in Meiliang Bay, Taihu Lake, China. *Acta Sci. Circumstantiae* 28, 24–30 (in Chinese with English Abstract).
- Kairesalo, T., 1980. Diurnal fluctuations within a littoral plankton community in oligotrophic Lake Pöräjärvi, Southern Finland. *Freshw. Biol.* 10, 533–537. <https://doi.org/10.1111/j.1365-2427.1980.tb01228.x>.
- Kalbitz, K., Geyer, W., 2001. Humification indices of water-soluble fulvic acids derived from synchronous fluorescence spectra - effects of spectrometer type and concentration. *J. Plant Nutr. Soil Sci.* 164, 259–265. [https://doi.org/10.1002/1522-2624\(200106\)164:3<259::AID-JPLN259>3.0.CO;2-T](https://doi.org/10.1002/1522-2624(200106)164:3<259::AID-JPLN259>3.0.CO;2-T).
- Kristiansen, J., 1996. Dispersal of freshwater algae – a review. *Biogeography of Freshwater Algae*. Springer Netherlands, Dordrecht, pp. 151–157 [https://doi.org/10.1007/978-94-017-0908-8\\_15](https://doi.org/10.1007/978-94-017-0908-8_15).
- Li, D., Wu, N., Tang, S., Su, G., Li, X., Zhang, Y., Wang, G., Zhang, J., Liu, H., Hecker, M., Giesy, J.P., Yu, H., 2018. Factors associated with blooms of cyanobacteria in a large shallow lake, China. *Environ. Sci. Eur.* 30. <https://doi.org/10.1186/s12302-018-0152-2>.
- Ma, X., 2017. The water quality has improved but cyanobacteria control is not ideal (Chinese). *Wuxi Dly.* 2.
- Paerl, H.W., Ustach, J.F., 1982. Blue green algae scums: an explanation for their occurrence during freshwater blooms. *Limnol. Ocean.* 27, 212–217.
- Peuravuori, J., Koivikko, R., Pihlaja, K., 2002. Characterization, differentiation and classification of aquatic humic matter separated with different sorbents: synchronous scanning fluorescence spectroscopy. *Water Res.* 36, 4552–4562. [https://doi.org/10.1016/S0043-1354\(02\)00172-0](https://doi.org/10.1016/S0043-1354(02)00172-0).
- Qin, B., Hu, W., Gao, G., Luo, L., Zhang, J., 2004. Dynamics of sediment resuspension and the conceptual schema of nutrient release in the large shallow Lake Taihu, China. *Artic. 54. Chin. Sci. Bull.* 49, 54–64. <https://doi.org/10.1360/03wd0174>.
- Rochelle-Newall, E.J., Fisher, T.R., 2002a. Chromophoric dissolved organic matter and dissolved organic carbon in Chesapeake Bay. *Mar. Chem.* 77, 23–41. [https://doi.org/10.1016/S0304-4203\(01\)00073-1](https://doi.org/10.1016/S0304-4203(01)00073-1).
- Rochelle-Newall, E.J., Fisher, T.R., 2002b. Production of chromophoric dissolved organic matter fluorescence in marine and estuarine environments: an investigation into the role of phytoplankton. *Mar. Chem.* 77, 7–21. [https://doi.org/10.1016/S0304-4203\(01\)00072-X](https://doi.org/10.1016/S0304-4203(01)00072-X).
- Schmidt, K.R., Aus Der Beek, T., Dai, X., Dong, B., Dopp, E., Eichinger, F., Hammers-wirtz, M., Haußmann, R., Holbach, A., Hollert, H., Illgen, M., Jiang, X., Koehler, J., Koester, S., Korth, A., Kueppers, S., Li, A., Lohmann, M., Moldaenke, C., Norra, S., Qin, B., Qin, Y., Reese, M., Riehle, E., Santiago-schuebel, B., Schaefer, C., Simon, A., Song, Y., Staaks, C., Steinhardt, J., Subklew, G., Tao, T., Wu, T., Yin, D., Zhao, F., Zheng, B., Zhou, M., Zou, H., Zuo, J., Tiehm, A., 2016. Since 2015 the SinoGerman research project SIGN supports water quality improvement in the Taihu region, China. *Environ. Sci. Eur.* 28. <https://doi.org/10.1186/s12302-016-0092-7>.
- Spigel R I J., 1980. The classification of Mixed-Layer Dynamics of Lakes of Small to Medium Size. *J. Phys. Oceanogr.* 10, 1104–1121. [https://doi.org/10.1175/1520-0485\(1980\)010<1104:TCOMLD>2.0.CO;2](https://doi.org/10.1175/1520-0485(1980)010<1104:TCOMLD>2.0.CO;2).
- Addressing water challenges and safeguarding water security: China's thought, action, and practice. In: World Water Council (Ed.), *Global Water Security*, pp. 53–83 [https://doi.org/10.1007/978-981-10-7913-9\\_3](https://doi.org/10.1007/978-981-10-7913-9_3).
- Xu, H., Paerl, H.W., Qin, B., Zhu, G., Gao, G., 2010. Nitrogen and phosphorus inputs control phytoplankton growth in eutrophic Lake. *Limnol. Oceanogr.* 55, 420–432.
- Xu, S., Huang, B., Wei, Z.B., Luo, J., Miao, A.J., Yang, L.Y., 2013. Seasonal variation of phytoplankton nutrient limitation in Lake Taihu, China: a monthly study from year 2011 to 2012. *Ecotoxicol. Environ. Saf.* 94, 190–196. <https://doi.org/10.1016/j.ecoenv.2013.05.006>.
- Xu, H., Paerl, H.W., Qin, B., Zhu, G., Hall, N.S., Wu, Y., 2015. Determining critical nutrient thresholds needed to control harmful cyanobacterial blooms in eutrophic Lake Taihu, China. *Environ. Sci. Technol.* 49, 1051–1059. <https://doi.org/10.1021/es503744q>.
- Ye, R., Shan, K., Gao, H., Zhang, R., Xiong, W., Wang, Y., Qian, X., 2014. Spatio-temporal distribution patterns in environmental factors, chlorophyll-a and microcystins in a large shallow lake, Lake Taihu, China. *Int. J. Environ. Res. Public Health* 11, 5155–5169. <https://doi.org/10.3390/ijerph110505155>.
- Ying, A., Yonghong, B., Zhengyu, H., 2015. Response of predominant phytoplankton species to anthropogenic impacts in Lake Taihu. *J. Freshw. Ecol.* 30, 99–112. <https://doi.org/10.1080/02705060.2014.992052>.
- Zhang, H., Shi, Y., Xu, Z., Ni, G., Li, J., 2017. The Health Status Report of Taihu Lake in 2016 [WWW Document]. Taihu Basin Auth. Minist. Water Resour URL <http://www.tba.gov.cn/tba/content/TBA/lygb/thjzkzkg/000000000013895.html>, Accessed date: 11 September 2017.
- Zhang, M., Shi, X., Yang, Z., Yu, Y., Shi, L., Qin, B., 2018. Long-term dynamics and drivers of phytoplankton biomass in eutrophic Lake Taihu. *Sci. Total Environ.* 645, 876–886. <https://doi.org/10.1016/j.scitotenv.2018.07.220>.

**Highly time-resolved analysis of seasonal water dynamics and algal kinetics based on *in-situ* multi-sensor-system monitoring data in Lake Taihu, China**

Jingwei Yang<sup>a\*</sup>, Andreas Holbach<sup>a</sup>, Andre Wilhelms<sup>a</sup>, Yanwen Qin<sup>b</sup>, Binghui Zheng<sup>b</sup>, Hua Zou<sup>c</sup>, Boqiang Qin<sup>d</sup>, Guangwei Zhu<sup>d</sup>, Stefan Norra<sup>a</sup>

<sup>a</sup>*Institute of Applied Geosciences, Working Group Environmental Mineralogy and Environmental System Analysis (ENMINSA)  
Karlsruhe Institute of Technology, Kaiserstraße 12, 76131 Karlsruhe, Germany*

<sup>b</sup>*Chinese Research Academy of Environmental Sciences, Dayangfang 8, Anwai Beiyuan, Beijing 100012, China*

<sup>c</sup>*School of Environmental and Civil Engineering, Jiangnan University, Wuxi 214122, People's Republic of China*

<sup>d</sup>*Nanjing Institute of Geography & Limnology, Chinese Academy of Sciences, 73 East Beijing Road, 210008 Nanjing, P.R.  
China*

\*Corresponding author

Email address: [Jingwei.yang@kit.edu](mailto:Jingwei.yang@kit.edu)

**SUPPORTING INFORMATION**

## **Content**

### **A. Sensors information and their specifications (P.2)**

BIOLIFT (Table A.1.)

Vaisala (Table A.2.)

### **B. Instrument detection limit (P.3)**

ICP-MS (Table B.1.)

IC (Table B.2.)

### **C. BIOLIFT statistic summary (P.4-5)**

Table C.1.

### **D. Matlab code for matrix calculation (P.6)**

### **E. Vertical-temporal data graph (P.7-10)**

2016-Summer (Fig.E.1., P.7)

2017-Winter (Fig.E.2., P.8)

2017-Autumn (Fig.E.3., P.9)

2018-Spring (Fig.E.4., P.10)

## A. Sensors information and their specifications (P.2)

**Table A.1.** Sensors installed on the BIOLIFT and their specifications

Parameters	Producer	Principle	Measuring range	Accuracy	Resolution	Response time
Pressure	ADM Elektronik	Piezo-resistive	0 - 200 dbar	±0.1 dBar	0.005 dbar	0.04 s
Oxygen	ADM Elektronik	Potentiometric (Clark electrode)	0 - 150 % sat	±2 % sat	0.02 % sat.	3 s (63 %)
Temperature	ADM Elektronik	Pt 100	-2 - 38 °C	±0.01 °C	0.001 °C	0.12 s
Electrical conductivity	ADM Elektronik	7-pole-cell	0 - 6 mS/cm	±2 µS/cm	0.1 µS/cm	0.05 s
pH	AMT GmbH	Potentiometric (Ag /AgCl)	0 - 14 pH	0.02 pH	0.02 pH	1 s (63 %)
Chlorophyll <i>a</i>	Turner designs	Fluorescence exc. 465 nm / fl. 696 nm	0.03 - 500 µg/L		0.01 µg/L	1 s
CDOM	Turner designs	Fluorescence exc. 325 nm / fl. 470 nm	0.15 - 1250 ppbQS	± 5 %	0.01 ppbQS	1 s
Turbidity	Seapoint sensors, Inc.	Mie backscattering	0 - 750 FTU	± 2 %	< 0.001 %	0.1 s
PAR (400-700 nm)	LI-COR®	Photon flux density	0 - 10 µmol/(s·m <sup>2</sup> )	± 5 %	0.01 µmol/(s·m <sup>2</sup> )	10 µs
Cyanobacteria (Freshwater, Phycocyanin)	Turner designs	Fluorescence exc. 590 nm / fl. ≥ 645 nm	0 - 4500 ppb		0.1 µg/L	1 s

**Table A.2.** Parameters specifications of weather station (Vaisala Weather Transmitter WXT520)

Instrument	Measuring range	Accuracy	Output Resolution	Response time
Wind speed	0 - 60 m/s	±3 % at 10 m/s	0.1 m/s	0.25 s
Wind direction	0 - 360°	±3.0°	1°	0.25 s
Rain amount	- (collecting area 60 cm <sup>2</sup> )	better than 5 %, weather dependent	0.01 mm	-
Rain intensity	0 - 200 mm/h	- (broader range with reduced accuracy)	-	-

### B. Instrument detection limit (P.3)

**Table B.1.** Instrument detection limit (IDL) ( $3 \cdot \sigma$ ) of inductively coupled plasma mass spectrometry (Dionex, ICS-1000)

Elements	Units	IDL	Elements	Units	IDL	Elements	Units	IDL
Li	µg/L	0.019	Cr	µg/L	0.008	Mo	µg/L	0.004
B	µg/L	0.322	Mn	µg/L	0.029	Cd	µg/L	0.000
Na	mg/L	0.005	Fe	µg/L	0.253	Sb	µg/L	0.016
Mg	mg/L	0.000	Co	µg/L	0.001	Cs	µg/L	0.003
Al	mg/L	0.251	Ni	µg/L	0.005	Ba	µg/L	0.013
P	µg/L	2.87	Cu	µg/L	0.052	Tl	µg/L	0.003
K	mg/L	0.005	Zn	µg/L	0.213	Pb	µg/L	0.004
Ca	mg/L	0.008	As	µg/L	0.005	U	µg/L	0.000
Ti	µg/L	0.054	Rb	µg/L	0.039			
V	µg/L	0.003	Sr	µg/L	0.005			

**Table B.2.** Instrumental detection limits (IDL) ( $2.82 \cdot \sigma$ ) of ion chromatography (X-Series 2, Thermo Fischer)

Ions	Fluoride	Chloride	Bromide	Nitrate	Phosphate	Sulfate
	mg/L	mg/L	mg/L	mg/L	mg/L	mg/L
IDL	0.02	0.06	0.14	0.07	0.09	0.05

**C. BIOLIFT statistic summary (P.4-5)**

**Table C.1.** BIOLIFT statistic summary in four scenarios

		<b>Max</b>	<b>Min</b>	<b>Mean</b>	<b>Median</b>	<b>Standard deviation</b>
<b>Temp</b> [°C]	<b>2016 Summer</b>	30.6	24.6	27.1	27.0	1.5
	<b>2017 Winter</b>	13.1	5.5	9.8	10.0	1.7
	<b>2017 Autumn</b>	27.8	22.9	24.8	24.7	1.1
	<b>2018 Spring</b>	24.0	10.8	17.1	17.3	2.3
<b>Chl<sub>a-f</sub></b> [µg/L]	<b>2016 Summer</b>	14.2	2.6	7.6	7.3	2.2
	<b>2017 Winter</b>	22.2	1.0	10.0	9.5	2.8
	<b>2018 Spring</b>	48.6	0.8	16.1	13.9	8.5
<b>Cyano<sub>PC</sub></b> [µg/L]	<b>2017 Autumn</b>	35.3	5.0	8.1	6.5	4.1
	<b>2018 Spring</b>	49.5	4.4	9.2	7.1	6.0
<b>EC<sub>25</sub></b> [µS/cm]	<b>2016 Summer</b>	443.6	311.1	394.4	387.4	26.3
	<b>2017 Winter</b>	486.1	416.4	447.8	444.2	11.0
	<b>2017 Autumn</b>	445.2	434.1	440.8	441.0	1.8
	<b>2018 Spring</b>	602.8	545.2	578.4	578.7	11.9
<b>Oxy-sat.</b> [%]	<b>2016 Summer</b>	206 %	42 %	108 %	103 %	33.8
		(> 150 % ultimate value)				
	<b>2017 Winter</b>	122 %	75 %	101 %	102 %	7.8
	<b>2017 Autumn</b>	182 %	52 %	82 %	80 %	21.4
		(>150 % ultimate value)				
	<b>2018 Spring</b>	243 %	49 %	88 %	76 %	33.2
		(> 150 %				

		<b>Max</b>	<b>Min</b>	<b>Mean</b>	<b>Median</b>	<b>Standard deviation</b>
		ultimate value)				
<b>pH</b>	<b>2016 Summer</b>	9.4	7.4	8.5	8.4	0.5
	<b>2017 Autumn</b>	9.5	6.5	7.9	7.9	0.4
	<b>2018 Spring</b>	9.3	7.6	8.2	8.1	0.3
<b>CDOM</b> [ $\mu\text{g/L}$ ]	<b>2016 Summer</b>	32.2	18.4	26.6	27.1	3.2
	<b>2017 Winter</b>	17.0	5.2	13.3	14.1	2.8
	<b>2017 Autumn</b>	16.2	10.9	13.6	13.8	1.2
	<b>2018 Spring</b>	14.8	1.9	9.2	9.3	2.2
<b>Turb</b> [FTU]	<b>2016 Summer</b>	10.0	1.9	4.5	4.3	1.6
	<b>2017 Winter</b>	75.8	3.6	12.9	8.3	12.8
	<b>2017 Autumn</b>	48.6	7.5	12.7	12.0	2.6
	<b>2018 Spring</b>	50.0	1.4	11.0	6.6	10.0
<b>PAR<sub>water</sub></b> [ $\mu\text{mol}/(\text{s}\cdot\text{m}^2)$ ] )]	<b>2016 Summer</b>	2196.0	0	36.7	0.5	128.0
	<b>2017 Winter</b>	1017.2	0	71.2	0.5	145.7
	<b>2018 Spring</b>	1943.8	0	104.5	9.9	221.2



#### **D. Matlab code for matrix calculation (P.6)**

*% Delete outliers*

Parameter (diff(Depth)==0)=NaN;

Parameter (Parameter<=0)=NaN;

*% Calculate matrix (0.1 m \* 3 hours)*

t\_q=(0 : 3/24 : Total days);

d\_q=(0 : 0.1 : Max depth);

Q\_Parameter (Max depth\*10, Total days \*24/3) = zeros;

for t\_loop=1 : days \*24/3

    for d\_loop=1 : depth\*10

        Q\_Parameter (d\_loop, t\_loop)=mean(Parameter (Parameter >= 0 & Time > (t\_loop.\*3/24 - 2/24) & Time <= (t\_loop.\*3/24 + 2/24) & Depth > (d\_loop.\*0.1 - 0.075) & Depth <= (d\_loop.\*0.1 + 0.075)));

    end

end

### E. Vertical-temporal data graph (P.7-10)

**Fig.E.1.** Vertical-temporal data measured by multi-sensor system (BIOLIFT) in 2016-Summer

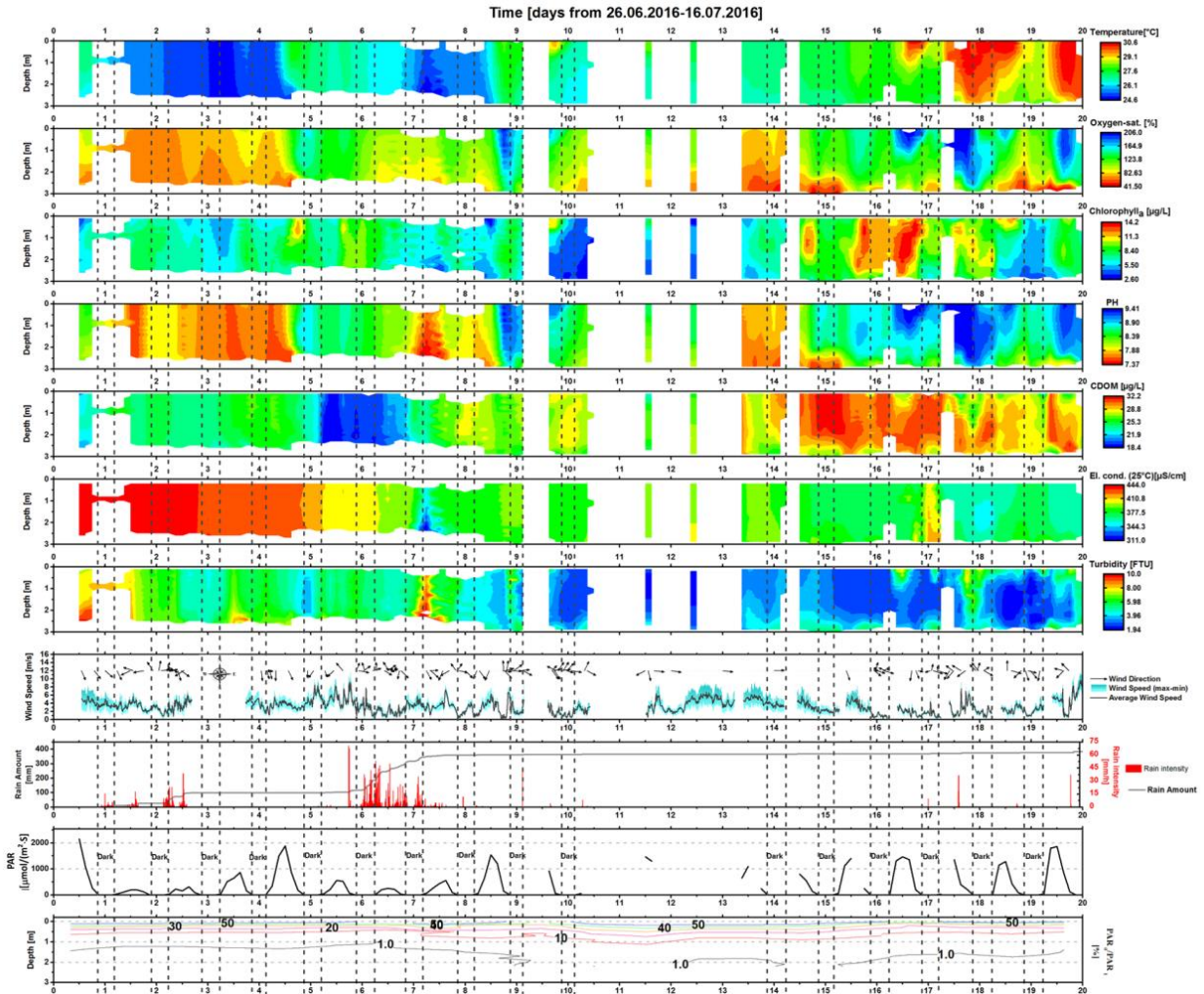
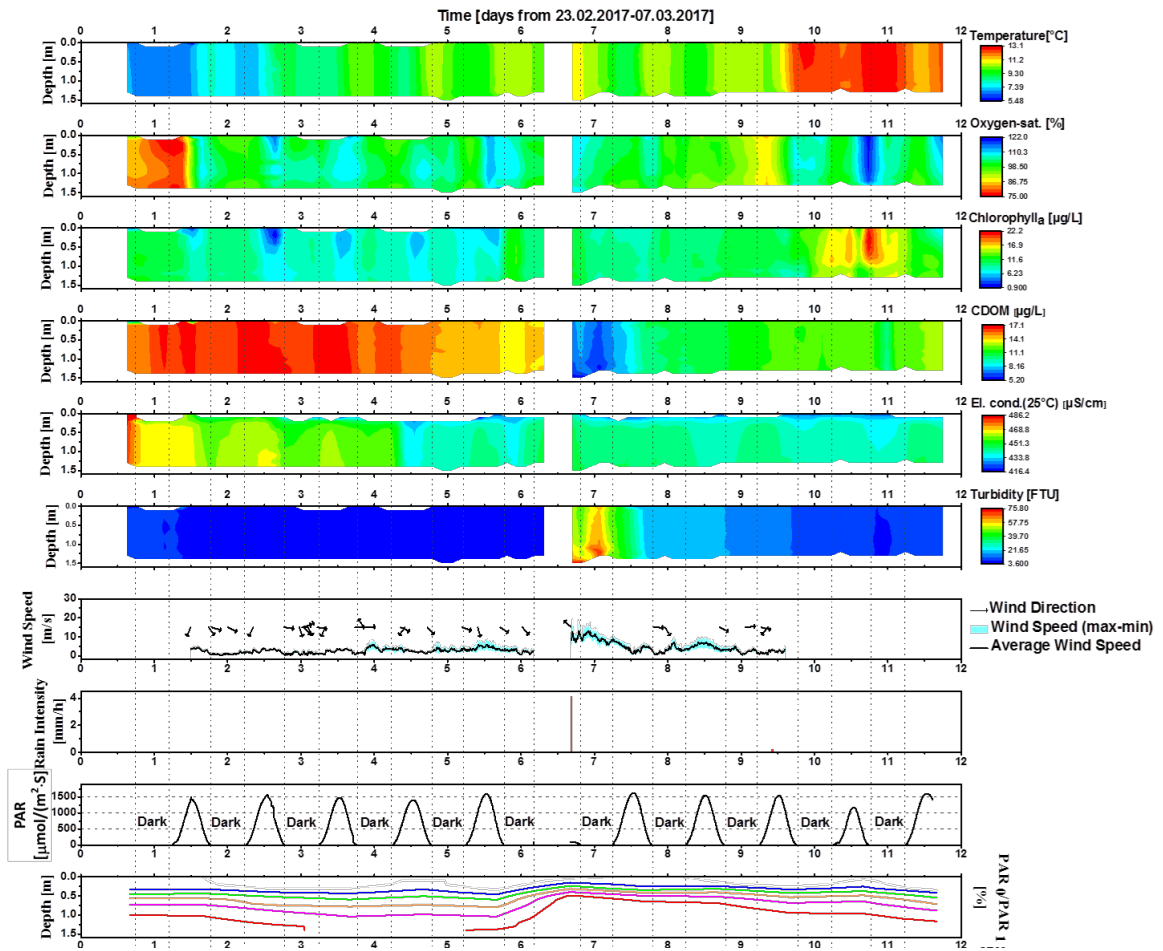
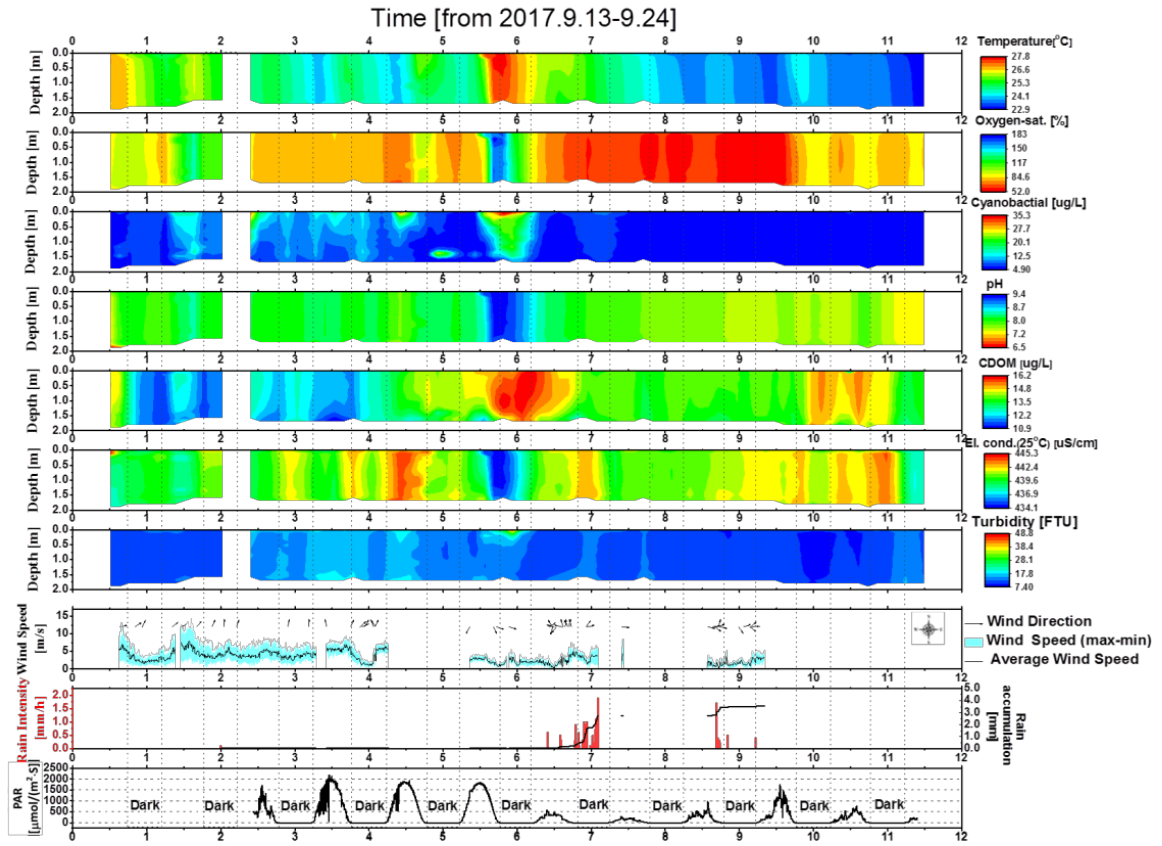


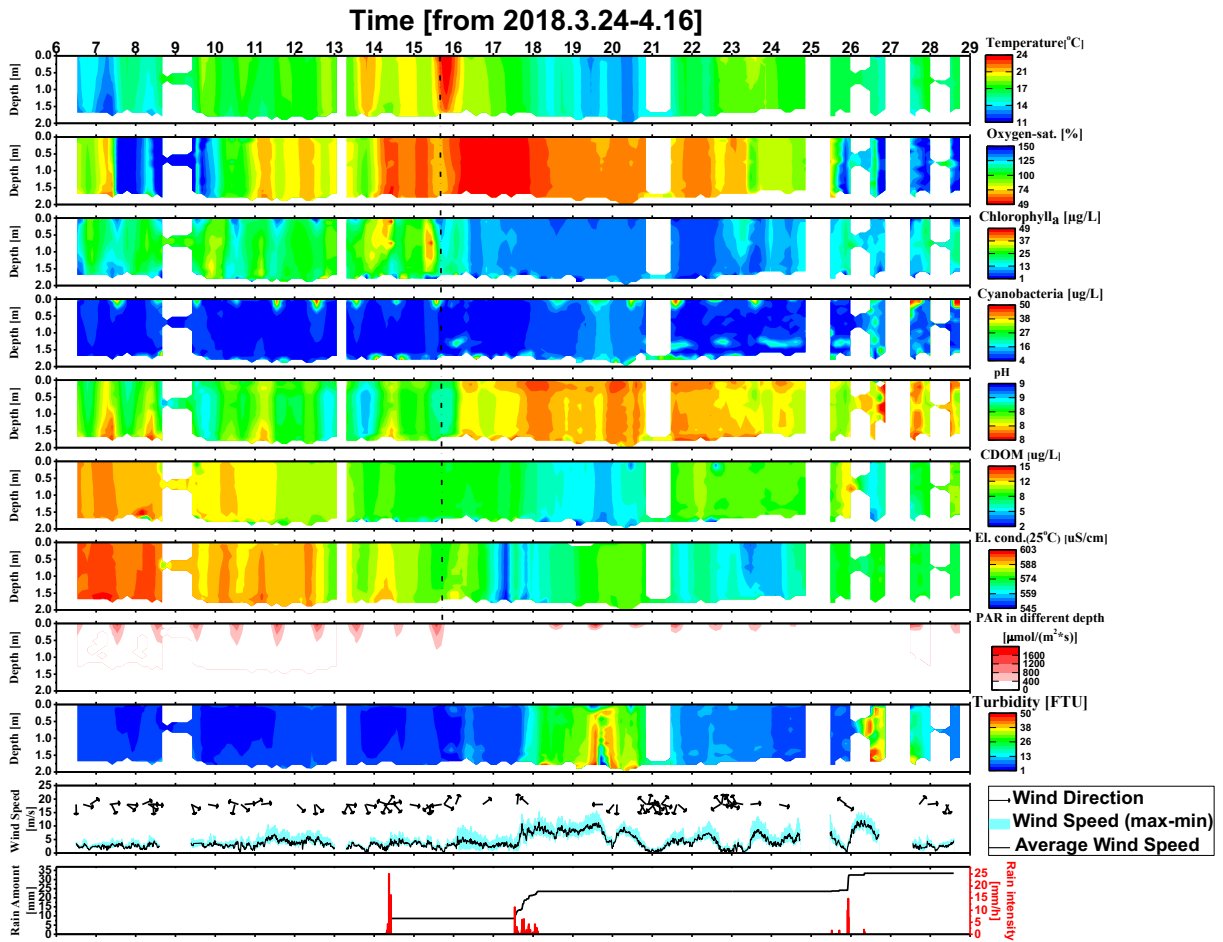
Fig.E.2. Vertical-temporal data measured by the multi-sensor system (BIOLIFT) in 2017-Winter



**Fig.E.3.** Vertical-temporal data measured by the multi-sensor system (BIOLIFT) in 2017-Autumn



**Fig.E.4.** Vertical-temporal data measured by the multi-sensor system (BIOLIFT) in 2018-Spring



## Appendix B.2 Identifying spatio-temporal dynamics of trace metals in shallow eutrophic lakes on the basis of a case study in Lake Taihu, China



ELSEVIER

Contents lists available at ScienceDirect

Environmental Pollution

journal homepage: [www.elsevier.com/locate/envpol](http://www.elsevier.com/locate/envpol)



## Identifying spatio-temporal dynamics of trace metals in shallow eutrophic lakes on the basis of a case study in Lake Taihu, China<sup>☆</sup>



Jingwei Yang<sup>a,\*</sup>, Andreas Holbach<sup>a,b</sup>, Andre Wilhelms<sup>a</sup>, Julia Krieg<sup>a</sup>, Yanwen Qin<sup>c</sup>, Binghui Zheng<sup>c</sup>, Hua Zou<sup>d</sup>, Boqiang Qin<sup>e</sup>, Guangwei Zhu<sup>e</sup>, Tingfeng Wu<sup>e</sup>, Stefan Norra<sup>a</sup>

<sup>a</sup> Institute of Applied Geosciences, Working Group Environmental Mineralogy and Environmental System Analysis (ENMINSA) Karlsruhe Institute of Technology, Kaiserstraße 12, 76131, Karlsruhe, Germany

<sup>b</sup> Department of Bioscience, Aarhus University, Frederiksborgvej 399, 4000, Roskilde, Denmark

<sup>c</sup> Chinese Research Academy of Environmental Sciences, Dayangfang 8, Anwai Beiyuan, Beijing, 100012, PR China

<sup>d</sup> School of Environmental and Civil Engineering, Jiangnan University, Wuxi, 214122, PR China

<sup>e</sup> Nanjing Institute of Geography & Limnology, Chinese Academy of Sciences, 73 East Beijing Road, 210008, Nanjing, PR China

### ARTICLE INFO

#### Article history:

Received 7 October 2019

Received in revised form

17 April 2020

Accepted 11 May 2020

Available online 14 May 2020

#### Keywords:

Sediment

Water quality

Pollution risk assessment

Cluster analysis

Online measurement

### ABSTRACT

In shallow eutrophic lakes, metal remobilization is closely related to the resuspension and eutrophication. An improved understanding of metal dynamics by biogeochemical processes is essential for effective management strategies. We measured concentrations of nine metals (Cr, Cu, Zn, Ni, Pb, Fe, Al, Mg, and Mn) in water and sediments during seven periods from 2014 to 2018 in northern Lake Taihu, to investigate the metal pollution status, spatial distributions, mineral constituents, and their interactions with P. Moreover, an automatic weather station and online multi-sensor systems were used to measure meteorological and physicochemical parameters. Combining these measurements, we analyzed the controlling factors of metal dynamics. Shallow and eutrophic northern Lake Taihu presents more serious metal pollution in sediments than the average of lakes in Jiangsu Province. We found chronic and acute toxicity levels of dissolved Pb and Zn (respectively), compared with US-EPA "National Recommended Water Quality Criteria". Suspended particles and sediment have been polluted in different degrees from uncontaminated to extremely contaminated according to German pollution grade by LAWA (Bund/Länder-Arbeitsgemeinschaft Wasser). Polluted particles might pose a risk due to high resuspension rate and intense algal activity in shallow eutrophic lakes. Suspended particles have similar mineral constituents to sediments and increased with increasing wind velocity. Al, Fe, Mg, and Mn in the sediment were rarely affected by anthropogenic pollution according to the geoaccumulation index. Among them, Mn dynamics is very likely associated with algae. Micronutrient uptake by algal will affect the migration of metals and intensifies their remobilization. Intensive pollution of most particulate metals were in the industrialized and down-wind area, where algae form mats and decompose. Moreover, algal decomposition induced low-oxygen might stimulate the release of metals from sediment. Improving the eutrophication status, dredging sediment, and salvaging cyanobacteria biomass are possible ways to remove or reduce metal contaminations.

© 2020 Elsevier Ltd. All rights reserved.

### 1. Introduction

Lakes are a sink for many trace metals. Naturally, metals contained in soil materials can be translocated into lake ecosystems by erosion and surface runoff (Garrett, 2000; Siegel, 2002). Erosion is a

large problem and might increase under climate change (more intensive precipitation events). Moreover, there is growing concern that the natural cycling rates of many metals are being altered by human activities. Pollutants from urban, industrial, and agricultural sources are released into the environment and entering the lake, which exacerbates the problem (Cai et al., 2015a).

Some metals are essential for biological systems, acting as both structural and catalytic components of proteins and enzymes, but they may be toxic when critical concentrations are exceeded. These include Zn, Cu, Fe, Mn, Mg, and Ni (Chen et al., 2018; Magnitskiy,

<sup>☆</sup> This paper has been recommended for acceptance by Maria Cristina Fossi.

\* Corresponding author.

E-mail address: [jingwei.yang@kit.edu](mailto:jingwei.yang@kit.edu) (J. Yang).

2011). Other metals, such as Pb and Cr, are harmful contaminants even in trace amounts (Zheng et al., 2013). Benthic biota and other organisms ingest metal particles by accumulating them in their tissues (Yin et al., 2011). This allows metals to enter food chains, which might ultimately affect humans through fish/shellfish consumption and drinking water (Tao et al., 2012).

We examined Lake Taihu in a case study of a shallow lake that has experienced accelerated nutrient and trace metal pollution accompanying rapid urban and agricultural expansion in its watershed. Accelerated nutrient loading and resultant algal bloom issues have caused great concern among researchers and the public, with numerous studies having addressed sources and impacts of excessive nutrient loading (Paerl et al., 2011; Qin et al., 2004a; Xu et al., 2008). The risks associated with metal pollution in eutrophic lakes are equally important but have rarely been addressed so far. Trace metals in organisms (e.g., fish, zoobenthos, microalgae) have been proved to pose a threat to human health in the Lake Taihu area (Fu et al., 2013; Hao et al., 2013; Kong et al., 2016; Yuan et al., 2015; Zeng et al., 2012). Therefore, it is necessary to investigate the ecological risks of trace metal pollution in lake water and sediments. Due to the lack of suspended particle and lake sediment criteria in current Chinese surface water standards, few studies have evaluated the particulate metal pollution risks of Lake Taihu.

In the Taihu basin, trace metals originate primarily from urban runoff and industrial discharge, such as from electrical machinery, pharmaceutical industry, chemical production, automobile exhausts, and waste incineration (Cai et al., 2015b; Cheung et al., 2003). Once metals have entered the lakes, they are easily deposited on the sediment surfaces through adsorption and coagulation and react as a source of secondary pollution (Liu et al., 2017).

Most of the suspended matter is due to resuspended surface sediments and algal biomass in the shallow eutrophic Lake Taihu, which is characterized by high resuspension rates and high biological activity (Wang et al., 2001; Yang et al., 2019; Zhu et al., 2015). In eutrophic lakes, heavy metal remobilization is often closely related to nutrient remobilization as both regularly adsorb to similar mineral fractions in the sediments (Bolan et al., 2003; Chen et al., 2017; Zan et al., 2011). Moreover, algal blooms may decrease the concentrations of dissolved metals in the water due to uptake by algae (Chen et al., 2008; Sunda, 2012).

A thorough understanding of metal pollution status and spatio-temporal dynamics is the prerequisite of effective water management and pollution prevention. This study assessed the metal pollution in water and sediments in Lake Taihu based on international standards. We investigated the concentrations of dissolved and particulate Fe, Mn, Mg, Al, Cu, Cr, Zn, Ni, and Pb in water samples, and the amount of these metals in sediment samples. Further, we examined metal spatial distributions and temporal dynamics in different seasons and studied the interaction between P and metals. Spatial-temporal water quality conditions were determined by using online multi-sensor arrays. The objectives of the current study are 1) the metal pollution status in water and sediments as well as their potential ecological risks; 2) the influence of lake shallowness on particulate metal dynamics; 3) the influence of lake eutrophication on metal spatial distributions and temporal dynamics.

## 2. Materials and methods

### 2.1. Study area

Northern Lake Taihu is the most polluted area due to discharge from industries mainly located in the Northwest (close to Zhushan Bay) (Li et al., 2011). Our study was conducted in northern Lake

Taihu, including Zhushan Bay, Meiliang Bay, and Gonghu Bay (Fig. 1). These bays have an average depth of 1.9 m. Due to the lake shallowness and frequent wind speeds, sediment resuspension rates in Lake Taihu are higher than many other lakes worldwide (Qi et al., 2019). The relatively long water residence times of about 300 days promote the accumulation of pollutants in the lake (Zhang et al., 2008).

Lake Taihu is facing severe eutrophication problems. From 2007 to 2017, the mean annual chlorophyll-*a* in the lake increased from 18 to 40  $\mu\text{g L}^{-1}$ , total N remained to exceed 2  $\text{mg L}^{-1}$ , and total P was over 75  $\mu\text{g L}^{-1}$  (Qin et al., 2019). Dominant southeasterly winds transport surface cyanobacterial blooms into the northern bays, aggravating water quality problems (Qin, 2008). Metals, which uptake by cyanobacteria, might also be carried to northern bays and settled in the local sediments.

### 2.2. Field methodology

The sampling area was divided into four sub-regions, including Zhushan Bay, Meiliang Bay, Gonghu Bay, and open lake (Fig. 1). We sampled the lake water and/or sediments during seven individual sampling campaigns from 2014 to 2018. Details can be found in Table 1.

#### 2.2.1. Water and sediment sample collection

In order to assess the spatial patterns of metals in northern Lake Taihu, we collected near-surface (0.2 m) water samples at 62 different locations by traditional organic glass water sampler.

To investigate the metal temporal dynamics, we collected water samples once per day from campaign four to seven at one location that 250 m away from the shoreline in outer Meiliang Bay (Fig. 1a). Specifically, the location is near the Taihu Laboratory for Lake Ecosystem Research (TLLER), which can offer electricity to the depth-profile multiple-sensor-system (BIOLIFT) for sampling. Sampling was done by a pump that connected to BIOLIFT at three different depths, surface ( $\sim 0.2$  m), intermediate (half of the depth), and bottom (depend on the depth). We collected 189 water samples at TLLER in total and calculated the mean value of three depths for subsequent analysis.

To assess the role of sediments as a source or sink for metal pollution in the lake, we applied two types of devices for collecting sediment samples (Fig. 1b). A Van Veen Grab Sampler (KC Denmark A/S, Silkeborg, Denmark) was used to obtain surface sediment samples at 20 locations throughout the northern lake. Moreover, a Uwitec Corer (Uwitec, Mondsee, Austria) was applied for taking 19 sediment cores. Limited by the sampling tubes, the maximal depth of the cores is 50 cm.

#### 2.2.2. Continuous online measurement of lake physicochemical parameters and meteorological data

In the meantime of pumping water samples, BIOLIFT measured physicochemical parameters in the water at TLLER station during campaign four to seven (Yang et al., 2019). The measured parameters used in this study were temperature (Temp) [ $^{\circ}\text{C}$ ], pH-value, oxygen saturation (Oxy-sat) [%], and electrical conductivity (EC) [ $\mu\text{S cm}^{-1}$ ]. EC was calculated and reported as at 25  $^{\circ}\text{C}$  (EC<sub>25</sub>), which is a proxy for dissolved ionic components (Reluy et al., 2004). The pH sensor broke in February 2017, so no data were available after that date.

To investigate the spatial differences in water quality, we applied a towed underwater multi-sensor system (BIOFISH) (Holbach et al., 2013), which was dragged behind a boat at 1 m depth at the junction of Meiliang Bay and Gonghu Bay on two days (29th November and December 2, 2015). The measured parameters were colored dissolved organic matter (CDOM) [ $\mu\text{g L}^{-1}$ ], turbidity



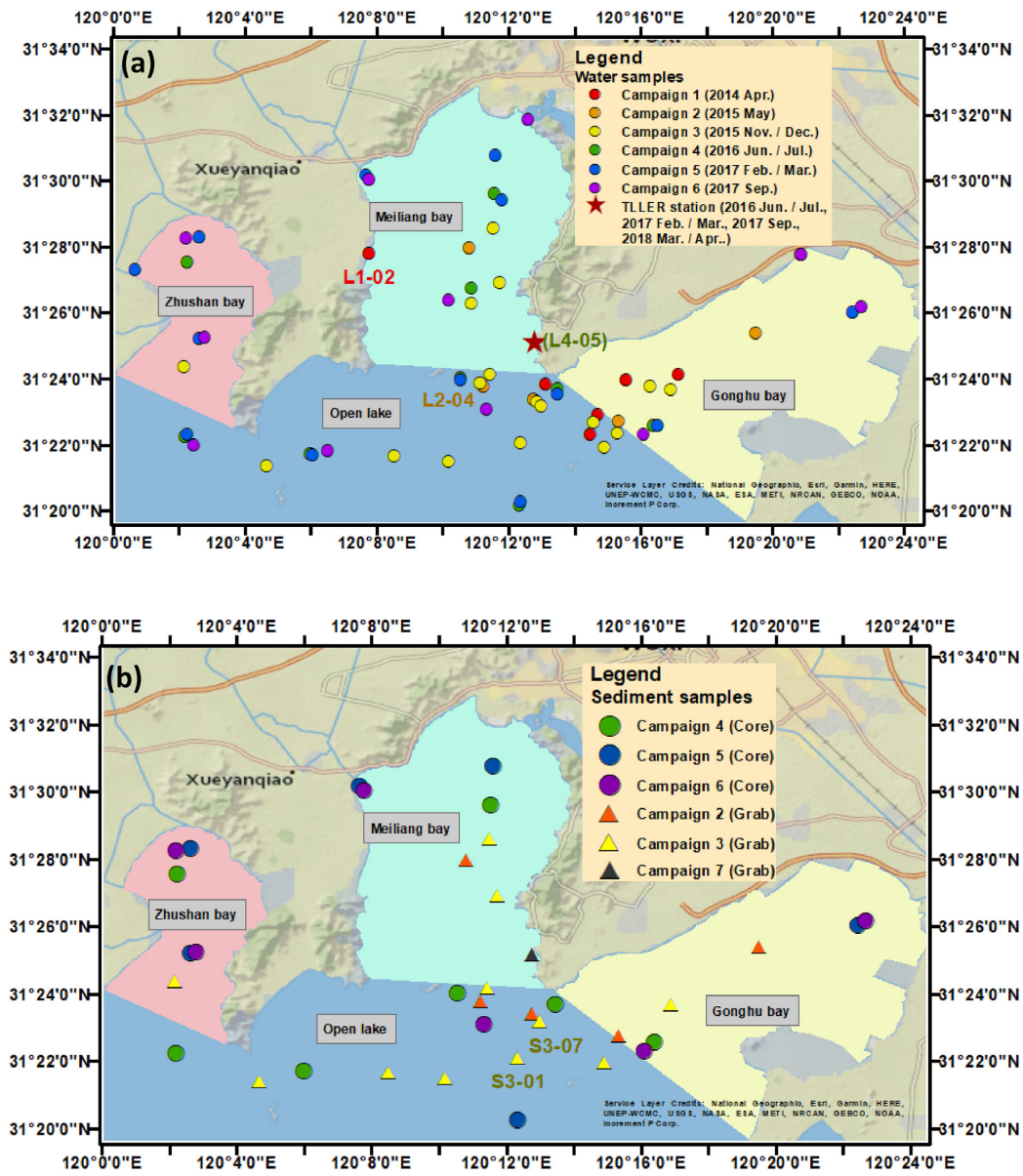


Fig. 1. a) Water samples locations and campaigns, campaign seven was only conducted at TLLER station; b) Sediment sampling sites (sediment core/grab) in different campaigns (map source: National Geographic Basemap).

Table 1  
 Sampling campaign details.

Campaign	Start Date	End Date	No. of Water Samples	No. of Sediment Samples	Location
1	2014-04-06	2014-04-08	17	–	TLLER, ML, GH
2	2015-05-09	2015-05-10	17	5	ML, GH
3	2015-11-03	2015-12-03	44	11	ML, GH, ZS
4	2016-06-27	2016-07-15	73	39	TLLER, ML, GH, ZS
5	2017-02-23	2017-03-06	38	40	TLLER, ML, GH, ZS
6	2017-09-14	2017-09-23	44	25	TLLER, ML, GH, ZS
7	2018-03-19	2018-04-16	80	1	TLLER

\*Taihu Laboratory for Lake Ecosystem Research station (TLLER), Meiliang Bay (ML), Gonghu Bay (GH), Zhushan Bay (ZS).

(Turb) [FTU], and EC [ $\mu\text{S cm}^{-1}$ ].

Meteorological data, including wind speed ( $\text{m s}^{-1}$ ), wind direction ( $^\circ$ ), and rainfall (mm), were recorded at an automatic weather station at TLLER every hour from campaign four to seven. Monthly average rainfall and wind speed were calculated for subsequent seasonal dynamics analysis.

### 2.3. Sample preparation

#### 2.3.1. Water samples

Water samples were pretreated, according to Yang et al. (2019). Cellulose-acetate filters with a pore size of  $0.45 \mu\text{m}$  were used to separate particles. For analyzing the dissolved Fe, Mn, Mg, Al, Cu, Cr, Zn, Ni, and Pb, filtered water samples were measured with ion chromatography (IC; ICS-1000, Thermo Fischer Scientific, Waltham, USA) and inductively coupled plasma mass spectrometry (ICP-MS; X-Series 2, Thermo Fischer Scientific, Waltham, USA).

To analyze the particulate Fe, Mn, Mg, Al, Cu, Cr, Zn, Ni, Pb and P, the filters were completely digested in 65%  $\text{HNO}_3$ , 40% HF, and 65%  $\text{HClO}_4$  (all super-pure grades) sequentially in Teflon beakers (Bock, 1974; Hu and Qi, 2013). The samples were constricted through the heating plate at  $175\text{--}200^\circ\text{C}$  in a fume hood. The digested samples were transferred into polypropylene bottles with 1%  $\text{HNO}_3$  in 10 mL and stored at  $4^\circ\text{C}$  until further analysis. Blank filters and certified standard soil and sediment material (GXR-2 and SL-1 (Govindaraju, 1994)) were also incorporated in digestion processes for quality control purposes.

#### 2.3.2. Sediment samples

The sediment cores were sliced into smaller layers directly after sampling. The first two layers were 2 cm and 3 cm, and the rest were 5 cm thick. One layer of sediment cores or one surface sediment sample collected by the Van Veen Grab Sampler is considered as one sample. A total of 121 samples were collected at 19 sampling points. Each layer was homogenized by stirring before freeze-drying (FreeZone 2.5, Labconco, Kansas, USA). Sediments were then sieved ( $<2 \text{ mm}$ ) and milled in a vibratory disc mill (Scheibenschwingmühle TS, SIEBTECHNIK, Mülheim an der Ruhr, Germany). Finally, sediment samples were analyzed by Wavelength Dispersive X-ray Fluorescence (WDX; S4 Explorer, Bruker, Billerica, USA) for Fe, Mn, Mg, Al, and P as well as Energy Dispersive X-ray Fluorescence (EDX; Epsilon 5, Malvern Panalytical, Malvern, UK) for Cr, Cu, Zn, Ni, and Pb. To explore the relationship between suspended particulate matter (SPM) and surface sediment, we measured their mineral composition in campaign three (11 sediment samples and 12 loaded filters). They were investigated with scanning electron microscopy (SEM-EDX; Quanta 650, Thermo Fischer Scientific, Waltham, USA) and X-ray diffraction (XRD; D8 Discover, Bruker, Billerica, USA).

### 2.4. Data processing and analysis

Shapiro-Wilk test (significance level 0.05) was first applied to test the assumption of normality for metal concentrations (Shapiro and Wilk, 1965). All the sample locations and water quality distribution were mapped with ArcGIS (10.5.1). Temporal diversity and cluster analysis graphs, as well as statistical analysis, were created and performed by OriginPro software (Origin Professional, 2016; OriginLab, Northampton, USA). Linear regressions were done between metals in SPM and sediment. Spearman's correlation coefficient was calculated to analyze the correlation between elements in two-tailed testing.

#### 2.4.1. Partition coefficients ( $K$ )

Partition coefficients of element M ( $K_M$ ) provide information on

the ratio changes between particulate and dissolved M (Comber et al., 1995; Feng et al., 2017),

$$K_M = C_{M(\text{SPM})} / C_{M(\text{diss})} \quad (1)$$

where  $C_{M(\text{SPM})}$  is the concentration of the element M in the SPM ( $\mu\text{g g}^{-1}$ ), and  $C_{M(\text{diss})}$  is the concentration in the dissolved phase ( $\mu\text{g L}^{-1}$ ).  $K_M$  integrates the effects of adsorption/desorption processes, external pollution, and sedimentation/resuspension of particles (Barreto et al., 2011; Pertsemli and Voutsas, 2007).

#### 2.4.2. Geoaccumulation index ( $I_{\text{geo}}$ )

Geoaccumulation index ( $I_{\text{geo}}$ ) developed by Müller (1986) was classified into seven groups and used to evaluate the anthropogenic influence levels of metal concentrations (Formula (2)).

$$I_{\text{geo}} = \log_2 (C_M / 1.5 \times B_M) \quad (2)$$

where  $C_M$  is the measured concentration of metal M in the sediment,  $B_M$  is the geochemical background of metal M reported by Zhu et al. and Zhao et al. (2014).

#### 2.4.3. Hierarchical cluster analysis

Cluster analysis was made to group the suspended Fe, Mn, Mg, and Al as well as sedimentary Fe, Mn, Mg, Al, Cr, Cu, Zn, Ni, Pb, and P according to their similarities. In a cluster analysis, the elements will be grouped according to the aim of having small differences between the object in a group and having significant differences between the groups. The Ward method of hierarchical cluster analysis (or minimum-variance method) (Ward, 1963) with minimal increase of the sum of squared errors and absolute correlation distance were used. The hierarchical methods start by placing its own cluster for each object and grouping different objects to a cluster, where the smallest difference is given.

## 3. Results

### 3.1. Metal pollution status

#### 3.1.1. Water and sediment pollution with dissolved and particulate metals

To assess the metal pollution status in water and sediments and its potential ecological risks, the minimum (Min), maximum (Max), median (Med), skewness (Skew) and kurtosis (Kurt) of the analyzed samples from all the campaigns were calculated (Table 2). Shapiro-Wilk's normality test revealed non-normal distributions of all metal concentrations in water and sediments.

The medians of dissolved metals decrease in order:  $\text{Al} > \text{Fe} > \text{Mg} > \text{Zn} > \text{Ni} > \text{Cu} > \text{Mn} > \text{Cr} > \text{Pb}$ . Data were compared to threshold values by EPA U.S., 2016. All the medians of dissolved metals were below the threshold values (Table 2). However, two samples from Meiliang Bay had a concentration of dissolved Pb above the threshold of  $2.5 \mu\text{g L}^{-1}$  ( $3.2 \mu\text{g L}^{-1}$  and  $7.7 \mu\text{g L}^{-1}$ ). Moreover, the maximum of dissolved Zn ( $164.4 \mu\text{g L}^{-1}$ ) was above the threshold of  $120 \mu\text{g L}^{-1}$ . The respective sample was taken near TLLER.

The medians of particulate metals decrease in order:  $\text{Al} > \text{Fe} > \text{Mg} > \text{Mn} > \text{Zn} > \text{Cr} > \text{Ni} > \text{Cu} > \text{Pb}$ . We assessed the metal pollution levels in SPM and sediments according to German pollution grades by LAWA (LAWA, 1998a). Because natural background concentrations of the Taihu basin are in the range of German background values, the evaluation method of LAWA can be applied for Lake Taihu (LAWA, 1998b). The LAWA-classification is divided into groups I to IV, from unpolluted to extremely polluted (Table 2). The pollution levels for the medians of metals in SPM

**Table 2**  
 Statistical parameters and criterion/background values of metals in water, suspended particles and bottom sediments of Lake Taihu.

Metals	Min	Max	Med	Skew	Kurt	Criterion & Background value						
Water ( $\mu\text{g L}^{-1}$ ) n = 313						CMC						CCC
Al	3.3	603.7	71.7	2.5	12.1	–	–	–	–	–	–	–
Mg	5.4	11.8	8.1	0.0	–1.1	–	–	–	–	–	–	–
Cr	0.1	1.4	0.4	2.1	6.2	16	–	–	–	–	–	11
Mn	0.2	163.3	1.7	10.2	121.3	–	–	–	–	–	–	–
Fe	1.3	652.8	49.3	4.9	43.8	–	–	–	–	–	–	1000
Ni	0.6	26.7	2.6	920.2	6.5	470	–	–	–	–	–	52
Cu	1.2	5.4	2.3	738.1	1.7	13	–	–	–	–	–	9
Zn	0.9	164.4	5.3	2719.1	6.0	120	–	–	–	–	–	120
Pb	0.0	7.8	0.1	57.3	12.4	65	–	–	–	–	–	2.5
<b>Suspended particles (SPM; <math>\text{mg kg}^{-1}</math>) n = 271</b>						LAWA						
						I (UC)	I–II	II (MC)	II–III	III (SC)	III–IV	IV (EC)
Al	6107.0	406057.6	98108.6	1.6	6.9	–	–	–	–	–	–	–
Mg	1169.9	41815.6	10704.7	1.8	7.4	–	–	–	–	–	–	–
Cr	4.7	531.4	129.5	2.0	5.8	$\leq 80$	$\leq 90$	$\leq 100$	$\leq 200$	$\leq 400$	$\leq 800$	$> 800$
Mn	115.6	4408.7	1425.8	1.1	2.6	–	–	–	–	–	–	–
Fe	3053.7	207510.1	45453.9	1.9	8.1	–	–	–	–	–	–	–
Ni	17.0	342.8	88.0	14.3	223.3	$\leq 30$	$\leq 40$	$\leq 50$	$\leq 100$	$\leq 200$	$\leq 400$	$> 400$
Cu	6.2	289.6	57.4	16.2	265.4	$\leq 20$	$\leq 40$	$\leq 60$	$\leq 120$	$\leq 240$	$\leq 480$	$> 480$
Zn	20.6	1813.8	337.1	5.6	48.0	$\leq 100$	$\leq 150$	$\leq 200$	$\leq 400$	$\leq 800$	$\leq 1600$	$> 1600$
Pb	0.2	240.5	45.0	2.6	9.6	$\leq 25$	$\leq 50$	$\leq 100$	$\leq 200$	$\leq 400$	$\leq 800$	$> 800$
<b>Sediment (<math>\text{mg kg}^{-1}</math>) n = 121</b>						$I_{\text{geo}}$ ( $\text{L g}^{-1}$ )		Background 1 <sup>a</sup>		Background 2 <sup>b</sup>		
						Med	Max	/Baseline ( $I_{\text{geo}}$ )				
Al	29493.5	47832.4	36412.9	0.5	–0.7	–2.2 (UC)	–1.8 (UC)	108,600 <sup>c</sup>		–		
Mg	4269.1	10099.9	6391.6	0.8	0.4	–0.4(UC)	0.3(UC/MC)	5600		–		
Cr	9.7	498.0	105.3	2.2	4.0	–0.2(UC)	2.1(MC/SC)	79.3		71.8		
Mn	387.3	2091.5	712.7	1.4	1.9	–0.1(UC)	1.4(MC)	511		–		
Fe	14517.2	33421.2	21249.8	0.4	–0.3	–1.4(UC)	–0.7(UC)	36,700		–		
Ni	30.2	153.2	49.7	2.0	3.6	–0.2(UC)	2.1(MC/SC)	19.5		19.8		
Cu	26.2	236.6	39.3	2.0	3.1	0.5 (UC/MC)	2.9(MC/SC)	18.9		15.4		
Zn	49.8	558.3	105.6	1.8	2.2	0.3 (UC/MC)	2.7(MC/SC)	59		65.1		
Pb	22.9	151.7	36.7	0.5	–0.2	0.6 (UC/MC)	2.6(MC/SC)	15.7		15.7		

CMC: criterion maximum concentration by US EPA – a measure of acute toxicity.  
 CCC: criterion continuous concentration by US EPA – a measure of chronic toxicity.  
 LAWA: Bund/Länder-Arbeitsgemeinschaft Wasser—a german criterion.  
 UC uncontaminated, MC moderately contaminated, SC strongly contaminated, EC extremely contaminated.  
<sup>a</sup> (Tao et al., 1983).  
<sup>b</sup> (Zhu et al., 2005).  
<sup>c</sup> (Zhao et al., 2014).

were ordered as  $\text{Zn} \approx \text{Ni} \approx \text{Cr}$  (II-III) >  $\text{Cu}$  (II) >  $\text{Pb}$  (I-II). The maximum value of  $\text{Pb}$  was classified as strongly polluted (III). The largest amounts of  $\text{Ni}$ ,  $\text{Cr}$ , and  $\text{Cu}$  were in the range of strongly to extremely polluted (groups III-IV), they were either located in Zhushan Bay or at TLLER station. Ten samples showed heavy pollution with  $\text{Zn}$  (IV), which were collected at TLLER station.

Median concentrations of  $\text{Cu}$ ,  $\text{Cr}$ ,  $\text{Ni}$ ,  $\text{Pb}$ ,  $\text{Zn}$ ,  $\text{Mg}$ ,  $\text{Mn}$ , and  $\text{Al}$  in the sediments were above the reported background values (Table 2) (Tao et al., 1983; Zhao et al., 2014; Zhu et al., 2005). Geo-accumulation index ( $I_{\text{geo}}$ ) for  $\text{Al}$ ,  $\text{Mg}$ ,  $\text{Cr}$ ,  $\text{Mn}$ ,  $\text{Fe}$ ,  $\text{Ni}$ ,  $\text{Cu}$ ,  $\text{Zn}$ , and  $\text{Pb}$  were calculated by reported background values. They were at uncontaminated to moderately contaminated levels. Among them,  $\text{Al}$ ,  $\text{Fe}$ ,  $\text{Mg}$ , and  $\text{Mn}$  were less affected by human activity ( $I_{\text{geo}} < 2$ ). The pollution levels by LAWA for the medians of metals in the sediment were ordered as  $\text{Cr}$  (II-III) >  $\text{Ni}$  (II) >  $\text{Zn} \approx \text{Cu} \approx \text{Pb}$  (I-II). The maxima values of  $\text{Cr}$ ,  $\text{Ni}$ ,  $\text{Zn}$ , and  $\text{Cu}$  were found in Zhushan Bay. The  $\text{Pb}$  maxima (group II) occurred at the junction of Meiliang Bay and Gonghu Bay.

### 3.1.2. Comparison with other lakes

Metal concentrations in the sediments, partition coefficient (K) of metals, and  $I_{\text{geo}}$  values were compared to that of the other lakes reported in the literature (Table 3).  $\text{Cr}$ ,  $\text{Ni}$ ,  $\text{Cu}$ ,  $\text{Zn}$ , and  $\text{Pb}$  in the sediments of Lake Taihu were slightly higher than the average value of lakes in China (Xu et al., 2017). In general,  $I_{\text{geo}}$  of  $\text{Cr}$ ,  $\text{Ni}$ ,  $\text{Cu}$ , and  $\text{Zn}$

in Lake Taihu was higher than the mean value of lakes in the same province (Jiangsu) (Xu et al., 2017), but they were still at the same level. Lake Taihu contained a higher level of  $\text{Pb}$  pollution (uncontaminated to moderately contaminated) than that in Jiangsu Province.  $\text{K}$  of  $\text{Cr}$ ,  $\text{Ni}$ ,  $\text{Cu}$ ,  $\text{Zn}$ ,  $\text{Pb}$ ,  $\text{Mn}$  and  $\text{Fe}$  in Lake Taihu were much higher than that in Lake Doirani and mean value of Loch Coire nan Arr, Loch Doilet, and Loch Urr (Gormley-Gallagher et al., 2015; Pertsemli and Voutsas, 2007). These lakes have deeper depth, bigger surface area, and lower nutrients levels.

### 3.2. The influence of lake shallowness on the particulate metal dynamics

To exclude regional differences, we only considered the data collected at TLLER station in the analysis of metal dynamics. Wind-induced resuspension from sediment is a vital source of SPM in shallow lakes. We compared the monthly average wind speed and monthly mean SPM over six months (Fig. 2a). The increase of SPM is in accordance with the increase in wind speed. According to XRD and SEM-EDX results, SPM mainly contains the minerals muscovite, chlorite, kaolinite, and quartz, which are also abundant in the sediments.

According to  $I_{\text{geo}}$  result,  $\text{Al}$ ,  $\text{Fe}$ ,  $\text{Mg}$ , and  $\text{Mn}$  were less affected by anthropogenic pollution. We did cluster analysis for particulate  $\text{Al}$ ,  $\text{Fe}$ ,  $\text{Mg}$ , and  $\text{Mn}$  (Fig. 2b). Among them,  $\text{Al}$ ,  $\text{Fe}$ , and  $\text{Mg}$  were grouped

**Table 3**  
Comparison of metals in sediments,  $I_{geo}$  and K in Lake Taihu with other lakes.

Name	Depth (m)	Area (km <sup>2</sup> )	Type	Cr	Ni	Cu	Zn	Pb	Mg	Mn	Fe
Sediment (mean; mg kg <sup>-1</sup> )											
Taihu	1.9	2250	HT	141.2	57.2	62.2	157.5	37.2	6666.5	823.9	21159.3
China <sup>a</sup>	—	—	—	77	40.5	39.1	112.6	34.1	—	—	—
$I_{geo}$ (mean; L g <sup>-1</sup> )											
Taihu	1.9	2250	HT	-0.04	-0.04	0.81	0.49	0.63	-0.36	0.003	-1.4
Jiangsu Prov. <sup>b</sup>	—	—	—	-0.8	-0.25	0.16	0.24	-0.5	—	—	—
K (mean; min-max)											
Taihu	1.9	2250	HT	375.3	58.2	322.3	120.7	514.7	1.3	1087.8	1351.0
Doirani <sup>c</sup>	5–8.5	28	EHT	0.01–0.79	0.02–0.63	0.01–0.63	0.04–0.13	0.03–0.79	—	2.51–100.00	2.51–31.62
Three Lakes in Scotland <sup>d</sup>	Max.11; 16; 13.2	0.13; 0.52; 0.47	OMT	2.2	1.2	3.2	—	270	—	31	—

HT: Hypertrophic; EHT: Eutro-hypertrophic; OMT: Oligio-mesotrophic

<sup>a</sup> Mean value of 110 lakes in China (Xu et al., 2017).

<sup>b</sup> Mean value of lakes in Jiangsu Province (Xu et al., 2017).

<sup>c</sup> Lake in Greece (Pertsemli and Voutsas, 2007).

<sup>d</sup> Loch Coire nan Arr, Loch Doilet, and Loch Urr in Scotland (Gormley-Gallagher et al., 2015).

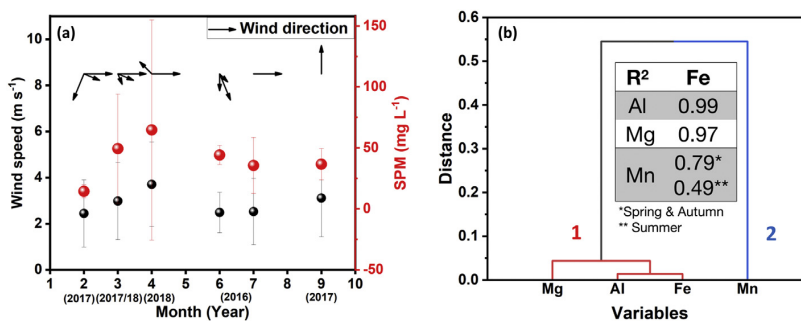


**Fig. 2.** a) Wind direction, wind speed and suspended particles (SPM) (The wind direction and frequency over 20% are marked as arrows, which point in the direction the wind is blowing towards.); b) Cluster analysis and linear relationship ( $R^2$ ) of particulate Al, Mg, Mn, and Fe.

together and had strong linear relationships (Table in Fig. 2b,  $R^2 \geq 0.97$ ).

### 3.3. The influence of lake eutrophication on the metal temporal dynamics

Metals uptake by floating cyanobacteria will be treated as SPM due to loaded on the filters with cyanobacteria together during sampling. Moreover, metal dynamics might be influenced by algae uptake, especially in cyanobacteria dominated summer (Duan et al., 2009). Algae uptake process and accumulation affinities are different depending on the type of metal and algal species (Jahan et al., 2004). This might be one reason for the weak correlation between particulate Fe and Mn in Fig. 2b. A strong linear relationship between Fe and Mn was found in spring and autumn (February, March, April, September) ( $R^2 = 0.79$ ), but not in summer (June and July) ( $R^2 = 0.49$ ) (Table in Fig. 2b).

P is an essential micronutrient in algal growth and dynamic. Different from N, particulate P is the dominant fraction and likely adsorbs on Fe-, Mn-, Mg- and Al- complexes in sediments (Selig, 2003; Weihrauch and Opp, 2018; Xu et al., 2015). Therefore, P dynamics are very likely associated with these metals. Partition coefficients (K) were calculated for the particulate and dissolved

**Table 4**  
Spearman's correlation coefficient between  $K_P$  and  $K_{Mg}$ ,  $K_{Al}$ ,  $K_{Mn}$ ,  $K_{Fe}$ .

	$K_{Mg}$	$K_{Al}$	$K_{Mn}$	$K_{Fe}$
$K_P$	0.04	-0.02	0.31	0.00

matter of P, Mg, Al, Mn, and Fe at TLLER station. In Table 4,  $K_P$  had a better correlation with  $K_{Mn}$  than  $K_{Mg}$ ,  $K_{Al}$ , and  $K_{Fe}$  by Spearman's correlation (non-normal distribution).

Eutrophication might result in changes in pH and oxygen and have effects on metal dynamics (Ansari et al., 2010). The average Oxy-sat in June, April, and September were below 100% (Fig. 3a). Both average pH and Oxy-sat values were high in March (8.3 and 112%) and July (8.5 and 117%). Influenced by the East Asian summer monsoon, rainfall was the highest from June to September, with its maximum (359.2 mm) in June 2016 (Fig. 3b). Temp was also the highest during this time, with an average of 25.7 °C. The temporal pattern of dissolved Mn was similar to EC<sub>25</sub>. Both show low values in June and July. The concentrations of dissolved Ni and Cu also decreased in June (Fig. 3d). Contrarily, the dissolved Pb, Cr, Fe, and Al were elevated at the same time.

### 3.4. The influence of lake eutrophication on metal spatial distributions

The regional discrepancy of cyanobacterial bloom and the location of pollution sources might influence the metal spatial distribution in the sediments. The cluster analysis was made for Pb, Fe, Mn, Cr, Cu, Zn, Ni, P, Al, and Mg in the surface sediment. The ten elements were divided into four groups (Fig. 4a). We found the spatial distributions of those elements were similar in surface sediments (Fig. 4b–f), with high values in Zhushan Bay.

Pb, Fe, and Mn were grouped into cluster 1. The highest concentration of Pb (151.7 mg kg<sup>-1</sup>), Fe (143,239.5 mg kg<sup>-1</sup>), and Mn (8738.0 mg kg<sup>-1</sup>) were found at the junction of Meiliang Bay and

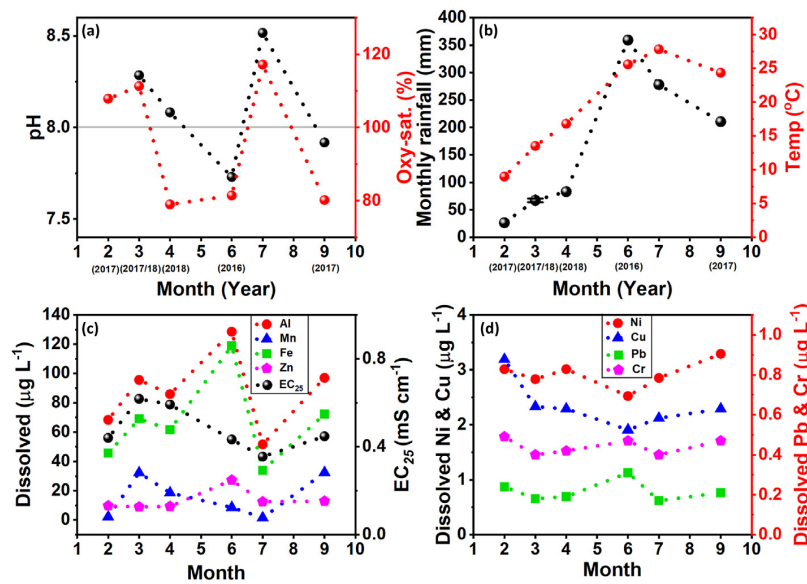


Fig. 3. a) Monthly average rainfall and temperature; b) Monthly average pH and oxygen saturation (the gray line represents 100% oxygen saturation); Temporal changes of c) dissolved Al, Mn, Fe, Zn, and electrical conductivity at 25 °C, d) dissolved Ni, Cu, Pb, and Cr.

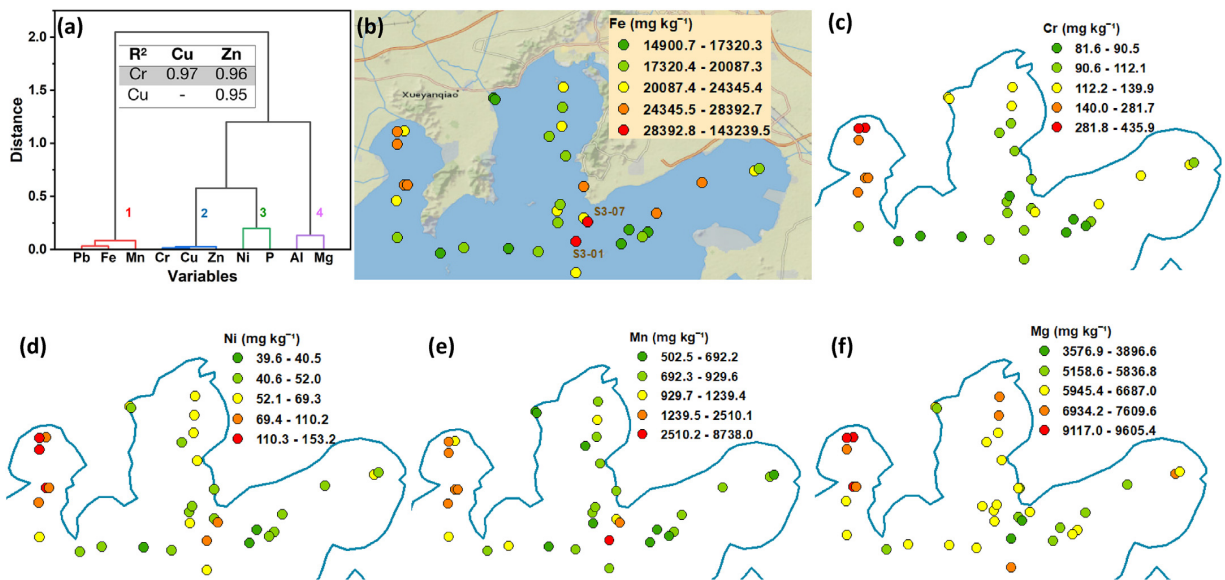


Fig. 4. a) Cluster analysis of Pb, Fe, Mn, Cr, Cu, Zn, Ni, P, Al and Mg and linear regression ( $R^2$ ) of Cu, Cr, and Cu; Spatial distribution of b) Fe, c) Cr, d) Ni, e) Mn, and f) Mg in the surface sediment.

Gonghu Bay in November 2015, where Ni ( $105.9 \text{ mg kg}^{-1}$ ) was also high at the same time. Cr, Cu, and Zn were grouped into cluster 2. They had excellent linear relationships, with  $R^2$  between each heavy metals were all above or equal to 0.95 (Table in Fig. 4a). P and Ni had closer relevance than other metals and merged into cluster 3. Moreover, Al and Mg were grouped into cluster 4.

To know the water quality differences in the small area at the

junction of Meiliang Bay and Gonghu Bay, water quality distribution maps measured by BIOFISH were presented in an area of less than  $10 \times 10 \text{ km}^2$  (Fig. 5). There were differences in the  $EC_{25}$  readings from 420 to  $490 \mu\text{S cm}^{-1}$ , CDOM from  $20 \text{ to } 38 \mu\text{g L}^{-1}$ , and Turb from 1 to 10 FTU. In general, in the two days, the distribution pattern of  $EC_{25}$ , CDOM, and Turb did not show pronounced differences. The spatial patterns indicate external pollution inflow into

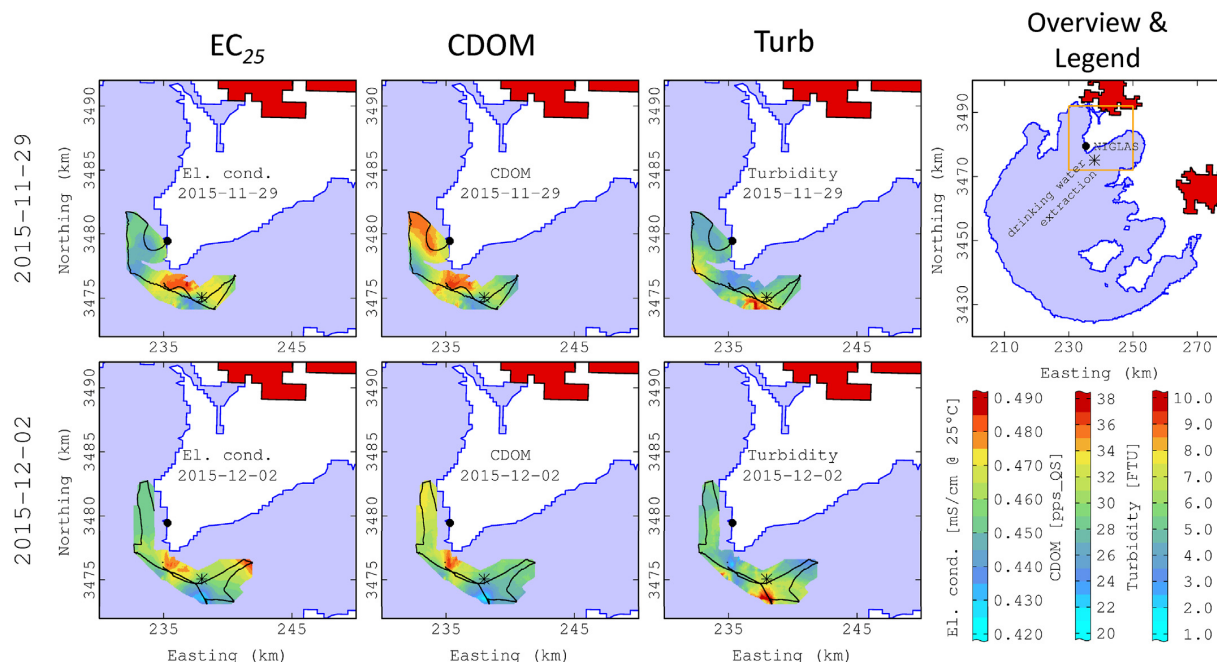


Fig. 5. Geostatistical modeling of the BIOFISH measured on November 29, 2015 and December 02, 2015. Parameters including electrical conductivity at 25 °C, colored dissolved organic matter, and turbidity.

the lake in this region during measurement, with high EC<sub>25</sub>, CDOM, and low Turb.

#### 4. Discussion

##### 4.1. Assessment of metal pollution risk

According to the water quality criteria by EPA U.S (2016) (Table 2), most of the dissolved metals are harmless for aquatic life in their current concentrations. With rare exceptions, two samples with dissolved Pb that exceeded CCC could cause chronic toxicity. One is located at a wetland outflow towards the Meiliang Bay (L1-02). The wetland linked to urban runoff has a connection to the lake, where the Pb pollution could originate. The other sample is located at the transition between Meiliang Bay and Gonghu Bay (L2-04) in May 2015, where the highest Pb in the sediment was observed in November 2015 (S3-01, S3-07) (Fig. 4). Combining BIOFISH data (Fig. 5), there might be Pb pollution input into the lake in this region, which is then adsorbed onto surface sediment or sedimented. Pb was the least contaminating heavy metal in the sediment and SPM, according to LAWA. However, Pb in the sediment was still more polluted than the majority of lakes in Jiangsu Province and China (Table 3).

Dissolved Zn at L4-05 (TLER) is considered acutely toxic. Zn contributes most to heavy metal pollution in SPM, which showed heavy pollution (grade IV) in ten samples from TLLER station. Heavily contaminated Zn was most likely coming from the wastewater of industrial plants.

The metal amounts in the sediment were higher than the reported background value and the average of lakes in Jiangsu Province and China (Tables 2 and 3), which indicates a strong influence of human activities in Lake Taihu. In general, the pollution levels of the evaluated heavy metals in the sediment covered the whole range from low (I-II) to heavy pollution (IV), according to

LAWA. The pollution status of SPM was more severe than that of surface sediment. This is likely because heavy metals tend to adsorb onto fine particles, which are easier to be resuspended (Qin et al., 2004b). Heavy metals can furthermore be accumulated in organic matter or inorganic colloidal matter, which are also enriched in SPM (Zhu et al., 2005). Strongly enriched particulate heavy metals can be a potential risk for aquatic life (Zhu et al., 2005).

##### 4.2. Lake shallowness accelerated metal remobilization

Lake shallowness is another reason for the accumulation of metals in SPM. Partition coefficient (K) of metals in shallow Lake Taihu was much higher than that of other reported deeper lakes (Lake Doirani, Loch Coire nan Arr, Loch Doilet, and Loch Urr) (Table 3). Due to the shallowness, wind-induced resuspension from sediment easily happens in Lake Taihu (Qi et al., 2019; Wang et al., 2001). The seasonal changes of SPM based on the water volume are highly related to wind speed, with a peak in April 2018 (Fig. 2a). At the same time, the maximum of particulate Cu, Cr, and Ni were measured, which might originate from sediment resuspension under strong wind.

Mineral compositions in SPM and sediment were similar, mainly muscovite, chlorite, kaolinite, and quartz. Because SPM is a basic material forms the bottom sediments (Kravchishina and Dara, 2014). Moreover, in shallow lakes, surface sediment is an essential source of SPM by resuspension. Al, Fe, Mg, and Mn were rarely affected by human activity, according to I<sub>geo</sub>. Particulate Fe, Al, and Mg had strong correlations ( $R^2 \geq 0.97$ ), which indicates their possible incorporation in chlorite.

##### 4.3. Lake eutrophication might affect metal dynamics

Eutrophication causes changes in the physical and chemical quality of water and sediments, which affects the whole

ecohydrology of lakes (Dubey and Dutta, 2019). Most of the dissolved elements decreased in June 2016 (Fig. 3c and d), which were likely related to the dilution of heavy rainfall produced by the summer monsoon. However, dissolved Pb, Cr, Fe, and Al were elevated in June 2016, which might be related to low Oxy-sat. Anaerobic conditions in June 2016, likely caused by algal death and consequent decomposition at the sediment surface, might have stimulated the mobilization of metals from sediments (Atkinson et al., 2007; Morford and Emerson, 1999; Zhu et al., 2013).

During the same time, particulate Fe and Mn had a weak correlation (Fig. 2b). The ratio of Fe/Mn varied in different seasons depending on the redox condition, are controlled by the processes of photosynthesis and decomposition (Naeher et al., 2013; Shen et al., 2007). Mn usually needs a slightly higher redox potential than Fe and can more easily be adsorbed on the surface of fine granules than Fe (Boyd, 2015; Song et al., 2009).

Moreover, algal activities might have a more significant effect on Mn dynamics than that of Fe.  $K_p$  had a better correlation with  $K_{Mn}$  than  $K_{Mg}$ ,  $K_{Al}$ , and  $K_{Fe}$  (Table 4), which might refer to the Mn-bound P. P and Mn might be subject to similar biochemical processes. Under the algal growth stage, P and Mn uptake by algae as micronutrients (Kong and Gao, 2005). Previous studies showed that phytoplankton has a great impact on the manganese cycle in freshwater, by transforming manganese from the soluble Mn(II) state to intracellularly bound Mn and particulate Mn(III/IV) oxides (Knauer et al., 1999).

#### 4.4. Lake eutrophication might change metal spatial distributions

Eutrophication of lakes is caused by over-enrichment with nutrients. Excess phosphorus inputs into lakes are mainly coming from agriculture (Bennett et al., 2001), whereas Ni can be incorporated in hydrated phosphates and are typical trace elements in phosphorites and phosphate fertilizers (Safa et al., 2013; Singh et al., 2017). This might explain the combined Ni and P in cluster 3 (Fig. 4a). In addition, we measured high concentrations of P, Ni, Fe, and Mn in the surface sediment at the junction of Meiliang Bay and Gonghu Bay in November 2015 (Fig. 4b, d, e). The BIOFISH data assessed at the same time and place (Fig. 5), indicate an inflow into the lake with high  $EC_{25}$ , CDOM, and low Turb. The potential pollution source is probably coming from phosphate fertilization contaminated by P and Ni (Safa et al., 2013; Singh et al., 2017). Moreover, P and Ni have an affinity to be bound on Fe and Mn oxides/hydroxides and might, therefore, have similar distribution patterns (Kabata-Pendias, 2010).

In the surface sediments, the concentrations of all evaluated metals were high in the sediments of Zhushan Bay (Fig. 4b–f). Among them, Cr, Cu, and Zn in cluster 2 showed strong linear correlations ( $R^2 \geq 0.95$ ) between any two of them in the sediments (Fig. 4a). Moreover, we observed a declining trend from the river mouths (connected to Zhushan Bay) to the open lake. This indicates possible severe pollution coming from inflowing rivers. Rivers in the northwest of Lake Taihu are closed to industrial parks, the metals most likely discharged from industrial wastewater (Bian et al., 2016; Yu et al., 2012).

According to  $I_{geo}$ , Mg, Al, Mn, and Fe were not affected much by human activity (Table 2). Therefore, sediment deposition difference might be a more important reason for the high metal concentrations in Zhushan Bay. According to a previous study (Luo et al., 2004), most of the sediments are deposited in the western shore area and the northern bays. Sediment regional depositions difference is likely related to the current circulation pattern induced by the prevailing wind forcing in Taihu (Luo et al., 2004). Furthermore, bioaccumulation of metals, particularly by bacteria and algae, can also affect their distributions. The dominating southeast wind in

summer makes the down-wind location of Zhushan Bay a favorable area for serious cyanobacteria accumulation (Wu et al., 2015; Zhang et al., 2017). The algae can act as a pollution transporter. By deposition of dead algae biomass, accumulated metals and P will be returned to the local sediments in Zhushan Bay (Monteiro et al., 2012; Webb et al., 2020).

## 5. Conclusions

Through a systematic assessment using criteria of USA-EPA and LAWA,  $I_{geo}$ , partition coefficient (K), cluster analysis, and online multi-sensor systems for meteorological and physicochemical parameters, this study analyzed dissolved, suspended, and sedimentary total Pb, Fe, Mn, Cr, Cu, Zn, Ni, Al, and Mg during seven periods from 2014 to 2018. During the measurement period, most of the dissolved trace metals posed no risk to aquatic life in Lake Taihu. Only Pb and Zn might cause chronic and acute toxicity, respectively. However, we consider particulate metals in SPM and bottom sediment risks in shallow eutrophic lakes.

Lake shallowness and eutrophication will aggravate the remobilization of metals. The sediments, as a pollution sink and source, are essential for the re-introduction of pollutants into the water column, especially in shallow lakes like Taihu. Wind-induced resuspension can easily lead to an increase of suspended metals in shallow lakes. In the eutrophic lakes, algal uptake has a great impact on the metal cycles and distributions. Sediment pollution in the down-wind location from blooms is worse. Moreover, algal decomposition might lower Oxy-sat. and accelerate the release of metals from sediment.

In general, in shallow eutrophic lakes, the improvement of the eutrophic state can alleviate the metal pollution problem. Controlling excessive fertilization can reduce nutrient and also metal inputs due to fertilizer impurities. Cyanobacteria salvaging and sediment dredging in down-wind areas might mitigate metal pollution by removing metals from aquatic systems. A future long-term study with intra- and extracellular metal extraction experiments should be conducted to help us understand the interaction mechanism between metals and different algal species.

## Author statement

**Jingwei Yang:** Data analyze, Laboratory work, Writing and editing; **Andreas Holbach:** Supervision, Methodology, Software; **Andre Wilhelms:** Field trip, Laboratory work; **Julia Krieg:** Part of Field trip, Laboratory work; **Yanwen Qin, Binghui Zheng, Hua Zou:** Project coordination and management, Reviewing and editing; **Boqiang Qin, Guangwei Zhu:** Providing monitoring data, Reviewing and editing; **Tingfeng Wu:** Help for field trip, Reviewing and suggestion; **Stefan Norra:** Supervision

## Declaration of competing interest

The authors declare that they have no known competing financial interests or personal relationships that could have appeared to influence the work reported in this paper.

## Acknowledgments

This work was supported by the Federal Ministry of Education and Research of Germany (BMBF, grant.-no.: 02WCL1336B) and National Natural Science Foundation of China (NSFC, grant.-no.: 41671494). The first author was supported by the China Scholarship Council. Thanks to the Taihu Laboratory for Lake Ecosystem Research (TLLER) for providing monitoring site and meteorological data. The authors also thank Prof. Hans W. Paerl (University of

North Carolina at Chapel Hill, Institute of Marine Sciences) for his critical reading and valuable comments.

### Appendix A. Supplementary data

Supplementary data to this article can be found online at <https://doi.org/10.1016/j.envpol.2020.114802>.

### References

Ansari, A.A., et al., 2010. Eutrophication: Causes, Consequences and Control. Springer, Dordrecht. <https://doi.org/10.1007/978-90-481-9625-8>.

Atkinson, C.A., et al., 2007. Effect of overlying water pH, dissolved oxygen, salinity and sediment disturbances on metal release and sequestration from metal contaminated marine sediments. *Chemosphere* 69, 1428–1437. <https://doi.org/10.1016/j.chemosphere.2007.04.068>.

Barreto, S.R.G., et al., 2011. Determination of partition coefficients of metals in natural tropical water. *Clean - Soil, Air, Water* 39, 362–367. <https://doi.org/10.1002/clen.201000271>.

Bennett, E.M., et al., 2001. Human impact on erodable phosphorus and eutrophication. *Bioscience* 51, 227–234.

Bian, B., et al., 2016. Distribution of heavy metals and benthic macroinvertebrates: impacts from typical inflow river sediments in the Taihu basin, China. *Ecol. Indic.* 69, 348–359. <https://doi.org/10.1016/j.ecolind.2016.04.048>.

Bock, R., 1974. *Aufschlußmethoden der Anorganischen und Organischen Chemie*. Wiley-VCH Verlag GmbH & Co. KGaA, Weinheim. <https://doi.org/10.1002/food.19740180622>.

Bolan, N.S., et al., 2003. Role of Phosphorus in (Im) mobilization and bioavailability of heavy metals in the soil-plant system. *Rev. Environ. Contam. Toxicol.* 177, 1–44. <https://doi.org/10.1007/0-387-21725-8>.

Boyd, C.E., 2015. *Water Quality*. Springer, Auburn.

Cai, Y., et al., 2015a. Comprehensive assessment of heavy metal contamination in surface sediments from the inflow rivers of Taihu basin. *Clean - Soil, Air, Water* 43, 1582–1591. <https://doi.org/10.1002/clen.201300886>.

Cai, Y., et al., 2015b. Influences of land use on sediment pollution across multiple spatial scales in Taihu basin. *Clean - Soil, Air, Water* 43, 1616–1622. <https://doi.org/10.1002/clen.201300888>.

Chen, C., et al., 2008. Mercury and arsenic bioaccumulation and eutrophication in Baiyangdian lake, China. *Water Air Soil Pollut.* 190, 115–127. <https://doi.org/10.1007/s11270-007-9585-8>.

Chen, L., et al., 2018. Heavy metals in food crops, soil, and water in the Lihe River watershed of the Taihu Region and their potential health risks when ingested. *Sci. Total Environ.* 615, 141–149. <https://doi.org/10.1016/j.scitotenv.2017.09.230>.

Chen, M., et al., 2017. An investigation of the effects of elevated phosphorus in water on the release of heavy metals in sediments at a high resolution. *Sci. Total Environ.* 575, 330–337. <https://doi.org/10.1016/j.scitotenv.2016.10.063>.

Cheung, K.C., et al., 2003. Assessment of metal and nutrient concentrations in river water and sediment collected from the cities in the Pearl River Delta, South China. *Chemosphere* 52, 1431–1440. [https://doi.org/10.1016/S0045-6535\(03\)00479-X](https://doi.org/10.1016/S0045-6535(03)00479-X).

Comber, S.D.W., et al., 1995. Comparison of the partitioning of trace metals in the Humber and Mersey estuaries. *Mar. Pollut. Bull.* 30, 851–860.

Duan, H., et al., 2009. Two-decade reconstruction of algal blooms in China's Lake Taihu. *Environ. Sci. Technol.* 43, 3522–3528. <https://doi.org/10.1021/es8031852>.

Dubey, D., Dutta, V., 2019. Environmental Concerns and Sustainable Development. Springer Singapore, Singapore. [https://doi.org/10.1007/978-981-13-6358-0\\_5](https://doi.org/10.1007/978-981-13-6358-0_5).

EPA U.S., 2016. National Recommended Water Quality Criteria (Aquatic Life Criteria Table) [WWW Document]. <https://www.epa.gov/wqc/national-recommended-water-quality-criteria-aquatic-life-criteria-table>.

Feng, C., et al., 2017. Heavy metal partitioning of suspended particulate matter-water and sediment-water in the Yangtze Estuary. *Chemosphere* 185, 717–725. <https://doi.org/10.1016/j.chemosphere.2017.07.075>.

Fu, J., et al., 2013. Risk and toxicity assessments of heavy metals in sediments and fishes from the Yangtze River and Taihu Lake, China. *Chemosphere* 93, 1887–1895. <https://doi.org/10.1016/j.chemosphere.2013.06.061>.

Garrett, R.G., 2000. Natural sources of metals to the environment. *Hum. Ecol. Risk Assess.* 6, 945–963. <https://doi.org/10.1080/10807030091124383>.

Gormley-Gallagher, A.M., et al., 2015. The applicability of the distribution coefficient, KD, based on non-aggregated particulate samples from lakes with low suspended solids concentrations. *PLoS One* 10. <https://doi.org/10.1371/journal.pone.0133069>.

Govindaraju, K., 1994. 1994 Compilation of working values and sample description for 383 geostandards. *Geostand. Newsl.* 18, 1–158. <https://doi.org/10.1046/j.1365-2494.1998.53202081.x-1>.

Hao, Y., et al., 2013. Trace elements in fish from Taihu Lake, China: levels, associated risks, and trophic transfer. *Ecotoxicol. Environ. Saf.* 90, 89–97. <https://doi.org/10.1016/j.ecoenv.2012.12.012>.

Holbach, A., et al., 2013. Processes and environmental quality in the Yangtze River system water mass interaction in the confluence zone of the Daning River and the Yangtze River—a driving force for algal growth in the Three Gorges Reservoir. *Environ. Sci. Pollut. Res.* 20, 7027–7037. <https://doi.org/10.1007/s11356-012-1373-3>.

Hu, Z., Qi, L., 2013. Sample digestion methods. *Treat. Geochem.* Second 15, 87–109. <https://doi.org/10.1016/B978-0-08-095975-7.01406-6>.

Jahan, K., et al., 2004. Metal uptake by algae. *Waste Manag. Environ. II*, 223–232.

Kabata-Pendias, A., 2010. *Trace Elements in Soils and Plants*. CRC Press, London.

Knauer, K., et al., 1999. Manganese uptake and Mn(II) oxidation by the alga *Senedesmus subspicatus*. *Aquat. Sci.* 61, 44–58. <https://doi.org/10.1007/s000270050051>.

Kong, F., Gao, G., 2005. Hypothesis on cyanobacteria bloom-forming mechanism in large shallow eutrophic lakes (in Chinese). *J. China Univ. Pet.* 25, 589–595.

Kong, M., et al., 2016. Accumulation and risk assessment of heavy metals in sediments and zoobenthos (*Bellamyia aeruginosa* and *Corbicula fluminea*) from Lake Taihu. *Water Sci. Technol.* 73, 203–214. <https://doi.org/10.2166/wst.2015.483>.

Kravchishina, M.D., Dara, O.M., 2014. Mineral composition of the suspended particulate matter in the White Sea. *Oceanology* 54, 327–337. <https://doi.org/10.1134/S000143701402012X>.

LAWA, 1998a. *Beurteilung der Wasserbeschaffenheit von Fließgewässern in der Bundesrepublik Deutschland - Chemische Gewässergüteklassifikation, first ed.* Kulturbuchverl. Berlin.

LAWA, 1998b. *Zielvorgaben Zum Schutz Oberirdischer Binnengewässer (Berlin)*.

Li, Y., et al., 2011. Spatiotemporal patterns in nutrient loads, nutrient concentrations, and algal biomass in Lake Taihu, China. *Lake Reserv. Manag.* 27, 298–309. <https://doi.org/10.1080/07438141.2011.610560>.

Liu, J., et al., 2017. Heavy metal pollution status and ecological risks of sediments under the influence of water transfers in Taihu Lake, China. *Environ. Sci. Pollut. Res.* 24, 2653–2666. <https://doi.org/10.1007/s11356-016-7909-1>.

Luo, L., et al., 2004. Sediment distribution pattern mapped from the combination of objective analysis and geostatistics in the large shallow Taihu Lake, China. *J. Environ. Sci.* 16, 908–911. [https://doi.org/10.1001/0742\(2004\)06.0908.04](https://doi.org/10.1001/0742(2004)06.0908.04).

Magnitskiy, S., 2011. Nickel: the last of the essential micronutrients. *Agron. Colomb.* 29, 49–56.

Monteiro, C.M., et al., 2012. Metal uptake by microalgae: Underlying mechanisms and practical applications. *Biotechnol. Prog.* 28, 299–311. <https://doi.org/10.1002/btpr.1504>.

Morford, J.L., Emerson, S., 1999. The geochemistry of redox sensitive trace metals in sediments. *Geochem. Cosmochim. Acta* 63, 1735–1750. [https://doi.org/10.1016/S0016-7037\(99\)00126-X](https://doi.org/10.1016/S0016-7037(99)00126-X).

Müller, G., 1986. Schadstoffe in sedimenten - sedimente als schadstoffe. *Mitteilungen der Österreichischen Geol. Gesellschaft* 79, 107–126. <https://doi.org/10.1055/s-2007-1023171>.

Naeher, S., et al., 2013. Tracing bottom water oxygenation with sedimentary Mn/Fe ratios in Lake Zurich, Switzerland. *Chem. Geol.* 352, 125–133. <https://doi.org/10.1016/j.chemgeo.2013.06.006>.

Paerl, H.W., et al., 2011. Controlling harmful cyanobacterial blooms in a hyper-eutrophic lake (Lake Taihu, China): the need for a dual nutrient (N & P) management strategy. *Water Res.* 45, 1973–1983. <https://doi.org/10.1016/j.watres.2010.09.018>.

Pertsemli, E., Vousta, D., 2007. Distribution of heavy metals in lakes Doirani and Kerkin, northern Greece. *J. Hazard Mater.* 148, 529–537. <https://doi.org/10.1016/j.jhazmat.2007.03.019>.

Qi, C., et al., 2019. In situ resuspension rate monitoring method in the littoral zone with multi-ecotypes of a shallow wind-disturbed lake. *Environ. Sci. Pollut. Res.* 26, 7476–7485. <https://doi.org/10.1007/s11356-018-04059-0>.

Qin, B., et al., 2019. Why Lake Taihu continues to be plagued with cyanobacterial blooms through 10 years (2007–2017) efforts. *Sci. Bull.* 64, 354–356. <https://doi.org/10.1016/j.scib.2019.02.008>.

Qin, B., 2008. *Lake Taihu, China: Dynamics and Environmental Change*. Springer Science & Business Media, Berlin.

Qin, B., et al., 2004a. Dynamics of sediment resuspension and the conceptual schema of nutrient release in the large shallow Lake Taihu, China. *Chin. Sci. Bull.* 49, 54–64. <https://doi.org/10.1360/03wd0174>.

Qin, B., et al., 2004b. Dynamics of sediment resuspension and the conceptual schema of nutrient release in the large shallow Lake Taihu, China. *Chin. Sci. Bull.* 49, 54–64. <https://doi.org/10.1007/BF02901743>.

Reluy, F.V., et al., 2004. Development of an equation to relate electrical conductivity to soil and water salinity in a Mediterranean agricultural environment. *Aust. J. Soil Res.* 42, 381–388. <https://doi.org/10.1071/SR03155>.

Safa, M.A. El, et al., 2013. Environmental geochemistry of trace metals in Egyptian phosphorites, phosphate fertilizers and soils. *Sedimentol. Egypt* 21, 221–242.

Selig, U., 2003. Particle size-related phosphate binding and P-release at the sediment-water interface in a shallow German lake. *Hydrobiologia* 492, 107–118.

Shapiro, S.S., Wilk, M.B., 1965. An analysis of variance test for normality (complete samples). *Biometrika* 52, 591. <https://doi.org/10.2307/2333709>.

Shen, J., et al., 2007. Distribution and chemical fractionation of heavy metals in recent sediments from Lake Taihu, China. *Hydrobiologia* 581, 141–150. <https://doi.org/10.1007/s10750-006-0523-3>.

Siegel, F.R., 2002. *Environmental Geochemistry of Potentially Toxic Metals*. Springer-Verlag Berlin Heidelberg, Berlin. <https://doi.org/10.1007/978-3-662-04739-2>.

Singh, D.P., et al., 2017. *Plant-Microbe Interactions in Agro-Ecological Perspectives*. Springer, New Delhi.

Song, C., et al., 2009. Seasonal variations in chlorophyll-a concentrations in relation to potentials of sediment phosphate release by different mechanisms in a large Chinese shallow eutrophic lake (Lake Taihu). *Geomicrobiol. J.* 26, 508–515.



- <https://doi.org/10.1080/01490450903061119>.
- Sunda, W.G., 2012. Feedback interactions between trace metal nutrients and phytoplankton in the ocean. *Front. Microbiol.* 3, 1–22. <https://doi.org/10.3389/fmicb.2012.00204>.
- Tao, D., et al., 1983. Research on the background of heavy metals along bank of the lake (in Chinese). *J. Shanghai Teach. Coll.* 95–111.
- Tao, Y., et al., 2012. Characterization of heavy metals in water and sediments in Taihu Lake, China. *Environ. Monit. Assess.* 184, 4367–4382. <https://doi.org/10.1007/s10661-011-2270-9>.
- Wang, J., et al., 2001. Taihu Lake, lower Yangtze drainage basin: evolution, sedimentation rate the sea level. *Geomorphology* 41, 183–193. [https://doi.org/10.1016/S0169-555X\(01\)00115-5](https://doi.org/10.1016/S0169-555X(01)00115-5).
- Ward, J.J.H., 1963. Hierarchical grouping to optimize an objective function. *J. Am. Stat. Assoc.* 58, 236–244. <https://doi.org/10.1198/016214503000000468>.
- Webb, A.L., et al., 2020. Sources of elevated heavy metal concentrations in sediments and benthic marine invertebrates of the western Antarctic Peninsula. *Sci. Total Environ.* 698, 134268. <https://doi.org/10.1016/j.scitotenv.2019.134268>.
- Wehrauch, C., Opp, C., 2018. Ecologically relevant phosphorus pools in soils and their dynamics: the story so far. *Geoderma* 325, 183–194. <https://doi.org/10.1016/j.geoderma.2018.02.047>.
- Wu, T., et al., 2015. The influence of changes in wind patterns on the areal extension of surface cyanobacterial blooms in a large shallow lake in China. *Sci. Total Environ.* 518–519, 24–30. <https://doi.org/10.1016/j.scitotenv.2015.02.090>.
- Xu, H., et al., 2008. Nitrogen pollution status of various types of passing-by water bodies in upper reaches of Taihu Lake (in Chinese). *Chinese J. Ecol.* 27, 43–49.
- Xu, Y., et al., 2017. The current status of heavy metal in lake sediments from China: pollution and ecological risk assessment. *Ecol. Evol.* 7, 5454–5466. <https://doi.org/10.1002/ece3.3124>.
- Xu, Y., et al., 2015. pH dependent phosphorus release from waste activated sludge: contributions of phosphorus speciation. *Chem. Eng. J.* 267, 260–265. <https://doi.org/10.1016/j.cej.2015.01.037>.
- Yang, J., et al., 2019. Highly time-resolved analysis of seasonal water dynamics and algal kinetics based on in-situ multi-sensor-system monitoring data in Lake Taihu, China. *Sci. Total Environ.* 660, 329–339. <https://doi.org/10.1016/j.scitotenv.2019.01.044>.
- Yin, H., et al., 2011. Distribution, sources and ecological risk assessment of heavy metals in surface sediments from Lake Taihu, China. *Environ. Res. Lett.* 6, 0444012 <https://doi.org/10.1088/1748-9326/6/4/0444012>.
- Yu, T., et al., 2012. Distribution and bioavailability of heavy metals in different particle-size fractions of sediments in Taihu Lake, China. *Chem. Speciat. Bioavailab.* 24, 205–215. <https://doi.org/10.3184/095422912X13488240379124>.
- Yuan, H., et al., 2015. The accumulation and potential ecological risk of heavy metals in microalgae from a eutrophic lake (Taihu Lake, China). *Environ. Sci. Pollut. Res.* 22, 17123–17134. <https://doi.org/10.1007/s11356-015-4891-y>.
- Zan, F., et al., 2011. A 100 year sedimentary record of heavy metal pollution in a shallow eutrophic lake, Lake Chaohu, China. *J. Environ. Monit.* 13, 2788–2797. <https://doi.org/10.1039/c1em10385g>.
- Zeng, J., et al., 2012. Metal accumulation in fish from different zones of a large, shallow freshwater lake. *Ecotoxicol. Environ. Saf.* 86, 116–124. <https://doi.org/10.1016/j.ecoenv.2012.09.003>.
- Zhang, Limin, et al., 2008. Eutrophication status and control strategy of Taihu Lake. *Front. Environ. Sci. Eng. China* 2, 280–290. <https://doi.org/10.1007/s11783-008-0062-4>.
- Zhang, W., et al., 2017. Spatiotemporal distribution of eutrophication in Lake Tai as affected by wind. *Water (Switzerland)* 9, 200. <https://doi.org/10.3390/w9030200>.
- Zhao, S., et al., 2014. Relationship of metal enrichment with adverse biological effect in the Yangtze Estuary sediments: role of metal background values. *Environ. Sci. Pollut. Res.* 21, 464–472. <https://doi.org/10.1007/s11356-013-1856-x>.
- Zheng, S., et al., 2013. Distribution of metals in water and suspended particulate matter during the resuspension processes in Taihu Lake sediment, China. *Quat. Int.* 286, 94–102. <https://doi.org/10.1016/j.quaint.2012.09.003>.
- Zhu, G.W., et al., 2005. Heavy-metal contents in suspended solids of Meiliang Bay, Taihu Lake and its environmental significances. *J. Environ. Sci.* 17, 672–675.
- Zhu, M., et al., 2015. The influence of macrophytes on sediment resuspension and the effect of associated nutrients in a shallow and Large Lake (Lake Taihu, China). *PLoS One* 10, 1–20. <https://doi.org/10.1371/journal.pone.0127915>.
- Zhu, M., et al., 2013. Influence of algal bloom degradation on nutrient release at the sediment-water interface in Lake Taihu, China. *Environ. Sci. Pollut. Res.* 20, 1803–1811. <https://doi.org/10.1007/s11356-012-1084-9>.

**Identifying spatio-temporal dynamics of trace metals in shallow eutrophic lakes on the  
basis of a case study in Lake Taihu, China**

Jingwei Yang<sup>a\*</sup>, Andreas Holbach<sup>a,b</sup>, Andre Wilhelms<sup>a</sup>, Julia Krieg<sup>a</sup>, Yanwen Qin<sup>c</sup>, Binghui Zheng<sup>c</sup>, Hua Zou<sup>d</sup>, Boqiang Qin<sup>e</sup>,  
Guangwei Zhu<sup>e</sup>, Tingfeng Wu<sup>e</sup>, Stefan Norra<sup>a</sup>

<sup>a</sup>*Institute of Applied Geosciences, Working Group Environmental Mineralogy and Environmental System Analysis (ENMINSA)  
Karlsruhe Institute of Technology, Kaiserstraße 12, 76131 Karlsruhe, Germany*

<sup>b</sup>*Department of Bioscience, Aarhus University, Frederiksborgvej 399, 4000 Roskilde, Denmark*

<sup>c</sup>*Chinese Research Academy of Environmental Sciences, Dayangfang 8, Anwai Beiyuan, Beijing 100012, P.R. China*

<sup>d</sup>*School of Environmental and Civil Engineering, Jiangnan University, Wuxi 214122, P.R. China*

<sup>e</sup>*Nanjing Institute of Geography & Limnology, Chinese Academy of Sciences, 73 East Beijing Road, 210008 Nanjing, P.R.  
China*

\*Corresponding author

Email address: [Jingwei.yang@kit.edu](mailto:Jingwei.yang@kit.edu)

**SUPPORTING INFORMATION**

## **Content**

- 1. Threshold values for LAWA. (P.3)**
- 2. Certified Reference Materials (CRM) (P.4)**
- 3. Instrument Detection Limit (IDL)(P.5)**
- 4. Procedures of filter digestion (P.6)**
- 5. Reference values and standard concentration (P.7)**
- 6. Minerals measured by XRD (P.10)**
- 7. SEM-image and EDX-spectrum of minerals in sediment (P.12)**
- 8. EDX-strata of minerals from sampling point L3-13 (SPM) (P.15)**
- 9. Spatial distribution of Cr, Zn, Cu, P and Pb in the surface sediment(P.17)**

### 1. Threshold values for LAWA. (P.3)

**Table 1-1: Threshold values for sediments/SPM as well as the natural background in Germany for the classification by LAWA. (unite: mg kg<sup>-1</sup>)**

<b>Element</b>	<b>Aquatic ecosystem, Soil, SPM, Sediments mg kg<sup>-1</sup></b>	<b>Natural background ranges (Germany) mg kg<sup>-1</sup></b>	<b>Natural background (Lake Taihu) mg kg<sup>-1</sup></b>
Pb	100	12.5 - 50	15.7
Cr	100	40 - 160	79.3
Cu	60	10 - 40	18.9
Ni	50	15 - 60	19.5
Zn	200	50 - 200	59

## 2. Certified Reference Materials (CRM) (P.4)

**Table 2-1** Overview of used Certified Reference Materials (CRM).

<b>CRM</b>	<b>Description</b>	<b>Applied Test</b>
<b>GXR-2</b>	Soil of the City Park in Utah Source: USGS-AEG, USA	EDX
<b>SL-1</b>	Lake Sediment- from 15 m depth in Sardis Reservoir Panola Country, Mississippi Source: IAEA	EDX
<b>PCC-1</b>	Peridotite Source: USGS, USA	WDX
<b>MRG-1</b>	Gabbro Source: CCRMP, Canada	WDX
<b>MAG-1</b>	Marine Mud- from Wilkinson Basin of the Gulf of Maine, 125 km east of Boston, Massachusetts Source: USGS, USA	WDX
<b>RW (Battle- 02)</b>	River Water, River Saskatchewan in 2002	IC
<b>TMDW-A</b>	Trace Elements in Drinking Water Source: High Purity Standard (HPS)	ICP

### 3. Instrument Detection Limit (P.5)

**Table 3-1.** Instrument Detection Limit (3\*Sigma) of Inductively Coupled Plasma Mass Spectrometry (Dionex, ICS-1000)

Elements	Units	IDL	Elements	Units	IDL
<b>Mg</b>	mg L <sup>-1</sup>	0.000	<b>Cr</b>	µg L <sup>-1</sup>	0.008
<b>Al</b>	mg L <sup>-1</sup>	0.251	<b>Mn</b>	µg L <sup>-1</sup>	0.029
<b>P</b>	µg L <sup>-1</sup>	2.87	<b>Fe</b>	µg L <sup>-1</sup>	0.253
<b>Ca</b>	mg L <sup>-1</sup>	0.008	<b>Ni</b>	µg L <sup>-1</sup>	0.005
<b>Pb</b>	µg L <sup>-1</sup>	0.004	<b>Cu</b>	µg L <sup>-1</sup>	0.052
<b>Zn</b>	µg L <sup>-1</sup>	0.213			

**Table 3-2.** Instrumental Detection Limits IDL of Energy Dispersive X-ray Fluorescence (EDX) (Epsilon 5, Malvern Panalytical). (unit: mg kg<sup>-1</sup>)

Element	D.L.	Element	D.L.
<b>Cr</b>	3.50	<b>Pb</b>	3.80
<b>Ni</b>	3.22	<b>Zn</b>	2.52
<b>Cu</b>	2.47		

#### 4. Procedures of filter digestion (P.6)

**Table 4-1** Instruction of acid digestion of filters with HNO<sub>3</sub>, HClO<sub>4</sub> and HF.

Step	Implementation	Repetition	Acid
1	Insert sample in Teflon beaker Add 2 mL HNO <sub>3</sub> → Constrict	1 ×	HNO <sub>3</sub> 65 % Suprapur®
2	Insert 0.25 mL HClO <sub>4</sub> + 1.5 mL HF → Constrict After third times constrict to almost dry	3 ×	HClO <sub>4</sub> 65 % Suprapur® HF 40 % Suprapur®
3	Add 2 mL HNO <sub>3</sub> → Constrict	1 ×	HNO <sub>3</sub> 65 % Suprapur®
4	Add 0.5 mL HNO <sub>3</sub> → Constrict	2 ×	HNO <sub>3</sub> 65 % Suprapur®
5	Add 2 mL HNO <sub>3</sub> (1%) → Constrict for 10 min	1 ×	HNO <sub>3</sub> 1 % Suprapur®
6	Transfer to volumetric flask and add HNO <sub>3</sub> to make 10 mL		HNO <sub>3</sub> 1 % Suprapur®

**5. Reference values and standard concentration (P.7)**

**Table 5-1.** Reference values and standard concentration of Inductively Coupled Plasma Mass Spectrometry for dissolved phase.

<b>HPS</b>	<b>26Mg</b> mg L <sup>-1</sup>	<b>27Al</b> µg L <sup>-1</sup>	<b>31P</b> µg L <sup>-1</sup>	<b>52Cr</b> µg L <sup>-1</sup>	<b>55Mn</b> µg L <sup>-1</sup>	<b>56Fe</b> µg L <sup>-1</sup>	<b>60Ni</b> µg L <sup>-1</sup>	<b>63Cu</b> µg L <sup>-1</sup>	<b>66Zn</b> µg L <sup>-1</sup>	<b>208Pb</b> µg L <sup>-1</sup>
Mean (n=25)	1.55	26.49		4.03	8.25	18.95	12.02	4.03	15.50	4.00
Standard Deviation	0.05	0.55		0.07	0.12	0.34	0.28	0.09	0.32	0.07
Reference Value	1.60	25.00		4.00	8.00	18.00	12.00	4.00	15.00	4.00
Recovery (%)	97.1	106.0		100.7	103.1	105.3	100.1	100.9	103.3	100.0
<b>CRM-RW</b>	<b>26Mg</b> mg L <sup>-1</sup>	<b>27Al</b> µg L <sup>-1</sup>	<b>31P</b> µg L <sup>-1</sup>	<b>52Cr</b> µg L <sup>-1</sup>	<b>55Mn</b> µg L <sup>-1</sup>	<b>56Fe</b> µg L <sup>-1</sup>	<b>60Ni</b> µg L <sup>-1</sup>	<b>63Cu</b> µg L <sup>-1</sup>	<b>66Zn</b> µg L <sup>-1</sup>	<b>208Pb</b> µg L <sup>-1</sup>
Mean (n=13)	21.18	4.77	35.08	0.12	0.51	4.28	3.14	3.27	6.58	0.19
Standard Deviation	0.67	1.47	8.29	0.05	0.28	0.41	0.39	0.58	2.40	0.11
Reference Value	21.7									
Recovery (%)	97.6									

**Table 5-2.** Reference values SL-1 and GXR-2 of ICP-MS for SPM

<b>SL-1</b>	<b>26Mg</b> mg L <sup>-1</sup>	<b>27Al</b> µg L <sup>-1</sup>	<b>31P</b> µg L <sup>-1</sup>	<b>52Cr</b> µg L <sup>-1</sup>	<b>55Mn</b> µg L <sup>-1</sup>	<b>56Fe</b> µg L <sup>-1</sup>	<b>60Ni</b> µg L <sup>-1</sup>	<b>63Cu</b> µg L <sup>-1</sup>	<b>66Zn</b> µg L <sup>-1</sup>	<b>208Pb</b> µg L <sup>-1</sup>
Mean (n=10)	6.02	101.17	1224.00	113.55	3567.01	65.85	51.05	33.39	244.61	39.59
Standard Deviation	0.122	2.467	56.193	2.502	74.658	1.494	1.396	1.323	38.839	1.954
Reference Value	<b>29.00</b>	<b>89</b>	<b>831</b>	<b>104.0</b>	<b>3460.0</b>	<b>67.4</b>	<b>44.9</b>	<b>30.0</b>	<b>223.0</b>	<b>37.7</b>
Recovery (%)	21	114	147	109	103	98	114	111	110	105
<b>GXR-2</b>	<b>26Mg</b> mg L <sup>-1</sup>	<b>27Al</b> µg L <sup>-1</sup>	<b>31P</b> µg L <sup>-1</sup>	<b>52Cr</b> µg L <sup>-1</sup>	<b>55Mn</b> µg L <sup>-1</sup>	<b>56Fe</b> µg L <sup>-1</sup>	<b>60Ni</b> µg L <sup>-1</sup>	<b>63Cu</b> µg L <sup>-1</sup>	<b>66Zn</b> µg L <sup>-1</sup>	<b>208Pb</b> µg L <sup>-1</sup>
Mean (n=4)	8.00	68.26	747.75	36.60	1097.40	19.33	20.23	88.99	638.63	737.12
Standard Deviation	0.449	4.020	65.975	2.045	56.965	0.528	1.063	4.455	46.621	9.678
Reference Value	<b>8.5</b>	<b>185.7</b>	<b>600</b>	<b>36.0</b>	<b>1010</b>	<b>18.6</b>	<b>21.0</b>	<b>76.0</b>	<b>530</b>	<b>690</b>
Recovery (%)	94	37	125	102	109	104	96	117	120	107

**Table 5-3.** Acid Blanks and Filter Blanks of ICP-MS for SPM

<b>SB</b>	<b>26Mg</b> mg L <sup>-1</sup>	<b>27Al</b> µg L <sup>-1</sup>	<b>31P</b> µg L <sup>-1</sup>	<b>52Cr</b> µg L <sup>-1</sup>	<b>55Mn</b> µg L <sup>-1</sup>	<b>56Fe</b> µg L <sup>-1</sup>	<b>60Ni</b> µg L <sup>-1</sup>	<b>63Cu</b> µg L <sup>-1</sup>	<b>66Zn</b> µg L <sup>-1</sup>	<b>208Pb</b> µg L <sup>-1</sup>
Mean (n=14)	0.02	0.11	10.22	2.95	1.77	0.12	0.34	0.81	29.40	0.77
Standard Deviation	0.029	0.170	3.489	0.810	0.643	0.270	0.203	0.702	23.700	0.647
<b>FB</b>	<b>26Mg</b> mg L <sup>-1</sup>	<b>27Al</b> µg L <sup>-1</sup>	<b>31P</b> µg L <sup>-1</sup>	<b>52Cr</b> µg L <sup>-1</sup>	<b>55Mn</b> µg L <sup>-1</sup>	<b>56Fe</b> µg L <sup>-1</sup>	<b>60Ni</b> µg L <sup>-1</sup>	<b>63Cu</b> µg L <sup>-1</sup>	<b>66Zn</b> µg L <sup>-1</sup>	<b>208Pb</b> µg L <sup>-1</sup>
Mean (n=14)	0.06	0.58	11.76	3.24	1.90	0.07	1.05	1.04	24.22	1.92
Standard Deviation	0.083	1.290	3.317	1.092	0.548	0.094	1.460	1.034	16.689	3.130



**Table 5-4. Reference values of MAG-1, MRG-1 and PCC-1 of WDX (unit: %)**

<b>PCC-1</b>	<b>MgO</b>	<b>Al<sub>2</sub>O<sub>3</sub></b>	<b>P<sub>2</sub>O<sub>5</sub></b>	<b>MnO</b>	<b>Fe<sub>2</sub>O<sub>3</sub></b>
<b>Reference Value</b>	43.43	0.68	0.00	0.12	8.25
<b>Mean (n=10)</b>	43.69	0.68	0.01	0.28	8.30
<b>Standard Deviation</b>	0.321	0.049	0.002	0.256	0.117
<b>Recovery (%)</b>	100.60	100.61	361.11	230.56	100.63
<b>MRG-1</b>	<b>MgO</b>	<b>Al<sub>2</sub>O<sub>3</sub></b>	<b>P<sub>2</sub>O<sub>5</sub></b>	<b>MnO</b>	<b>Fe<sub>2</sub>O<sub>3</sub></b>
<b>Reference Value</b>	13.55	8.47	0.08	0.17	17.94
<b>Mean (n=9)</b>	13.43	8.38	0.07	0.19	17.94
<b>Standard Deviation</b>	0.110	0.137	0.003	0.051	0.182
<b>Recovery (%)</b>	99.10	98.96	90.28	112.61	100.03
<b>MAG</b>	<b>MgO</b>	<b>Al<sub>2</sub>O<sub>3</sub></b>	<b>P<sub>2</sub>O<sub>5</sub></b>	<b>MnO</b>	<b>Fe<sub>2</sub>O<sub>3</sub></b>
<b>Reference Value</b>	3.00	16.37	0.16	0.10	6.80
<b>Mean (n=9)</b>	3.10	16.52	0.17	0.11	7.21
<b>Standard Deviation</b>	0.041	0.246	0.005	0.021	0.234
<b>Recovery (%)</b>	103.48	100.93	106.94	112.78	106.05

**Table 5-5. Reference values of GXR-2 and SL-1 of EDX (unit: mg kg<sup>-1</sup>)**

<b>GXR-2</b>	<b>Cr</b>	<b>Ni</b>	<b>Cu</b>	<b>Pb</b>	<b>Zn</b>
<b>Reference Value</b>	36.00	21.00	76.00	690.00	530.00
<b>Mean (n=9)</b>	33.85	15.44	74.84	690.95	549.10
<b>Standard Deviation</b>	2.741	1.787	1.044	4.053	6.325
<b>Recovery (%)</b>	94.04	73.54	98.48	100.14	103.60
<b>SL-1</b>	<b>Cr</b>	<b>Ni</b>	<b>Cu</b>	<b>Pb</b>	<b>Zn</b>
<b>Reference Value</b>	104.00	44.90	30.00	37.70	223.00
<b>Mean (n=9)</b>	130.22	49.56	33.55	37.93	202.57
<b>Standard Deviation</b>	6.163	2.036	1.792	2.162	9.267
<b>Recovery (%)</b>	125.22	110.38	111.84	100.62	90.84

**6. Minerals measured by XRD (P.10)**

**6.1 Surface sediment**

S3-01	S3-02	S3-03	S3-04	S3-05	S3-06	S3-07	S3-08	S3-09	S3-10	S3-11	
Quartz	Quartz	Quartz	Quartz	Quartz	Quartz	Quartz	Quartz	Quartz	Quartz	Quartz	
Muscovite	Muscovite	Muscovite	Muscovite	Muscovite	Muscovite	Muscovite	Muscovite	Muscovite	Muscovite	Muscovite	
Albite (Plagioclase)	Albite (Plagioclase)	Albite (Plagioclase)	Albite (Plagioclase)	Albite (Plagioclase)	Albite (Plagioclase)	Albite (Plagioclase)	Albite (Plagioclase)	Albite (Plagioclase)	Albite (Plagioclase)	Albite (Plagioclase)	
Goethite	Goethite	Goethite	Goethite	Goethite	Goethite	Goethite	Goethite	Goethite	Goethite	Goethite	
	Chlorite	Chlorite	Chlorite	Chlorite	Chlorite	Chlorite	Chlorite	Chlorite	Chlorite	Chlorite	
Kaolinite	Kaolinite	Kaolinite	Kaolinite		Kaolinite	Kaolinite	Kaolinite	Kaolinite	Kaolinite	Kaolinite	
				Illite				Illite			
Dolomite	Dolomite	Dolomite	Dolomite	Dolomite	Dolomite	Dolomite	Dolomite	Dolomite	Dolomite	Dolomite	
Rutile	Rutile	Rutile	Rutile	Rutile	Rutile	Rutile	Rutile	Rutile	Rutile	Rutile	
	Hornblende	Anorthite	Zircon Sanidine (Kalifeldspat)	Zircon	Zircon		Orthoclase (Kalifeldspat)	Zircon	Zircon	Zircon	Calcite
	Anorthite			Sanidine Hornblende				Anorthite Amphibole	Hornblende Calcite		

**6.2 SPM**

Filter	L3-09c	L3-10c	L3-11c	L3-12c	L3-13c	L3-14c	L3-15c	L3-16c	L3-17c	L3-18c	L3-19c	L3-20c
Minerals	Muscovite	Muscovite	Muscovite	Muscovite	Muscovite	Muscovite	Muscovite	Muscovite	Muscovite	Muscovite	Muscovite	Muscovite
	Chlorite-serpentine	Chlorite-serpentine	Chlorite-serpentine	Chlorite-serpentine	Chlorite-serpentine	Chlorite-serpentine	Chlorite-serpentine	Chlorite-serpentine	Chlorite-serpentine	Chlorite-serpentine	Chlorite-serpentine	Chlorite-serpentine
	Kaolinite	Kaolinite	Kaolinite	Kaolinite	Kaolinite	Kaolinite	Kaolinite	Kaolinite	Kaolinite	Kaolinite	Kaolinite	Kaolinite
	Quartz	Quartz	Quartz	Quartz	Quartz	Quartz	Quartz	Quartz	Quartz	Quartz	Quartz	Quartz

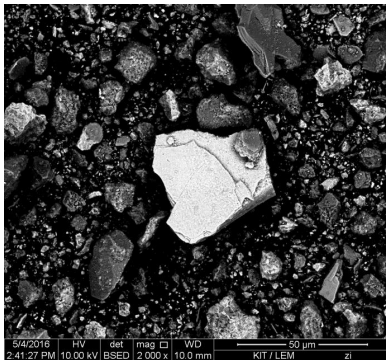
\* S3-01 and L3-09c were taken at same time and location, the same to S3-02 and L3-10c, S3-03 and L3-11c, S3-04 and L3-12, S3-05 and L3-13, S3-06 and L3-14, S3-07 and L3-15, S3-08 and L3-16, S3-09 and L3-17, S3-10 and L3-18, S3-11 and L3-19, S3-12 and L3-20.

## 7. SEM-image and EDX-spectrum of minerals in sediment (P.12)

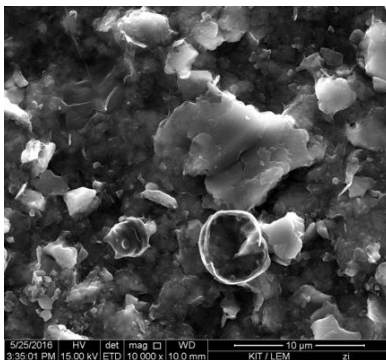
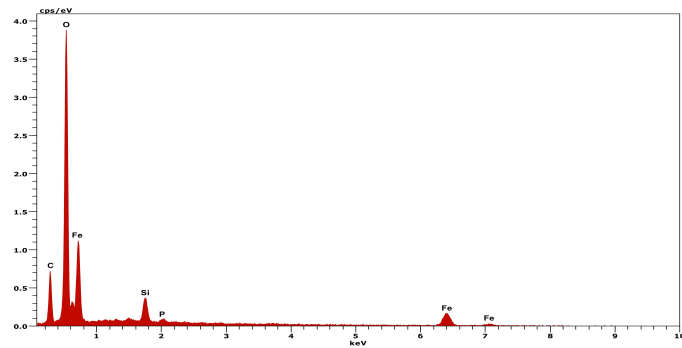
### 7.1 Mineral summary

Sampling Site	S3-01 (Sediment)	L3-10c (filter)	S3-06 (Sediment)
Minerals	illite zircon feldspar Mn-Oxide Fe-Oxide quartz	Muscovite Quartz Dolomite rutile Fe/Mn Oxide zircon feldspar (orthoclase) monazite illite montmorillonite apatite chlorite	ilmenite Fe-Oxide Magnesiochromite xenotime zircon quartz amphibole (Ti-hornblende) fly ash monazite allanite

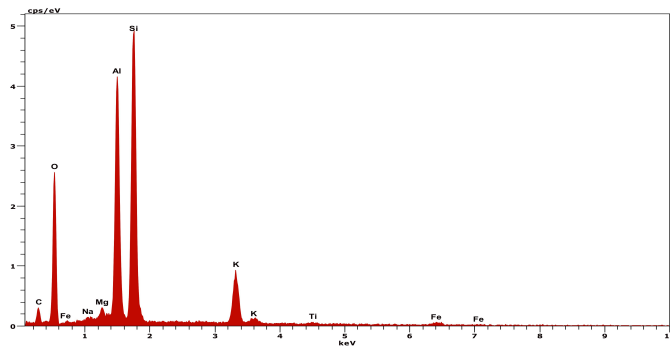
### 7.2 S3-01

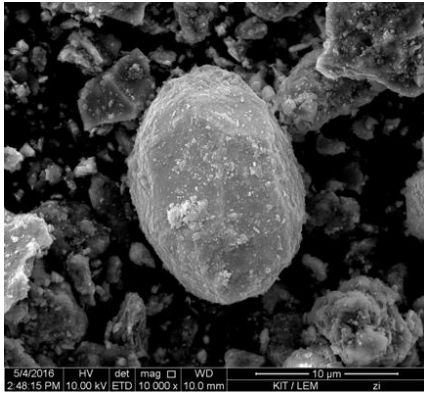


Iron-Oxide

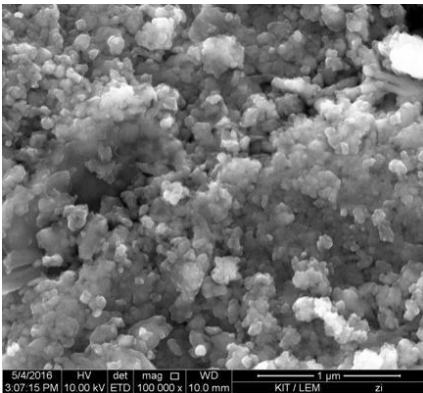
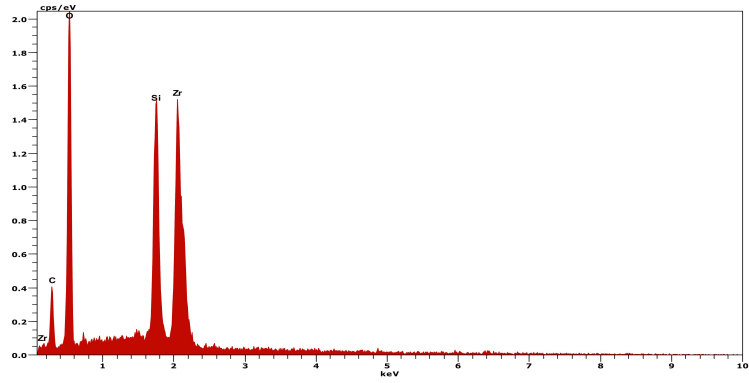


Muscovite

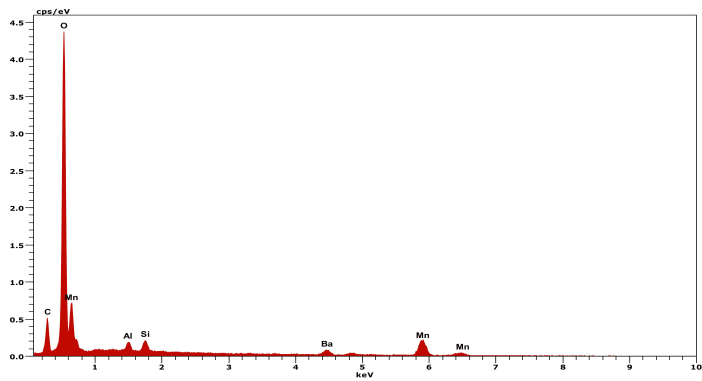




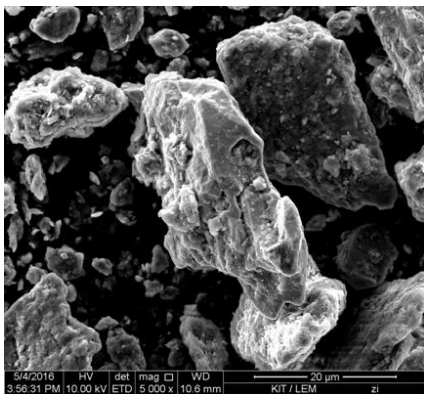
**Zircon**



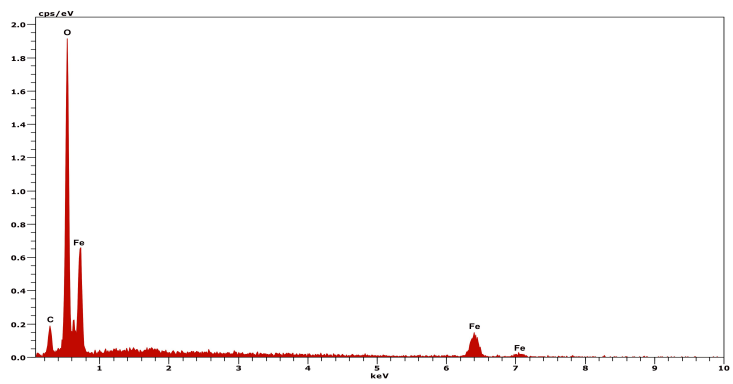
**Mn-Oxide coating**

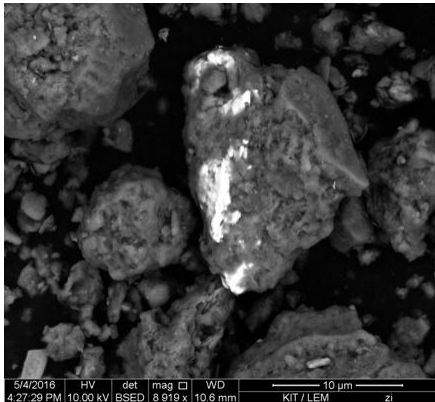


### 7.3 S3-06

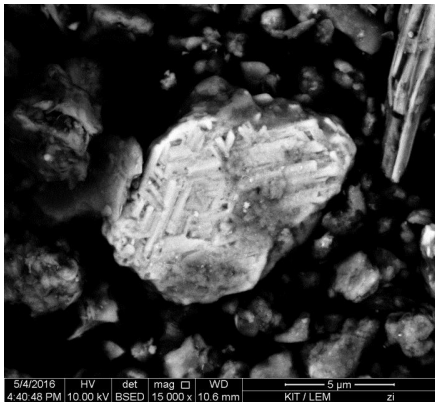
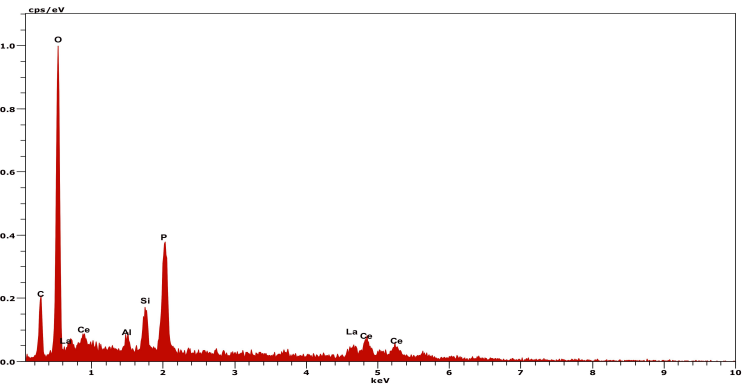


**Magnetite**

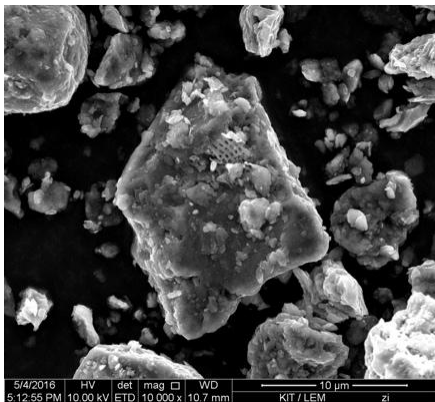
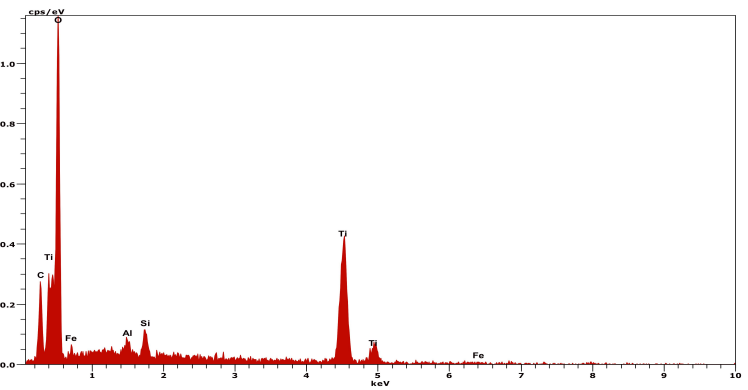




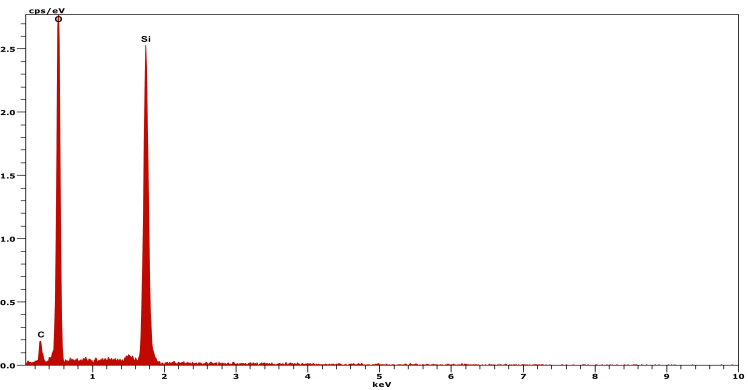
**Monazite**

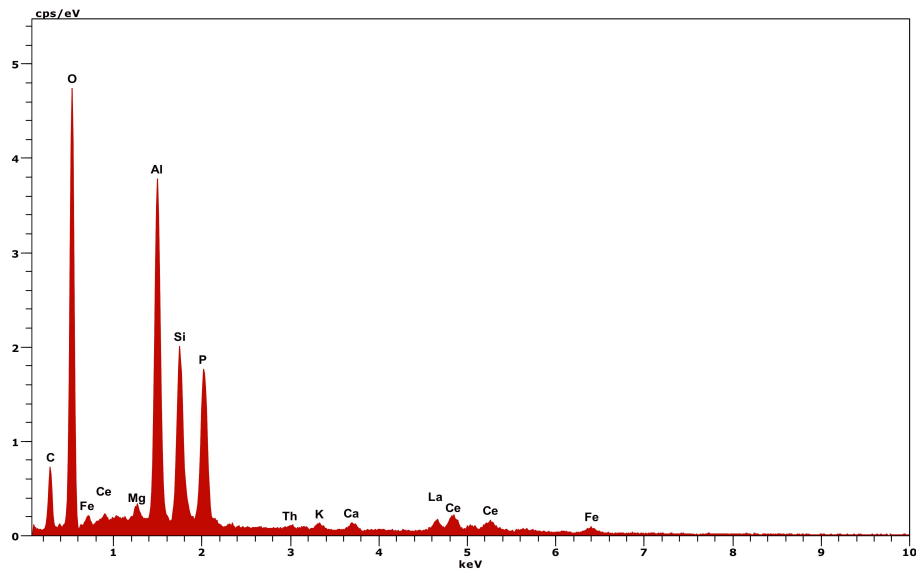


**Amphibole (titano hornblende) of L3-18. Cleavage planes of 120°**

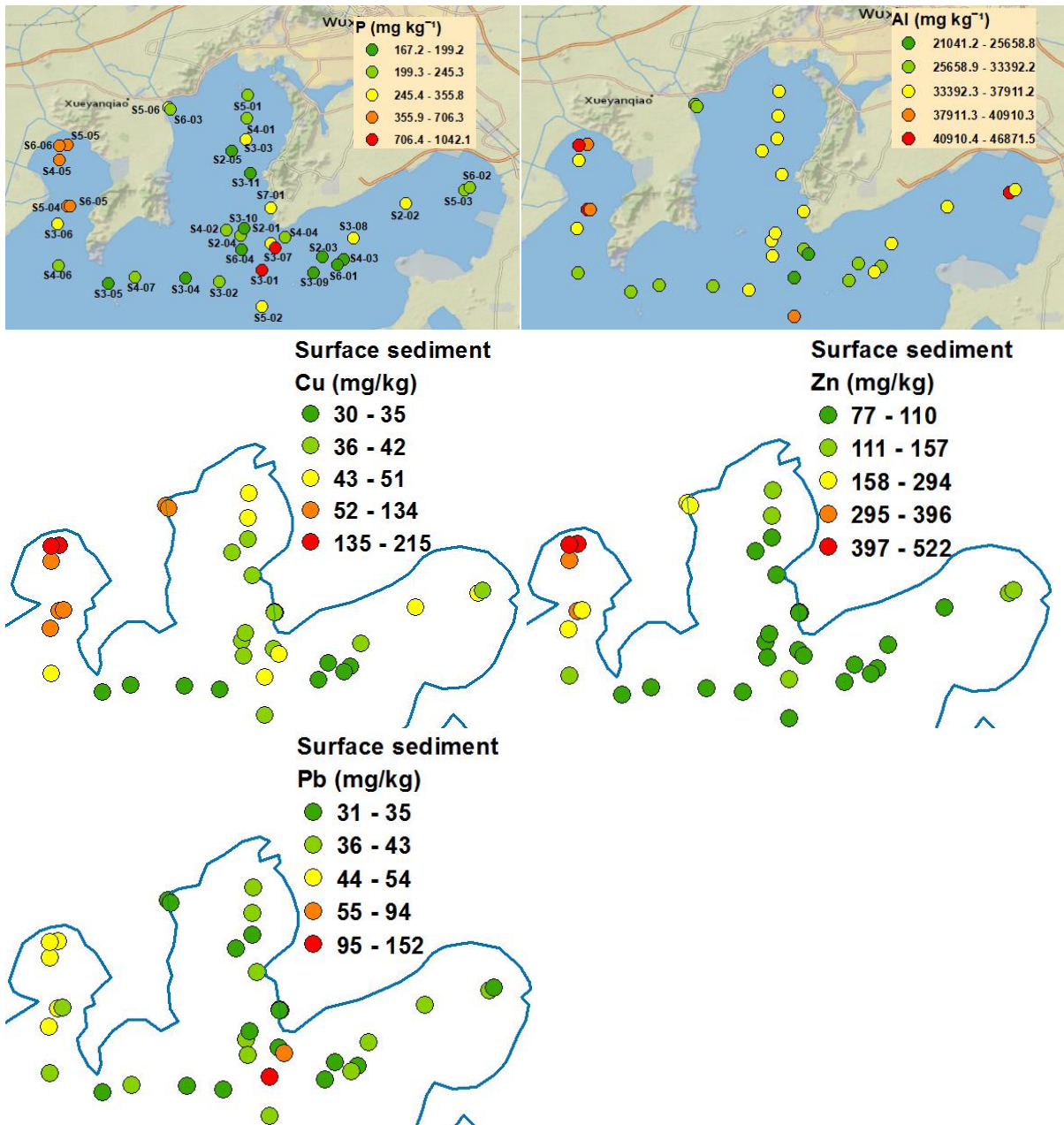


**Quartz**





### 9. Spatial distribution of Cr, Zn, Cu, P and Pb in the surface sediment (P. 17)



## Appendix B.3 Simulating chlorophyll-a fluorescence changing rate and phycocyanin fluorescence by using a multi-sensor system in Lake Taihu, China





Contents lists available at ScienceDirect

Chemosphere

journal homepage: [www.elsevier.com/locate/chemosphere](http://www.elsevier.com/locate/chemosphere)



## Simulating chlorophyll-*a* fluorescence changing rate and phycocyanin fluorescence by using a multi-sensor system in Lake Taihu, China



Jingwei Yang<sup>a,\*</sup>, Andreas Holbach<sup>a,b</sup>, Michael J. Stewardson<sup>c</sup>, Andre Wilhelms<sup>a</sup>, Yanwen Qin<sup>d</sup>, Binghui Zheng<sup>d</sup>, Hua Zou<sup>e</sup>, Boqiang Qin<sup>f</sup>, Guangwei Zhu<sup>f</sup>, Christian Moldaenke<sup>g</sup>, Stefan Norra<sup>a</sup>

<sup>a</sup> Institute of Applied Geosciences, Working Group Environmental Mineralogy and Environmental System Analysis (ENMINSA), Karlsruhe Institute of Technology, Kaiserstraße 12, 76131, Karlsruhe, Germany

<sup>b</sup> Department of Bioscience, Aarhus University, Frederiksborgvej 399, 4000, Roskilde, Denmark

<sup>c</sup> Department of Infrastructure Engineering, Melbourne School of Engineering, The University of Melbourne, 3010, Victoria, Australia

<sup>d</sup> Chinese Research Academy of Environmental Sciences, Dayangfang 8 Anwai Beiyuan, Beijing, 100012, China

<sup>e</sup> School of Environmental and Civil Engineering, Jiangnan University, Wuxi, 214122, China

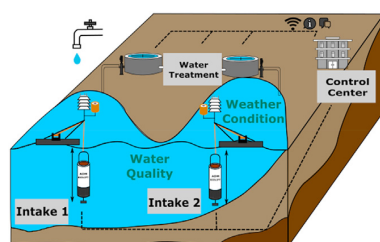
<sup>f</sup> Nanjing Institute of Geography & Limnology, Chinese Academy of Sciences, 73 East Beijing Road, 210008, Nanjing, China

<sup>g</sup> bbe Moldaenke GmbH, Preetzer Chaussee 177, 24222, Schwentinental, Germany

### HIGHLIGHTS

- Chlorophyll-*a* and phycocyanin fluorescence can be predicted using on-line sensor data.
- Wave is the leading factor for the short-term changes of algae in shallow lakes.
- Nutrients are not important factors in short-term algal simulation in eutrophic lakes.

### GRAPHICAL ABSTRACT



### ARTICLE INFO

#### Article history:

Received 9 June 2020

Received in revised form

23 September 2020

Accepted 25 September 2020

Available online 5 October 2020

Handling Editor: Jim Lazorchak

#### Keywords:

Eutrophic shallow lakes

Online monitoring

Algal classes

Stepwise multiple regression

Short-term simulation

### ABSTRACT

Algal pollution in water sources has posed a serious problem. Estimating algal concentration in advance saves time for drinking water plants to take measures and helps us to understand causal chains of algal dynamics. This paper explores the possibility of building a short-term algal early warning model with online monitoring systems. In this study, we collected high-frequency data for water quality and weather conditions in shallow and eutrophic Lake Taihu by an *in situ* multi-sensor system (BIOLIFT) combined with a weather station. Extracted chlorophyll-*a* from water samples and chlorophyll-*a* fluorescence differentiated according to different algal classes verified that chlorophyll-*a* fluorescence continuously measured by BIOLIFT only represent chlorophyll-*a* of green algae and diatoms. Stepwise linear regression was used to simulate the chlorophyll-*a* fluorescence changing rate of green algae and diatoms together ( $\Delta\text{Chl}_{a-f}\%$ ) and phycocyanin fluorescence concentration (blue-green algae) on the water surface layer (CyanoS). The results show that nutrients (total N,  $\text{NO}_3\text{-N}$ ,  $\text{NH}_4\text{-N}$ , total P) were not necessary parameters for short-term algal models.  $\Delta\text{Chl}_{a-f}\%$  is greatly influenced by the seasons, so seasonal partition of data before modeling is highly recommended.  $\text{CyanoS}_{\text{max}}$  and  $\Delta\text{Chl}_{a-f}\%$  were simulated by only using multi-sensor and meteorological data ( $R^2 = 0.73; 0.75$ ). All the independent variables (wave, water temperature, relative humidity, depth, cloud cover) used in the model were measured online and predictable. Wave height is the most important independent variable in the shallow lake. This paper offers a

\* Corresponding author.

E-mail address: [jingwei.yang@kit.edu](mailto:jingwei.yang@kit.edu) (J. Yang).

new approach to simulate and predict the algal dynamics, which also can be applied in other surface water.

© 2020 Elsevier Ltd. All rights reserved.

## 1. Introduction

Lake eutrophication is a persistent challenge in Lake Taihu. Despite considerable research and management efforts in the lake, the average chlorophyll-*a* concentration (Chl<sub>a</sub>) increased between 2009 and 2017 (Zhu et al., 2020). In May 2017, a blue-green algal bloom extended over 1580 km<sup>2</sup> of the lake, the largest bloom so far recorded for the lake (Qin et al., 2019). Continued blue-green algal blooms in Lake Taihu are attributed to ineffective nutrient reduction strategies and also to climate change (Qin et al., 2019; Yang et al., 2016). In particular, warmer air temperature, increased precipitation, wind patterns alternation, and water acidification produced by climate changes are expected to cause changes in vertical mixing, and phytoplankton community structure and composition (Paerl and Huisman, 2009; Wells et al., 2015).

In 2007, blue-green algal blooms produced odor and taste compounds, which led to over one week of undrinkable tap water and influenced more than one million residents in Wuxi supplied from Lake Taihu (Zheng et al., 2016). Algal bloom leads to the high organic content in malodorous or unpalatable raw water, as well as the formation of disinfection by-products, and clogging of filter beds during drinking water treatment processes. Drinking water plants often have online water monitoring systems at the raw water extraction point to assist in water treatment optimization. However, this monitoring concept is insufficient to notify the algal biomass and species changes in time where phytoplankton grows rapidly under suitable conditions. Algae doubling time depends on algal species and environmental conditions. Doubling time of *Microcystis*, which is the dominant cyanobacteria in Lake Taihu, ranges from 1.5 to 5.2 days, with a mean value of 2.8 days (Wilson et al., 2006). Hence, it is strongly recommended to identify an emerging algal bloom in the earliest stages of growth to avoid shortage of drinking water. Thus, in the future, drinking water plants require estimates of algal bloom development in advance (2–3 days) to adapt drinking water processing timely enough, involving degree and period of the usage of water intake wells and pumps, and treatment processes. Forecasting algal blooms based on online monitoring data can be a valuable measure for securing the drinking water supply at Lake Taihu (Qin et al., 2015), and other eutrophic drinking water source lakes.

Many studies produced algal forecast models worldwide (Huang et al., 2012; Ogashawara et al., 2013). However, traditional algal models often require large numbers of input data, and are only applicable when there is sufficient data (Rajaei and Boroumand, 2015). Moreover, recent studies have found that wind pattern changes and extreme weather increase the algal bloom formation in shallow Lake Taihu (Wu et al., 2015; Yang et al., 2016). Traditional long-term prediction models do not provide sufficient temporal resolution to respond to the rapid environmental changes. In this case, high-frequency data of weather and water quality is necessary for understanding short-term responses of phytoplankton biomass and issuing early warnings of harmful algal blooms in aquatic ecosystems (Huang et al., 2014).

Nutrient sensors are not equipped in the high-frequency online multi-sensor system. Because no sensor-based technology has, so far, been validated to replace the standard laboratory technique for determining nutrient contents with fast reaction time (less than

2 min) and high accuracy (Bodini et al., 2015; Hsu et al., 2016). Moreover, in the short-term, the climatic parameters (extreme conditions) are more critical than nutrients (Singh and Singh, 2015).

Accordingly, this study examines an alternative approach that considers extreme conditions and uses fewer independent variables, although in a highly time resolution. We used an online and *in situ* multi-sensor systems to collect continuous high-frequency meteorological and water quality data. Subsequently, the recorded online multi-sensor data were used for stepwise linear regression to evaluate the possibility of simulating and predicting the Chl<sub>a</sub> changing rate of green algae and diatoms together ( $\Delta\text{Chl}_a$ , %) and phycocyanin concentrations (blue-green algae) on the water surface layer (CyanoS<sub>max</sub>). Compared to traditional methods, sensor technology saves efforts and avoids significant time delays (Zulkifli et al., 2018). Accompanying lab analyses of nutrients (total P, dissolved P, NO<sub>3</sub>-N, NH<sub>4</sub>-N, total N) were done to discuss the necessity of involving nutrients in the short-term algal simulation model.

## 2. Materials and methods

### 2.1. Study area

Lake Taihu, a large and shallow lake, experienced eutrophication problems for more than a decade. Wind-induced resuspension easily changes water chemistry and vertical algal distribution in this shallow lake (average water depth: 1.9 m) (Yang et al., 2019). Moreover, vertical stratification frequently forms in the warm summer, when blue-green algae dominate the phytoplankton community.

As a preliminary study, single-point water quality measurements were carried out at Taihu Laboratory for Lake Ecosystem Research (TLER) (Fig. 1a), which is located at outer Meiliang bay and belongs to the Nanjing Institute of Geography and Limnology (NIGLAS). Due to this monitoring location, only 250 m west from the shore, easterly winds rarely generate waves (Fig. 1b).

### 2.2. *In situ* physicochemical parameter monitoring

The continuous physicochemical water quality measurements were recorded by the multi-sensor-system 'BIOLIFT' (ADM Elektronik, Sauerlach, Germany) for the entire water column. The BIOLIFT measures depth profiles of water depth (Depth, [m]), water temperature (WTemp, [°C]), pH-value (pH), chlorophyll-*a* fluorescence (Chl<sub>a-f</sub>, [μg L<sup>-1</sup>]), phycocyanin fluorescence (Cyano, indicative of blue-green algae, [μg L<sup>-1</sup>]), oxygen saturation (Oxy-sat, [%]), turbidity (Turb, [FTU = Formazan Turbidity Unit]), and colored dissolved organic matter (CDOM, [μg L<sup>-1</sup>]). Furthermore, photo-synthetically active radiation sensors (PAR, [μmol (m<sup>2</sup> × s)<sup>-1</sup>]) were installed at the BIOLIFT and on the buoy system at ca. 2 m above the water surface, which determined the PAR above water.

Hourly meteorological data were directly recorded by a multi-weather sensor (WXT520, Vaisala, Vantaa, Finland) near to the BIOLIFT, operation point including air temperature (ATemp) [°C], wind direction ( $\vec{v}$ ) [°], wind speed (*v*) [m s<sup>-1</sup>], rainfall (Ra) [mm], and relative humidity (RH) [%]. Cloud cover (Cloudcover, [%]) was

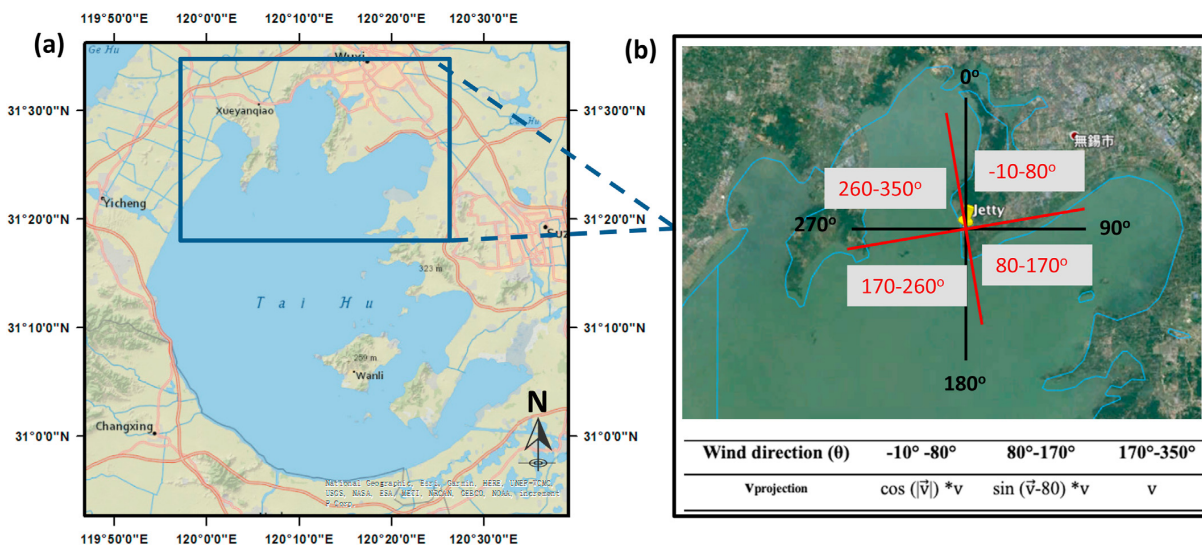


Fig. 1. Map of the a) Lake Taihu and b) monitoring point (TLER, Taihu Laboratory for Lake Ecosystem Research) in northern lake Taihu and the site adapted classification of wind directions (Vprojection).

obtained from the China meteorological administration. On day N, the daily cloud cover is the average of Cloudcover from 8 p.m. on day N-1 till 8 p.m. on day N.

Data were collected from five campaigns, including 2016–June/July, 2017–February/March, 2018–March/April, 2018–August/September, and 2018–November. The interval time between each depth-profile was 10 min, and the measuring frequency is 3–5 datasets per second and every 2–3 cm per dataset. One depth-profile (downwards and upwards) takes around 2 min in the shallow Lake Taihu. In this setup, the system generates around 37,000 data points per day. In total, we monitored 98 days across all five campaigns. However, we only used data from 67 days, where all 24 h were covered, for the simulation model of the  $Chl_{a-f}$  changing rate. Only since 2018–March/April, the BIOLIFT was equipped with a phycocyanin fluorescence sensor. Thus, 47 days of data were used for the blue-green algae simulation model (Cyano).

### 2.3. Water sample collection and treatment

Water samples were collected once per day in the morning at three different depths, including the surface layer (0.2 m), the bottom layer, and the intermediate layer (half of the water depth). We calculated daily mean values across the water column for each parameter.

The water samples were filtered through 0.45  $\mu\text{m}$  Cellulose Acetate membrane filters (Sartorius, Goettingen, Germany). Ion chromatography ((IC; ICS-1000, Thermo Fischer Scientific, Waltham, USA) and inductively coupled plasma mass spectrometry ((ICP-MS; X-Series 2, Thermo Fischer Scientific, Waltham, USA) was used to measure the  $\text{NO}_3\text{-N}$  and dissolved P (Yang et al., 2019). The particles on the filters were fully digested and followed by ICP-MS measurement for the total P in the particulate phase (Yang et al., 2020). Moreover, total N and  $\text{NH}_4\text{-N}$  were measured by quick test without filtration in 2018 (Merck Group, Darmstadt, Germany; Product Number. 1006130001 and 1147390001).

Chlorophyll-a was extracted from the water samples ( $Chl_{a-e}$ ) using the hot-ethanol extraction method with 90% ethanol (95%

ethanol diluted by distilled water) at 80–85  $^{\circ}\text{C}$  and measured by UV–Visible Spectrophotometer (UV-1100; Mapada Instruments, Shanghai, China) for all samples from the three campaigns in 2018 (Bartram and Chorus, 1999; Chen et al., 2006; Lorenzen Carl, 1967). Three parallel experiments ( $Chl_{a-e}$ ) were done for each water sample in three campaigns in 2018. Daily average value of  $Chl_{a-e}$  was calculated and then used to verify the accuracy of  $Chl_{a-f}$ .

$Chl_{a-f}$  signal measured by  $Chl_a$  sensor equipped on BIOLIFT (Turner, Cyclops-7, blue excitation) is only excited by blue light. An *ex situ* device, PhycoLA (resolution: 0.01  $\mu\text{g L}^{-1}$ ; bbe moldaenke, Schwentinal, Germany), equipped with seven excitation illuminants (LEDs) and two detection photomultipliers, measured the same water samples as was done for the  $Chl_{a-e}$ . PhycoLA differentiates five algal classes by their specific excitation-fluorescence spectrum, including green algae, diatoms, blue-green algae, cryptophyta, and planktonthrix (Moldaenke et al., 2019). A stirrer is kept running during the measurement to keep the solution uniform, which is important for the measurement of blue-green algae due to their buoyancy.

### 2.4. Data processing

As it can be seen from the Fig.S.3, the  $Chl_{a-f}$  can have rapid changes in relatively short time intervals. Therefore, we chose 3-h time intervals to calculate average values across the entire water column for  $Chl_{a-f}$  and all other physicochemical parameters measured by the BIOLIFT before analysis and simulation. All the data graphs were plotted and Shapiro-Wilk test (significance level 0.05) was applied to test the assumption of normality (Shapiro and Wilk, 1965) using the software OriginPro (Origin Professional, 2016; OriginLab, Northampton, USA). We calculated the interquartile range (IQR) and used  $1.5 \times \text{IQR}$  to find outliers for high-frequency BIOLIFT data. Moreover, for data that follows a normal distribution, we used Z-scores (3 standard deviations of the mean) to get rid of outliers over a window length of 1000 data (ca. 3 profiles) by the function of “movmean” in software MATLAB (R2018a; MathWorks, Natick, USA).

2.4.1. Chlorophyll-a 3-h changing rate ( $\Delta\text{Chl}_{a-f}\%$ ) and water temperature changes ( $\Delta\text{WTemp}$ )

$\text{Chl}_{a-f}$  of every 3-h was calculated based on BIOLIFT data.  $\Delta\text{Chl}_{a-f}\%$  was used to represent the changing rate of  $\text{Chl}_{a-f}$  per 3-h. The calculation was started from 0 o'clock following formula (1):

$$\Delta\text{Chl}_{a-f(t_{n+3})}[\%] = \left( \text{Chl}_{a-f(t_{n+3})} - \text{Chl}_{a-f(t_n)} \right) / \text{Chl}_{a-f(t_n)} \times 100 \quad (1)$$

Analogously, the changes of WTemp for every 3-h ( $\Delta\text{WTemp}$ ) was calculated as follows:

$$\Delta\text{WTemp}_{t_{n+3}} = \text{WTemp}_{t_{n+3}} - \text{WTemp}_{t_n} \quad (2)$$

The daily mean of  $\Delta\text{Chl}_{a-f}\%$ , WTemp and  $\Delta\text{WTemp}$  were used in the further stepwise regression.

2.4.2. Wave calculation and wind projection

The BIOLIFT sensor module will stay on the lake bottom for 20 s during each depth-profile. The water depth changes in these 20 s in each profile is recorded by the pressure sensor and the depth difference is defined as wave height ( $\text{Wave}_h$ ). The equation is as follows:

$$\text{Wave}_h = \text{Depth}_{\max} - \text{Depth}_{\min} \quad (3)$$

The water depth strongly affects wave shapes. The wave heights will be smaller and wave periods will be shorter if the generation takes place in shallow water rather than in deep water. Basically, the water depth and  $\text{Wave}_h$  have logarithmic relationships (Pascolo et al., 2018). For a shallow lake, the speed of waves is influenced by gravitational attraction and water depth (Garrison, 2012). The  $\text{Wave}_h$  is adjusted by water depth and defined as  $\text{Wave}_d$  (Formula (4)).

$$\text{Wave}_d = \text{Wave}_h \times 0.1 / \log(\text{Depth}) \quad (4)$$

According to the geographical location of the monitoring point (TLER), for instance, wind from the east hardly generates waves (Fig. 1b). We introduced  $v_{\text{projection}}$  to modify wind speed ( $v$ ) by wind direction ( $\vec{v}$ ) according to projection method (Fig. 1b). The specific calculation angle and equation is adjusted according to the monitoring location, and the method can be applied at other monitoring locations or lakes.

2.4.3. Stepwise linear regression

Stepwise linear regression was carried out for the simulation using the software of SPSS (SPSS Statistics 24.0; IBM, New York, USA). Stepwise regression is a procedure for automatically selecting independent variables, by successively adding variables based solely on the t-statistics of their estimated coefficients and maximizing the squared multiple correlations coefficient ( $R^2$ ) of the dependent variable with the set of selected independent variables. The p-value ( $p$ ; 0.05) for each independent variable tests the null hypothesis. The independent variables would not be included in the simulation if the null hypothesis proved that there is no correlation between the independent and dependent variables.

Homoscedasticity was used to checked whether residuals of regressions are equally distributed in SPSS. AICc (Akaike information criterion for the model with small sample size) was used to estimate the relative amount of information lost by models, which provides a means for model selection (Cavanaugh, 1997). RMSE (root mean square error) was also calculated between observed and simulated dependent variables.

3. Results

3.1. Chlorophyll-a measurement and algal classes

As can be seen from Fig. 2a, the total  $\text{Chl}_{a-f}$  measured by PhycoLA ( $\text{Chl}_{a-f}\text{-PhycoLA}$ ) shows a very strong correlation with chlorophyll-a concentration measured by extraction procedure ( $\text{Chl}_{a-e}$ ) in three different depths during two measured campaigns (2018–March/April & 2018–November),  $R^2$  was 0.88 ( $p < 0.05$ ).  $\text{Chl}_{a-f}\text{-PhycoLA}$  and  $\text{Chl}_{a-e}$  were measured in the same water samples.

However, the correlations between  $\text{Chl}_{a-e}$  and chlorophyll-a fluorescence measured by BIOLIFT ( $\text{Chl}_{a-f}\text{-BIOLIFT}$ ) at the corresponding water sampling time were seasonally different (Fig. 2b–d). This is because, in principle, the Turner Cyclops 7 sensor on the BIOLIFT only measures fluorescence after excitation with blue light, and so does not well represent blue-green algae. However, the composition of algal classes varies between different seasons, which led to the discrepancy between  $\text{Chl}_{a-e}$  and  $\text{Chl}_{a-f}\text{-BIOLIFT}$  relationships.

The variation ranges of  $\text{Chl}_{a-e}$  were similar to  $\text{Chl}_{a-f}\text{-BIOLIFT}$  in 2018–March/April (Fig. 2b). In this period from day seven to 27 (Fig. 2e), the fraction of  $\text{Chl}_{a-f}$  of blue-green algae is less than 15% of the total  $\text{Chl}_{a-f}\text{-PhycoLA}$ . In blue-green algae dominated summer (2018–August/September),  $\text{Chl}_{a-e}$  was much higher than the  $\text{Chl}_{a-f}\text{-BIOLIFT}$ , especially after day 16 (Fig. 2c). Similarly, in 2018–November (Fig. 2d), the ratio of  $\text{Chl}_{a-e}$  and  $\text{Chl}_{a-f}\text{-BIOLIFT}$  changed after day eight. During this period, algal classes vary greatly and the  $\text{Chl}_{a-f}$  of blue-green algae ranged from 15% to 63% of the total  $\text{Chl}_{a-f}\text{-PhycoLA}$  (Fig. 2f). The occurrence of different algal classes can change very fast. For example, in campaign 2018–March/April (Fig. 2e), the fractions of blue-green algae had a rapid decrease on day 14 and increased again on day 17, and diatoms dropped on day 19.

From the result, in the campaign 2018–March/April and 2018–November (Fig. 2g and h), the changes of  $\text{Chl}_{a-f}\text{-BIOLIFT}$  ( $\Delta\text{Chl}_{a-f}\text{-BIOLIFT}$ ) showed better correlations with the changes of diatoms and green algae together ( $\Delta\text{Chl}_{a-f}\text{-Green algae} + \text{Diatoms}$ ) instead of with  $\Delta\text{Chl}_{a-f}$  of PhycoLA. Therefore,  $\Delta\text{Chl}_{a-f}\text{-BIOLIFT}$  is used to represent the  $\text{Chl}_{a-f}$  changes of diatoms and green algae.

3.2. Stepwise linear regression of  $\text{Chl}_{a-f}\text{-BIOLIFT}$  and Cyano

Daily mean rates of change (3-h averages) in  $\text{Chl}_{a-f}\text{-BIOLIFT}$  ( $\Delta\text{Chl}_{a-f}\%$ ) is the dependent variable, which represents the changes of green algae and diatoms together.  $\text{WTemp}_{\text{mean}}$ ,  $\Delta\text{WTemp}_{\text{mean}}$ ,  $\text{PAR}_{\max}$ ,  $\text{Ra}_{\text{mean}}$  (rain amount),  $\text{RH}_{\text{mean}}$  (relative humidity),  $\text{Cloud-cover}_{\text{mean}}$ ,  $\text{Wave}_{d\max}$  were set as independent variables in the stepwise linear regression simulation.  $\text{WTemp}_{\text{mean}}$ ,  $\Delta\text{WTemp}_{\text{mean}}$ , and  $\text{Wave}_{d\max}$  were selected to be the independent variables for the final regression model ( $p < 0.05$ ).  $R^2$  was 0.37 and RMSE was 2.7. As can be seen from Fig. 3a, the simulated  $\Delta\text{Chl}_{a-f}\%$  fits better to the observed  $\Delta\text{Chl}_{a-f}\%$  in spring and autumn than summer. The result is consistent with the fact that the  $\Delta\text{Chl}_{a-f}\%$  calculated by BIOLIFT mainly represents the changes in green algae and diatoms, which are dominant in spring and autumn. Therefore,  $\Delta\text{Chl}_{a-f}\%$  simulation model should be differentiated between the seasons.

According to the fit quality of the previous analysis (Fig. 3a), we separated the five campaigns into two classes. Class-S included 2016–June/July and 2018–August/September represent for summer, normally dominated by blue-green algae. The rest of the campaigns (2017–February/March, 2018–March/April, and 2018–November) were classified as Class-SF and represent spring and fall. Stepwise linear regression was applied individually for these two classes. Seven independent variables with daily mean/max values were considered in the stepwise linear regressions of

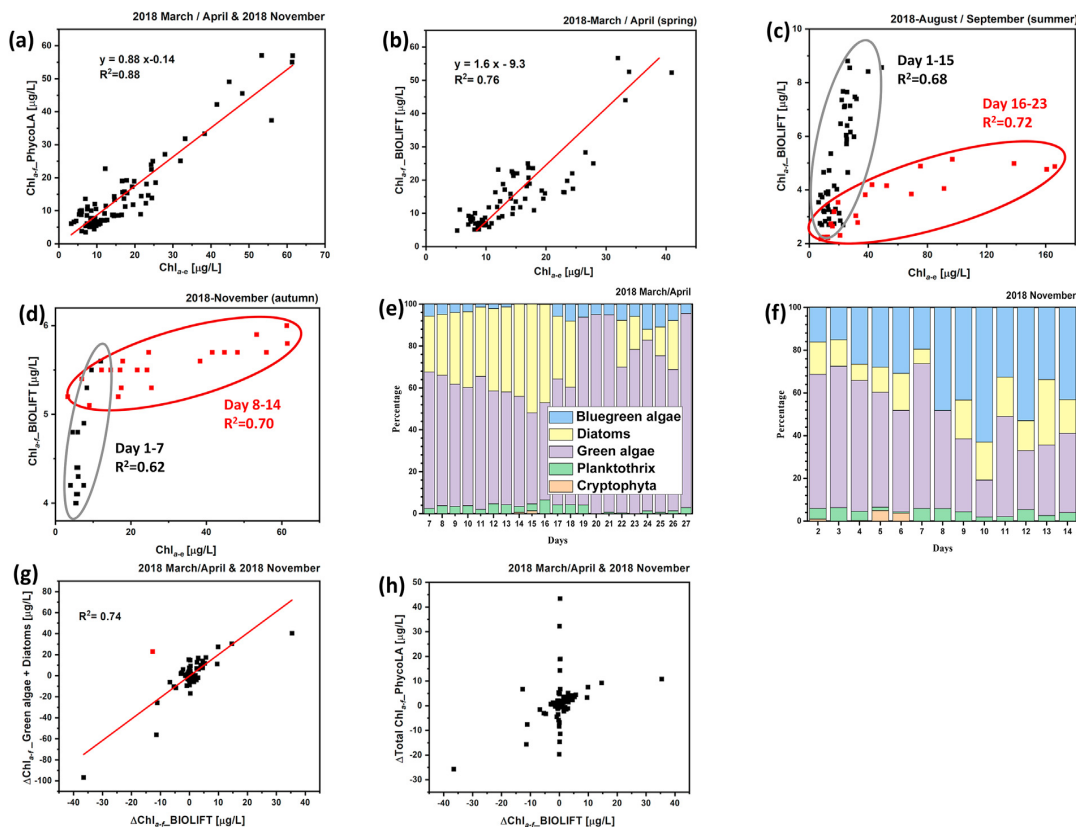


**Fig. 2.** a) Correlation between chlorophyll-a fluorescence concentrations ( $\mu\text{g L}^{-1}$ ) measured by Phycocyanin ( $\text{Chl}_{a-f}$ -Phycocyanin) and chlorophyll-a concentrations ( $\mu\text{g L}^{-1}$ ) measured by extraction experiments ( $\text{Chl}_{a-e}$ ) in 2018–March/April (spring) and 2018–November (autumn); Correlation between chlorophyll-a fluorescence concentrations ( $\mu\text{g L}^{-1}$ ) measured by BIOLIFT ( $\text{Chl}_{a-f}$ -BIOLIFT) and  $\text{Chl}_{a-e}$  by extraction in different seasons b) 2018–March/April (spring); c) 2018–August/September (summer); d) 2018–November (autumn); Daily chlorophyll-a ratio changes of different algal species in campaign e) 2018–March/April (spring); f) 2018–November (autumn); Correlation between g) the changes of  $\text{Chl}_{a-f}$ -BIOLIFT and  $\text{Chl}_{a-f}$ -Phycocyanin of green algae and diatoms; h) the changes of  $\text{Chl}_{a-f}$ -BIOLIFT and total  $\text{Chl}_{a-f}$ -Phycocyanin in campaign 2018–March/April and 2018–November.

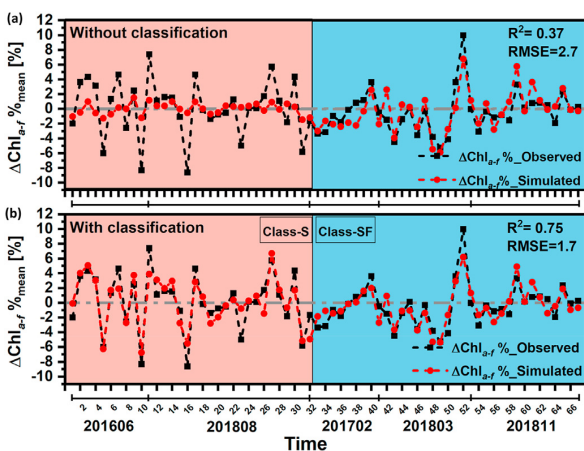


**Fig. 3.** Time series of observed and simulated chlorophyll-a fluorescent changing rate ( $\Delta\text{Chl}_{a-f}\%$ ) a) without classification; b) after classification.

$\Delta\text{Chl}_{a-f}\%$  as well. The selection process for variables in the two classes is shown in Table 1. Finally, we chose model No.2 in Class-S and model No.3 in Class-SF,  $R^2$  were 0.75 and 0.74 respectively.

Model No.3 in Class-S with  $R^2$  of 0.78 was not chosen in the final model because the  $p$  of  $\text{RH}_{\text{mean}}$  in Class-S was 0.07 (over 0.05). Moreover, AICc value was the same in model No. 2 and No. 3, in this case, the model with fewer parameters (model No.2) was chosen. The regressions' residuals follow a normal distribution according to the Shapiro-Wilk test and are equally distributed (Fig.S.3, S.4). Both of  $\Delta\text{WTemp}_{\text{mean}}$  and  $\text{Wave}_{\text{dmax}}$  were selected independent variables in two different classes. However,  $\text{RH}_{\text{mean}}$  was only used in Class-SF.

After putting the simulation result of the two classes together, the time-series of both observed and simulated  $\Delta\text{Chl}_{a-f}\%$  are presented in Fig. 3b. The overall  $R^2$  was 0.75, and the RMSE was 1.7.

Blue-green algae scum is one of the main issues for the algal problem. It appears and varies very fast and causes oxygen depletion, which is harmful to aquatic animals (Sahoo and Seckbach, 2015). Therefore, we focus on the daily maximum of Cyano on the surface layer (0–0.3 m) ( $\text{CyanoS}_{\text{max}}$ ) instead of its changing rate in the whole water column.  $\text{WTemp}_{\text{max}}$  and  $\Delta\text{WTemp}_{\text{max}}$  on the surface layer were calculated and named as  $\text{WTempS}_{\text{max}}$  and  $\Delta\text{WTempS}_{\text{max}}$ . Stepwise linear regressions were carried out by setting  $\text{WTempS}_{\text{max}}$ ,  $\Delta\text{WTempS}_{\text{max}}$ ,  $\text{PAR}_{\text{max}}$ ,  $\text{Ra}_{\text{mean}}$ ,  $\text{Depth}_{\text{mean}}$ ,  $\text{RH}_{\text{mean}}$ , and  $\text{Wave}_{\text{dmax}}$ ,  $\text{Cloudcover}_{\text{mean}}$  as alternative independent variables.  $\text{Cloudcover}_{\text{mean}}$ ,  $\text{Depth}_{\text{mean}}$  and  $\text{Wave}_{\text{dmax}}$  were left after stepwise regression. The stepwise regression procedure was shown in Table S.3. Residuals of regression are homoscedastic and follow a

**Table 1**  
 Summary of  $\Delta\text{Chl}_{a-f}$  % simulation model of Class-S and Class-SF ( $p < 0.05$ ).

No.	Variables	$R^2$	Coefficients	AICc	No.	Variables	$R^2$	Coefficients	AICc
Class-S: 2016 June/July & 2018 August/September (n = 32)					Class-SF: 2017 February/March 2018 March/April 2018 November (n = 35)				
1	(Constant)	0.43	- 6.7	3.2	1	(Constant)	0.45	- 3.5	2.6
2	Wave <sub>dmax</sub>	0.75	134.0	2.5	2	Wave <sub>dmax</sub>	0.67	7.4	2.1
	(Constant)		- 6.4			(Constant)		- 3.6	
3	Wave <sub>dmax</sub>	0.78	123.0	2.5	3	Wave <sub>dmax</sub>	0.74	7.1	1.9
	$\Delta\text{WTemp}_{\text{mean}}$		50.5			(Constant)		9.9	
	(Constant)		- 11.5			(Constant)		0.3	
	Wave <sub>dmax</sub>		133.0			Wave <sub>dmax</sub>		6.9	
	$\Delta\text{WTemp}_{\text{mean}}$		50.8			$\Delta\text{WTemp}_{\text{mean}}$		9.1	
	RH <sub>mean</sub>	0.06			RH <sub>mean</sub>	- 0.05			

Dependent Variable:  $\Delta\text{Chl}_{a-f}$  %.

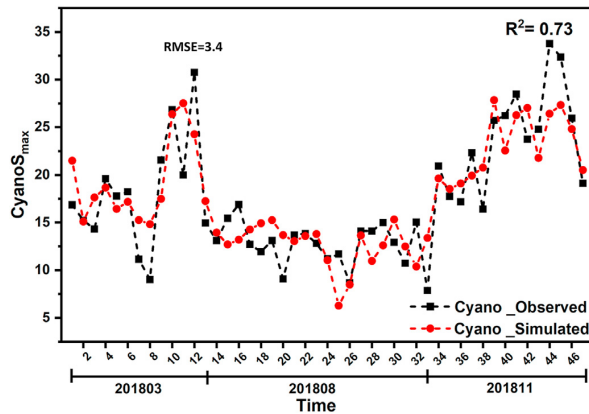


**Fig. 4.** Time series of observed and simulated maximum of phycochlorophyll concentrations on the water surface layer (0–0.3 m) ( $\text{CyanoS}_{\text{max}}$ ).

normal distribution. The selected model (No.3) has the lowest AICc value (3.6), and  $R^2$  between observed and simulated Cyano was 0.73, RMSE was 3.4. The observed and simulated  $\text{CyanoS}_{\text{max}}$  of 47 days were plotted in Fig. 4.

3.3. Correlation between independent variables and simulation objects ( $\Delta\text{Chl}_{a-f}$  % &  $\text{CyanoS}_{\text{max}}$ )

The correlation between simulation objects ( $\Delta\text{Chl}_{a-f}$  % &  $\text{CyanoS}_{\text{max}}$ ) and chosen independent variables are shown in Fig. 5.  $\text{Wave}_{\text{dmax}}$  was the most important factor for both  $\Delta\text{Chl}_{a-f}$  % and  $\text{CyanoS}_{\text{max}}$  model.  $R^2$  between  $\text{Wave}_{\text{dmax}}$  and Class-S of  $\Delta\text{Chl}_{a-f}$  %, Class-SF of  $\Delta\text{Chl}_{a-f}$  % and  $\text{CyanoS}_{\text{max}}$  were 0.43, 0.44 and 0.59.  $\Delta\text{Chl}_{a-f}$  % and  $\text{CyanoS}_{\text{max}}$  increased with the raise of  $\text{Wave}_{\text{dmax}}$ .

$\Delta\text{WTemp}_{\text{mean}}$  was more important for  $\Delta\text{Chl}_{a-f}$  % model in summer (Class-S) than in spring/autumn (Class-SF),  $R^2$  were 0.39 and 0.26.  $\text{RH}_{\text{mean}}$  had a slight linear correlation with  $\Delta\text{Chl}_{a-f}$  % in spring/autumn ( $R^2 = 0.15$ ) and  $\Delta\text{Chl}_{a-f}$  % decreased with the increase of  $\text{RH}_{\text{mean}}$ . Almost no correlation ( $R^2 = 0.002$ ) was found between

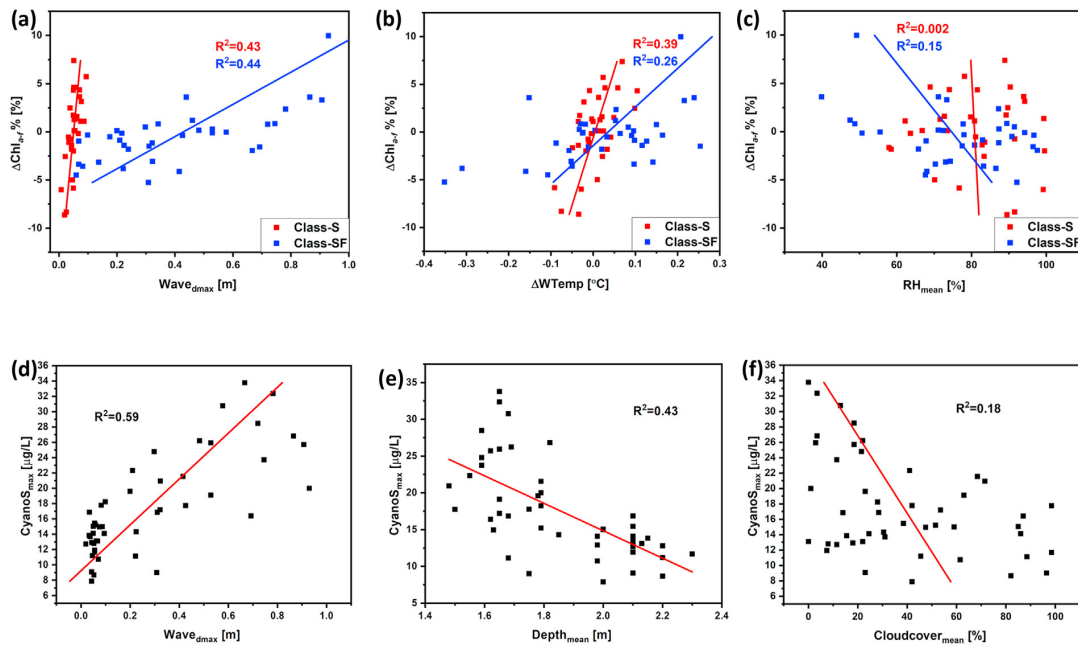


**Fig. 5.** Correlation between a)  $\text{Wave}_{\text{dmax}}$  and  $\Delta\text{Chl}_{a-f}$  %; b)  $\Delta\text{WTemp}$  and  $\Delta\text{Chl}_{a-f}$  %; c)  $\text{RH}_{\text{mean}}$  and  $\Delta\text{Chl}_{a-f}$  %; d)  $\text{Wave}_{\text{dmax}}$  and  $\text{CyanoS}_{\text{max}}$ ; e)  $\text{Depth}_{\text{mean}}$  and  $\text{CyanoS}_{\text{max}}$ ; f)  $\text{Cloudcover}_{\text{mean}}$  and  $\text{CyanoS}_{\text{max}}$ .

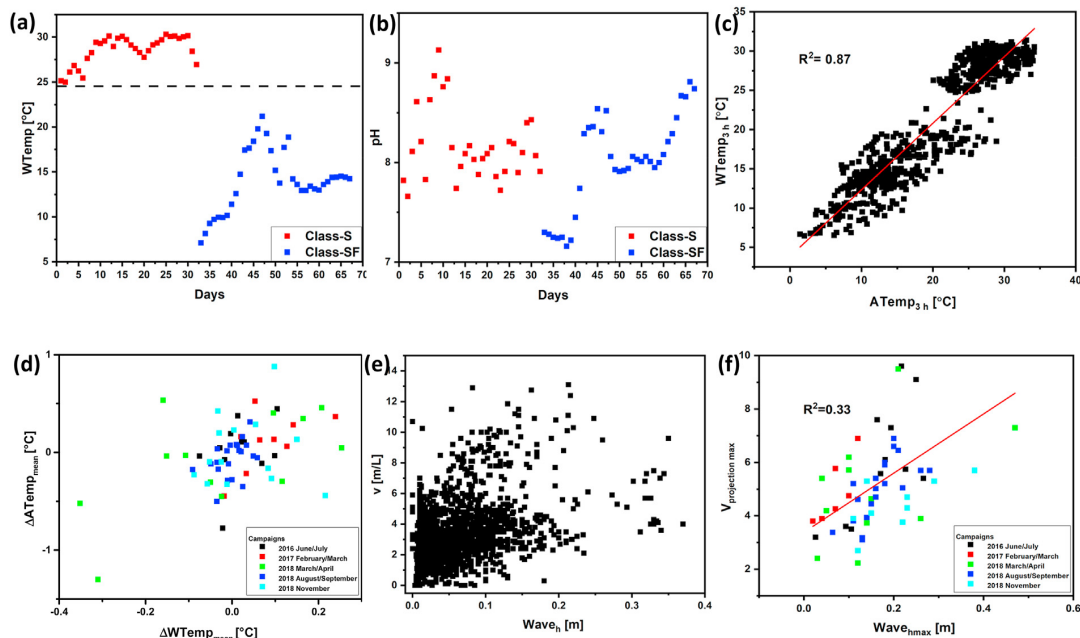


**Fig. 6.** a) Daily WTemp in Class-S and Class-SF; a) Daily pH in Class-S and Class-SF; Correlations between c) mean values of every 3-h water temperature (WTemp<sub>3h</sub>) and air temperature (ATemp<sub>3h</sub>); d) daily mean values of water temperature and air temperature 3-h changes (ΔWTemp<sub>mean</sub> & ΔATemp<sub>mean</sub>); e) mean values of every 3-h wave height (Wave<sub>h</sub>) and wind speed (v); f) daily maximum value of every 3-h Wave<sub>h</sub> and v<sub>projection</sub>.

RH<sub>mean</sub> and ΔChl<sub>a-f</sub>% in summer (Class-S), therefore it is not used in the model as independent variable ( $p > 0.05$ ). CyanoS<sub>max</sub> was lower under deeper water.  $R^2$  was 0.43 between Depth<sub>mean</sub> and CyanoS<sub>max</sub>. Weak linear correlation was found between Cloudcover<sub>mean</sub> and CyanoS<sub>max</sub> ( $R^2 = 0.18$ ). High CyanoS<sub>max</sub> appeared under low cloud cover (high irradiation).

### 3.4. Algal community succession and potential to predict ΔChl<sub>a-f</sub>% and CyanoS<sub>max</sub> by meteorological parameters

To know when algal classes' change from green algae/diatoms dominated to blue-green algae dominated is essential for water management and drinking water plants. In Fig. 6a, blue-green algae dominated Class-S (summer) had higher WTemp than Class-SF. Moreover, in general more blue-green algae were observed during periods of high pH.

Every 3-h ATemp had a strong correlation with that of WTemp in five campaigns,  $R^2$  was 0.87 (Fig. 6c). ΔWTemp<sub>mean</sub> also had a positive trend with ΔATemp<sub>mean</sub> (Fig. 6d).

No correlation between Wave<sub>h</sub> and Wind speed (v) was found within three-hourly mean observations (Fig. 6e). The wind direction ( $\vec{v}$ ) corrected wind speed (v<sub>projection</sub>) were calculated as shown in Fig. 1b. The daily maximum of v<sub>projection</sub> and Wave<sub>h</sub> had a positive correlation, and  $R^2$  was 0.33 (Fig. 6f).

## 4. Discussion

### 4.1. ΔChl<sub>a-f</sub>% simulation model

Instead of focusing on simulating the absolute values of Chl<sub>a-f</sub>, we decided to model changing rates of Chl<sub>a-f</sub> (ΔChl<sub>a-f</sub>) across the whole water column and to identify the possible factors that lead to rapid changes of ΔChl<sub>a-f</sub>. This is because stronger correlations were

found between measured parameters and ΔChl<sub>a-f</sub> than with Chl<sub>a-f</sub>. After seasonal differentiation of the model, the ΔChl<sub>a-f</sub>% simulation model improved significantly ( $R^2$  from 0.37 to 0.75). ΔChl<sub>a-f</sub>% simulation in summer had a dramatic improvement by classification. Classification is related to seasonal differences in algal species composition (Fig. 2e and f), because ΔChl<sub>a-f</sub>% for most parts represents for the changes of green algae and diatoms, which dominated in spring/autumn. A more detailed seasonal differentiation can be gained after collecting more representative long-term monitoring data.

Wave<sub>d</sub>, ΔWTemp and RH were the three parameters used in the ΔChl<sub>a-f</sub>% simulation model. Wave<sub>d</sub> reflects wind-induced mixing and resuspension, which leads to an increase in ΔChl<sub>a-f</sub>%. Strong enough wind can fully mix the water body in shallow Lake Taihu (Cao et al., 2006) and leads to extensive sediment resuspension, which disperses algae across the whole water column (Qin et al., 2004). Green algae and diatoms do not regulate their buoyancy. However, waves help them to circulate between the bottom and surface water, where they find better growth conditions, for example, warmer WTemp and stronger irradiation. Moreover, mixing induces higher bottom water temperatures, which also benefits algae (Pettersson et al., 2003). In short, mixing creates better conditions for the growth and activity of green algae and diatoms. WTemp is a vital factor for green algae and diatoms in all seasons, especially in summer. The increase of water temperature leads to the enhancement of metabolism of organisms and promotes the reproduction of algae to a certain limit (Feng et al., 2015).

Wave<sub>d</sub> and ΔWTemp were more important than RH in the ΔChl<sub>a-f</sub>% simulation model. RH was only used in Class-SF and with weak relationship between RH and ΔChl<sub>a-f</sub>%. It is generally believed that RH has little direct connection to algal growth, but many factors related to RH (temperature, rainfall and irradiation) might influence the algae (Sherwood et al., 2010; Vicente-Serrano et al., 2018). For example, rainfall, which is not beneficial for algal

growth (Allott, 1986), might lead to an increase of RH. High RH is also related to strong water evaporation, due to the increase in irradiation. The relationship between irradiation and algae is not linear. The optimum irradiation depends on the corresponding temperature and algal species (Chen et al., 2017; Latała et al., 2009). Few studies have been carried out on the principle behind the relationship between RH and algae. Even though RH was chosen by the stepwise linear regression, the changes of  $\Delta\text{Chl}_{a-f}\%$  might not be directly affected by RH. More data across different seasons should be collected to confirm respective relationships.

#### 4.2. CyanoS<sub>max</sub> simulation model

The majority of the maximum of surface Cyano (CyanoS<sub>max</sub>, 0–0.3 m) can be estimated by Wave<sub>d</sub>, Cloudcover, and Depth ( $R^2 = 0.73$ ). The blue-green algae have a strong ability to move towards the water surface to get better living conditions. This is a particular problem for drinking water production plants. An increase of CyanoS<sub>max</sub> can either represent blue-green algae movement to the water surface and subsequent accumulation, or growth of blue-green algae, or a combination of both.

Similar to the  $\Delta\text{Chl}_{a-f}\%$  model, Wave<sub>d</sub> formed the most important independent variable in the CyanoS<sub>max</sub> model. Stronger waves appear to be related to increased surface blue-green algae in the shallow lake (Fig. 5d). This could be related to corresponding mixing and resuspension. Moreover, blue-green algae accumulated at the water surface cannot be well measured by the BIOLIFT sensor. Wind mixing could distribute the blue-green algae better across the upper 0.3 m and make them measurable for the sensor. The days with deeper water resulted in lower CyanoS<sub>max</sub>. Because it takes more time for the algae to float to the water surface layer in deeper water (Oliver et al., 2016), moreover, the volume concentration of CyanoS<sub>max</sub>, which is at depth from 0 to 0.3 m, should be related to water depth. The irradiation promotes the growth of blue-green algae and might also affect its vertical distribution (Fig. 5f). Moreover, gas vesicles enable blue-green algae to adjust their vertical position for suitable irradiation in the water column (Ding et al., 2013). WTemp is not so important to CyanoS<sub>max</sub> in studied campaigns (2018 March/April, 2018 August/September, and 2019 November). During these periods, the mean and maximum of WTemp were 21.7 °C and 30.3 °C. More data with different WTemp of different seasons will be deeper insight into influence of WTemp to blue-green algae on the water surface layer.

#### 4.3. Eliminated independent variables and predictability of selected independents

Even though from previous studies, Oxy-sat, pH, Turb, and CDOM have quite good correlations with Chl<sub>a</sub> (Huang et al., 2010; Wang et al., 2017), the algal activity can inversely affect these parameters. Therefore, they are not suitable to be considered as independent variables that cause changes in algae abundance. However, pH and WTemp are important factors for algal community succession. Blue-green algae bloom usually develop during summer when WTemp and pH are higher (Fig. 6a and b). Nutrients are not used in either of the models, since only weak correlations were found between nutrients (total P, dissolved P, total N, NH<sub>4</sub>-N, NO<sub>3</sub>-N) and CyanoS<sub>max</sub>/ $\Delta\text{Chl}_{a-f}\%$  (Fig.S.6). For modeling long-term phytoplankton dynamics, nutrients still remain the primary predictors (Cai et al., 2012; Shi et al., 2017). However, nutrients in Lake Taihu are constantly at levels sufficient for intense algal growth, especially in the northern part of the lake (Qin et al., 2015). Hence nutrient dynamics do not show significant effects on algae growth in the short-term (Ye et al., 2011). They only would do if they become strict limiting factors, which currently is not the case in

Lake Taihu (Yang et al., 2019). Moreover, there is (Lorenzen Carl, 1967) still a lack of quick response and high-accuracy on-line sensors for nutrients (Havlik et al., 2013; Huang et al., 2010). Therefore, nutrients were not considered in this simulation model with respect to model simplification and feasibility.

The independent variables used in the two simulation models are  $\Delta\text{WTemp}_{\text{mean}}$ ,  $\text{RH}_{\text{mean}}$ ,  $\text{Depth}_{\text{mean}}$ ,  $\text{Cloudcover}_{\text{mean}}$ , and  $\text{Wave}_{\text{dmax}}$ . The increase in air temperature will be directly reflected in the lake water temperature (Fig. 6c and d). Previous studies showed that WTemp could be estimated from ATemp (Erickson and Stefan, 2000; Wood and Wood, 2005). In addition, wind dynamics controlled wave dynamics (Bengtsson and Hellström, 1992; Chao et al., 2008), and thus wave dynamics can be deduced from respective wind data (Goda, 2003; Jin and Ji, 2001). After correction by wind direction according to the specific location, the maximum wind speed had a positive correlation with the maximum of Wave<sub>h</sub> with  $R^2$  equal to 0.33 (Fig. 6f). The projection angle can be regulated and then be applied in other locations by projecting wind speed into two directions considering the effect of the wind direction in this location. In summer, during strong stratification, higher wind speed is required to induce the same level of mixing compared to non-stratified conditions in other seasons. Therefore, in Fig. 5a, the slope between  $\Delta\text{Chl}_{a-f}\%$  and  $\text{Wave}_{\text{dmax}}$  was higher in summer (Class-S) than in spring/autumn (Class-SF). The parameters  $\vec{v}$ ,  $v$ , Cloudcover and RH can be acquired from BIOLIFT and weather forecast data. Water depth was collected by the multi-sensor system BIOLIFT in real-time and is unlikely to show remarkable changes in a short time, except for heavy rainfall events.

## 5. Conclusions

In summary, it is feasible by only using the multi-sensor and meteorological data to explain most of the variance of CyanoS<sub>max</sub> and  $\Delta\text{Chl}_{a-f}\%$ . Among them, classification of the  $\Delta\text{Chl}_{a-f}\%$  model by seasons was required to considerably improve the simulation quality. Moreover, the independent variables used in the models can be acquired from the weather forecast data or can be estimated. However, the certainty of the prediction will then depend on the weather forecast accuracy. It is therefore possible to use BIOLIFT or similar instruments to generate forecasts for next day's algal status, which may provide additional information for water management.

For example, the online monitoring data and the corresponding prediction results will be available for the drinking water plant before the occurrence of algal blooms. They can consider respective data for implementing short-term reaction schemes of their water treatment process. The World Health Organization (WHO) has established guidance levels for recreational water, which is a reference for the drinking water plants. Specifically, the thresholds for low health alert are 500 blue-green algae cells mL<sup>-1</sup> ( $\approx 4 \mu\text{g L}^{-1}$  phycocyanin), most of our data were within this level. Where blue-green algae are not present at bloom levels, but environmental conditions are sufficiently favorable for rapid algal growth. The drinking water plants and local governments should prepare for potential medium alert within several weeks. The thresholds for a moderate health alert are 2000 bluegreen algae cells mL<sup>-1</sup> ( $\approx 30 \mu\text{g L}^{-1}$  phycocyanin) or  $1 \mu\text{g L}^{-1}$  Chl<sub>a</sub>. Where drinking water plants should prepare for additional sampling, assessment of toxicity, additional water treatment (e.g., activated carbon), and have to think about using alternative drinking water supply. Next stage, thresholds for high health alert are 100,000 bluegreen algae cells/ml ( $\approx 90 \mu\text{g L}^{-1}$  phycocyanin) or  $50 \mu\text{g L}^{-1}$  Chl<sub>a</sub>. Where the operators and health authorities should decide to issue a health warning or notice in relation to the suitability of the water for



consumption, drinking water plants must seek an alternative water supply (Bartram and Chorus, 1999; Brient et al., 2008). Predicted  $Chl_{a-f}$  can be calculated by the current  $Chl_{a-f}$  concentration measured by BIOLIFT and the predicted  $\Delta Chl_{a-f}$ . Significantly, what we predicted for blue-green algae is the maximum value of phycocyanin on the water surface layer, which is higher than the mean value in the whole water column, but it will be treated as an alert value. Specific measures need to be regulated according to actual conditions in water plant operations. This can be applied not only in Lake Taihu but also potentially in other aquatic systems in the world.

Nutrients cannot be well measured by online and *in situ* sensor systems and are hardly necessary to be used in short time algal models for Lake Taihu. Wave characteristic was the most important factor for the  $\Delta Chl_{a-f}$  and  $CyanoS_{max}$  simulation models, because the wind-induced mixing and resuspension easily happen in shallow Lake Taihu. More representative monitoring data across seasons, also including extreme conditions as can now occur due to climate change, should be collected to optimize the classification and simulation. This knowledge can be used in other shallow and eutrophic lakes as well.

Based on this study, real-time weather forecast data combined with *in situ* multi-sensor data will be used to create an algal forecast model in a follow-up study. Moreover, an *in situ* algal class sensor will be equipped within the multi-sensor system in the near future. So, total  $Chl_{a-f}$  and  $Chl_{a-f}$  of different algal classes (green algae, blue-green algae, diatoms) can be measured and most probably also estimated. Furthermore, the wind-induced waves might also lead to the physical movement of algae. To take this into account, we will install more BIOLIFTS in combination with a velocimeter in different locations. In the near future, potential current direction and algal physical movement will also be considered in the model.

#### Author contributions

**Jingwei Yang:** Fieldwork, Laboratory work, Data analyze, Writing and editing, **Andreas Holbach:** Supervision, Fieldwork, Reviewing and editing, **Michael J. Stewardson:** Simulation suggestion, Reviewing and editing, **Andre Wilhelms:** Fieldwork, **Yanwen Qin; Binghui Zheng:** Project coordination and management, **Hua Zou:** Field trip assistance in Wuxi, **Boqiang Qin, Guangwei Zhu:** Fieldwork arrangement in TLLER, **Christian Moldaenke:** Technical support for PhycoLA instrument, **Stefan Norra:** Project coordination and outline, Supervision.

#### Declaration of competing interest

The authors declare that they have no known competing financial interests or personal relationships that could have appeared to influence the work reported in this paper.

#### Acknowledgments

This work was supported by the Federal Ministry of Education and Research of Germany (BMBF, grant-no.: 02WCL1336B). The first author was supported by the China Scholarship Council. Michael Stewardson acknowledges support for his contribution to this research from the Australian Research Council provided for Discovery Project (DP130103619).

#### Appendix A. Supplementary data

Supplementary data to this article can be found online at <https://doi.org/10.1016/j.chemosphere.2020.128482>.

#### References

- Allott, N.A., 1986. Temperature, oxygen and heat-budgets of six small western Irish lakes. *Freshw. Biol.* 16, 145–154. <https://doi.org/10.1111/j.1365-2427.1986.tb00959.x>.
- Bartram, J., Chorus, I., 1999. Toxic Cyanobacteria in Water: A Guide to Their Public Health Consequences, Monitoring and Management. CRC Press. <https://doi.org/10.1017/CBO9781107415324.004>.
- Bengtsson, L., Hellström, T., 1992. Wild-induced resuspension in a small shallow lake. *Hydrobiologia* 241, 163–172. <https://doi.org/10.1007/BF00028639>.
- Bodini, S., Sanfilippo, L., Savino, E., Moschetta, P., 2015. Automated micro Loop Flow Reactor technology to measure nutrients in coastal water: state of the art and field application. In: MTS/IEEE OCEANS 2015 - Genova: Discovering Sustainable Ocean Energy for a New World. IEEE, pp. 1–7. <https://doi.org/10.1109/OCEANS-Genova.2015.7271720>.
- Brient, L., Lengronne, M., Bertrand, E., Rolland, D., Sipel, A., Steinmann, D., Baudin, I., Legeas, M., Le Rouzic, B., Bormans, M., 2008. A phycocyanin probe as a tool for monitoring cyanobacteria in freshwater bodies. *J. Environ. Monit.* 10, 248–255. <https://doi.org/10.1039/b714238b>.
- Cai, L.L., Zhu, G.W., Zhu, M.Y., Xu, H., Qin, B.Q., 2012. Effects of temperature and nutrients on phytoplankton biomass during bloom seasons in Taihu Lake. *Water Sci. Eng.* 5, 361–374. <https://doi.org/10.3882/j.issn.1674-2370.2012.04.001>.
- Cao, H.-S., Kong, F.-X., Luo, L.-C., Shi, X.-L., Yang, Z., Zhang, X.-F., Tao, Y., -ong, F.-X., 2006. Effects of wind and wind-induced waves on vertical phytoplankton distribution and surface blooms of *Microcystis aeruginosa* in Lake Taihu. *J. Freshw. Ecol.* 21, 231–238. <https://doi.org/10.1080/02705060.2006.9664991>.
- Cavanaugh, J.E., 1997. Unifying the derivations for the Akaike and corrected Akaike information criteria. *Stat. Probab. Lett.* 33, 201–208. [https://doi.org/10.1016/s0167-7152\(96\)00128-9](https://doi.org/10.1016/s0167-7152(96)00128-9).
- Chao, X., Jia, Y., Shields, F.D., Wang, S.S.Y., Cooper, C.M., 2008. Three-dimensional numerical modeling of cohesive sediment transport and wind wave impact in a shallow oxbow lake. *Adv. Water Resour.* 31, 1004–1014. <https://doi.org/10.1016/j.advwatres.2008.04.005>.
- Chen, C., Mao, Z., Han, G., Li, T., Wang, Z., Tao, B., Wang, T., Gong, F., 2017. Optimal PAR intensity for spring bloom in the Northwest Pacific marginal seas. *Ecol. Indic.* 72, 428–435. <https://doi.org/10.1016/j.ecolind.2016.08.044>.
- Chen, Y., Chen, K., Hu, Y., 2006. Discussion on possible error for phytoplankton chlorophyll-a concentration analysis using hot-ethanol extraction method. *J. Lake Sci.* 18, 550–552.
- Ding, Y., Song, L., Sedmak, B., 2013. UVB radiation as a potential selective factor favoring microcystin producing bloom forming cyanobacteria. *PLoS One* 8, e73919. <https://doi.org/10.1371/journal.pone.0073919>.
- Erickson, T.R., Stefan, H.G., 2000. Linear air/water temperature correlations for streams during open water periods. *J. Hydrol. Eng.* 5, 317–321. [https://doi.org/10.1061/\(ASCE\)1084-0699\(2000\)5](https://doi.org/10.1061/(ASCE)1084-0699(2000)5).
- Feng, L., Chen, B., Hayat, T., Alsaedi, A., Ahmad, B., 2015. Modelling the influence of thermal discharge under wind on algae. *Phys. Chem. Earth* 79 (82), 108–114. <https://doi.org/10.1016/j.pce.2014.12.003>.
- Garrison, T.S., 2012. *Essentials of Oceanography*. Cengage Learning.
- Goda, Y., 2003. Revisiting Wilson's formulas for simplified wind-wave prediction. *J. Waterw. Port. Coast. Ocean Eng.* 129, 93–95. [https://doi.org/10.1061/\(ASCE\)0733-950X](https://doi.org/10.1061/(ASCE)0733-950X).
- Havlik, I., Lindner, P., Scheper, T., Reardon, K.F., 2013. On-line monitoring of large cultivations of microalgae and cyanobacteria. *Trends Biotechnol.* 31, 406–414. <https://doi.org/10.1016/j.tibtech.2013.04.005>.
- Hsu, L.H.H., Aryasomayajula, A., Selvaganapathy, P.R., 2016. A review of sensing systems and their need for environmental water monitoring. *Crit. Rev. Biomed. Eng.* 44, 357–382. <https://doi.org/10.1615/CritRevBiomedEng.2017019704>.
- Huang, C., Li, Y., Yang, H., Sun, D., Yu, Z., Zhang, Z., Xia, 2014. Detection of algal bloom and factors influencing its formation in Taihu Lake from 2000 to 2011 by MODIS. *Environ. Earth Sci.* 71, 3705–3714. <https://doi.org/10.1007/s12665-013-2764-6>.
- Huang, J., Gao, J., Hörmann, G., 2012. Hydrodynamic-phytoplankton model for short-term forecasts of phytoplankton in Lake Taihu, China. *Limnologia* 42, 7–18. <https://doi.org/10.1016/j.limno.2011.06.003>.
- Huang, M.Z., Wan, J.Q., Ma, Y.W., Li, W.J., Sun, X.F., Wan, Y., 2010. A fast predicting neural fuzzy model for on-line estimation of nutrient dynamics in an anoxic/oxic process. *Bioresour. Technol.* 101, 1642–1651. <https://doi.org/10.1016/j.biortech.2009.08.111>.
- Jin, K.R., Ji, Z.G., 2001. Calibration and verification of a spectral wind wave model for Lake Okeechobee. *Ocean. Eng.* 28, 571–584. [https://doi.org/10.1016/S0029-8018\(00\)00009-3](https://doi.org/10.1016/S0029-8018(00)00009-3).
- Latała, A., Jodłowska, S., Pniewski, F., 2009. Culture Collection of Baltic Algae (CCBA) and characteristic of some strains by factorial experiment approach. *Arch. Hydrobiol. Suppl. Algol. Stud.* 122, 137–154. <https://doi.org/10.1127/1864-1318/2006/0122-0137>.
- Lorenzen Carl, J., 1967. Determination of chlorophyll and pheophytin pigments: spectrophotometric equations. *Plant Physiol.* 12, 343–346.
- Moldaenke, C., Fang, Y., Yang, F., Dahlhaus, A., 2019. Early warning method for cyanobacteria toxin, taste and odor problems by the evaluation of fluorescence signals. *Sci. Total Environ.* 667, 681–690. <https://doi.org/10.1016/j.scitotenv.2019.02.271>.
- Ogashawara, I., Mishra, D.R., Mishra, S., Curtarelli, M.P., Stech, J.L., 2013. A performance review of reflectance based algorithms for predicting

- phycocyanin concentrations in inland waters. *Rem. Sens.* 5, 4774–4798. <https://doi.org/10.3390/rs5104774>.
- Oliver, S.K., Soranno, P.A., Emi Fergus, C., Wagner, T., Winslow, L.A., Scott, C.E., Webster, K.E., Downing, J.A., Stanley, E.H., 2016. Prediction of lake depth across a 17-state region in the United States. *Inl. Waters* 6, 314–324. <https://doi.org/10.5268/1W-6.3.957>.
- Paerl, H.W., Huisman, J., 2009. Climate change: a catalyst for global expansion of harmful cyanobacterial blooms. *Environ. Microbiol. Rep.* 1, 27–37. <https://doi.org/10.1111/j.1758-2229.2008.00004.x>.
- Pascolo, S., Petti, M., Bosa, S., 2018. On the Wave Bottom Shear Stress in Shallow Depths: the Role of Wave Period and Bed Roughness. *Water, Switzerland*. <https://doi.org/10.3390/w10101348>.
- Pettersson, K., Grust, K., Weyhenmeyer, G., Blenckner, T., 2003. Seasonality of chlorophyll and nutrients in Lake Erken – effects of weather conditions. *Hydrobiologia* 506–509, 75–81. <https://doi.org/10.1023/B:HYDR.0000008582.61851.76>.
- Qin, B., Hu, W., Gao, G., Luo, L., Zhang, J., 2004. Dynamics of sediment resuspension and the conceptual schema of nutrient release in the large shallow Lake Taihu, China. *Chin. Sci. Bull.* 49, 54–64. <https://doi.org/10.1007/BF02901743>.
- Qin, B., Li, W., Zhu, G., Zhang, Y., Wu, T., Gao, G., 2015. Cyanobacterial bloom management through integrated monitoring and forecasting in large shallow eutrophic Lake Taihu (China). *J. Hazard Mater.* 287, 356–363. <https://doi.org/10.1016/j.jhazmat.2015.01.047>.
- Qin, B., Paerl, H.W., Brookes, J.D., Liu, J., Jeppesen, E., Zhu, G., Zhang, Y., Xu, H., Shi, K., Deng, J., 2019. Why Lake Taihu continues to be plagued with cyanobacterial blooms through 10 years (2007–2017) efforts. *Sci. Bull.* 64, 354–356. <https://doi.org/10.1016/j.scib.2019.02.008>.
- Rajaei, T., Boroumand, A., 2015. Forecasting of chlorophyll-a concentrations in South San Francisco Bay using five different models. *Appl. Ocean Res.* 53, 208–217. <https://doi.org/10.1016/j.apor.2015.09.001>.
- Sahoo, D., Seckbach, J., 2015. *The Algae World*, vol. 26. Springer, Dordrecht. [https://doi.org/10.1007/978-94-017-7321-8\\_8](https://doi.org/10.1007/978-94-017-7321-8_8).
- Shapiro, S.S., Wilk, M.B., 1965. An analysis of variance test for normality (complete samples). *Biometrika* 52, 591. <https://doi.org/10.2307/2333709>.
- Sherwood, S.C., Ingram, W., Tsushima, Y., Satoh, M., Roberts, M., Vidale, P.L., O’Gorman, P.A., 2010. Relative humidity changes in a warmer climate. *J. Geophys. Res. Atmos.* 115, 1–11. <https://doi.org/10.1029/2009JD012585>.
- Shi, W., Yu, N., Jiang, X., Han, Z., Wang, S., Zhang, X., Wei, S., Giesy, J.P., Yu, H., 2017. Influence of blooms of phytoplankton on concentrations of hydrophobic organic chemicals in sediments and snails in a hyper-eutrophic, freshwater lake. *Water Res.* 113, 22–31. <https://doi.org/10.1016/j.watres.2017.01.059>.
- Singh, S.P., Singh, P., 2015. Effect of temperature and light on the growth of algae species: a review. *Renew. Sustain. Energy Rev.* 50, 431–444. <https://doi.org/10.1016/j.rser.2015.05.024>.
- Vicente-Serrano, S.M., Nieto, R., Gimeno, L., Azorin-Molina, C., Drumond, A., El Kenawy, A., Dominguez-Castro, F., Tomas-Burguera, M., Peña-Gallardo, M., 2018. Recent changes of relative humidity: regional connections with land and ocean processes. *Earth Syst. Dyn.* 9, 915–937. <https://doi.org/10.5194/esd-9-915-2018>.
- Wang, Y., Xie, Z., Lou, L., Ung, W., Mok, K., 2017. Algal bloom prediction by support vector machine and relevance vector machine with genetic algorithm optimization in freshwater reservoirs. *Eng. Comput.* 34, 664–679.
- Wells, M.L., Trainer, V.L., Smayda, T.J., Karlson, B.S.O., Trick, C.G., Kudela, R.M., Ishikawa, A., Bernard, S., Wulff, A., Anderson, D.M., Cochlan, W.P., 2015. Harmful algal blooms and climate change: learning from the past and present to forecast the future. *Harmful Algae* 49, 68–93. <https://doi.org/10.1016/j.hal.2015.07.009>.
- Wilson, A.E., Wilson, W.A., Hay, M.E., 2006. Intraspecific variation in growth and morphology of the bloom-forming cyanobacterium *Microcystis aeruginosa*. *Appl. Environ. Microbiol.* 72, 7386–7389. <https://doi.org/10.1128/AEM.00834-06>.
- Wood, D.J., Wood, D.J., 2005. Waterhammer analysis—essential and easy (and efficient). *J. Environ. Eng.* 131, 1123–1131. [https://doi.org/10.1061/\(ASCE\)0733-9372\(2005\)131](https://doi.org/10.1061/(ASCE)0733-9372(2005)131).
- Wu, T., Qin, B., Brookes, J.D., Shi, K., Zhu, G., Zhu, M., Yan, W., Wang, Z., 2015. The influence of changes in wind patterns on the areal extension of surface cyanobacterial blooms in a large shallow lake in China. *Sci. Total Environ.* 518–519, 24–30. <https://doi.org/10.1016/j.scitotenv.2015.02.090>.
- Yang, J., Holbach, A., Wilhelms, A., Krieg, J., Qin, Y., Zheng, B., Zou, H., Qin, B., Zhu, G., Wu, T., Norra, S., 2020. Identifying spatio-temporal dynamics of trace metals in shallow eutrophic lakes on the basis of a case study in Lake Taihu, China. *Environ. Pollut.* 264, 114802. <https://doi.org/10.1016/j.envpol.2020.114802>.
- Yang, J., Holbach, A., Wilhelms, A., Qin, Y., Zheng, B., Zou, H., Qin, B., Zhu, G., Norra, S., 2019. Highly time-resolved analysis of seasonal water dynamics and algal kinetics based on in-situ multi-sensor-system monitoring data in Lake Taihu, China. *Sci. Total Environ.* 660, 329–339. <https://doi.org/10.1016/j.scitotenv.2019.01.044>.
- Yang, Z., Zhang, M., Shi, X., Kong, F., Ma, R., Yu, Y., 2016. Nutrient reduction magnifies the impact of extreme weather on cyanobacterial bloom formation in large shallow Lake Taihu (China). *Water Res.* 103, 302–310. <https://doi.org/10.1016/j.watres.2016.07.047>.
- Ye, C., Li, C.H., Yu, H.C., Song, X.F., Zou, G.Y., Liu, J., 2011. Study on ecological restoration in near-shore zone of a eutrophic lake, Wuli Bay, Taihu Lake. *Ecol. Eng.* 37, 1434–1437. <https://doi.org/10.1016/j.ecoleng.2011.03.028>.
- Zheng, Y., Zhao, L.Y.T.S., 2016. *China’s Great Urbanization*. Taylor & Francis.
- Zhu, G., Zou, W., Guo, C., Qin, B., Zhang, Y., Xu, H., Zhu, M., 2020. Long-term variations of phosphorus concentration and capacity in Lake Taihu, 2005–2018: implications for future phosphorus reduction target management. *J. Lake Sci.* 32, 21–35. <https://doi.org/10.18307/2020.0103>.
- Zulkifli, S.N., Rahim, H.A., Lau, W.J., 2018. Detection of contaminants in water supply: a review on state-of-the-art monitoring technologies and their applications. *Sensor. Actuator. B Chem.* 255, 2657–2689. <https://doi.org/10.1016/j.snb.2017.09.078>.

## **Simulating chlorophyll-a fluorescence changing rate and phycocyanin fluorescence by using a multi-sensor system in Lake Taihu, China**

Jingwei Yang<sup>\*,a</sup>, Andreas Holbach<sup>a,b</sup>, Michael J. Stewardson<sup>c</sup>, Andre Wilhelms<sup>a</sup>, Yanwen Qin<sup>d</sup>, Binghui Zheng<sup>d</sup>, Hua Zou<sup>e</sup>,  
Boqiang Qin<sup>f</sup>, Guangwei Zhu<sup>f</sup>, Christian Moldaenke<sup>g</sup>, Stefan Norra<sup>a</sup>

<sup>a</sup>*Institute of Applied Geosciences, Working Group Environmental Mineralogy and Environmental System Analysis (ENMINSA)  
Karlsruhe Institute of Technology, Kaiserstraße 12, 76131 Karlsruhe, Germany*

<sup>b</sup>*Department of Bioscience, Aarhus University, Frederiksborgvej 399, 4000 Roskilde, Denmark*

<sup>c</sup>*Department of Infrastructure Engineering, Melbourne School of Engineering, The University of Melbourne, 3010 Victoria,  
Australia*

<sup>d</sup>*Chinese Research Academy of Environmental Sciences, Dayangfang 8, Anwai Beiyuan, Beijing 100012, P.R. China*

<sup>e</sup>*School of Environmental and Civil Engineering, Jiangnan University, Wuxi 214122, P.R. China*

<sup>f</sup>*Nanjing Institute of Geography & Limnology, Chinese Academy of Sciences, 73 East Beijing Road, 210008 Nanjing, P.R.  
China*

<sup>g</sup>*bbe Moldaenke GmbH, Preetzer Chaussee 177, 24222 Schwentinental, Germany*

**\*Corresponding author**

Email address: [Jingwei.yang@kit.edu](mailto:Jingwei.yang@kit.edu)

**SUPPORTING INFORMATION**

## Content

1. Campaign and sample information (P.3)
2. BIOLIFT instrument (P.4)
3. Comparing cell density and  $\text{Chl}_{a-f}$  in different algal classes (P.5)
4.  $\text{Chl}_{a-f}$  in campaign 2018-November from day 2 to day 6 (P.5)
5.  $\Delta\text{Chl}_{a-f}\%$  stepwise linear regression before classification (P.6)
6.  $\text{CyanoS}_{\max}$  stepwise linear regression (P.8)
7. The correlations between nutrients and  $\text{CyanoS}_{\max} / \Delta\text{Chl}_{a-f}\%$  (P.9)

## 1. Campaign and sample information (P.3)

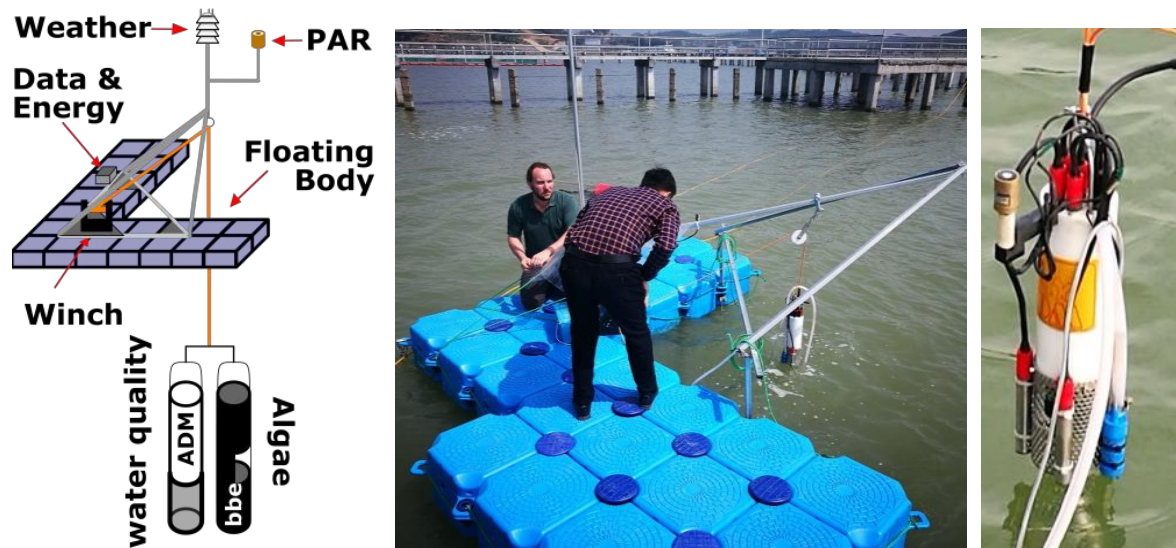
Table S.1. Campaign and sample information.

Campaign	Start Date (YY-MM-DD)	End Date (YY-MM-DD)	Measuring Days	Days for model	Campaign name
1	2016-06-27	2016-07-15	20	11	2016-June/July
2	2017-02-23	2017-03-06	12	9	2017-February/March
3	2018-03-24	2018-04-15	23	12	2018-March/April
4	2018-08-15	2018-09-09	26	21	2018-August/September
5	2018-11-15	2018-12-01	17	14	2018-November

---

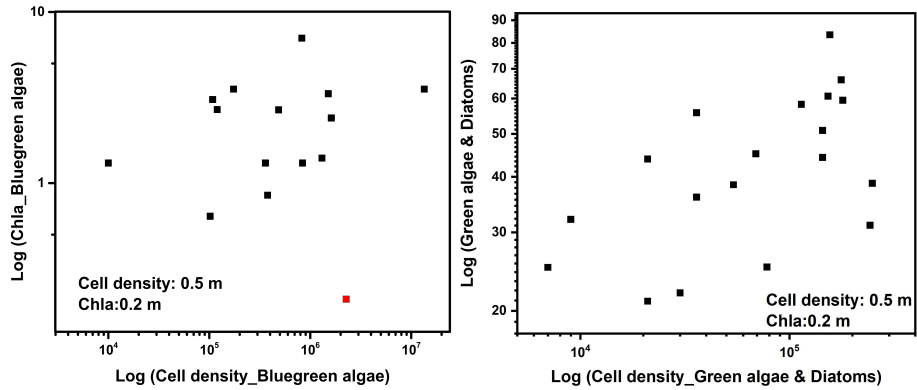
## 2. BIOLIFT instrument (P.4)

Fig. S.1. Structure of BIOLIFT-buoy system (Left) ; BIOLIFT-buoy system in the field (Middle);  
BIOLIFT (Right)



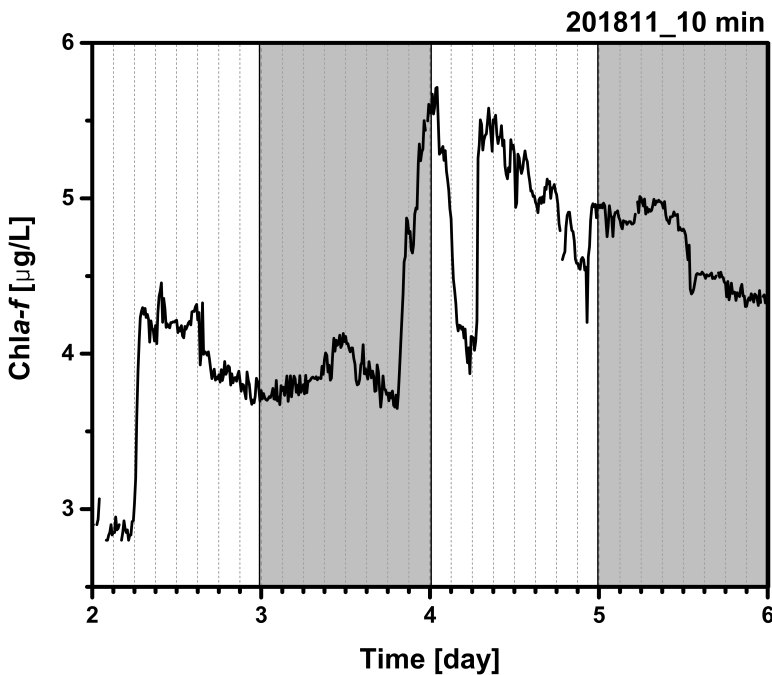
### 3. Comparing cell density and Chl<sub>a-f</sub> in different algal classes (P.5)

Fig. S.2. Correlation between logged cell density and logged Chl<sub>a-f</sub> of bluegreen algae as well as diatoms & green algae.



### 4. Chl<sub>a-f</sub> in campaign 2018-November from day 2 to day 6 (P.5)

Fig. S.3. Chl<sub>a-f</sub> in campaign 2018-November from day 2 to day 6.



### 5. $\Delta\text{Chl}_{a-f}\%$ stepwise linear regression before classification (P.6)

Table. S.2. Summary of  $\Delta\text{Chl}_{a-f}\%$  simulation model before classification.

	Variables	R <sup>2</sup>	Coefficients	P
1	(Constant)	0.19	-0.4	
	$\Delta\text{WTemp}_{\text{mean}}$		14.1	0.00
2	(Constant)	0.23	-1.0	
	$\Delta\text{WTemp}_{\text{mean}}$		13.4	0.00
	$\text{Wave}_{\text{dmax}}$		2.9	0.05
3	(Constant)	0.37	-6.4	
	$\Delta\text{WTemp}_{\text{mean}}$		14.9	0.00
	$\text{Wave}_{\text{dmax}}$		6.8	0.00
	$\text{WTemp}_{\text{mean}}$		0.2	0.00

Fig.S.4 Homoscedasticity graph for  $\Delta\text{Chl}_{a-f}\%$  simulation model in Class-S

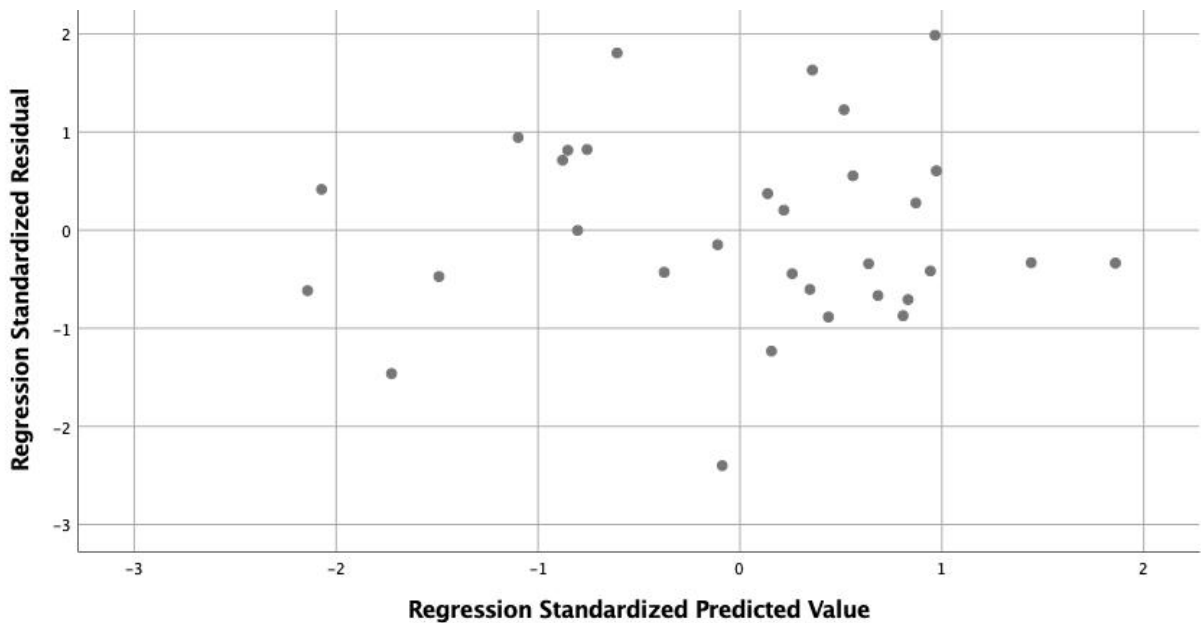
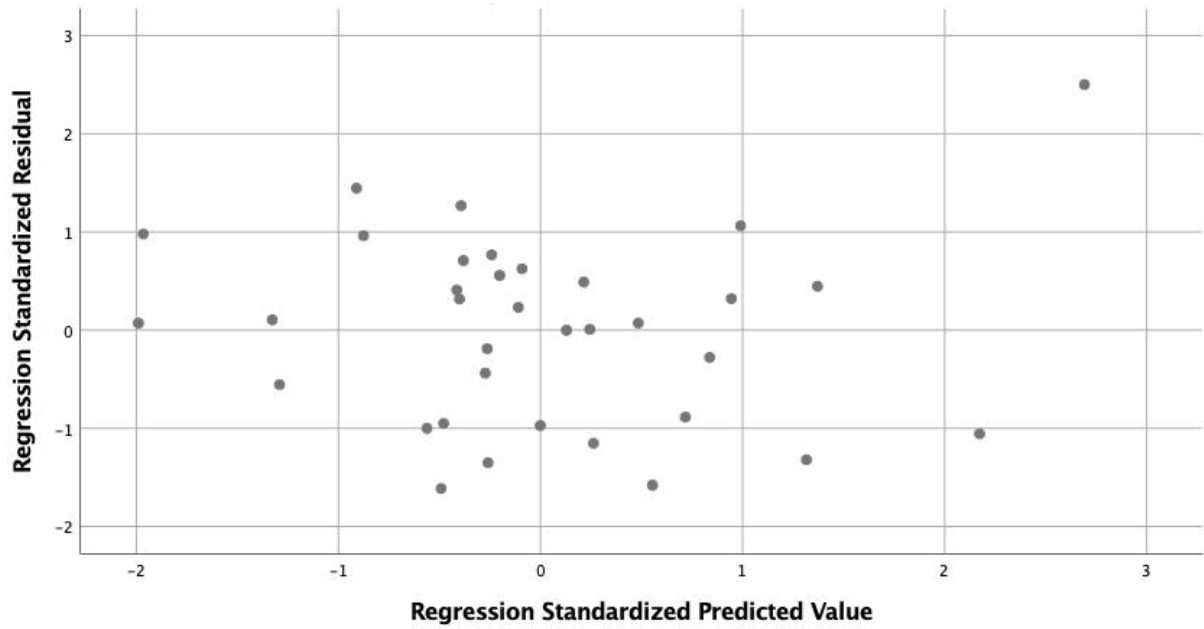




Fig.S.5 Homoscedasticity graph for  $\Delta\text{Chl}_{a-f}\%$  simulation model in Class-SF

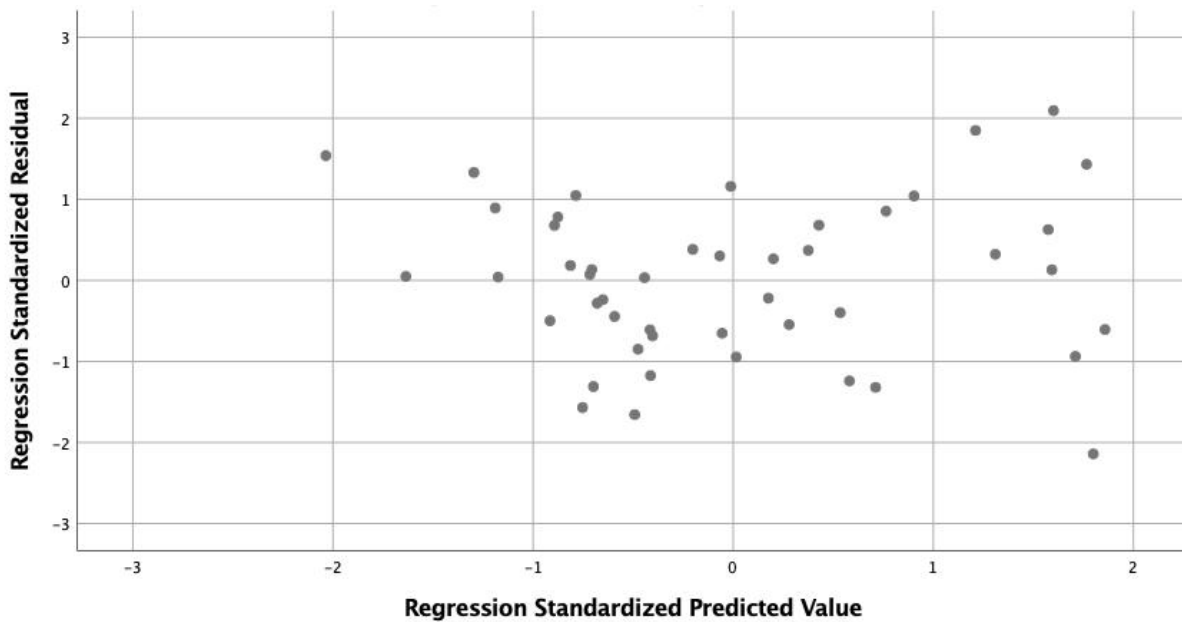


### 6. CyanoS<sub>max</sub> stepwise linear regression (P.8)

Table. S.3. The model summary of CyanoS<sub>max</sub> linear regression simulation ( $p < 0.05$ )

No.	Variables	R <sup>2</sup>	Coefficients	AICc
1	(Constant)	0.59	12.6	3.9
	Wave <sub>dmax</sub>		17.7	
2	(Constant)	0.66	15.1	3.8
	Wave <sub>dmax</sub>		16.3	
	Cloudcover		-0.06	
3	(Constant)	0.73	37.2	3.6
	Wave <sub>dmax</sub>		10.1	
	Cloudcover		-0.07	
	Depth		-10.6	

Fig.S.6 Homoscedasticity graph for CyanoS<sub>max</sub> simulation model



### 7. The correlations between nutrients and $\text{CyanoS}_{\max} / \Delta\text{Chl}_{a-f}\%$ (P.9)

Fig. S.7. The correlation between dissolved P (TDP) and  $\Delta\text{Chl}_{a-f}\%$ .

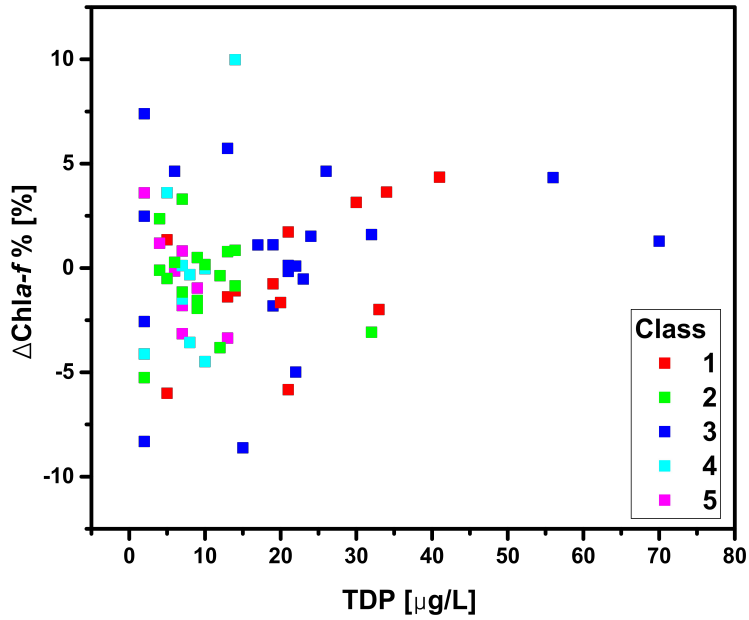


Fig. S.8. The correlation between total N (TN) and  $\Delta\text{Chl}_{a-f}\%$ .

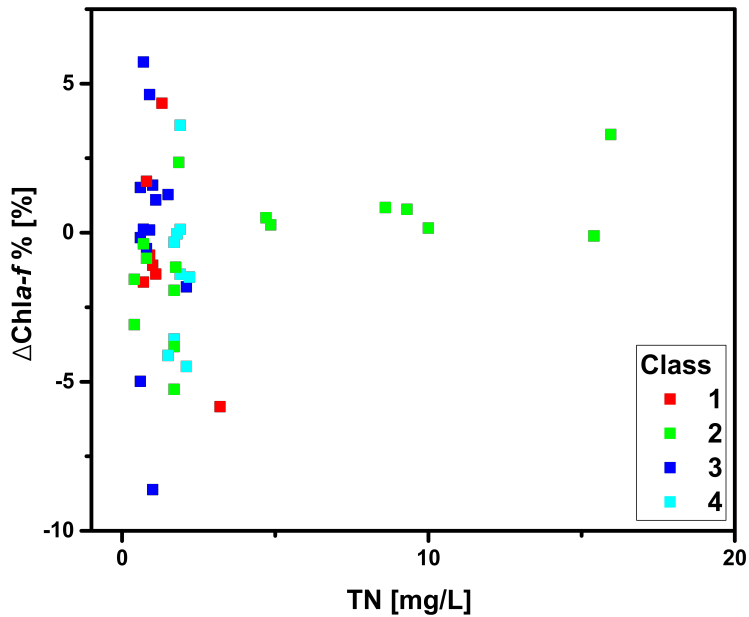


Fig. S.9. The correlation between  $\text{NH}_4^+\text{-N}$  and  $\Delta\text{Chl}_{a-f}\%$ .

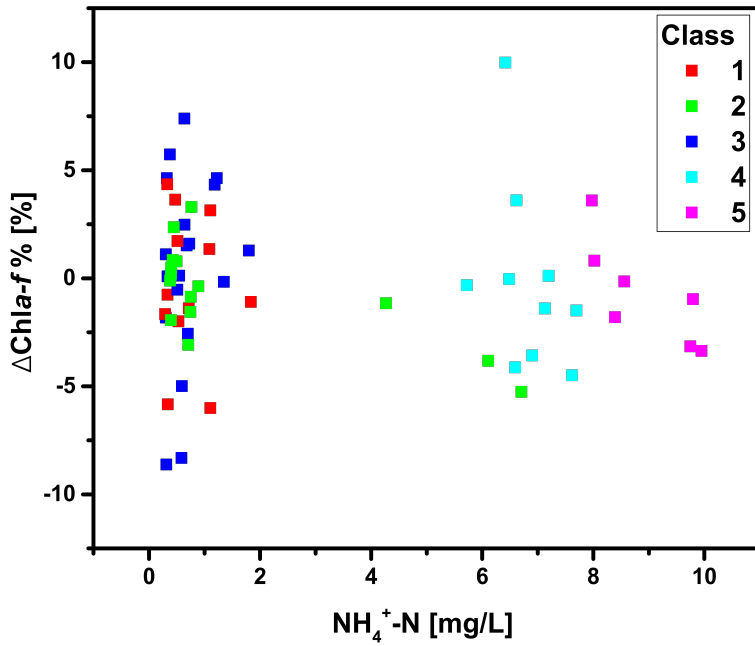


Fig. S.10. The correlation between  $\text{NO}_3^-$  and  $\Delta\text{Chl}_{a-f}\%$ .

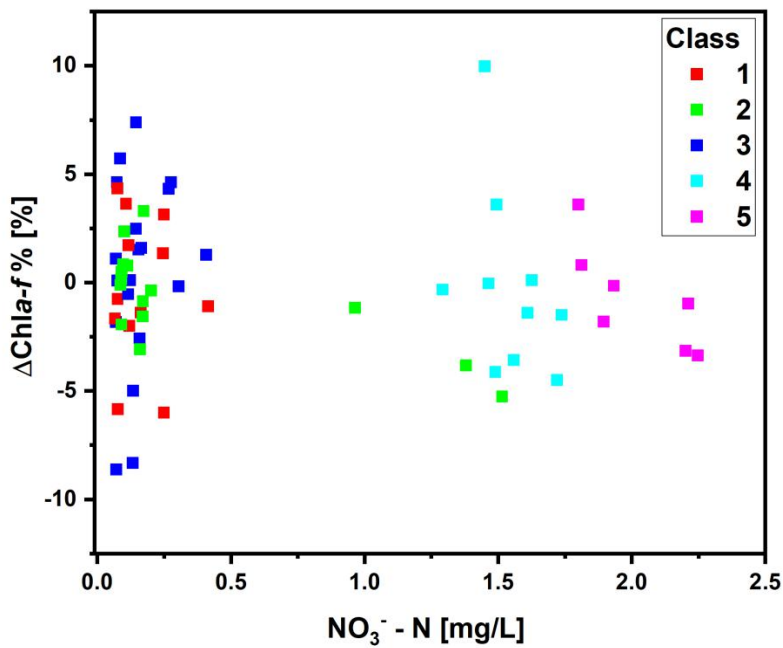


Fig. S.11. The correlation between  $\text{NO}_3^-$  and  $\text{CyanoS}_{\text{max}}$ .

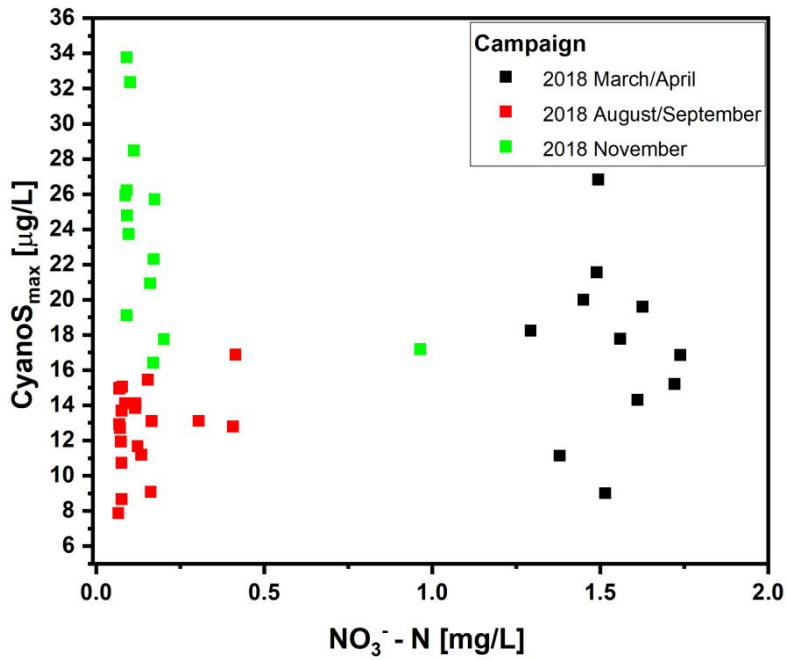


Fig. S.12. The correlation between dissolved P (TDP) and  $\text{CyanoS}_{\text{max}}$ .

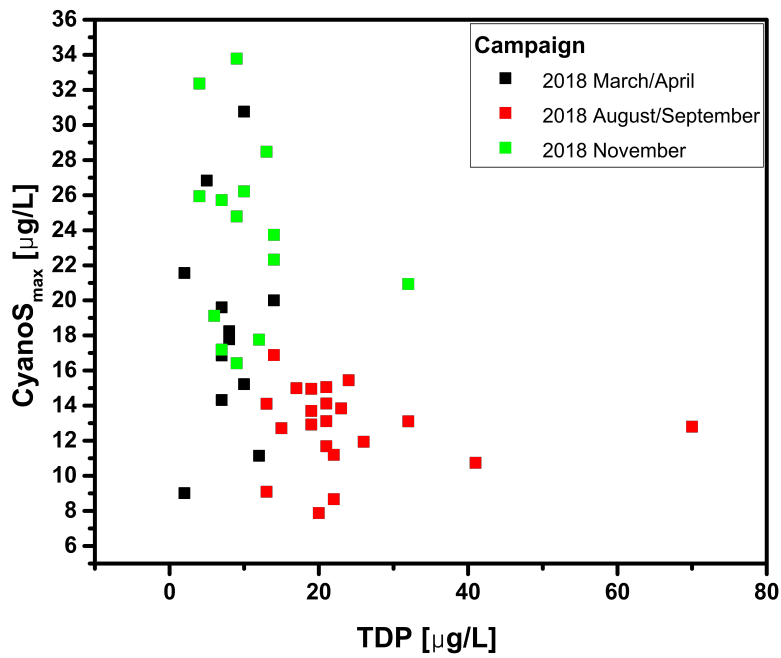


Fig. S.13. The correlation between  $\text{NH}_4^+\text{-N}$  and  $\text{CyanoS}_{\text{max}}$ .

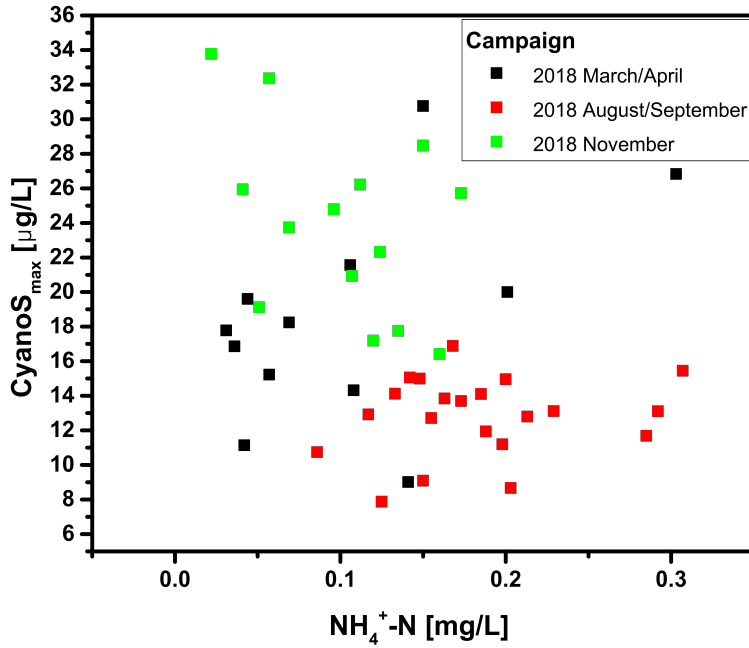


Fig. S.14. The correlation between total N (TN) and  $\text{CyanoS}_{\text{max}}$ .

